



Provided by the author(s) and University of Galway in accordance with publisher policies. Please cite the published version when available.

Title	Regulation of cell fate by microRNAs during unfolded protein response and its role in cancer
Author(s)	Arabkari, Vahid
Publication Date	2018-12-20
Publisher	NUI Galway
Item record	<a href="http://hdl.handle.net/10379/14750">http://hdl.handle.net/10379/14750</a>

Downloaded 2024-05-21T01:25:31Z

Some rights reserved. For more information, please see the item record link above.





**Regulation of cell fate by microRNAs during unfolded protein  
response and its role in cancer**

A thesis submitted to the National University of Ireland, Galway in fulfillment of  
the requirement for the degree of

**Doctor of Philosophy**

By

**Vahid Arabkari**

Discipline of Pathology, School of Medicine, College of Medicine,  
National University of Ireland Galway, Ireland

Thesis supervisor: Dr. Sanjeev Gupta

October 2018

# Contents

<b>Dedication</b> .....	<b>i</b>
<b>Acknowledgments</b> .....	<b>ii</b>
<b>Declaration</b> .....	<b>iii</b>
<b>Communications arising from this work</b> .....	<b>iv</b>
<b>List of figures</b> .....	<b>v</b>
<b>List of tables</b> .....	<b>viii</b>
<b>List of abbreviations</b> .....	<b>ix</b>
<b>Abstract</b> .....	<b>xiii</b>
<b>Chapter 1</b> .....	<b>1</b>
<b>1-0. Introduction</b> .....	<b>2</b>
1-1. The Endoplasmic Reticulum.....	2
1-2. Endoplasmic Reticulum Stress and the Unfolded Protein Response (UPR) Signalling Pathway .....	3
1-2-1. ATF6 signalling pathway .....	5
1-2-2. PERK signalling pathway .....	7
1-2-3. IRE1 signalling pathway .....	11
1-3. Human Cancer .....	13
1-4. Breast Cancer.....	15
1-4-1. Overview .....	15
1-4-2. Molecular classification of breast cancer .....	15
1-4-3. Signalling pathways in breast cancer .....	17
1-4-4. Inherited breast cancer.....	21
1-4-5. Breast cancer treatment .....	22
1-5. UPR signalling pathway and its role in cancer .....	26
1-6. UPR signalling pathway in breast cancer .....	31
1-6-1. IRE1-XBP1 axis and breast cancer .....	31
1-6-2. PERK and breast cancer .....	32
1-6-3. ATF6 and breast cancer.....	33

1-6-4. GRP78 and breast cancer .....	34
1-7. UPR signalling pathway and breast cancer therapy resistance.....	35
1-8. UPR targeting drugs and cancer treatment .....	36
1-9. MicroRNAs .....	37
1-9-1. MicroRNAs nomenclature .....	38
1-9-2. MicroRNAs biogenesis: Canonical pathway.....	38
1-9-3. MicroRNAs biogenesis: Non-canonical pathway .....	40
1-9-4. MicroRNAs function.....	41
1-9-5. MicroRNAs as cancer therapeutics and targets.....	41
1-9-6. The role of microRNAs in cancer development.....	43
1-9-7. Tumour suppressive and oncogenic roles of microRNAs .....	45
1-10. MicroRNAs and breast cancer.....	48
1-11. MicroRNAs and the unfolded protein response .....	49
1-12. Rationale of the study .....	54
1-13. Aims of the study.....	57
<b>Chapter 2.....</b>	<b>58</b>
<b>2-0. Materials and Methods .....</b>	<b>59</b>
2-1. Cell culture .....	59
2-2. Drug treatments .....	60
2-3. RNA preparation.....	63
2-4. Reverse transcription reaction .....	63
2-5. Conventional Polymerase Chain Reaction (PCR) assay.....	64
2-6. Real-Time Quantitative PCR (RT-qPCR) .....	65
2-6-1. Real-time quantitative PCR assay for mRNAs .....	65
2-6-2. Real-time quantitative PCR assay for miRNAs .....	66
2-7. Plasmids.....	66
2-7-1. PERK, ATF6 and XBP1 shRNA plasmids.....	66
2-7-2. miR-378, miR-616, XBP1s, VAV1 and c-MYC overexpressing plasmids .....	67
2-7-3. Transformation of plasmids.....	69
2-7-4. Transient transfection of spliced XBP1 in MCF7 cells.....	70
2-7-5. Transient transfection of miR-616, VAV1, and c-MYC in HEK 293T cells.....	70



2-8. Preparation of lentivirus .....	71
2-9. Lentivirus transduction .....	72
2-10. Protein extraction and western blotting .....	73
2-11. Colony formation assay .....	77
2-12. Scratch wound healing assay .....	78
2-13. MTS cell proliferation assay .....	78
2-14. Cell death analysis by Flow cytometry .....	79
2-15. mRNA expression profiling by next-generation sequencing technology .....	79
2-16. Analysis of oncomine cancer gene microarray database .....	81
2-17. Preparation of conditioned media .....	81
2-18. Survival analysis for miR-378 .....	81
2-19. Survival analysis for miR-378 signature .....	82
2-20. Statistical analysis of data .....	82
<b>Chapter 3.....</b>	<b>83</b>
<b>3-0. Results chapter 1.....</b>	<b>84</b>
3-1. Background.....	84
3-2. Hypothesis .....	87
3-3. Aims .....	87
3-4. Results .....	88
3-4-1. MiR-378 is downregulated during conditions of EnR stress and UPR activation .....	88
3-4-2. MiR-378 is downregulated in MCF7 human breast cancer cells during conditions of EnR stress and UPR activation .....	92
3-4-3. MiR-378 host gene (PPARGC1B) is downregulated in colorectal and breast cancer cells during conditions of EnR stress and UPR activation .....	93
3-4-4. The expression level of miR-378 and PPARGC1B are downregulated in breast cancer .....	94
3-4-5. Generation of stable pools of human colorectal and breast cancer cells with knockdown of UPR sensors .....	95
3-4-6. XBP1 is required for downregulation of miR-378 and its host gene (PPARGC1B) during UPR.....	99
3-4-7. The expression of XBP1 and PPARGC1B has a negative correlation in breast cancer patients. ....	102
3-4-8. Generation of stable overexpressing miR-378 clones in colorectal and breast cancer cells ..	103

3-4-9. MiR-378 reduced proliferation of luminal breast cancer cells .....	105
3-4-10. MiR-378 reduced colony formation of luminal breast cancer cells .....	106
3-4-11. MiR-378 reduced migration of luminal breast cancer cells .....	108
3-4-12. MiR-378 enhanced the sensitivity of MCF7 cells toward the anti-estrogen compounds.....	110
3-4-13. MiR-378 enhanced the sensitivity of MCF7 cells toward the EnR stress-inducing compounds .....	111
3-4-14. MiR-378 does not have any effect on UPR sensors during conditions of EnR stress and UPR activation.....	111
3-4-15. MiR-378 dependent gene signature was identified by the transcriptomic and bioinformatic analysis.....	114
3-4-16. Confirmation of selected miR-378 dependent genes expression by RT-qPCR assay .....	116
3-4-17. Type I interferon signalling pathway plays a role to reduce MCF7 cell proliferation through miR-378 .....	119
3-4-18. High expression of miR-378 has a good outcome in ER-positive breast cancer patients ....	121
3-4-19. MiR-378 dependent gene signature is associated with good outcome in breast cancer .....	123
<b>Chapter 4.....</b>	<b>124</b>
<b>4-0. Results Chapter 2 .....</b>	<b>125</b>
4-1. Background.....	125
4-2. Hypothesis .....	128
4-3. Aims .....	128
4-4. Results .....	128
4-4-1. MiR-616 is upregulated during conditions of EnR stress in colorectal and breast cancer cells .....	128
4-4-2. MiR-616 host gene (CHOP) is upregulated during conditions of EnR stress in colorectal and breast cancer cells .....	130
4-4-3. Expression level of miR-616 in breast cancer cell lines.....	131
4-4-4. PERK is required for regulation of primary miR-616 during conditions of EnR stress.....	132
4-4-5. Generation of stable overexpressing miR-616 pools in colorectal and breast cancer cells....	134
4-4-6. MiR-616 reduced proliferation of colorectal and luminal breast cancer cells.....	136
4-4-7. MiR-616 reduced colony formation of colorectal and luminal breast cancer cells.....	137
4-4-8. MiR-616 reduced migration of colorectal and luminal breast cancer cells.....	139
4-4-9. MiR-616 enhanced the sensitivity of MCF7 cells towards the anti-estrogen compounds ....	141

4-4-10. MiR-616 did not have any effect on the sensitivity of MCF7 cells towards the EnR stress-inducing compounds .....	142
4-4-11. MiR-616 reduced CHOP expression during conditions of EnR stress.....	142
4-4-12. MiR-616 dependent gene signature was identified by the transcriptomic and bioinformatic analysis.....	145
4-4-13. Confirmation of selected miR-616 dependent genes expression by RT-qPCR assay .....	147
4-4-14. MiR-616 targets the coding sequence region (CDS) of VAV1 and c-MYC transcripts .....	151
4-4-15. Generation of stable overexpressing VAV1 and c-MYC clones in overexpressing miR-616 MCF7 cells.....	153
4-4-16. VAV1 and c-MYC reversed the growth inhibition effect of miR-616 in MCF7-miR-616 cells .....	154
4-4-17. VAV1 and c-MYC reversed miR-616 effect in colony formation on MCF7-miR-616 cells .....	155
4-4-18. VAV1 and c-MYC reversed miR-616 effect in migration on MCF7-miR-616 cells.....	157
4-4-19. Generation of stable overexpressing VAV1 and c-MYC pools in parental MCF7 cells.....	158
4-4-20. VAV1 and c-MYC increased the proliferation of parental MCF7 cells.....	159
4-4-21. VAV1 and c-MYC increased colony formation of parental MCF7 cells.....	160
4-4-22. VAV1 and c-MYC increased migration of parental MCF7 cells.....	161
<b>Chapter 5.....</b>	<b>163</b>
<b>5-0. Discussion .....</b>	<b>164</b>
5-1. MiRNA-378 is downregulated by XBP1 and inhibits growth and migration of luminal breast cancer cells.....	164
5-2. CHOP-intronic miR-616 inhibits cell growth and migration by targeting c-MYC and VAV1.....	172
5-3. Limitations of the study and future directions .....	181
5-3-1. Limitations of the study.....	181
5-3-2. Future directions of the study.....	182
<b>Chapter 6.....</b>	<b>184</b>
<b>6-0. Appendix .....</b>	<b>185</b>
6-1. Cell lines .....	185
6-2. MiRNA-specific primer sequences for RT-qPCR assay .....	185
6-3. Cell culture medium and chemical reagents .....	186
6-4. Reverse transcription reagents.....	187

6-5. IDT primer and probe sequences for UPR signalling pathway genes .....	188
6-6. IDT primer and probe sequences for miR-616 dependent genes.....	189
6-7. IDT primer and probe sequences for miR-378dependent genes.....	190
6-8. MiR-378 upregulated dependent genes .....	191
6-9. MiR-378 downregulated dependent genes .....	192
6-10. Kaplan-Meier plots for miR-378 in ER-positive breast cancers.....	193
6-11. Kaplan-Meier plots for selected miR-378 gene signature .....	194
6-12. MiR-616 upregulated dependent genes .....	196
6-13. MiR-616 downregulated dependent genes .....	197
6-14. Permission letter for figure 1-4.....	198
6-15. Submitted manuscripts. ....	199
6-16. Results for two uncompleted projects.....	232
<b>Bibliography .....</b>	<b>236</b>

# **Dedication**

This thesis is dedicated to my parents Saeid and Homai for their  
unwavering love and support

# Acknowledgments

I would sincerely like to thank my supervisor Dr. Sanjeev Gupta for giving me the opportunity to work in his lab and for all his help and support over the course of my Ph.D.

I would like to thank my lab mates Muhammad Mosaraf Hossain and David Barua for their help and support over the course of my Ph.D. I would also like to thank the Department of Pathology technical staff member Mr. Mark Webber for his help and support.

# Declaration

The data described in this thesis is the result of my work, which has been carried out in Dr. Sanjeev Gupta's laboratory, Department of Pathology, School of Medicine, College of Medicine, National University of Ireland Galway from January 2016 to July 2018. The material is not substantially similar to any other work that has been submitted for any other degree or qualification at NUIG or any other university.

Signed: \_\_\_\_\_

# Communications arising from this work

## Peer-reviewed publications:

- 1- Hossain, M. M., D. Barua, **V. Arabkari**, N. Islam, A. Gupta and S. Gupta (2018). "Hyperactivation of nuclear receptor coactivators induces PERK-dependent cell death." Oncotarget **9**(14): 11707-11721.
- 2- Clancy, E., M. Burke, **V. Arabkari**, T. Barry, H. Kelly, R. M. Dwyer, M. J. Kerin and T. J. Smith (2017). "Amplification-free detection of microRNAs via a rapid microarray-based sandwich assay." Anal Bioanal Chem **409**(14): 3497-3505.

## Submitted manuscripts:

- 1- **V. Arabkari**, Hossain, M. M., D. Barua, M. Webber, T. Smith, A. Gupta and S. Gupta. miRNA-378 is downregulated by XBP1 and inhibits growth and migration of luminal breast cancer cells. BMC Cancer.
- 2- **V. Arabkari**, E. Clancy, R.M. Dwyer, M. J. Kerin, J. Newell and T. J. Smith. Relative and Absolute Expression Analysis of MicroRNAs Associated with Luminal A Breast Cancer- A Comparison. Pathology & Oncology Research.

## Poster presentations:

- 1- **Vahid Arabkari**, Muhammad Mosaraf Hossain, Ananya Gupta and Sanjeev Gupta. Regulation of cell fate by unfolded protein response-regulated microRNAs in cancer. 21-23 Feb, Annual meeting 2017. Irish Association for Cancer Research, Kilkenny, Ireland.
- 2- **Vahid Arabkari**, Muhammad Mosaraf Hossain, Ananya Gupta and Sanjeev Gupta. XBP1 regulated miR-378 has tumour suppressor role in breast cancer. 22-24 Feb, Annual meeting 2018. Irish Association for Cancer Research, Dublin, Ireland.



# List of figures

Figure 1-1. The UPR signalling pathway

Figure 1-2. Adaptive responses of the UPR signalling pathway during conditions of EnR stress

Figure 1-3. Pro-apoptotic responses of UPR signalling pathway during conditions of EnR stress

Figure 1-4. The hallmarks of cancer

Figure 1-5. The pathophysiological and pharmacological inducers of EnR stress and cancer cell responses

Figure 1-6. The UPR signalling pathway and cell fate decisions

Figure 1-7. The canonical microRNA biogenesis pathway

Figure 3-1. Cytogenetic location of miR-378 in its host gene (PPARGC1B) sequence

Figure 3-4-1-1. MiRNA expression profiles in HCT116 cells during conditions of EnR stress.

Figure 3-4-1-2. MiR-378 and miR-1908 are downregulated in HCT116 cells during conditions of EnR stress

Figure 3-4-1-3. MiR-378 is downregulated in RKO cells during conditions EnR stress

Figure 3-4-2. MiR-378 is downregulated in MCF7 breast cancer cells during conditions of EnR stress

Figure 3-4-3. PPARGC1B is downregulated in cancer cells during conditions of EnR stress

Figure 3-4-4. Expression of miR-378 and PPARGC1B are downregulated in breast cancer

Figure 3-4-5-1. Schematic images of lentiviral vector map and shRNA construct

Figure 3-4-5-2. PERK, ATF6, and XBP1 expression were reduced in HCT116 knockdown pools

Figure 3-4-5-3. PERK, ATF6, and XBP1 expression were reduced in MCF7 knockdown pools

Figure 3-4-6-1. XBP1 is required for downregulation of miR-378 during UPR

Figure 3-4-6-2. Downregulation of miR-378 and its host gene (PPARGC1B) are dependent on the IRE1-XBP1 axis during EnR stress

Figure 3-4-6-3. Downregulation of miR-378 and its host gene (PPARGC1B) are dependent on spliced XBP1

Figure 3-4-7. The negative relationship between XBP1 and PPARGC1B expression in breast cancer patients

Figure 3-4-8-1. Schematic image of lentivirus vector map for cloning and expression of precursor miR-378

Figure 3-4-8-2. Generation of stable overexpressing miR-378 pools in colorectal and breast cancer cells

Figure 3-4-9. The effect of miR-378 on colorectal and breast cancer cells proliferation

Figure 3-4-10-1. The effect of miR-378 in colony formation of colorectal and breast cancer cells

Figure 3-4-10-2. The effect of miR-378 on size and number of colorectal and breast cancer cells

Figure 3-4-11. The effect of miR-378 on breast cancer cells migration

Figure 3-4-12. The effect of miR-378 on MCF7 cells response to the anti-estrogen compounds

Figure 3-4-13. The effect of miR-378 on MCF7 cells response to the EnR stress-inducing compounds

Figure 3-4-14. MiR-378 has no effect on UPR sensors during conditions of EnR stress

Figure 3-4-15. Identification of miR-378 dependent gene signature

Figure 3-4-16-1. Confirmation of miR-378 upregulated dependent genes by RT-qPCR assay

Figure 3-4-16-2. Confirmation of miR-378 downregulated dependent genes by RT-qPCR assay

Figure 3-4-17. Type I interferon signalling pathway regulates MCF7 cell proliferation through miR-378

Figure 3-4-18. High expression of miR-378 has a good outcome in ER + breast cancer

Figure 3-4-19. MiR-378 dependent gene signature is associated with good outcome in breast cancer

Figure 4-1. Cytogenetic location of miR-616 and in its host gene (DDIT3) sequence

Figure 4-4-1. MiR-616 is upregulated in colorectal and breast cancer cells during EnR stress

Figure 4-4-2. CHOP (miR-616 host gene) is upregulated in colorectal and breast cancer cells during conditions of EnR stress

Figure 4-4-3. Endogenous level of miR-616 is downregulated in several breast cancer cell lines

Figure 4-4-4-1. PERK is required for regulation of primary miR-616 during UPR

Figure 4-4-4-2. PERK is required for regulation of primary miR-616 but not for mature miR-616 during UPR

Figure 4-4-5-1. Schematic image of lentivirus vector map for cloning and expression of precursor miR-616

Figure 4-4-5-2. Generation of stable overexpressing miR-616 pools in colorectal and breast cancer cells

Figure 4-4-6. The effect of miR-616 on cells proliferation of colorectal and breast cancer

Figure 4-4-7-1. The effect of miR-616 on colony formation of colorectal and breast cancer cells

Figure 4-4-7-2. The effect of miR-616 on colony formation of colorectal and breast cancer cells

Figure 4-4-8. The effect of miR-616 on colorectal and breast cancer cells migration

Figure 4-4-9. The effect of miR-616 on MCF7 cells response to the anti-estrogen compounds

Figure 4-4-10. The effect of miR-616 on MCF7 cells response to the EnR stress-inducing compounds

Figure 4-4-11. MiR-616 has no effect on UPR sensors during conditions of EnR stress

Figure 4-4-12. Identification of miR-616 dependent gene signature

Figure 4-4-13-1. Confirmation of downregulated miR-616 dependent genes by RT-qPCR assay

Figure 4-4-13-2. VAV1 and c-MYC proteins are reduced in miR-616 expressing HCT116 and MCF7 cells

Figure 4-4-13-3. Confirmation of upregulated miR-616 dependent genes by RT-qPCR assay

Figure 4-4-14-1. Identification of a potential miR-616 binding site in VAV1 and c-MYC transcripts

Figure 4-4-14-2. MiR-616 targets the coding sequence region (CDS) of VAV1 and c-MYC transcripts

Figure 4-4-15. Generation of stable clones expressing VAV1 and c-MYC in MCF7-miR-616 cells

Figure 4-4-16. The effect of VAV1 and c-MYC on miR-616 expressing MCF7 cells proliferation

Figure 4-4-17. The effect of VAV1 and c-MYC on MCF7-miR-616 cells colony formation

Figure 4-4-18. The effect of VAV1 and c-MYC on MCF7-miR-616 cells migration

Figure 4-4-19. Generation of stable clones expressing VAV1 and c-MYC on parental MCF7 cells

Figure 4-4-20. The effect of VAV1 and c-MYC on parental MCF7 cells proliferation

Figure 4-4-21. The effect of VAV1 and c-MYC on parental MCF7 cells colony formation

Figure 4-4-22. The effect of VAV1 and c-MYC on parental MCF7 cells migration.

Figure 5-1. Graphical abstract of UPR regulated miR-378

Figure 5-2. Graphical abstract of UPR regulated miR-616

# List of tables

- Table 1-1. Molecular breast cancer subtypes and their hormone receptor status
- Table 1-2. MiRNAs and their expression in malignancy
- Table 1-3. Common dysregulated miRNAs in breast cancer subtypes
- Table 1-4. Summary of microRNA effects on UPR signaling pathway and their target genes
- Table 2-1. Pharmacological compounds for cell treatment
- Table 2-2. Recipes for cell lysis buffer
- Table 2-3. Recipes for Laemmli's SDS-PAGE
- Table 2-4. Recipes for immunoblotting gels
- Table 2-5. Recipes for running buffer
- Table 2-6. Recipes for transfer buffer
- Table 2-7. Optimum conditions for different antibodies in western blotting

# List of abbreviations

AIDS	Acquired immunodeficiency syndrome
ASK1	Apoptosis signal regulation kinase 1
AGO	Argonaute
ARE	Antioxidant response element
ATF4	Activated transcription factor 4
ATF6	Activating transcription factor 6
ATP	Adenosine triphosphate
BAD	BCL-2-antagonist of cell death
BAK	BCL-2 homologous antagonist/killer
BAX	BCL-2 associated protein X
BCL-2	B-cell lymphoma 2
BCL-xL	B-cell lymphoma 2- extra large
BID	BH3-interacting domain death agonist
BIM	BCL-2-interacting mediator of cell death
BFA	Brefeldin A
CHOP	CCAAT enhancer-binding protein homologous protein
CLL	Chronic lymphocytic leukaemia
CIMP	CpG island methylator phenotype
CIN	Chromosomal instability
CDK4	Cyclin-dependent kinase 4
DGCR8	DiGeorge Syndrome Critical Region Gene 8
DISC	Death inducing signalling complex
DNA	Deoxyribonucleic acid
DTX	Docetaxol
eIF2 $\alpha$	Eukaryotic translation initiation factor 2 $\alpha$
EMT	Epithelial-to-mesenchymal transition
EnR	Endoplasmic Reticulum
ER $\alpha$	Estrogen receptor-alpha

ER $\beta$	Estrogen receptor-beta
ERAD	ER-associated degradation
ERK	Extracellular signal-regulated kinase
ERO-1	ER oxidoreductin 1
ERP72	Endoplasmic reticulum resident protein 72
ERSEI/ II	EnR Stress Response Element I/ II
GADD34	Growth arrest and DNA damage-inducible protein
GWAS	Genome-wide association studies
GLS	Golgi localization signals
GRP78	Glucose-regulated protein 78
HCV	Hepatitis C virus
HCC	Hepatocellular carcinoma
HSP72	Heat shock protein 72
HER2	Human epidermal growth factor receptor-2
IHC	Immune-histochemical staining
IRE1 $\alpha$	Inositol-requiring enzyme-1
JNK	c-JUN terminal kinase
KEAP1	Kelch-like ECH-associated protein
LIMK1	LIM domain kinase-1
LTED	Long-term estrogen-deprived
M7G 5'	7 methylguanosine
MCL-1	Myeloid cell leukemia sequence 1
MEF	Mouse embryonic fibroblast
miRNA	MicroRNA
MGB	Minor groove binder
MSI	Microsatellites instability
MMR	Mismatch repair
NRF2	Nuclear factor (erythroid-derived 2)-like 2
OS	Overall survival
PAK-2	P21-activated kinase-2
PCR	Polymerase chain reaction

PDIA5	Protein disulphide isomerase A5
PPARGC1B	Peroxisome proliferator-activated receptor $\gamma$ coactivator-1 $\beta$
PERK	(PKR)-like ER kinase
PKR	Protein kinase R
Pre-miRNA	Precursor miRNA
Pri-miRNA	Primary miRNA
PUMA	p53 up-regulated modulator of apoptosis
PS	Phosphatidylserine
RIDD	Regulated Ire1-dependent decay
RT-qPCR	Reverse transcription quantitative polymerase chain reaction
RISC	RNA-induced silencing complex
RNA	Ribonucleic acid
RNAi	RNA interference
ROS	Reactive oxygen species
S1P	Site-1 protease
S2P	Site-2 protease
SERDs	Selective estrogen receptor degraders
SERMs	Selective estrogen receptor modulator
siRNA	small interfering RNA
SNPs	Single nucleotide polymorphism
TamR	Tamoxifen-resistant
TG	Thapsigargin
TXNIP	Thioredoxin-interacting protein
TILs	Tumour infiltrating lymphocytes
TNF	Tumour necrosis factor
TRAF2	TNF-receptor associated factor 2
TRBP	Transactivator RNA-binding protein
TNBC	Triple-negative breast cancer
TM	Tunicamycin
uORFs	Upstream open reading frames
UPR	Unfolded protein response

UPRE	Unfolded Protein Response Element
UTR	Untranslated region
VAV1	Vav guanine nucleotide exchange factor 1
WHO	World Health Organization
XBP1	X-box binding protein
XBP1s	X-box binding protein spliced
XIAP	X-linked inhibitor of apoptosis protein



# Abstract

The endoplasmic reticulum (EnR) stress is a common phenomenon in various cancers such as breast, colorectal, skin and hepatocellular carcinoma. Several pathophysiological events (e.g., radiation, aneuploidy, oncogenic transformation and tumour microenvironment) and pharmacological inducers (e.g., thapsigargin, tunicamycin and brefeldin A) can induce EnR stress and initiate the unfolded protein response (UPR) signalling pathway. Tumour microenvironmental factors such as low pH, hypoxia, nutrient starvation, and elevated levels of free radicals cause UPR activation in cancer cells. The UPR signalling pathway has three major sensors which are localised at the EnR membrane, including IRE1, ATF6 and PERK. These three molecules sense any changes in protein folding capacity (accumulation of misfolded proteins) and activate a variety of transcription factors such as ATF6, ATF4, CHOP and XBP1. These downstream effectors of the UPR induce the expression of a wide array of target genes including EnR chaperones and genes involved in ERAD (endoplasmic reticulum associated degradation) to enhance the protein folding capacity of the cell and to decrease the unfolded protein load of the EnR. However, if the primary stimulus causing protein misfolding in the EnR is prolonged or excessive, apoptosis ensues. The exact mechanism involved in transition of the UPR from a cell survival to cell death response is not clearly understood.

MicroRNAs are a class of endogenous, short (19-22 nucleotides in length) non-coding RNAs that play a pivotal role in gene expression regulation by translational repression or degradation of target transcripts. MicroRNAs usually interact with the 3' untranslated region (UTR) of their target mRNA to downregulate its expression. Computational analysis predicts that more than 30% of animal genes may be subject to regulation by miRNAs, suggesting a role for miRNA-mediated gene regulation during UPR. Several studies have shown that miRNA expression is globally repressed in tumour tissues as compared with the tumour adjacent normal tissue. Three potential mechanisms responsible for miRNA dysregulation in cancer are: (i) the miRNAs loci are frequently localized in fragile chromosomic sites and are often altered (methylation, deletion, amplification and translocation) in human cancers (ii) the change in activities of transcription factors (e.g., MYC and P53) that control miRNA expression and (iii) miRNA biogenesis could be affected by the altered expression of DICER, DROSHA and XPO5. MicroRNAs have been shown to act as tumour suppressor and/or oncogene in human cancers. Gain or loss of miRNA functions has been reported in different cancers, with pathological roles in tumour cell proliferation, progression of tumours and metastatic process. Hence, we hypothesize that UPR-regulated microRNAs can influence the cellular response during EnR stress and may contribute to cancer progression. The role of miRNAs in the regulation of the UPR is an emerging area and further research is required to gain an understanding of the pathways involved, which will provide additional therapeutic opportunities. In this study, we identified two UPR regulated miRNAs (miR-378 and miR-616) and determined their effect on cell growth, proliferation, migration and cell fate during conditions of EnR stress.

In Chapter 3, we show that miR-378 and its host gene (PPARGC1B) are downregulated during UPR through the IRE1-XBP1 axis. Overexpression of XBP1s significantly reduced the expression of miR-378 and PPARGC1B. Furthermore, we found that overexpression of miR-378 strongly suppressed cell proliferation, colony formation and migration of ER $\alpha$ -positive breast cancer cells (MCF7, ZR-75-1). Moreover, our results show that miR-378 enhanced sensitivity of MCF7 cells towards EnR stress inducing compounds and anti-estrogens. We also demonstrated that high expression of miR-378 was associated with good outcome in ER $\alpha$ -positive breast cancer patients. We found that ectopic expression of miR-378 increased the expression of several type I interferon signalling pathway genes. Analysis of separate cohorts of breast cancer patients showed that a gene-signature derived from miR-378 upregulated genes showed a strong association with improved overall and recurrence free survival in breast cancer. Our findings show that XBP1s may contribute to the development of endocrine-resistant breast cancer, in part, by downregulating the expression of miR-378.

In Chapter 4, we show that the expression level of miR-616 and CHOP (the host gene of miR-616) is increased during UPR signalling through the PERK pathway. Our results showed that overexpression of miR-616 strongly reduced cell proliferation, colony formation and migration of cancer cells (MCF7, ZR-75-1 and HCT116). Additionally, miR-616 enhanced the sensitivity of MCF7 cells to anti-estrogens. We found that miR-616 directly targeted the protein coding sequences of c-MYC and VAV1 transcripts. Furthermore, we showed that miR-616 inhibited MCF7 cell proliferation and migration by suppressing the expression of c-MYC and VAV1. Ectopic expression of c-MYC and VAV1 reversed the inhibitory effects of miR-616 on cell growth and migration in MCF7 cells. In summary, our results suggest that the CHOP locus generates two gene products, CHOP protein and miR-616, that can act together to inhibit cancer progression.

# Chapter 1

## **1-0. Introduction**

### **1-1. The Endoplasmic Reticulum**

The Endoplasmic Reticulum (EnR) is a major eukaryotic cellular organelle which has various functions, including lipid/steroid biosynthesis, protein biosynthesis (post-translational modification, protein translocation, and protein folding) and storage/regulation of calcium ions in its lumen [1]. The EnR consists of a tube-like structure named cisternae or EnR lumen. The cisterna is a flattened membrane disk that is connected to other cisternae. This structure is also seen in the Golgi apparatus that is formed from three to twenty cisternae [2].

There are two kinds of EnR in eukaryotic cells, the rough EnR and the smooth EnR. The rough or granular EnR has ribosomes on its cytosolic side which are needed for protein synthesis. The rough EnR is mostly seen in cells that secrete proteins. Proteins which are synthesised by ribosomes on the rough EnR are translocated into the EnR lumen for further modifications [2]. Both free and membrane-bounded ribosomes are the same in function and structure with the only difference being in the proteins that they generate [1]. On the other hand, the smooth EnR does not have any ribosomes and plays roles in metabolism and production of lipids and hormones. They are frequently found in specific cell types such as muscle, liver, neurons and steroid synthesising cells with distinct functions [2].

## **1-2. Endoplasmic Reticulum Stress and the Unfolded Protein Response (UPR)**

### **Signalling Pathway**

The EnR stress response is induced by multiple pathophysiological and pharmacological inducers. For instance, glucose deprivation [3] and hypoxia [4] are common events in a tumour microenvironment which cause EnR stress and UPR activation in cancer cells. It has been found that cancer cells engage UPR signalling to adapt to stressful conditions within the tumour microenvironment [5]. The UPR is also activated in other diseases such as neurodegenerative disorders, [6], diabetes [7] and viral infections [8]. Furthermore, pharmacological inducers such as thapsigargin, tunicamycin and brefeldin A can induce EnR stress and activate UPR signalling, a common approach used in laboratories for research purposes [9].

The EnR stress response activates the UPR signalling pathway in order to maintain cellular homeostasis [10]. The UPR signalling pathway has three major sensors which are localised at the EnR membrane including inositol-requiring protein-1 (IRE1), activating transcription factor-6 (ATF6) and protein kinase RNA (PKR)-like ER kinase (PERK) [11]. These three molecules sense any changes in protein folding capacity in the EnR lumen and pass the information across the EnR membrane to the cytosol in order to activate downstream effectors (Figure 1-1). For instance, UPR activation induces the phosphorylation of eIF2 $\alpha$  to block general protein translation, reducing the client protein load entering the EnR, and increases the function of several transcription factors such as ATF4, XBP1 and ATF6f which translocate to the nucleus and consequently induce various genes such as endoplasmic reticulum-resident chaperones, endoplasmic reticulum-associated degradation (ERAD) machinery, amino acid transport and metabolism proteins, phospholipid biosynthesis enzymes and autophagy genes to restore EnR homeostasis [12].

The UPR initially tries to restore normal EnR homeostasis, however, if the damage is too severe cell death pathways are activated [13]. The molecular mechanisms involved in the transition of the UPR from a protective to an apoptotic phase are unclear.

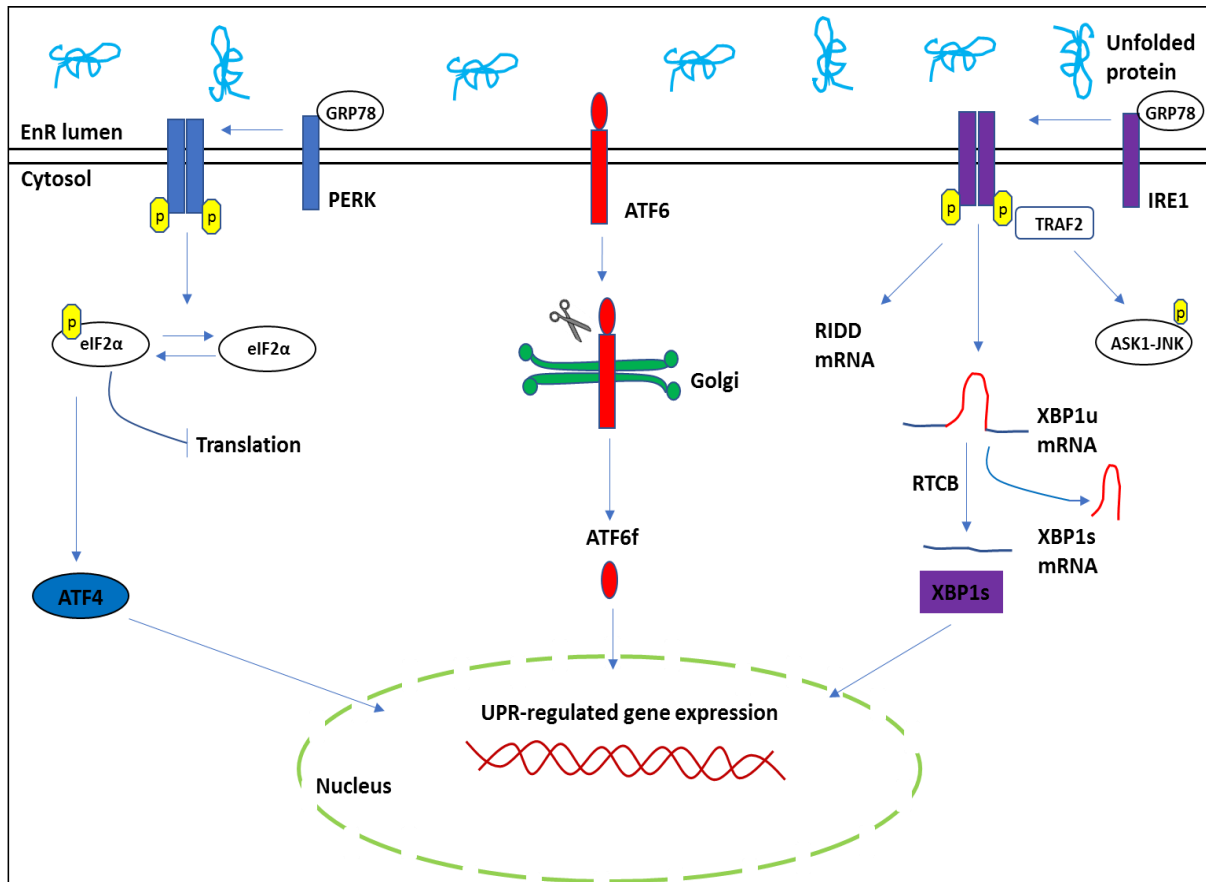


**Figure 1-1. The UPR signalling pathway.** UPR sensors including PERK, ATF6, and IRE1 are activated by accumulation of unfolded and misfolded proteins in the EnR lumen. PERK forms dimers and is auto-phosphorylated after dissociation from GRP78. Activated PERK phosphorylates eIF2 $\alpha$  and consequently, p-eIF2  $\alpha$  blocks general mRNA translation and increases the translation ATF4 transcript. IRE1 also forms dimers and is auto-phosphorylated like PERK during activation. Phosphorylation of IRE1 causes activation of its endoribonuclease domain. IRE1 then cleaves 26 nucleotides of XBP1 mRNA to generate spliced XBP1. IRE1 also activates two other mechanisms, RIDD and TRAF2 signalling to induce mRNA degradation and EnR stress-induced apoptosis respectively. ATF6 translocates from the EnR lumen to the Golgi apparatus after activation and is cleaved by two proteases (S1P, S2P) to generate a 50 kDa fragment (ATF6f). ATF4, XBP1s and ATF6f then translocate to the cell nucleus and induce the expression of multiple genes to restore EnR homeostasis.

### **1-2-1. ATF6 signalling pathway**

ATF6 is a type II transmembrane glycoprotein with two subtypes, ATF6  $\alpha$  (90 kDa) and ATF6  $\beta$  (110 kDa, also known as cAMP-response-element-binding protein (CREB)-related protein; CREB-RP) [12]. The C-terminal domain of ATF6 is located in the EnR lumen and the N-terminal domain is suspended in the cytoplasm [11]. In unstressed cells, ATF6 is localized at the EnR membrane, intermolecular disulphide bonds keep ATF6 in a dimeric form and bound to GRP78. In response to EnR stress, ATF6 dissociates from GRP78 and the disulphide bonds of ATF6 are reduced to generate the monomeric ATF6 form [12]. This event exposes regions in ATF6, named Golgi localization signals (GLS), which facilitate the translocation of ATF6 to the Golgi apparatus [14]. In the Golgi apparatus, ATF6 is cleaved by two Golgi-resident proteases, firstly with S1P (site 1 proteases) and secondly with S2P (site 2 proteases) to form a 50 kDa cytosolic, bZIP containing transcription factor named ATF6f [11]. ATF6f moves to the nucleus and induces the expression of different genes involved in EnR homeostases such as chaperones and EnR-associated degradation (ERAD) proteins (Figure 1-2). There is also a study that has shown that ATF6f induces the expression of XBP1 which in turn is processed by IRE1 to generate spliced XBP1 [15]. Moreover, ATF6 induces the expression of two other proteins including protein disulphide isomerase-associated 6 (PDIA6) and ER degradation-enhancing  $\alpha$ -mannosidase-like protein 1 (EDEMI) in order to increase the degradation of misfolded proteins [16]. To regulate the expression of UPR target genes, ATF6f binds to the ATF/cAMP response element (CRE) [17], the EnR stress response elements (ERSE-I and -II) and Unfolded Protein Response Element (UPRE) [18]. These sequences are present in the promoter region of UPR regulated genes such as GRP78, GRP92, ERP72 and Calreticulin [19].



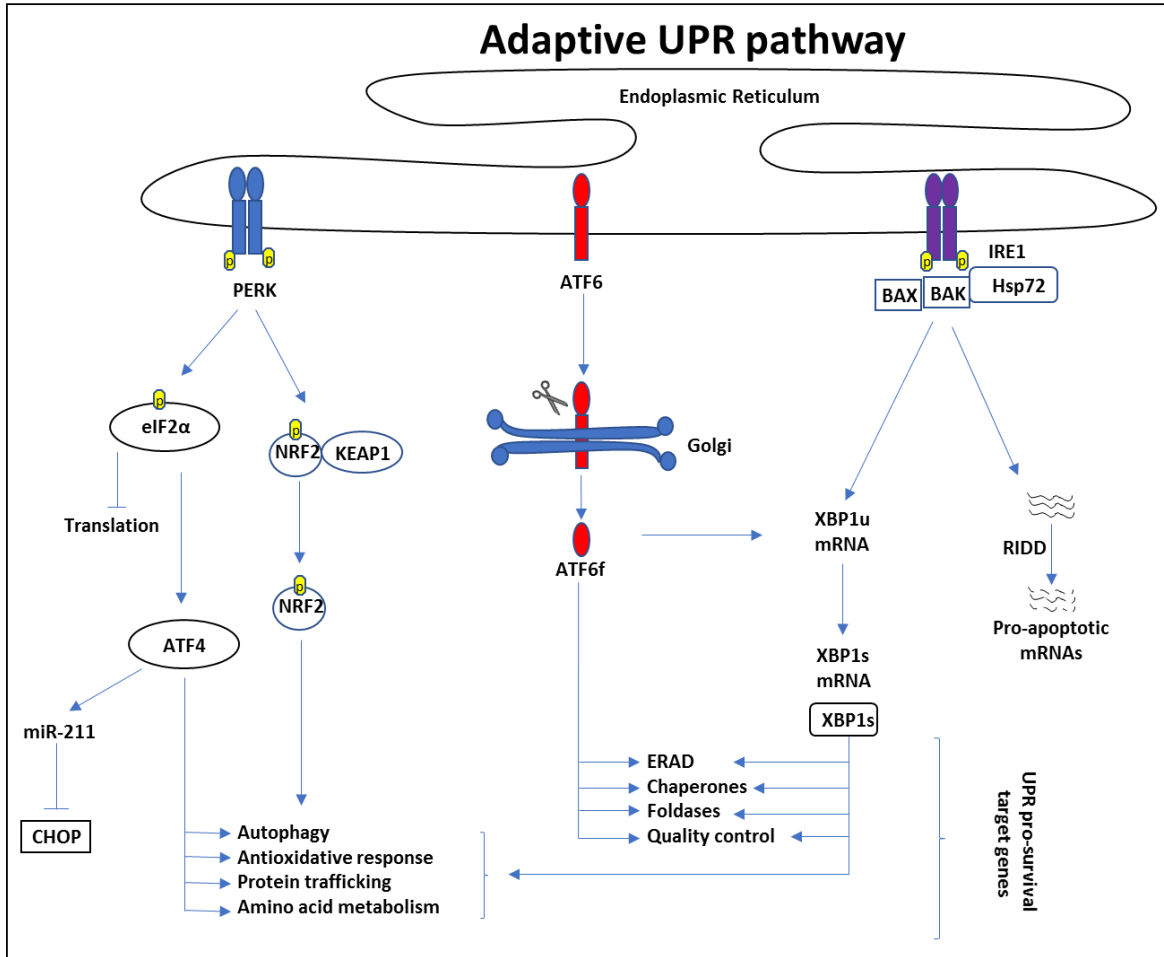


**Figure 1-2. Adaptive responses of UPR signalling pathway during conditions of EnR stress.** PERK phosphorylates eIF2 $\alpha$  to block general protein translation. It activates the ATF4 transcription factor to induce the expression of multiple UPR adaptive target genes which are involved in autophagy, protein trafficking and amino acid metabolism. ATF4 can upregulate miRNA levels (e.g., miR-211) to block the expression of the pro-apoptotic transcription factor CHOP. PERK also phosphorylates NRF2 to induce antioxidative responses. IRE1 initiates its adaptive responses through XBP1 splicing and RIDD. IRE1 recruits BAK, BAX and HSP72 to increase XBP1 splicing. Activated ATF6 (ATF6f) increases the expression level of XBP1u and induces several mechanisms involved in the UPR adaptive pathway with the help of XBP1s.

It is also reported that ATF6 needs the nuclear factor Y (NF-Y)/CCAAT-binding factor (CBF) to bind to the EnR stress response elements (ERSE-I and -II) [20].

ATF6 has a pro-survival role during EnR stress (Figure 1-2) as ATF6f translocates to the nucleus to induce the expression of multiple genes which consequently lead to increased protein folding capacity [21]. However, the pro-death role of ATF6 has been shown, where ATF6 contributes to UPR-induced apoptosis by decreasing the expression of pro-survival BCL-2 family member myeloid cell leukaemia 1 (MCL1) [22].

### **1-2-2. PERK signalling pathway**

PERK is a type I transmembrane protein and has a cytosolic domain with serine/threonine kinase activity [23]. PERK is associated with chaperone GRP78 in an inactive state, and upon EnR stress, GRP78 is dissociated from the luminal domain of PERK. This event first causes PERK dimerization and subsequently leads to the trans-autophosphorylation of PERK on threonine-980 present in cytosolic domain [11]. The activated loop of PERK then phosphorylates the  $\alpha$  subunit of eukaryotic translation initiation factor-2 (eIF2) at serine 51 and leads to blockade of general protein translation [24]. In addition, phosphorylated eIF2 $\alpha$  paradoxically increases translation of some selected mRNAs such as activated transcription factor 4 (ATF4; also known as CREB2). ATF4 has two upstream open reading frames (uORFs) including uORF1 (positive acting element) and uORF2 (inhibitory element) [25]. During conditions of EnR stress, when level of phosphorylated eIF2 $\alpha$  is high, the scanning ribosomes pass through the inhibitory uORF2 and initiate translation in the ATF4 coding region. However, during resting conditions, ribosomes which are downstream of uORF1, start to scan through the uORF2 and uORF2 blocks the translation of ATF4 [24].

ATF4 is a transcription factor which has a pro-survival role (Figure 1-2) activating multiple genes which are involved in cell's response to antioxidant and amino acid synthesis [12]. ATF4 can also increase the expression of growth arrest and DNA damage-inducible protein 34 (GADD34) transcript which is a regulator of protein phosphatase 1 (PP1). PP1 then dephosphorylates eIF2  $\alpha$  and restores general mRNA translation [26].

PERK also activates another transcription factor named nuclear factor (erythroid-derived 2)-like 2 (NRF2) (Figure 1-2). NRF2 is a member of the cap 'n' collar family of basic leucine zipper and redox-regulated transcription factors which regulates cellular responses to the high level of reactive oxygen species (ROS) [27]. In normal conditions, NRF2 is bound to an inhibitor protein named Kelch-like ECH-associated protein (KEAP1) in the cytoplasm and stays in an inactive state [28]. Under conditions of oxidative stress and upon phosphorylation by PERK, NRF2 is activated and separated from KEAP1. NRF2 is then translocated into the nucleus and heterodimerizes with small Maf proteins [29] to form transactivation complexes on antioxidant response elements (AREs) and induces the expression of various genes such as anti-oxidative and cytoprotective enzymes [30]. Furthermore, the PERK arm activates nuclear factor Kappa B (NF- $\kappa$ B) through the phosphorylation of eIF2 $\alpha$ . It has been shown that p-eIF2 $\alpha$  translational repression activity leads to the attenuation of the amount of I $\kappa$ B in the protein complex and consequently activates the NF- $\kappa$ B protein [31].

The PERK arm has both adaptive and pro-apoptotic roles depending on EnR stress intensity and duration. Prolonged PERK activation causes switching of the PERK's adaptive role to its apoptotic role [32]. Under these circumstances, PERK upregulates the transcription factor CHOP (also known as GADD153) which can regulate the expression of multiple target genes that contributes to the cell apoptosis (Figure 1-3). For example, it has been reported that CHOP downregulates the expression of the anti-apoptotic BCL2 protein to induce cell death [33].

CHOP also increases the expression level of pro-apoptotic BCL2 family proteins such as BIM and PUMA to promote apoptosis [34-36]. Although clearly important for EnR stress-induced apoptosis in many scenarios, CHOP is not uniformly essential for cell death induced by EnR stress, as demonstrated by the observation that PERK<sup>-/-</sup> and EIF2 $\alpha$  (Ser51Ala) knock-in cells are hypersensitive to EnR stress-induced apoptosis but fail to induce CHOP gene expression.

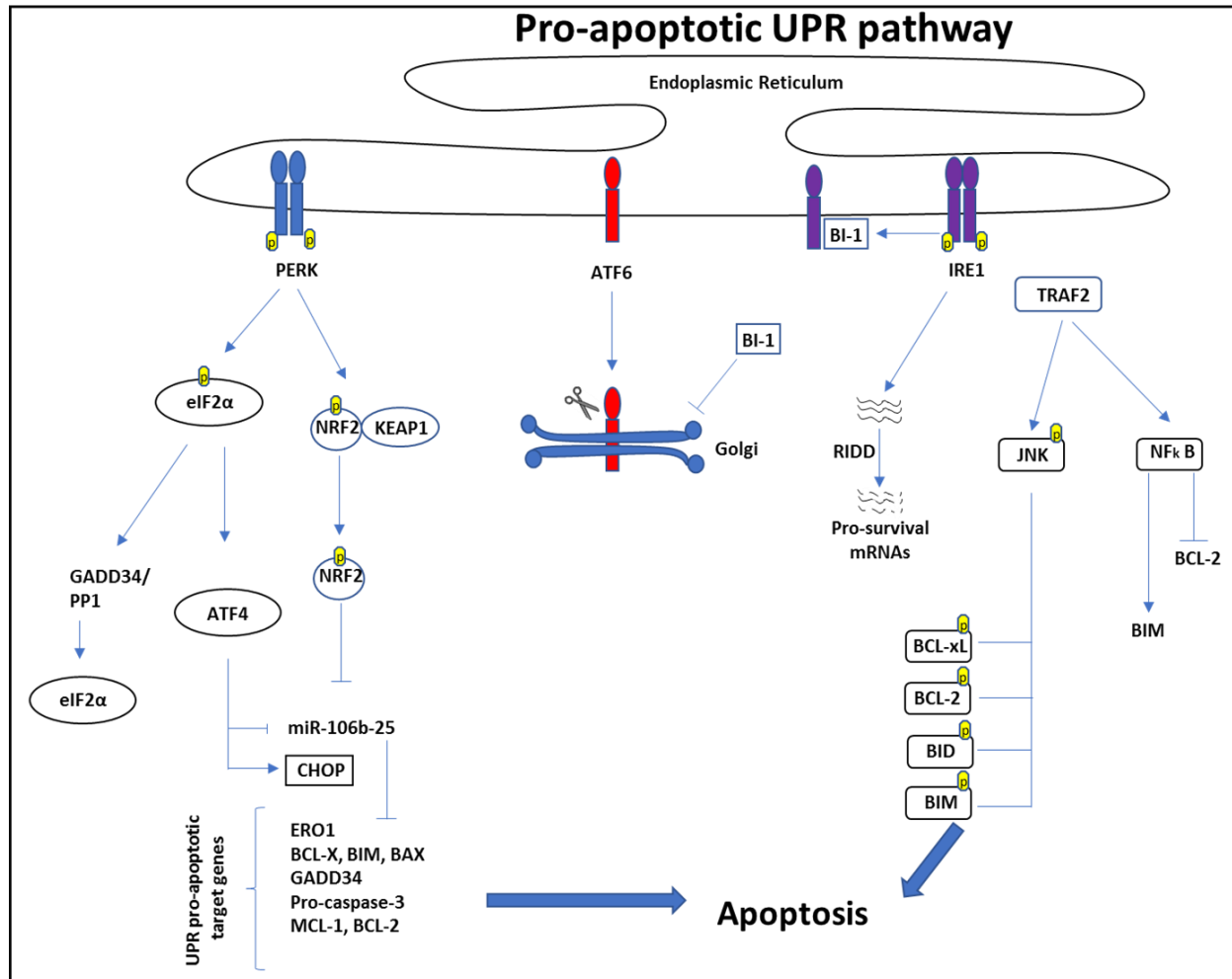


**Figure 1-3. Pro-apoptotic responses of UPR signalling pathway during conditions of EnR stress.** Prolonged EnR stress activates pro-death responses of PERK arm. ATF4 upregulates expression of CHOP and consequently induces the UPR pro-apoptotic target genes. ATF4 and NRF2 block expression level of miRNAs (e.g., miR-106b-25) to increase the UPR pro-apoptotic target genes. GADD34/PP1 complex dephosphorylates p-eIF2 $\alpha$  to increase general protein translation. IRE1-TRAF2 complex activates NF- $\kappa$ B and JNK transcription factors which lead to activation of pro-apoptotic BCL-2 proteins and inhibition of anti-apoptotic BCL-2 proteins. IRE1 increases the RIDD pathway activity to degrade adaptive UPR target mRNAs. BI-1 transmembrane protein blocks splicing of XBP1u and cleavage of ATF6 to reduce the adaptive responses of the UPR signalling pathway.

### **1-2-3. IRE1 signalling pathway**

Inositol-requiring protein-1 (IRE1) is the most conserved signalling branch of the UPR [37]. IRE1, like the PERK sensor, is a type I transmembrane protein and has cytoplasmic domains with kinase and endoribonuclease activity [21]. The two isoforms of IRE1 in mammals, IRE1 $\alpha$  (expressed in most cells and tissues) and IRE1 $\beta$  (mostly expressed in intestinal epithelial cells), are activated by oligomerization and trans-autophosphorylation of their kinase domains upon EnR stress [11, 38]. Upon activation, IRE1 forms higher oligomeric complexes, which leads to trans-autophosphorylation of its kinase domain which in turn engages its RNase activity [37]. During EnR stress, ATF6 (one of three major UPR sensors) induces the expression of XBP1 mRNA [15]. Activated IRE1 excises a 26-nucleotide sequence from unspliced XBP1 (XBP1u) mRNA. IRE1-mediated XBP1 mRNA splicing causes a shift in the reading frame, such that spliced XBP1 (XBP1s) mRNA encodes the XBP1s protein, which has 376 amino acids (in humans) and possesses a potent transcriptional transactivation domain in its C-terminal region (Figure 1-2) [11]. The 5' and 3' mRNA fragments that are created from XBP1u cleavage are joined by an RNA ligase named RTCB [39]. This procedure is known as an unconventional cytosolic splicing reaction which depends on IRE1 endoribonuclease and RTCB ligase activities and does not follow the general nuclear spliceosome-mediated processing rule. The XBP1s protein generated from spliced XBP1 mRNA, binds to cis-acting promoter motifs including the EnR stress response element (ERSE) and the unfolded protein response element (UPRE), and leads to the transactivation of target genes [14]. XBP1s regulates a wide range of UPR target genes (Figure 1-2) involved in protein folding capacity, ERAD, autophagy, lipid biogenesis and redox metabolism [40, 41]. There is also a study that found that XBP1s plays a role in the regulation of various EnR resident chaperone genes such as the DnaJ/Hsp40-like genes, p58IPK, ERdj4 and EDEM [42].

Furthermore, there is an XBP1-independent function of IRE1 during EnR stress known as regulated IRE1-dependent decay (RIDD) [43]. In this procedure the RNase activity of IRE1 degrades various mRNAs encoding secreted and membrane proteins, thereby preventing their translation, an additional measure to aid in relieving EnR stress [44] (Figure 1-2). It has been reported that IRE1 $\alpha$  is responsible for XBP1 mRNA splicing while IRE1 $\beta$  is required for RIDD activity [45]. RIDD induces degradation of EnR related mRNAs by cleaving a specific site to generate the free 5' and 3' ends. These free 5' and 3' ends are recognised and degraded by an exoribonuclease enzyme [46]. It has been shown that RIDD activity contributes to cell apoptosis (Figure 1-3) by degradation of Caspase-2 (CASP2) targeting pre-miRNAs including miR-96, miR-125b, miR-34a, and miR-17 which then leads to increase in CASP2 activity [47]. Moreover, tumour necrosis factor receptor (TNFR)-associated factor-2 (TRAF2) can be recruited by phosphorylated IRE1 and begin to activate the apoptosis signal regulation kinase 1 (ASK1) and Jun N-terminal kinase (JNK) (Figure 1-3) [48].

IRE1 activity, which leads to XBP1 mRNA splicing and RIDD, plays both pro-apoptotic and pro-survival roles in diseases. However, it has been reported that the pro-survival output is mostly seen in cancer and the pro-apoptotic output is seen in other diseases [41]. Overall, via its endoribonuclease activity, the functional outputs of active IRE1 are tailored to the stimulus. This occurs through the combination of unconventional splicing of XBP1 mRNA and RIDD. While splicing of XBP1 mRNA is a cytoprotective response to UPR, RIDD has revealed many context dependent outcomes.

### **1-3. Human Cancer**

Cancer is a general term used to describe a large group of diseases that can affect any part of the body, characterised by the rapid production of abnormal cells that fail to properly regulate their proliferation and grow beyond their usual boundaries. These cells can then spread from the tissue of origin to other organs in a process referred to as metastasis. Metastases are the major cause of cancer-related death. Cancer is associated with several signs and symptoms such as unexplained weight loss, bleeding, lumps, diarrhoea, nausea, vomiting and fatigue. Globally, about 1 in 6 deaths is due to cancer based on the world health organization (WHO) estimates with 14.2 million new cancer cases and 8.5 million deaths from cancer reported in 2012 [49]. These include 3.5 million new cases and 1.80 million deaths within the European Union during that same period [50].

Cancer arises from the transformation of normal cells into tumour cells in a multistage process that generally progresses from a pre-cancerous lesion to a malignant tumour. Usually, normal cells evolve progressively into a cancerous state, as they do this, there are a series of changes, known as hallmarks, that they acquire along the way. This allows cancer cells to acquire traits leading to the formation of tumours and malignancy. The hallmarks of cancer were first described by Douglas Hanahan and Robert Weinberg in 2000, where they attempted to organize the acquired properties of cancer cells into six major hallmarks: (Figure 1-4) including activating invasion and metastasis, avoiding growth suppressors, resisting cell death, increased angiogenesis, immortality and sustaining proliferative signalling. [51]. A decade later, they added two emerging hallmarks, the reprogramming of energy metabolism and evading the immune response, and two enabling traits, genome instability and mutation, and tumour-promoting inflammation [52].



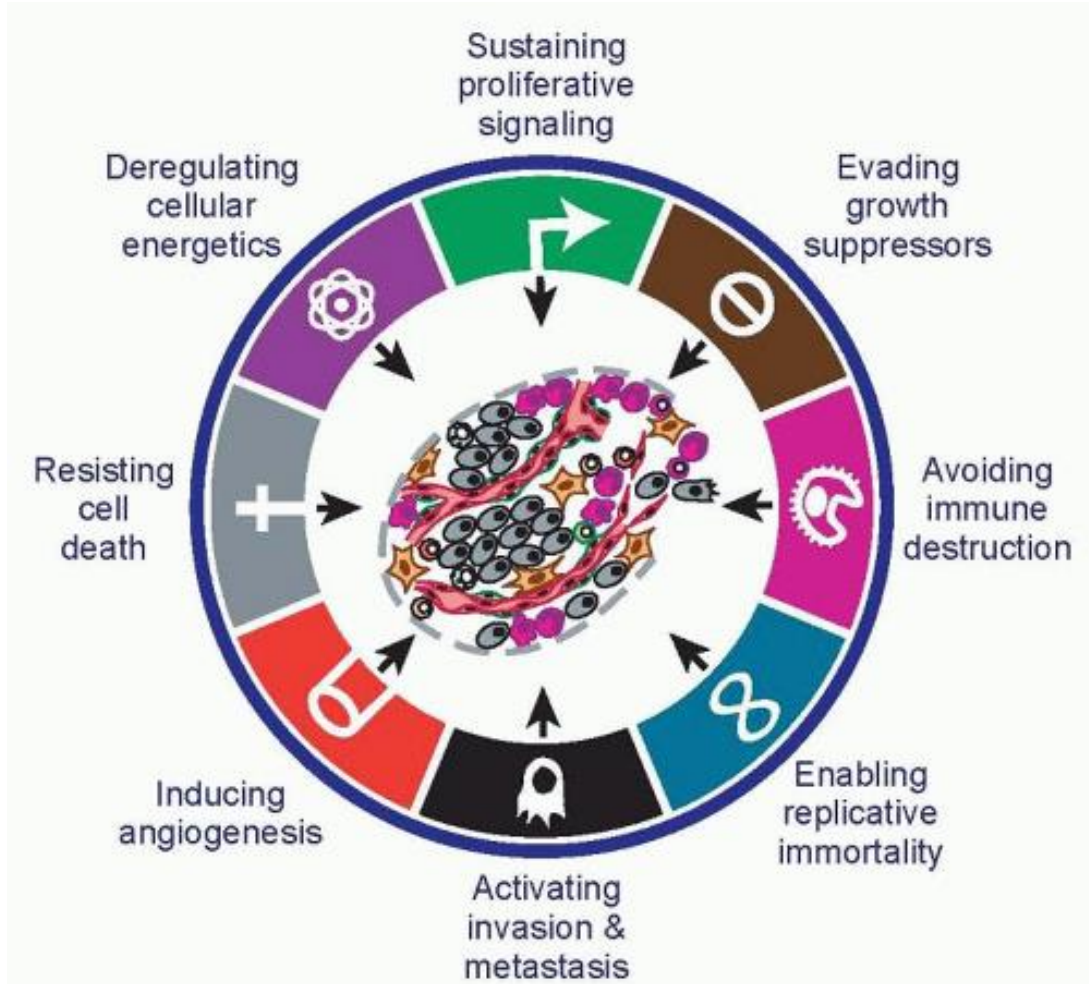


**Figure 1-4. The hallmarks of cancer.** The essential properties that tumours acquire, which are important in malignant growth. The illustration is reproduced from Hanahan *et al.* published article, 2011 [52]. Permission to reuse this figure has been granted by Elsevier and the copyright clearance centre. Permission letter is in Appendix 6-14.

## **1-4. Breast Cancer**

### **1-4-1. Overview**

Breast cancer is one of the most common causes of death in women in developed nations, with approximately 1.75 million new cases and 550,000 deaths recorded in 2012 [53]. A higher incidence is observed in north and western European countries while more deaths occur in less developed countries such as eastern Africa, central America and eastern Asia [54]. Breast cancer is the most common female cancer in Ireland with approximately 2800 new cases diagnosed annually [55]. Epidemiological studies have shown that postmenopausal women constitute the majority of breast cancer patients with the average age of diagnosis being around 58 years [56, 57]. Currently, breast cancer diagnosis, classification and treatment are based on a range of factors such as gender, age, menopausal status, lymph node status, tumour size, histopathological features, hormone receptor status and proliferation index.

### **1-4-2. Molecular classification of breast cancer**

Different studies have categorised breast cancer in several biologically distinct subtypes. According to tumour histology and morphology, breast cancer has been categorized into major subtypes including infiltrating ductal and lobular carcinomas, tubular carcinoma, mucinous carcinoma, medullary carcinoma, invasive papillary carcinoma and metaplastic carcinoma [58]. This classification has some limitations, therefore, other methods have been developed based on immunohistochemistry and gene expression profiling. Several groups have used microarray-based gene expression profiling to study breast cancer at the molecular level [59-61].

In a published study by Perou *et al.*, hierarchical clustering analysis of genes revealed four molecular breast cancer subtypes including luminal A, luminal B, human epidermal growth factor receptor 2 (HER2) overexpressing and basal-like tumours (Table 1-1) [59].

Table 1-1. Molecular breast cancer subtypes and their hormone receptor status

<b>Molecular subtypes</b>	<b>Hormone receptor status</b>
<b>Luminal A</b>	ER-positive (+) and/or PR-positive/HER2-
<b>Luminal B</b>	ER-positive and/or PR+/HER2+
<b>HER2 overexpressing</b>	ER-/PR-/HER2+
<b>Basal-like</b>	ER-/PR-/HER2-

The estrogen receptor  $\alpha$  (ER) positive tumours consists of two subtypes; luminal A (ER and/or PR positive, HER2/neu negative) and luminal B (ER, PR, and HER2/neu positive). Luminal breast cancers are the most common subtype of breast cancer. They express luminal cytokeratin 8/18, ER $\alpha$ / $\beta$  and some genes associated with ER activation (LIV1, CCND1) [59, 62]. Luminal A breast cancers express ER-regulated genes more than luminal B while luminal B breast cancers express higher levels of proliferative genes [60, 63].

15% to 30% of all breast cancer cases are HER2-positive [64]. It has been reported that the growth factor receptor-bound protein 7 (GRB7) gene is associated with the HER2 amplicon which plays a pivotal role in tumour progression and cell migration in invasive breast cancer [65]. HER2 positive tumours are negative for the ER (low expression of ER and their regulated genes) and have a high incidence (40-80 %) of p53 mutations [66].

In basal-like tumours, the morphology of the tumour cells is similar to that of other basal epithelial cells and normal breast epithelial cells [59]. This group does not express the ER and ER-regulated genes, has low expression of HER2, but has high expression of basal cytokeratin 5, 6, and 17 [67]. Based on IHC staining, this subtype is also called triple negative breast cancer (TNBC) as they are negative for ER, PR and HER2. TNBC tumours also have a high rate (80%) of p53 mutation [68].

In another study by the Caldas group at the University of Cambridge, they introduced a new classification for breast cancer. Based on the genomic and transcriptomic profiles of 2000 breast tumours from the METABRIC [Molecular Taxonomy of Breast Cancer International Consortium] cohort they classified breast tumours into ten groups, termed integrative clusters (IntClust/s) [69]. Ten clusters identified by METABRIC partly capture subgroups defined by other approaches but importantly also groups tumours into more novel subtypes.

### **1-4-3. Signalling pathways in breast cancer**

Multiple pathways play crucial roles in promoting breast cancer progression and survival such as ER, HER2, Notch, Wnt and Cyclin dependent kinase (CDK) signalling pathways [70-73]. Here we describe the mechanism of action of these important pathways.

#### **-ER signalling pathway:**

ER $\alpha$  is the main ER subtype expressed in mammary epithelial cells and has important roles in mammary gland biology as well as in breast cancer progression. ER $\alpha$  contains an N-terminal AF1 domain, a DNA-binding domain, and a C-terminal ligand-binding region that contains an AF2 domain [74]. Estrogen receptors (ERs) act by regulating transcriptional processes.

The important mechanism of ER $\alpha$  action involves estrogen binding to receptors in the nucleus, after which the receptors dimerize, bind to estrogen response elements (EREs) located in the promoters of target genes and regulate their expression [74]. In addition, ER $\alpha$  can modulate the functions of other transcription factors, by protein-protein interactions in the nucleus and activation of signal transduction pathways at the plasma membrane. It has been shown that ER $\alpha$  activates several extranuclear signalling pathways such as protein kinase C, Src kinase, phosphatidylinositol 3-kinase (PI3K) and mitogen-activated protein kinase (MAPK) pathways, which play crucial roles in breast cancer cell proliferation and metastasis [75, 76]. ER $\beta$ , like ER $\alpha$ , is activated by estrogen to mediate multiple physiological responses.

Several published studies have suggested a tumour suppressor role of ER $\beta$  by repressing cell proliferation and invasion in cancer cells [77, 78]. Lindberg *et al.* reported that ectopic expression of ER $\beta$  increased the level of integrin  $\alpha$ 1 and integrin  $\beta$ 1 and consequently enhanced breast cancer cell adhesion [79]. The role of ER $\alpha$  has been well established in human breast cancer whereas the role of ER $\beta$  is still unclear in all cancers including breast cancer [80].

### **-HER2 signalling pathway:**

The HER family are type I transmembrane proteins with extracellular, transmembrane and a cytosolic tyrosine kinase domain [81]. It consists of four receptors including HER1 (EGFR), HER2 (neu, C-erbB2), HER3 and HER4. Activation of these receptors triggers other downstream signalling pathways such as the PI3K/Akt (pro-survival) and RAS/MAPK (proliferation) pathways [82]. The HER2 proto-oncogene is expressed in both normal and tumour breast tissues [81].

HER2 is overexpressed in 15-30% of human breast tumours and it is associated with poor prognosis and outcome in patients [64]. Overexpression of HER2 has also been reported in other cancers such as ovarian, cervix, colon, stomach, lung and bladder [66].

**-CDKs signalling pathway:**

Cyclin dependent kinases (CDK) are responsible for cell cycle progression [83, 84]. Interactions between CDKs and cyclins play a key role in maintaining control of progression through the cell cycle. Loss of control, leading to unrestricted growth, is a classic hallmark of cancer. Dysregulation of these proteins has been seen in many cancers including breast cancer. Almost 60% of all breast cancer show cyclin D1 amplification and it has been reported that estrogen increases breast cancer cell growth by inducing cyclin D1 expression [85]. It has been shown that overexpression of cyclin D1 is associated with poor prognosis and reduced recurrence free-survival rate in inflammatory breast cancer [86]. Stendahl and colleagues found that overexpression of cyclin D1 can predict resistance to tamoxifen in ER-positive breast cancer patients [87]. Thus, using CDK inhibition in an effort to regain cell cycle control has been a tempting option in the development of targeted cancer therapy.

### **-Notch signalling pathway:**

The Notch signalling pathway plays a key role in breast cancer pathogenesis. A Notch mutation was first discovered in human pre-T-cell acute lymphoblastic leukaemias (T-ALL) which came from the chromosomal translocation [t(7:9)(q34; q34.3)] [88]. Notch mutations have also been found in breast cancer cell lines. Stylianou *et al.* reported that from eight investigated cell lines, two have a mutation in NOTCH4 and all eight cell lines have a NOTCH1 mutation [89]. It has been reported that overexpression of JAG1 and NOTCH1 are associated with poor outcome in breast cancer patients [90]. In a recently published study, it has been shown that NOTCH1 expression inhibits a PTEN-ERK1/2 signalling pathway in breast cancer stem cells (BCSCs) and increases cell proliferation. NOTCH1 expression is also associated with a poor survival rate in HER2 breast cancer patients [91].

### **- Wnt/ $\beta$ -catenin signalling pathway:**

Published studies have reported that the Wnt/ $\beta$ -catenin signalling pathway role in several cancers including colon, ovarian and breast cancer [92]. The Wnt/ $\beta$ -catenin signalling pathway plays a key role in determining cell fate and disruption of this pathway can increase cell proliferation [93]. Hyperactivation of Wnt/ $\beta$ -catenin signalling is seen in TNBC with poor outcome [94]. Bilir and colleagues found that inhibition of Wnt signalling pathway significantly reduced migration and proliferation of BT-549 cell [95]. Moreover, Zhou *et al.* reported that downregulation of Dickkopf-related protein 1 (DDK-1) (an inhibitor of Wnt/ $\beta$ -catenin signalling) significantly increased MCF7 breast cancer cell proliferation [96].

#### **1-4-4. Inherited breast cancer**

Family history of breast cancer is an important risk factor for patients. Mutations in breast cancer 1 and 2 (BRCA1 and BRCA2) genes have been reported in familial breast cancer. Mutation in BRCA1 (70%) and BRCA2 (16-23 %) genes have been associated with TNBC [97]. BRCA1 consists of 22 exons that encodes a 270 kDa nuclear protein [98]. Multiple tissues including breast and ovarian express the BRCA1 gene, and different mutations have been reported including base pair insertions, missense substitutions, an 11-base pair deletion and a stop codon mutation. The BRCA2 gene which is larger than BRCA1 encodes a 384 kDa nuclear protein [99]. Mutation of BRCA2 increases the risk of melanoma, stomach, bile duct and gall bladder cancers. Both BRCA1 and BRCA2 are tumour suppressor genes which play key roles in the repair of damaged DNA [100].

Tumours with a BRCA1 mutation are mainly basal-like and most of the BRCA1- related breast cancers are negative for hormone receptors and positive for Ki67 and basal-like markers (e.g., p53, P-cadherin, EGFR and CK5/6/14) [101]. X-chromosome abnormalities have been seen frequently in basal-like breast cancers with a poor outcome similar to patients with BRCA1-related tumours [102]. Mutation of other genes in inherited breast cancer includes PALB2, STK11, TP53, ATM, BARD1, MUTYH, NBN, NF1, RAD50, PTEN, STK11, CDH1, CHEK2, MRE11A and BRIP1[103]. For instance, PALB2 gene mutations are associated with an elevated risk of familial breast cancer similar to BRCA1/BRCA2 gene mutations. It has been reported that almost 33% of women with a mutation in PALB2 will have breast cancer by the age of 70 years [104].



### **1-4-5. Breast cancer treatment**

Treatment for breast cancer patients is a combination of radiotherapy, hormonal therapy, surgical therapy and chemotherapy, depending on tumour subtype. The first line of treatment for breast cancer is usually surgery. The type of surgery depends on the type of breast cancer. There are two types of surgery for breast cancer. These surgeries are done to remove the cancerous tissue (tumour), known as breast-conserving surgery, and surgery to remove the whole breast (mastectomy). Listed below are the common treatment options based on the molecular subtypes of breast cancer.

#### **-Treatment options for ER-positive breast cancer subtype**

Drugs targeting estrogen signalling are predominantly used for the treatment of ER-positive breast cancer. Several inhibitors of ER signalling have been introduced including drugs which reduce endogenous estrogen levels (e.g., aromatase inhibitors) and drugs that antagonise the ER by competing with estrogen such as selective estrogen receptor modulators (SERMs) and selective estrogen receptor degraders (SERDs) [105].

There are three compounds that act as SERMs including 4-hydroxytamoxifen (tamoxifen), raloxifene and toremifene. SERMs act by binding to the ER and blocking ER signalling pathway activity [106]. Depending on the target tissue, these compounds can act as both antagonists and agonists. For example, tamoxifen has a potential antagonistic effect in breast cancer cells while it shows an agonistic effect in the endometrium [107]. On the other hand, SERDs are anti-estrogens that bind and degrade the ER and consequently block the ER signalling pathway.

Fulvestrant or Faslodex<sup>®</sup> (7 $\alpha$ -alkylsulphinyl) is an analogue of 17 $\beta$ -estradiol with higher affinity for the ER compared to endogenous estradiol, which competitively binds to and blocks the ER and enhances its degradation [108].

Furthermore, aromatase inhibitors (AIs) such as anastrozole, letrozole and exemestane are frequently used in the treatment of ER-positive breast cancer in postmenopausal women [109]. Aromatase inhibitors inhibit the aromatase enzyme activity which converts androgens to estrogens [110]. Compared with tamoxifen, treatment with anastrozole has a significantly better overall survival rate, fewer metastases and prolonged time to recurrence in ER-positive breast cancer patients [111].

#### **-Treatment options for HER2 positive breast cancer subtype**

A substantial number of drugs have been introduced for the treatment of HER2 positive breast cancer. Trastuzumab (Herceptin<sup>®</sup>) is a monoclonal antibody that binds to the extracellular domain of the HER2 receptor and blocks HER2–HER3 dimerization and consequently HER2 signalling [112]. It also initiates an immune response against cancer cells through antibody-dependent cellular cytotoxicity (ADCC) [113]. Pertuzumab (Perjeta<sup>®</sup>) is another monoclonal antibody for HER2 positive breast cancer treatment. Similar to trastuzumab, it binds to the extracellular domain of HER2 and inhibits HER2–HER3 dimerization and consequently blocks activation of downstream pathways such as PI3K/Akt [114]. Lapatinib (Tykerb<sup>®</sup>) is another option for HER2 positive breast cancer treatment. It blocks the receptor tyrosine kinase activity of both HER1 & HER2 and leads to the interruption of MAPK/Erk1/2 and PI3K/Akt signalling pathways [115]. It has been reported that combination therapy with lapatinib and trastuzumab can increase apoptosis in HER2-positive cancers [116].

### **-Treatment options for TNBC**

Compared to other breast cancer subtypes, TNBC is very aggressive with worse outcomes. Current treatment options for TNBC is a combination of surgical therapy, radiotherapy, and cytotoxic chemotherapy [117]. Several chemotherapeutic compounds are used for the treatment of TNBC including platinum compounds (e.g., cisplatin and carboplatin) which target DNA repair pathways, taxanes (e.g., paclitaxel and docetaxel) which stabilize tubulin protein in the microtubule and anthracycline-based therapy (e.g., doxorubicin and daunorubicin) which inhibits DNA synthesis [118].

### **-Endocrine therapy resistance in breast cancer**

Endocrine therapy is one of the most effective kinds of therapy for ER-positive breast cancer patients. However, some patients do not respond (de novo resistance) or acquire resistance to the therapy. One-third of patients with ER-positive breast cancer develop resistance to treatment with tamoxifen [119]. Several mechanisms have been shown to play a key role in endocrine resistance therapy such as ER mutations, loss of ER expression and cross-talk between the ER and other cellular signalling pathways [120]. Two major signalling pathways are involved in endocrine therapy resistance including cyclin D1/CDK4/6 and PI3K/AKT/mTOR cell signalling pathways. The PI3K/AKT/mTOR signalling pathway plays pivotal roles in glucose metabolism, protein synthesis, cell growth and survival. Dysregulation of this pathway has been seen in many types of cancer including breast cancer [121]. It has been found that upregulation of the PI3K/AKT/mTOR signalling pathway can increase ER activity and contribute to the development of resistance to endocrine therapy [122].

Several inhibitors have been developed and tested to target PI3K/AKT/mTOR signalling in ER-positive breast cancer. Combination of the mTOR inhibitor Everolimus and the aromatase inhibitor exemestane showed better overall survival when used for the treatment of patients with ER+/HER2- tumours [123]. In another study by Ribas and colleagues, they reported that AZD5363, an AKT inhibitor, sensitised long-term estrogen-deprived (LTED) and tamoxifen resistant (TamR) breast cancer cell line variants (MCF7, ZR-75-1, HCC1428 and T47D) to tamoxifen [124].

The Cyclin D1/CDK4/6 signalling pathway, an essential signalling cascade regulating cell cycle, is another important pathway that promotes endocrine resistance [83]. CDK4/6 inhibitors have been introduced and employed in the treatment of ER+ breast cancer patients with resistance to anti-estrogen agents [125]. For example, palbociclib (PD 0332991; Pfizer) was approved by the US Food and Drug Administration (FDA) in 2015 for the treatment of advanced post-menopausal ER+, HER2- breast cancer [126].

## **1-5. UPR signalling pathway and its role in cancer**

Reduced oxygen and glucose availability are key features of the tumour microenvironment. Since the delivery of nutrients to the tumour is determined in part by fluctuating blood flow, different regions of the tumour must constantly respond to fluctuating levels of EnR stress to survive. The EnR stress is a common phenomenon in various cancers such as breast, colorectal, skin and hepatocellular carcinoma [127]. Several pathophysiological events (e.g., radiation, aneuploidy, oncogenic transformation and tumour microenvironment) initiate EnR stress and UPR activation [128].

Tumour microenvironmental factors such as low pH, hypoxia, nutrient starvation and elevated levels of free radicals can also induce EnR stress and UPR activation in cancer cells [129, 130]. In the tumour microenvironment, cancer cells induce UPR to promote cell survival through multiple mechanisms such as cell proliferation, metastasis, angiogenesis and therapy resistance [128, 131] (Figure 1-5).

A few studies have found somatic mutations in UPR pathway genes in cancer. For instance, IRE1 mutation has been seen in glioblastoma multiforme [132] and hepatocellular carcinoma [133]. Upregulation of XBP1s has been reported in several tumours and is associated with poor prognosis [134, 135]. Moreover, Ramirez *et al.* found that tumour cells increased the expression level of XBP1s during hypoxia to promote cancer cell proliferation [136]. It has been reported that the IRE1 $\alpha$  arm of UPR induces the expression of vascular endothelial growth factor (VEGF) in cancer cells to promote angiogenesis [137].

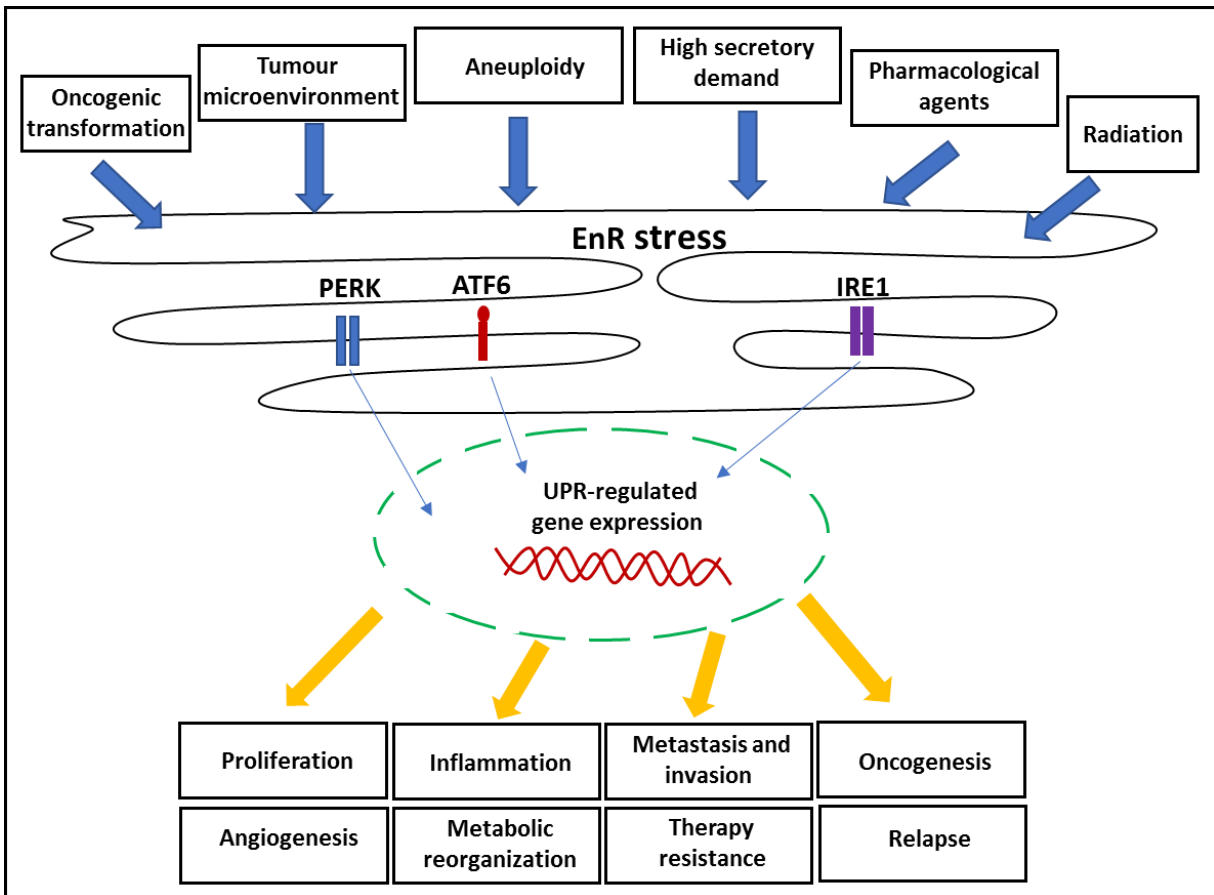


**Figure 1-5. The pathophysiological and pharmacological inducers of EnR stress and cancer cell responses.** Multiple pathophysiological events and factors (e.g., radiation, aneuploidy, oncogenic transformation and tumour microenvironment) and pharmacological agents (e.g., thapsigargin, tunicamycin, and brefeldin A) initiate EnR stress in cells. Cancer cells activate the UPR signalling pathway to adapt to stressful conditions and dictate cell fate by modulating cell proliferation, metastasis, angiogenesis, and therapy resistance.

The PERK signalling pathway also plays a pivotal role in cancer progression. Hart and colleagues found that c-MYC /N-MYC increased PERK/eIF2 $\alpha$  /ATF4 expression and consequently promoted cell survival through the induction of autophagy in lymphoma [138]. Kim *et al.* found that PERK and p-eIF2 $\alpha$  are significantly upregulated in HER2 positive breast cancer and associated with high histological grade and high numbers of tumour infiltrating lymphocytes (TILs) [139].

ATF4, as a downstream gene of the PERK sensor, is upregulated in many cancers. Horiguchi and colleagues found that overexpression of the ATF4 transcript suppresses the cyclin-dependent kinase inhibitor 2A (p16/CDKN2A) and consequently increases cell survival in primary embryonic fibroblasts [140]. Furthermore, activation of the NRF2 transcription factor through the PERK arm causes resistance to several chemotherapeutic drugs such as 5'fluorouracil, doxorubicin, etoposide and cisplatin [141]. Thus, using NRF2 inhibitors as adjuvants can increase the efficacy of chemotherapeutic drugs in cancer treatment.

Not much is known about the role of the ATF6 signalling pathway in human cancer. Depending on the cellular context, ATF6 has both pro-survival and pro-death functions. Two separate studies have investigated the role of ATF6f in tumourgenesis of lung cancer [142, 143] . Furthermore, it has been reported that ATF6 $\alpha$  is upregulated in chronic myeloid leukaemia cells and ATF6 $\alpha$  activation contributes to carcinogenesis and chemoresistance [144].

Depending on the EnR stress intensity and duration, cells activate the UPR signalling pathway to restore EnR homeostasis or induce apoptosis (Figure 1-6). Activation of the three arms of the UPR promotes pro-survival signalling. If activation of the UPR is successful in removing the accumulated misfolded proteins in the EnR, then normal protein translation is resumed and the cell recovers. Although the UPR is primarily a pro-survival response, in the event of prolonged EnR stress that remains unresolved, the UPR switches to initiate apoptosis.

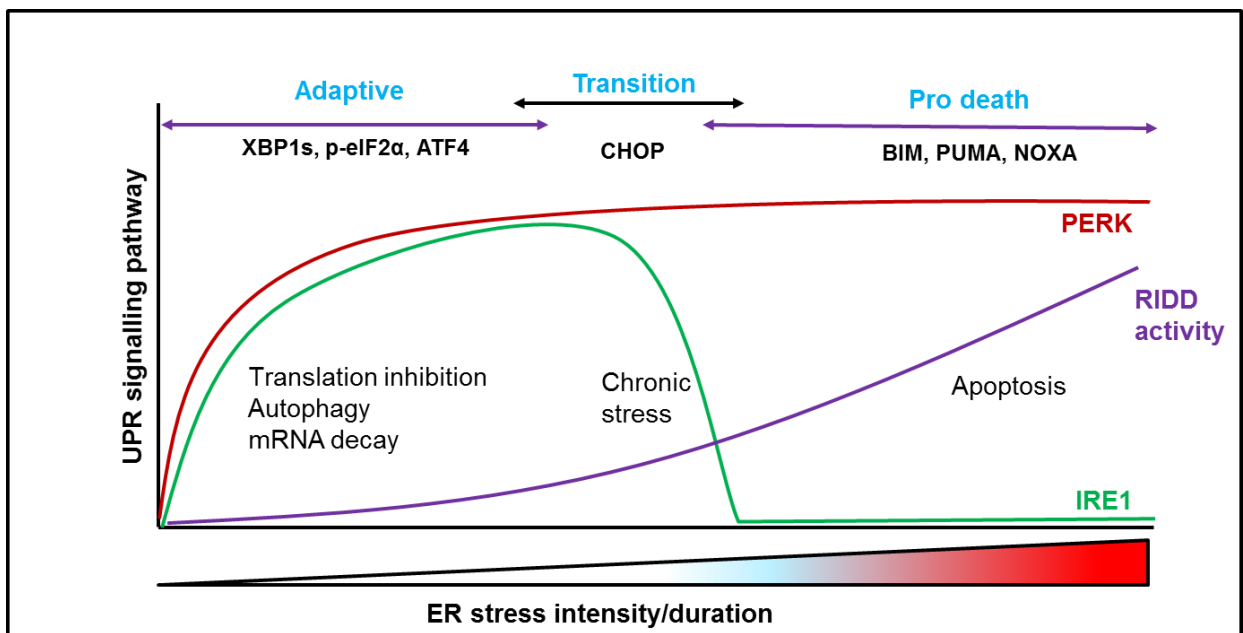


**Figure 1-6. The UPR signalling pathway and cell fate decisions.** Accumulation of unfolded or misfolded proteins initiates UPR. Two major UPR arms (IRE1 and PERK) play adaptive and pro-death roles depending on the EnR stress intensity and duration. Both IRE1 and PERK trigger an adaptive phase by activation of their downstream targets including XBP1s, p-eIF2 $\alpha$  and ATF4. This leads to the upregulation of multiple genes to reduce protein translation, increase autophagy and mRNA degradation. Prolonged EnR stress (chronic stress) turns off the IRE1 signalling pathway and downregulates XBP1s expression. CHOP, which is activated by ATF4, is an important transcription factor in the transition phase. In pro-death phase, the expression level of several genes from the pro-apoptotic BCL-2 protein family (e.g., BIM, PUMA and NOXA) are increased and leads to the cell apoptosis. The increased RIDD activity of IRE1 also contributes to induce cell apoptosis.



The IRE1 and PERK arms initially exhibit a pro-survival role through activation of their downstream targets. One of the main targets of active PERK is eIF2 $\alpha$ , whose phosphorylation leads to inhibition of cap-dependent protein translation. This rapidly reduces the load of nascent proteins being channelled into the EnR (Figure 1-6). Cap-independent translation persists, however, allowing the synthesis of key proteins that mediate the UPR. One such protein is ATF4, a transcription factor which induces EnR chaperones (e.g., GRP78 and GRP94), proteins involved in regulation of amino acid metabolism and resistance to oxidative stress which promote survival, in addition to the transcription factor CHOP which is known to promote apoptotic cell death. Thus, although PERK activation is initially protective, it later promotes cell death. Thus, PERK activation is initially protective, although it later promotes cell death.

IRE1 is a key component of cell fate switch during UPR signalling. Production of XBP1s promotes cell survival (Figure 1-6). However, if the stress is intensive or prolonged, the IRE1 $\alpha$ -XBP1 pathway fades out gradually with the RIDD pathway reinforcing. Basal RIDD activity of IRE1 is necessary for maintaining EnR homeostasis. The extent of RIDD activity is regulated proportionally with stress intensity or duration, eventually leading to apoptosis by degrading pro-survival protein-encoding mRNAs under irremediable EnR stress (Figure 1-6). Furthermore, IRE1 is also able to cleave several mircoRNAs, which may lead to an enhancement in cell death.

## **1-6. UPR signalling pathway in breast cancer**

### **1-6-1. IRE1-XBP1 axis and breast cancer**

Several studies have shown an association between UPR activation and poor clinical outcome in breast cancer [145, 146]. It has been reported that mediators of UPR signalling pathway are activated in breast cancer [135]. Gene expression profiling of primary tumour samples have revealed that increased XBP1 expression is associated with ER $\alpha$  in luminal breast cancer [147]. In another study by Scriven and colleagues, overexpression of XBP1 protein was reported in 90% of breast adenocarcinoma samples [148]. In another published study by Chen *et al*, they found that overexpression of XBP1 is correlated with poor prognosis and recurrence free survival rate in TNBC [135]. They demonstrated that XBP1 interacts with hypoxia-inducing factor 1 $\alpha$  (HIF1 $\alpha$ ) to regulate its target genes thereby promoting TNBC tumourgenicity. They also showed overexpression of total XBP1 and XBP1s in luminal tumours and TNBC respectively [135]. In another study, overexpression of XBP1s was traced through a bioluminescence indicator in mammary epithelial tumours in a transgenic mouse model, and increased expression of XBP1s was reported in hypoxic tumours [131]. Furthermore, the MYC proto-oncogene has been found to increase the expression and function of IRE1 thereby leading to increased splicing of XBP1 mRNA to augment XBP1s protein in TNBC [149].

The Cancer Genome Atlas (TCGA) consortium reported that the most dominant feature of luminal/ER-positive breast cancers is increased mRNA and protein levels of ESR1, GATA3, FOXA1, XBP1 and MYC [150]. Most notably, ESR1 and XBP1 were typically highly expressed but infrequently mutated, suggesting an important functional role.

Gene expression profiling of primary tumour samples has revealed overexpression of XBP1 is associated with ER $\alpha$  in luminal breast cancer [147]. The expression of XBP1 is upregulated by ER $\alpha$  which in turn, potentiates ER $\alpha$ -dependent transcriptional activity [151]. Ectopic expression of XBP1s in ER-positive breast cancer cells can lead to estrogen-independent growth and reduced sensitivity to anti-estrogens [145]. The expression of XBP1s is upregulated in endocrine resistant breast cancer cells and tumours [146, 148]. More recently, an IRE1 inhibitor (STF-083010) has been shown to restore tamoxifen sensitivity to tamoxifen-resistant MCF7 cells in a xenograft model [152]. Moreover, it has been found that increased expression of both un-spliced and spliced XBP1 enhanced resistance of ER-positive breast cancer cells to fulvestrant and tumour-associated macrophages through the activation of NF- $\kappa$ B [153]. The relationship between the UPR and the estrogen signalling pathway has also been reported in breast cancer [154]. Our lab found that NCOA3 is a target of XBP1s and upregulation of NCOA3 plays an important role in providing resistance against anti-estrogenic compounds through the IRE1-XBP1 axis [155].

### **1-6-2. PERK and breast cancer**

Activation of the PERK signalling pathway has been reported in several cancer types including breast cancer [156]. High tumour grade and poor prognosis have been associated with a PERK activation gene signature in cancer patients [157]. Blocking PERK signalling has been shown to reduce the tumour size after injecting MDA-MB-468 (TNBC) and HER2-driven mammary carcinoma cells into mice [156]. ATF4, a downstream target of PERK, is upregulated in hypoxic conditions in the tumour microenvironment [158]. Nagelkerke and colleagues found that the PERK/ATF4 pathway increased the invasion of breast cancer cells by activation of lysosomal-associated membrane protein 3 (LAMP3) [4].

It has been shown that LAMP3 on the surface of cancer cells interacts with E-selectin expressing cells within the tumour microenvironment, and knockdown of LAMP-3 reduces cancer cell invasion [4, 159]. It has also been reported that ATF4 mediates breast cancer progression by activating tribbles homolog 3 (TRIB3) and unc-51-like autophagy activating kinase 1 (ULK1) in hypoxic conditions and knockdown of ATF4 can reduce cell proliferation through TRIB3 and ULK1 [160]. Furthermore, the PERK signalling arm has been shown to be required for EMT leading to enhanced invasion and metastasis [161]. Moreover, mammary gland-specific knockout of PERK in the MMTV-Neu breast cancer model delayed tumour progression and reduced metastatic lesions. PERK mediates significant pro-survival effects on extracellular matrix (ECM)-detached mammary epithelial cells. PERK is activated upon cell detachment and induces autophagy via AMPK/mTORC1 regulation, thereby protecting cells from anoikis. Additional pathways through which PERK likely contributes to cell survival are the PI3K-Akt and NF $\kappa$ B networks, however, these mechanisms have not yet been fully elucidated.

### **1-6-3. ATF6 and breast cancer**

ATF6 is another arm of UPR signalling pathway which is activated during conditions of ER stress. Our knowledge about ATF6's role in breast cancer is very limited. ATF6-regulated genes have not yet been described in breast cancer. COSMIC analysis of 2000 breast cancer tumours has revealed a few rare mutations of the ATF6 gene [162]. It has been shown that there is a connection between the ATF6 and PERK sensors as prolonged activation of ATF6 leads to activation of the pro-death transcription factor CHOP [163]. It has also been reported that ATF6 knockdown significantly suppresses the estrogen-induced cell growth in ER $\alpha$ + breast cancer [154] and reduces tumour volume and angiogenesis in patient-derived xenograft (PDX) animal models [164].

#### **1-6-4. GRP78 and breast cancer**

GRP78, as an EnR resident chaperone, is associated with all three sensors of UPR during normal cell conditions. Upregulation of this major chaperone of the EnR has been seen in several cancers including breast cancer. Tissue microarray analysis has shown upregulation of GRP78 in breast cancer [148]. It has been found that upregulation of GRP78 reduced estrogen starvation-induced apoptosis through suppressing the endoplasmic reticulum BIK (BCL-2-interacting killer) in MCF7 cells [165].

Expression level of GRP78 is higher in HER2 positive breast cancer compared to HER2 negative disease [166] and is also upregulated in various breast cancer cell lines [167]. Zhao and colleagues showed that GRP78 plays a pro-survival role in breast tumours [168].

It functions by inhibiting pro-apoptotic BCL2-family proteins [165] and reducing pro-caspase-7 enzyme cleavage [169]. It has also been reported that GRP78 knockdown significantly reduced cell migration and invasion whereas ectopic expression of GRP78 increased these properties in breast cancer cells [170].

## **1-7. UPR signalling pathway and breast cancer therapy resistance**

Several studies have reported a role for the UPR in breast cancer therapy resistance including resistance to the endocrine therapy [153], chemotherapeutic drugs [171, 172] and radiation therapy [173]. However, there are also studies that show UPR signalling promotes breast cancer cell death in response to some chemotherapeutic compounds [174, 175]. Vecchio and colleagues reported that activated PERK phosphorylates NRF2 to reduce levels of ROS and consequently promotes breast cancer cell resistance to doxorubicin and paclitaxel [157]. The PERK/ATF4/LAMP3 pathway is activated after radiation therapy in breast cancer cells and knockdown of this pathway can promote radiation induced cell death by attenuating the DNA damage response [176].

The IRE1-XBP1 axis also plays an important role in induction of breast cancer therapy resistance. It has been shown that ectopic expression of XBP1s can promote resistance to tamoxifen in ER+ breast cancer cells [153]. In another study, Gomez *et al.* found that overexpression of XBP1s increased expression of the anti-apoptotic BCL2 protein in an ER+ breast cancer cell line which when treated with fulvestrant and tamoxifen [145].

Moreover, GRP78 plays a pivotal role in breast cancer therapy resistance. Cook *et al.* found that tamoxifen treatment upregulates GRP78 expression in breast tumours and knockdown of GRP78 can attenuate cancer cell resistance to tamoxifen [177]. In a separate study, it has been found that breast cancer treatment with two microtubules-targeted agents (vinblastine and taxol) increased GRP78 expression, and blocking of GRP78 by its inhibitor epigallocatechin gallate (EGCG) promotes ER+ breast cancer cell death [172].

## 1-8. UPR targeting drugs and cancer treatment

UPR targeting compounds have not yet been approved for patient treatment, however, animal model studies have demonstrated their potential therapeutic impact in cancer treatment. These drugs target all three UPR arms by different mechanisms. Multiple IRE1 RNase inhibitors (such as 4 $\mu$ 8C, STF-083010, MKC3946, Toyocamycin and 3-methoxy-6-bromosalicylaldehyde) that block both XBP1 splicing and RIDD have been reported. For example, Zhao and colleagues showed that MKC3946 can reduce breast tumour size in a genetically engineered mouse model [149].

In a separate study by Samali's group, the IRE1 $\alpha$  RNase inhibitor MKC8866 alone did not show any effect on tumour size in MDA-MB-231 xenograft models, however, its addition potentiated paclitaxel-mediated tumour suppression [178]. In a published study, it has been reported that XBP1s is increased in tamoxifen resistant MCF7 cells and treatment with STF-083010 compound, which blocks total XBP1 splicing, enhanced sensitivity to tamoxifen [152].

PERK inhibitors including AMG PERK 44, GSK2606414 and GSK2656157 block its kinase activity in the cytosolic domain [179, 180]. Feng *et al.* found that GSK2606414 significantly inhibited migration and invasion in breast cancer cells [161]. In a recently published study, Gallagher and colleagues introduced a new ATF6 signalling pathway inhibitor, Ceapins, which selectively targets the ATF6 $\alpha$  arm [181].

Moreover, there are two compounds that directly bind GRP78 and reduce its activity including HA15 [182] and VER-155008 [183]. Xu et al. showed that anti-GRP78scFv has an anti-tumour activity and can significantly reduce breast tumour size in a xenograft model [184]. Liu and colleagues have introduced a monoclonal antibody, MAB159, that specifically targets GRP78 and changes PI3K pathway function. They showed that MAB159 significantly suppressed TNBC cell growth and invasion [185]. There is also another monoclonal immunoglobulin M antibody, PAT-SM6, targeting GRP78 which is in phase I clinical trials for myeloma treatment [186]. In another recently published study, it has been shown that plumbagin, an organic compound, inhibits GRP78 activity and increases breast cancer cell death in response to tamoxifen [187].

## **1-9. MicroRNAs**

MicroRNAs are a class of endogenous, short (19-22 nucleotides in length) non-coding RNAs that play a pivotal role in gene expression regulation by translational repression or degradation of target transcripts. MicroRNAs were first discovered in the nematode *Caenorhabditis elegans* by Lee *et al.* in 1993 [188]. MicroRNAs are expressed in multiple tissues, cells and body fluids, and their expression profiles can change in various circumstances, for instance during developmental stages [189], in response to pathogens or due to diseases [190, 191]. Each individual miRNA may have thousands of mRNA targets, with it being estimated that 30-80% of human genes may be regulated by one or more miRNA [192]. Thus, these small non-coding RNAs play pivotal roles in a wide range of normal physiological processes such as cellular differentiation, proliferation and metabolism [193]. As with mRNAs, miRNA profiles may vary significantly between different tissues and cell types [194, 195]. In addition, cells also selectively release specific miRNAs into body fluids (e.g., blood) via exosomes, microvesicles, apoptotic bodies [196-198].



### **1-9-1. MicroRNAs nomenclature**

The nomenclature system used to name individual microRNAs includes an uncapitalised ‘mir’ prefix and a unique number to show the pre-microRNA (e.g., mir-1, mir-2, mir-3, mir-4) and a capitalised ‘miR’ prefix for mature microRNAs. In addition, the name of each miRNA has three letters to show the specific species. For instance, ‘hsa’ is used for humans (Homo sapiens- e.g., hsa-miR-616), ‘mmu’ is used for a mouse (Mus musculus- e.g., mmu-miR-451), and ‘rno’ refers to the rat microRNAs (Rattus norvegicus- e.g., rno-miR-14) [199]. To distinguish multiple microRNAs from the same family, a letter is used after the number of the microRNA such as hsa-miR-10a and hsa-miR-10b. To show which double-stranded microRNA the mature sequence comes from a ‘3p’ or ‘5p’ tag follows the name of the microRNA (e.g., hsa- miR-616-3p or hsa-miR-616-5p) and the unstable strand of miRNAs is given a \* sign (e.g., has-miR-378\*) after the numerical identifier [200].

### **1-9-2. MicroRNAs biogenesis: Canonical pathway**

Half of all known miRNAs are intragenic and are processed from introns of a host gene, while other miRNAs are intergenic and processed independently [201]. MicroRNA biogenesis is categorised in two pathways, the canonical and non-canonical pathways. The canonical pathway is known as the main process by which miRNA processing is initiated in the nucleus of cells (Figure 1-7). RNA polymerases II and III (pol II/pol III) are responsible for transcribing miRNA genes into long primary transcripts, named Pri-miRNAs [202]. Pol II generates most of the mRNAs and non-coding RNAs while pol III produces the shorter non-coding RNAs (5S ribosomal RNA, tRNAs and the U6 snRNA) and miRNAs [203].

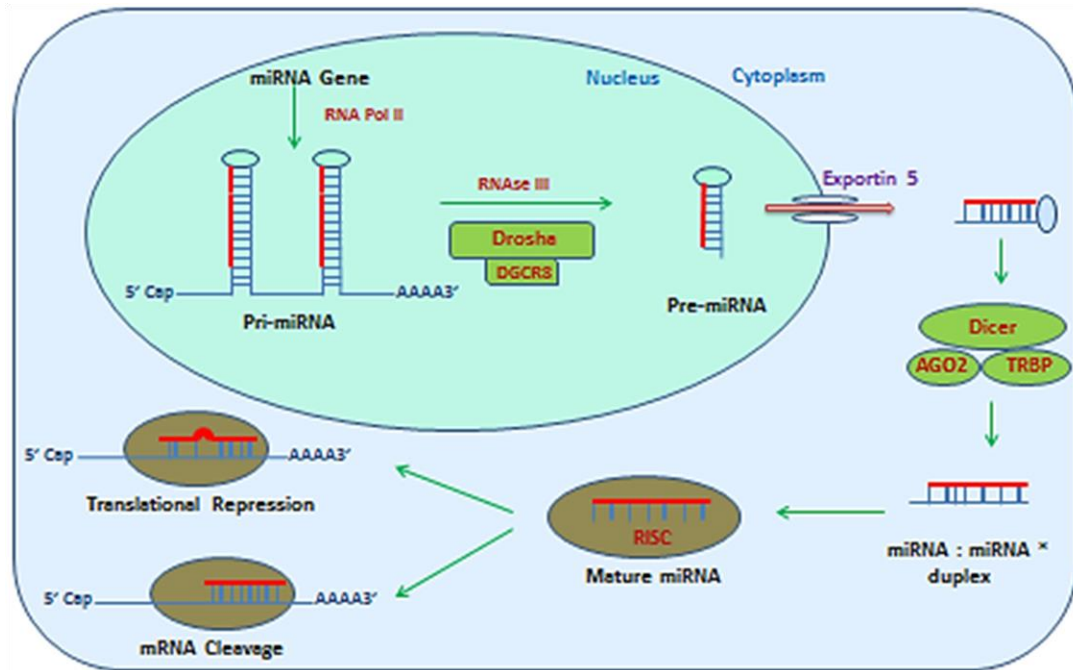


**Figure 1-7. The canonical microRNA biogenesis pathway.** MicroRNA biogenesis initiates in the nucleus where RNA polymerase II transcribes microRNA genes into pri-miRNAs. Droshe (RNase III-type enzyme) and its co-factor DGCR8 cleave pri-miRNAs into precursor miRNAs (pre-microRNAs). Pre-miRNAs are then transported into the cytoplasm by the XPO5/RanGTP complex, which are then processed by DICER, trans-activator RNA-binding protein (TRBP), and AGO2 to produce double-strand RNA (miRNA: miRNA\* duplex). Finally, the mature microRNA is translocated into the RISC to mediate gene silencing by endonucleolytic cleavage or translational repression mechanisms.

Pri-miRNA is processed by the RNase III-type enzyme, DROSHA, and its co-factor DGCR8 (microprocessor complex) and converted into a 70-nucleotide precursor miRNA (pre-microRNA) which has the stem-loop structure [204, 205]. Pre-miRNA is then transported into the cytoplasm by the Exportin-5 (XPO5)/Ran-GTP complex and processed by DICER (a second RNase III enzyme) that works in association with the transactivator RNA-binding protein (TRBP) and Argonaute2 (AGO2) [206]. This complex then removes the terminal loop and generates double-stranded RNA duplexes (miRNA: miRNA\* duplex) consisting of a mature microRNA (guide strand) and its complementary (passenger) strand [207, 208].

Thermodynamic features of double-stranded miRNAs determine which strand would be a passenger or guide strand. The guide strand has U-bias at its 5'-end and passenger strands have C-bias at their 5'-end [209]. The miRNA strand, which generally exhibits weaker 5' base pairing is selected as a guide strand. Guide strands of 21-nt duplexes preferentially enter the RNA-induced silencing complex (RISC) protein complex. The proteins in RISC are involved in pairing the single-stranded mature miRNA with the target mRNA. The core components of every RISC complex are several Argonaute (AGO) proteins (AGO1, 2, 3, and 4). RISC, which includes a mature miRNA, mediates gene silencing by endonucleolytic cleavage or translational repression [210].

### **1-9-3. MicroRNAs biogenesis: Non-canonical pathway**

There are two main non-canonical miRNA biogenesis pathways, the DICER-independent and DROSHA/DGCR8-independent pathways [211]. For example, mirtrons, which are generated from the introns of mRNA during splicing, are produced by the DROSHA/DGCR8-independent pathway [212]. Mirtrons were initially discovered in *Drosophila melanogaster* and *Caenorhabditis elegans* in 2007 [212]. The expression of mirtrons depends on the host gene as mirtrons are associated with the sequence of their host genes while the expression of other intragenic miRNAs is regulated independently [213]. Another example of the non-canonical miRNA biogenesis is 7-methylguanosine (m7G)-capped pre-miRNA. There are two types of pre-miRNA hairpins which consist of phosphate or a m7G-cap at the 5' region [202]. RNA polymerase II transcribes the m7G capped pre-miRNAs which are directly transported to the cytoplasm by exportin 1 with no need for the DROSHA cleavage [214]. Both mirtrons and m7G-capped pre-miRNAs require processing by DICER to complete their cytoplasmic maturation.

Another example of a non-canonical miRNA biogenesis pathway is the production of endogenous short hairpin RNAs (shRNA). RNA polymerase III is responsible for transcribing endogenous shRNA and further processing is performed by the DROSHA/DGCR8 complex followed by transportation in to the cytoplasm by XPO5/Ran-GTP. Finally, endogenous shRNA is processed by an AGO2 protein with no need for DICER [215].

#### **1-9-4. MicroRNAs function**

miRNAs have been shown to be involved in diverse biological processes, including development, cellular differentiation, proliferation, apoptosis, and oncogenesis. MicroRNAs play pivotal roles in gene expression regulation by translational repression or degradation of target transcripts [216]. MicroRNAs usually interact with 3' untranslated region (UTR) of their target mRNA(s) to downregulate expression [202]. However, miRNAs can interact with other regions of target mRNA such as the 5' UTR, gene promoters and protein-coding sequences [217]. Indeed, some studies indicate that miRNAs may also promote translation of target mRNAs [218-221] or increase transcription via the binding sites present in the promoter region of target genes [222].

#### **1-9-5. MicroRNAs as cancer therapeutics and targets**

MicroRNAs play a pivotal role in various diseases including cancer, making them valuable drug targets. There are two possible approaches for the use of miRNAs as a therapeutic strategy in cancer, blocking oncogenic miRNAs by antimiRs or the use of tumour suppressor miRNA mimetics. The activity of miRNAs can be suppressed by anti-miRNA oligonucleotides (AMOs) which are sufficiently stable in the body and bind strongly to their miRNA target(s) [223].

There are two types of chemical modifications that have been introduced in AMOs to confer strong binding to miRNAs, including 2'-O-methylation of RNA nucleotides [223] and locked nucleic acid (LNA) DNA nucleotides [224]. miRNA mimetics are RNA molecules similar to the corresponding miRNA sequence which can enter the miRNA biogenesis pathway post DICER processing and become incorporated into the RISC complex.

Several studies have investigated the therapeutic efficacy of miRNAs in human cancer. For instance, miR-16 mimetics have been introduced to treat patients with malignant pleural mesothelioma and advanced lung carcinoma and are in phase I clinical trials [225]. Multiple preclinical studies have found therapeutic effects of miR-34 mimetics in various tumour tissues including lung, prostate, and liver in mice models [226, 227]. In another study, it has been reported that treatment with miR-200c mimetics significantly enhanced sensitivity of lung cancer cells to the radiotherapy and was associated with better overall survival in a mouse model [228]. They found that miR-200c directly targeted multiple mRNAs including sestrin 1 (SESN1), peroxiredoxin 2 (PRDX2) and NRF2 which lead to apoptosis.

Moreover, Ma and colleagues reported that inhibition of miR-10b by AMOs significantly suppressed breast cancer cell migration and invasion in a mouse model. They found that inhibition of miR-10b increased the expression level of the anti-metastatic gene HODX10 [229]. The therapeutic role of other miRNAs has also been investigated in these tumours; miR-26a/-221 in Hepatocellular carcinoma (HCC) [230, 231], miR-506/-520/-630 in ovarian cancer [232, 233], miR-15/16 in leukaemia [234], miR-155 in lymphoma [235] and miR-145/-33a in colon cancer [236].

## 1-9-6. The role of microRNAs in cancer development

Cancer is a group of diseases caused by genetic alterations which leads to dysregulated cell growth, causing malignant tumour formation which may invade other tissues and vital organs. At a molecular level, this is normally characterised by changes in gene expression profiles [237]. Like other genes, miRNA expression profiles also change in cancer cells [238]. The first report of abnormalities in miRNA expression was demonstrated in B-cell chronic lymphocytic leukaemia (B-CLL), where miR-15 and miR-16 were downregulated in approximately 68% of B-CLL patients [239]. These miRNAs regulate the expression of BCL2 transcripts. In fact, downregulation of miR-15 and miR-16 was responsible for increased expression of BCL2 in B-CLL and ectopic expression of miR-15 and miR-16 induced apoptosis by targeting BCL2 mRNA [240]. It has been shown that miRNAs are linked to the etiology and progression of numerous cancers (Table 1-2) [241] and different cancer types can be classified by miRNA expression patterns [242].

Table 1-2. MiRNAs and their expression in malignancy

Cancer	Up-regulated	Down-regulated	Reference
<b>Breast</b>	miR-21,miR-451,miR-205 miR-29b-2,miR-155	miR-145,miR-497,miR-125b miR-10b,miR-27b,miR-17-5p	[243],[244] [245]
<b>Lung</b>	miR-21,miR-7,miR-200b,miR-210	miR-126,miR-451,miR-30a,miR-486	[246]
<b>Gastric</b>	miR-21,miR-223,miR-103-2	miR-218-2	[242], [247]
<b>Prostate</b>	let-7d,miR-195,miR-203	miR-128a	[242]
<b>Colon</b>	miR-135b,miR-92,miR-222 miR-95,miR-17-3p	miR-143, miR-145, let-7	[248], [242] [247]
<b>Pancreatic</b>	miR-103-1,2, miR-107, miR-125-1	miR-375	[242], [247]
<b>Ovarian</b>	miR-200a,miR-141 miR-200c,miR-200b	miR-199a, miR-140 miR-145,miR-125b1	[249]

Moreover, Volinia *et al.* characterised miRNA expression profiles in six different cancers (breast, lung, prostate, stomach, pancreas and colon) using a large cohort of patient and control samples, and reported 43 dysregulated miRNAs [250].

Mitchell *et al.* showed that miR-141 is upregulated in human prostate cancer patients compared to healthy controls [251]. Furthermore, Iorio *et al.* examined the miRNA expression profile in human ovarian cancer and found four overexpressed (miR-200a, miR-141, miR-200c, and miR-200b) and four downregulated miRNAs (miR-199a, miR-140, miR-145, and miR-125b1) [249]. Table 1-2 shows some miRNAs known to be dysregulated in malignant solid tumours.

It has been proven that regions of the human genome which are associated with cancer (fragile sites) harbour half of the miRNAs genes [252, 253]. There are many cancer-associated regions in the human genome which comprise miRNA genes [254]. Although several miRNAs are dysregulated in specific tumours, a global reduction of miRNA abundance appears to be a general trait of human cancers, playing a causal role in the transformed phenotype. The loss of miRNAs biogenesis and aberrant expression of proteins, associated with miRNA biogenesis, has been observed in various cancer types [255]. For example, downregulation of DICER has been found in several cancers such as breast, colorectal and lung cancers [256-258]. Kumar and colleagues found that downregulation of DICER, DROSHA, and DGCR8 in LKR13 cells (mouse adenocarcinoma cell line) increased cellular transformation and tumourigenesis and upregulated the expression of key oncogenic genes such as c-MYC, K-Ras and E2F1 [241]. Mutation of the Exportin 5 gene, which is responsible for transporting precursor miRNA from the nucleus to the cytoplasm, causes miRNAs to accumulate in the nucleus and leads to tumour formation [259]. Somatic mutations in AGO2 have been found in gastric and colon cancers [260]. Moreover, upregulation of AGO2 by EGFR and MAPK signalling has been reported in ER-positive breast cancer cell lines [261].

### **1-9-7. Tumour suppressive and oncogenic roles of microRNAs**

MicroRNAs have both tumour suppressor and oncogenic functions [262, 263] and gain or loss of these functions has been documented in different cancers, with pathological roles in tumour cell proliferation, progression and the metastatic process [264, 265]. Tumour suppressive miRNAs target the mRNA transcript of genes that normally function as oncogenes. For instance, expression of BCL-2 and MCL-1 (anti-apoptotic proteins) are increased in human cancer and are responsible for chemotherapeutic resistance and relapse [266]. Several studies have reported the role of miRNAs in regulation of these anti-apoptotic proteins in cancer cells. Singh *et al.* found three tumour suppressive miRNAs (miR-365-2, miR-195 and miR-24-2) which directly target the 3'UTR of BCL-2 mRNA and induce apoptosis in MCF7 cells [267]. In another published study, the expression level of miR-15a and miR-16-1 clusters were found to be downregulated in chronic lymphocytic leukaemia (CLL) [240]. They reported that these miRNAs target BCL-2 and modulate apoptosis in leukemic cell line models.

Moreover, the let-7 family is known as a tumour suppressor miRNA in breast cancer. It has been shown that the expression levels of let-7a, let-7b, and let-7g were significantly downregulated in breast cancer patients, and ectopic expression of let-7b strongly reduced cell migration and invasion [268]. In addition, miR-378 has been demonstrated to play a tumour suppressor role in various cancers including colorectal cancer by targeting SDAD1, vimentin, BRAF and CDC40 [269-272]; gastric cancer by inhibiting expression of MAPK1, CDK6 and VEGF transcripts; prostate cancer by targeting MAPK1, KLK2 and KLK4 [273, 274]; pituitary adenoma by inhibiting RNF31 [275]; medulloblastoma by inhibiting UHRF1 [276] and myelodysplastic syndrome (MDS) by inhibiting BCL-W and CDC40 [277].



On the other hand, a substantial number of studies have reported an oncogenic function of miRNAs (Oncomirs) in multiple cancers. Some of these miRNAs target the mRNAs of tumour suppressor genes and contribute to cancer progression. For example, an oncogenic function of miR-17-92 cluster has been reported in Burkitt's lymphoma, diffuse large B-cell lymphoma and lung cancer [278, 279]. In another published study, miR-31 was identified as an oncogenic miRNA in cervical cancer which directly targets BRCA1-associated protein-1 (BAP1), and inhibition of miR-31 expression strongly promoted EMT [280]. Moreover, it has been reported that overexpression of miR-548d-2-3p is associated with poor prognosis in TNBC by directly targeting the 3'UTR of TP53BP2 mRNA. Ectopic expression of miR-548d-2-3p in MDA-MB231 cells significantly increased cell growth, and knockdown of this miRNA strongly reduced cell proliferation and increased apoptosis [281]. Several studies have indicated that miR-378 plays a role as an oncomiR in multiple cancer types such as cervical cancer [282, 283]; lung cancer [284-286] and glioblastoma by targeting vimentin, Sufu, Fus and VEGFR2 [287-289], and nasopharyngeal carcinoma by targeting TOB2 [290]. Furthermore, it has been reported that miR-616 acts as an oncomiR in multiple human cancers [291-295]. miR-616 expression is upregulated in prostate cancer, gastric cancer, non-small cell lung cancer (NSCLC), hepatocellular carcinoma (HCC) and glioblastoma. miR-616 directly targets TFPI-2 mRNA in prostate cancer [291], PTEN mRNA in HCC and gastric cancer [292], SOX7 in glioblastoma [293] and NSCLC [294].

In addition, some miRNAs have both oncogenic and tumour suppressive roles in human cancer [296] in a context dependent manner. For example, the miR-17-92 family has been found to be upregulated in various cancers including lung cancer, diffuse large B-cell lymphoma, follicular lymphoma, Burkitt's lymphoma and mantle cell lymphoma [278, 279]. miR-17-92 is known mostly as an oncogenic miRNA which increases cancer cell proliferation, migration and invasion. However, tumour suppressor activity of miR-17-92 has also been reported in human cancers [279, 297]. For example, miR-17-92 expression is downregulated in prostate cancer, and ectopic expression of this miRNA significantly reduced prostate cancer cell growth [298]. Another example of miRNAs with both oncogenic and tumour suppressive function is miR-155. For instance, miR-155 is dysregulated in different cancers including gastric and pancreatic cancers, playing a tumour suppressive role by reducing cell proliferation [247, 299]. However, miR-155 was found to be a tumour promoting miRNA in breast cancer. It has been shown that miR-155 is overexpressed in breast cancer and reduces the expression of tumour suppressor gene suppressor of cytokine signalling 1 (SOCS1), and consequently promotes cancer cell proliferation [300]. This apparent paradox can be reconciled by taking into account the fact that a single miRNA molecule has the capacity to target numerous different mRNAs, some of which may have opposing oncogenic or tumour suppressive functions [301].

## 1-10. MicroRNAs and breast cancer

Several studies have been conducted to identify the miRNAs that are differentially expressed and regulate initiation and progression in different breast cancer subtypes. Blenkiron and colleagues were the first group that described a miRNA signature in breast cancer subtypes [302]. They profiled 309 miRNAs in 93 breast tumours including all four breast cancer subtypes. In another study, Lowery and colleagues identified miRNAs related to the estrogen (miR-217, miR-190, miR-135b, miR-218, miR-342, miR-299), progesterone (miR-527-518a, miR-520g, miR-377, miR-520f-520c) and HER2/ neu (miR-181c, miR-302c, miR-520d, miR-376b, miR-30e) receptor status of breast cancer patients based on artificial neural networks (ANN) analysis and qRT-PCR. They also showed that miR-342 was upregulated in ER and HER2/neu-positive luminal B and downregulated in triple-negative subtypes with miR-520g expression being increased in ER and PR-negative subtypes [303]. The most commonly dysregulated miRNAs from three independent studies in breast cancer subtypes are listed in table 1-3.

Table 1-3. Commonly dysregulated miRNAs in breast cancer subtypes.

<b>Luminal</b>	<b>Basal</b>	<b>HER2</b>	<b>Normal-like</b>
let-7c	hsa-miR-18a	hsa-miR-142-3p	hsa-miR-145
hsa-miR-10b	hsa-miR-135b	hsa-miR-150	hsa-miR-99a
let-7f	hsa-miR-93		hsa-miR-100
	hsa-miR-155		hsa-miR-130a

These miRNAs are derived from three independent studies by Rinaldis *et al.* [304], Dvinge *et al.* [305], and Blenkiron *et al.* [302].

There are also some published studies which have reported miRNA signatures in breast cancer cell lines. In one such example, Riaz and colleagues carried out a comprehensive study to characterise the miRNA expression profiles in 51 human breast cancer cell lines [306].

They explored the expression level of 725 human miRNAs by microarrays containing LNA<sup>TM</sup> capture probes. Based on miRNA signatures, they divided 51 human breast cell lines into two groups: a minor cluster that included 18 cell lines and a major cluster that included 33 cell lines. Based on intrinsic subtyping, 17 out of 18 cell lines present in the minor cluster belonged to the basal-like subtype, and 16 of them lacked ER, PR and ERBB2 protein expression (triple-negative). On the other hand, 29 out of 33 breast cancer cell lines present in the major cluster were of the luminal-type. Among the 87 most-variably expressed miRNAs across the entire panel, a set of 15 miRNAs was significantly higher in the basal-like subtype and a set of 17 miRNAs showed significantly higher expression in luminal subtype. Taken together, this indicates that microRNAs have the potential to be diagnostic and prognostic markers in breast cancer.

### **1-11. MicroRNAs and the unfolded protein response**

Several studies have shown alterations in miRNA-expression profiles during conditions of EnR stress and UPR activation (Table 1-4). MiRNAs, as modulators of gene expression, affect the induction of UPR target genes and influence the cell's response to EnR stress. Based on their functional effects, UPR-regulated miRNAs can be divided into two groups: pro-adaptive and pro-apoptotic miRNAs [307, 308]. The miRNAs that have a pro-adaptive role contribute to increasing the folding capacity and reducing protein loading into the EnR lumen. On the other hand, the pro-apoptotic related miRNAs play a role in modulating UPR-induced apoptosis and cell death.

Table 1-4. Summary of microRNA effects on the UPR signalling pathway and their target genes.

MicroRNA	UPR arm	Targets	Reference
miR-221/222	PERK(CHOP)	p <sup>27kip</sup>	[309]
miR-204	PERK	BIP, CHOP	[310]
miR-23a~27a~24-2	PERK-IRE1	ATF4, TRAF2, JNK, ASK1, ATF3	[311]
miR-122	PERK	Calreticulin, ERp29	[312]
miR-346	IRE1(XBP1s)	TAP1	[313]
miR-708	PERK(CHOP)	Rhodopsin	[314]
miR-30c-2*	IRE1	XBP1	[315]
miR-455	ATF6	Calreticulin	[316]
miR-106b-25	PERK (ATF4)	BIM	[317]
miR-211	PERK	CHOP	[318]
miR -17,34a, 96a,125b	IRE1	Caspase-2	[47]
miR-17	IRE1	TXNIP	[319]
miR-663	PERK	ATF4, VEGF	[320]
miR-214	IRE1	XBP1	[321]
miR-30d, miR-181a	ATF6	GRP78/BIP	[322]
miR-1291	IRE1	Glypican-3	[323]
miR-199-5p	IRE1, ATF6	AP-1, BIP	[322, 324, 325]
miR-297	IRE1	Xbp1s, GRP78	[326]
miR-495	IRE1 (XBP1)	GRP78	[325]
miR-29a	PERK, IRE1	CHOP, XBP1s	[327]
miR-200c-3p	IRE1 $\alpha$ , ATF6	LC3-II	[328]

### **-Pro adaptive role of miRNAs during UPR signalling**

The first UPR regulated miRNA was identified by Dai and colleagues in 2010. They showed that the expression of miR-221/222 is regulated by CHOP during prolonged EnR stress. They found that p27<sup>kip1</sup> is a target of miR-221/222 and upregulation of this miRNA can prevent the loading of p27<sup>kip1</sup> protein into the EnR [309]. Byrd and colleagues found that miR-30c-2-3p is upregulated during UPR and is dependent on the kinase activity of PERK. Furthermore, miR-30c-2-3p limits the expression of XBP1, and expression of anti-miR-30c-2-3p protected cells against UPR-induced death [315]. Moreover, Chitnis *et al.* (2012) found that miR-211 has a pro-survival activity during UPR. They showed that miR-211 was induced by the PERK sensor and reduced the expression of CHOP [318]. In another study by Bartoszewski and colleagues, they reported that miR-346 expression was regulated by XBP1 during an early stage of the EnR stress and UPR [313]. They found that antigen peptide transporter 1 (TAP1) is a direct target of this miRNA, inhibiting the loading of MHC class I in the EnR and consequently reducing the EnR protein load. ATF6 has been shown to downregulate miR-455 expression during UPR activation in cardiomyocytes [316]. Furthermore, it is reported that calreticulin is a target of miR-455, and its upregulation restores the calcium homeostasis to improve the EnR folding capacity. Yang *et al.* (2011) showed that inhibition of miR-122 leads to accumulation of the EnR stress protein 29 (EnRp29), calreticulin and cyclin-dependent kinase 4 (CDK4) protein in the EnR lumen of hepatoma cells [312]. CDK4 then increases the stability of non-ATPase regulatory subunit 10 (PSMD10) of the 26S proteasome and increases cell survival. Thus, upregulation of miR-122 can increase apoptosis in these liver cell lines (Huh7 and HepG2 cells). These reports provide evidence for the interplay between miRNAs and the pro-adaptive activity of UPR-associated transcription factors.

### **-Pro-apoptotic role of miRNAs during UPR signalling**

miRNAs have been shown to be critically involved in the control of cell survival and cell death decisions. Several studies have shown alterations in miRNA expression during UPR activation, which have implications for regulation of cell fate. The contribution of miR-106b-25 to the UPR pro-apoptotic response was demonstrated by our laboratory [317].

We showed that downregulation of the miR-106b-25 cluster (miR-106b, miR-25 and miR-93), which are regulated by ATF4 and NRF2, increases the level of BIM, a pro-apoptotic molecule of the BH3-only family of proteins. In another study we reported that miR-424(322)503 cluster is downregulated in a PERK-dependent manner during UPR activation. In addition, we showed that miR-424 regulates cell fate during UPR by influencing the activation of ATF6 (as its direct target) and RIDD activity of IRE1 [329].

A new alternative miRNA degradative mechanism was reported during UPR activation by Upton and colleagues [318]. They showed that the RNase activity of IRE1 $\alpha$  can degrade four precursor miRNAs including miR-17, miR-34a, miR-96a and miR-125b. These miRNAs target and repress the Caspase 2 (C-2) transcript which is an activator for the mitochondrial apoptosis pathway. Thus, activation of the endoribonuclease activity of IRE1 increases C-2 protein levels and promotes cell apoptosis.

There is also another study that showed that the degradation of miR-17 through IRE1 $\alpha$  RNase activity elevates the thioredoxin-interacting protein (TXNIP) level and causes the programmed cell death in pancreatic  $\beta$  cells [319]. Su *et al.* (2013) have reported downregulation of three miRNAs (miR-30a, miR-181a, and miR-199a-5p) in prostate, colon and bladder tumours. They showed that these miRNAs directly targeted the 3' UTR of GRP78/BiP in C42B prostate cancer cells, and their induction promoted apoptosis during UPR activation [322].

Taken together, UPR-regulated miRNAs can affect both pro-adaptive and pro-apoptotic cellular signaling during UPR activation. Because miRNAs can target many distinct mRNA targets, the physiological consequence of UPR-regulated miRNAs are likely to be context and/or tissue-dependent. Therefore, it will be crucial to identify which miRNAs constitute the essential signalling nodes in this network. The advances in understanding how miRNAs take part in UPR-mediated adaptive and apoptotic signaling will reveal novel therapeutic potential for diseases associated with the UPR.



## 1-12. Rationale of the study

The stressful conditions of the tumour microenvironment, including low oxygen supply, nutrient deprivation and pH changes, activate a range of cellular stress-response pathways [330]. Tumour hypoxia is a common microenvironmental factor that adversely influences tumour phenotype and treatment response [331]. Cellular adaptation to hypoxia occurs through multiple mechanisms, including activation of the UPR. The UPR is an intracellular signalling network activated in response to EnR stress. A variety of transcription factors including ATF6, ATF4, CHOP and XBP1, are activated during UPR. They collaborate to induce the expression of a wide array of targets, including EnR chaperones and genes involved in ERAD, to enhance the protein folding capacity of the cell and to decrease the unfolded protein load of the EnR [10, 332]. However, if the primary stimulus causing protein unfolding in the EnR is protracted or excessive, apoptosis ensues.

At present, it is unclear how tumour cells adapt to long-term EnR stress *in vivo* - whether the protective elements of the response are enhanced, the destructive components suppressed, or if the compromised apoptotic machinery (a common occurrence in tumour cells) is sufficient to protect them from UPR-induced apoptosis. Given that the UPR can trigger pro-survival and pro-apoptotic signals, it is important to understand how modulation of the UPR alters the balance between these processes and contributes to carcinogenesis in different cell types. The upregulation of the UPR in cancers may be beneficial for tumour cells by increasing the protein folding capacity and prolonging life. On the contrary, downregulation of the UPR may allow cells to escape the apoptotic pathway, favouring tumourigenesis. The exact mechanisms involved in the transition of the UPR from a cell survival to cell death response is not clearly understood.

Computational analysis predicts that more than 30% of animal genes may be subject to regulation by miRNAs [338, 339], suggesting a role for miRNA-mediated gene regulation during UPR. Several studies have shown that miRNA expression is globally repressed in tumour tissues compared to the tumour adjacent normal tissue. There are three possible mechanisms responsible for miRNA dysregulation in cancer:

- (i) miRNAs loci are frequently localized in fragile chromosomic sites and are often altered (methylation, deletion, amplification and translocation).
- (ii) Changes in transcription factor activities that control miRNA expression (e.g., MYC and P53).
- (iii) miRNA biogenesis could be affected by the altered expression of DICER, DROSHA and XPO5 or mutations in these genes.

Hence, we hypothesise that UPR-regulated microRNAs can influence the cellular response during EnR stress and may contribute to cancer progression. The role of miRNAs in regulation of the UPR is an emerging area and further research is required to gain an understanding of the pathways involved, which may provide additional therapeutic opportunities.

In this study, we identified two UPR regulated miRNAs (miR-378 and miR-616) during conditions of EnR stress and UPR. miR-378 was identified in preliminary studies performed to identify UPR-regulated miRNAs by global miRNA expression profiling during conditions of UPR. Several studies have indicated that miR-378 is upregulated and acts as an oncomiR in: cervical cancer by targeting *ST7L* and *ATG12* [282, 283]; lung cancer by inhibiting the expression of *RBX1*, *HMOX1*, *TP53* and *FOXG1* [284-286]; glioblastoma by inhibiting vimentin, *Sufu*, *Fus* and *VEGFR2* [287-289]; nasopharyngeal carcinoma by targeting *TOB2* [290].

However, miR-378 has been shown to play a tumour suppressor role in: colon cancer by inhibiting SDAD1, vimentin, BRAF and CDC40 [269-272]; gastric cancer by inhibiting MAPK1, CDK6 and VEGF; prostate cancer by inhibiting MAPK1, KLK2 and KLK4 [273, 274]; pituitary adenoma by inhibiting RNF31 [275]; medulloblastoma by inhibiting UHRF1 [276] and myelodysplastic syndrome by inhibiting BCL-W and CDC40 [277]. These observations underscore the context-dependent behaviour of miR-378 in human cancers.

The presence of the miRNA genes within the introns of protein-coding genes suggests a possible functional relationship between the intronic miRNA and its host gene. Therefore, we hypothesise that miR-616 (originating from the CHOP locus) may influence the cellular response during conditions of EnR stress and dysregulation of miR-616 may contribute to cancer progression. Several studies have shown that miR-616 acts as a tumour promoting miRNA in human cancers [291-295]. The expression of miR-616 has been shown to be upregulated in androgen-independent prostate cancer, non-small cell lung cancer (NSCLC), hepatocellular carcinoma (HCC) and gliomas. MiR-616 targets the tissue factor pathway inhibitor (TFPI-2) in prostate cancer [291], PTEN in HCC and gastric cancer [292] and SOX7 in glioma [293] and NSCLC [294].

### **1-13. Aims of the study**

MiRNAs have been shown to be critically involved in the control of cell survival and cell death decisions [308]. During the past few years, work from several groups have revealed that all three branches of the UPR regulate specific subsets of miRNAs (Table 1-4). The modes of regulation include induction/repression by UPR-regulated transcription factors such as ATF6, XBP1, ATF4 and NRF2, as well as IRE1-mediated miRNA degradation [11, 333]. The outcome of UPR-dependent miRNA expression is a fine tuning of the EnR stress machinery to modulate cellular adaptation to stress and regulation of cell fate [333]. Since a given miRNA can target several distinct RNA transcripts, the physiological consequence of altered miRNA expression is likely to be context- and/or tissue-dependent. It is still not clear whether UPR regulated miRNAs are differentially expressed depending on the UPR activation status in tumours, and in turn whether they contribute to adaptive responses in tumours.

Collectively, in this study, we aimed to:

- 1- Identify UPR regulated miRNAs and validate the expression levels of candidate miRNAs (miR-378 and miR-616) during conditions of EnR stress in human cancer cells.
- 2- Determine the mechanisms regulating the expression of miR-378 and miR-616 during conditions of EnR stress and UPR.
- 3- Evaluate the effect of miR-378 and miR-616 on cell growth, proliferation, migration and cell fate during conditions of EnR stress and UPR.
- 4- Identify the functional targets of miR-378 and miR-616.

## Chapter 2

## **2-0. Materials and Methods**

### **2-1. Cell culture**

Cell culture refers to the process by which cells grow in an artificial environment under controlled conditions. These conditions may vary for each cell type but usually contain essential factors such as growth factors, hormones, amino acids, carbohydrates, minerals and vitamins. Depending on the cell type, they may need a surface for growing, known as adherent cells while other cell types can be grown floating in the medium (suspension cells).

Human breast cancer cells (MCF7, MDA-MB-231 and ZR-75-1) were purchased from (ATCC) American Type Culture Collection (Manassas, VA). Colorectal cancer cells (HCT116 and RKO) were a kind gift from Dr. Victor E. Velculescu, Johns Hopkins University, USA. HEK 293T cells were from Indiana University National Gene Vector Biorepository. All tissue culture work was performed under the tissue culture class II biological safety cabinet (ESCO, GB Ltd, UK) sterilised with UV and wiped with 70 % v/v ethanol before and after use. The MCF7, MDA-MB-231 and HEK 293T cells were maintained in Dulbecco's modified eagle's medium (DMEM) (Sigma, UK, Cat #D6429). HCT116 and RKO cells were maintained in McCoys 5A modified medium (Sigma, UK, Cat #M9309) and ZR-75-1 cells were maintained in RPMI 1640 (Invitrogen, UK, Cat #11879). Cells were grown using appropriate medium supplemented with 10% heat-inactivated fetal bovine serum (FBS) and 100 U/ml penicillin and 100 µg/ml streptomycin (Sigma, UK, Cat #P0781) in a humidified atmosphere with 5% CO<sub>2</sub> at 37°C.

To start the cell culture, frozen stocks of cells were removed from liquid nitrogen storage and were immediately thawed at 37 °C in a water bath and seeded in T-75 tissue culture flasks (75 cm<sup>2</sup>, Sarstedt, Germany, Cat # 83.182.002). When the cultured cells reached the 70-80 % confluency, they were trypsinised by addition of 3 ml of 1X Trypsin/ EDTA (Sigma, UK, Cat # T4174) in HANKS balanced salt solution (Sigma, UK, Cat # H6648) and kept at 37°C for 5 minutes to obtain the single cells. Then, 7 ml of fresh medium were added, cells were mixed and counted by Haemocytometer to estimate the number of cells per millilitre. An appropriate number of cells were then seeded into the tissue culture flasks for further experiments.

## 2-2. Drug treatments

Several pharmacological compounds were used in this study including EnR stress inducers (tunicamycin, thapsigargin, and brefeldin A), UPR pathway inhibitors (PERK and IRE1 inhibitors) and chemotherapeutic compounds (tamoxifen, fulvestrant, and docetaxel) at the indicated concentrations for the indicated time points (Table 2-1).

**Tunicamycin** is an antiviral antibiotic derived from *Streptomyces lysisuperificus* which inhibits the UDP-N-acetylglucosamine-dolichol phosphate N-acetylglucosamine-1-phosphate transferase (GPT). Consequently, it blocks the initial step of glycoprotein biosynthesis and leads to accumulation of glycoproteins in the EnR lumen [334].

**Thapsigargin** which is derived from the plant named *Thapsia garganica*. *Linnaeus* decreases calcium levels in the EnR by blocking the sarcoendoplasmic reticulum Ca<sub>2+</sub>-ATPases (SERCAs). The EnR chaperone functions are dependent on the calcium level. Thus, a low level of calcium hinders their activity, leading to the accumulation of unfolded proteins in the EnR lumen [335].

**Brefeldin A**, which is also named Cyanein or Decumbin, is produced by some fungi such as Penicillium, Penicillium Brefeldianum and Penicillium cyanium. This compound prevents protein transportation from the EnR to the Golgi apparatus and reverses protein transport from the Golgi apparatus to the EnR which causes protein accumulation in the EnR lumen [336].

**PERK inhibitor (GSK 2606414)**, which is also named EIF2AK1 Inhibitor, is a cell-permeable compound that inhibits EIF2AK3/PERK by targeting PERK in its inactive DFG motif conformation in the ATP-binding region [179].

**IRE1 inhibitor (4 $\mu$ 8c)** is a cell-permeable compound that targets IRE1 Lys907 via Schiff base formation and inhibits IRE1 RNase activity in a time- and dose-dependent manner and prevents EnR stress-induced site-specific mRNA splicing [337].

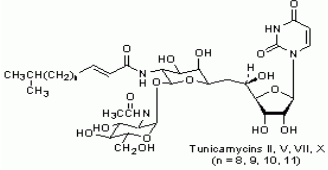
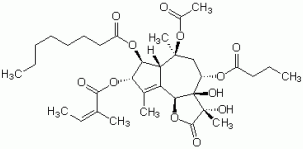
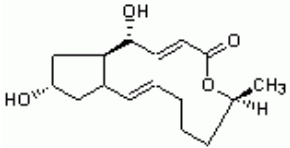
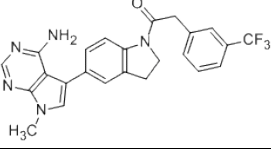
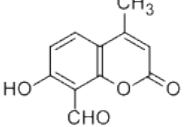
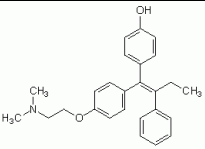
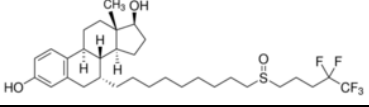
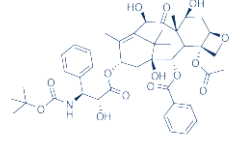
**Tamoxifen (4-Hydroxytamoxifen, 4-OH-TAM)**, which is also known as an estrogen receptor signalling regulator II, is an anti-estrogen drug that is commonly used for breast cancer treatment. Depending on the target tissue, tamoxifen acts as estrogenic and anti-estrogenic compounds. For this reason, tamoxifen is also named as a selective estrogen receptor modulator (SERM) [338].

**Fulvestrant (ICI 182,780)** is a cell-permeable compound that downregulates estrogen receptors and is known as a selective estrogen receptor degrader (SERD). Fulvestrant is a high-affinity ER antagonist. It does not have estrogen agonist activity and is more effective than tamoxifen in reducing estrogen receptors in breast tumour cells [339].

**Docetaxel** is a chemotherapeutic compound which is used for several cancer treatments including breast, prostate, head and neck, stomach and non-small lung cancers. It inhibits depolymerisation of microtubules by binding to stabilized microtubules and causes the failure of chromosomes to segregate to the daughter cells [340].



Table 2-1. Pharmacological compounds for cell treatment.

Compound Name	Chemical Formula	Structure formula Image	Catalogue Number
<b>Tunicamycin</b>	$C_{39}H_{64}N_4O_{16}$		# 3516 Tocris Bioscience
<b>Thapsigargin</b>	$C_{34}H_{50}O_{12}$		# 1138 Tocris Bioscience
<b>Brefeldin A</b>	$C_{16}H_{24}O_4$		# 1231 Tocris Bioscience
<b>PERK inhibitor (GSK- 2606414)</b>	$C_{24}H_{20}F_3N_5O$		# 516535 Millipore
<b>IRE1 inhibitor (4μ8c)</b>	$C_{11}H_8O_4$		#412512 Millipore
<b>Tamoxifen</b>	$C_{26}H_{29}NO_2$		# T5648 Sigma
<b>Fulvestrant</b>	$C_{32}H_{47}F_5O_3S$		# I4409 sigma
<b>Docetaxel</b>	$C_{43}H_{53}NO_{14}$		# 01885 Sigma

Depending on the experiments, cells were treated with Tunicamycin (TM) 1.0  $\mu$ g/ml, Brefeldin A (BFA) 0.5  $\mu$ g/ml, Thapsigargin (TG) 1 $\mu$ M, PERK inhibitor (100nM), IRE1 inhibitor (10  $\mu$ M), Tamoxifen (10 $\mu$ M), Fulvestrant (100 $\mu$ M) and Docetaxel (100 nM) for different time periods.

### **2-3. RNA preparation**

The total RNA from cultured cells was purified using the Trizol reagent (Invitrogen, UK, Cat #15596-018). Briefly, after removing growth media, 1 ml of Trizol reagent was added directly to the cells in a T-75 flask and cells were lysed by pipetting several times. Then lysate was collected into the 1.5 ml microtube (Eppendorf, Germany, Cat #72.706.400) and incubated at room temperature for 5 minutes. After that, 0.2 ml of chloroform was added, mixed and incubated for 5 minutes and then centrifuged at 12000 X g for 15 minutes. After this step, the upper clear phase was carefully pipetted into a 1.5 ml tube and the total RNA was precipitated using 0.5 ml of absolute isopropanol. After incubation at -20°C overnight, samples were centrifuged at 12,000g for 10 minutes and the RNA pellet was washed in 75% Ethanol. All the ethanol was carefully removed and the pellet was air dried. Finally, the RNA was resuspended in 50 µl of nuclease-free water. Following purification, the total RNA was quantified by UV spectrophotometry (NanoDrop, ThermoFisher, UK) and gel agarose electrophoresis to determine its integrity. Samples were then stored at -80°C until required.

### **2-4. Reverse transcription reaction**

For messenger RNA (mRNA), the ImProm-II™ reverse transcription system (Promega Cat #A3800) was used to generate complementary DNA (cDNA). 2 µg (2 µl) of total RNA was mixed with 2 µl of random primer and 1 µl of nuclease-free water and heated at 70°C for 5 minutes. The reverse transcription reaction mix was prepared in a sterile 1.5 µl microcentrifuge tube on ice using 7.5 µl nuclease free water, 4 µl ImProm-II™ 5X reaction buffer, 1 µl MgCl<sub>2</sub>, 1µl dNTP mix, 1 µl ImProm-II™ reverse transcriptase and 0.5 µl ribonuclease inhibitor (total volume 15 µl).

The 15 µl aliquots of reverse transcription reaction mix were added into the 5 µl RNA and primer mix to have a final reaction volume of 20 µl per tube. The samples were kept at 25°C for 5 minutes followed by 42°C for 60 minutes and finally inactivated at 70°C for 15 minutes. The non-template controls (NTC) which consisted of all reagents except the RNA sample were also used to monitor any contamination during the RT reaction process. The cDNA samples were then stored at -20°C until required.

For microRNA reverse transcription, 1µg of the total RNA from each sample was used to generate cDNA using the TaqMan microRNA reverse transcription kit (Cat. No. 4366596, Life Technologies, Paisley, UK) according to the manufacturer's instructions. Briefly, the reverse transcription reaction consisted of 7 µL master mix [4.16 µL nuclease-free water, 1.5 µL 10X RT buffer, 1 µL multitranscribe RT enzyme (50 U/ µL), 0.19 µL RNase inhibitor (20U/ µL) and 0.15 µL dNTP mix (100mM total)], 3 µL miRNA specific primer and 1µg RNA were added to the PCR microtube (total volume 15 µL). Reverse transcription thermocycling conditions were 16°C for 30 min, 42°C for 30 min and 85°C for 5 min. The resultant cDNA was stored at -20°C until required.

## **2-5. Conventional Polymerase Chain Reaction (PCR) assay**

Conventional PCR for human GAPDH was carried out using 1 µl of cDNA to check cDNA quality with 2x Go Taq master mix (Promega) and with the following primers (Sigma):

GAPDH Fwd 5'ACCACAGTCCATGCCATC3'

GAPDH Rev 5'TCCACCCTGATATTGCTG3'

PCR cycle conditions include 94°C for 3 minutes, then 25 cycles in 94°C for the 30s, 55°C for 30 s, 72°C for 30 s, and 72°C for 10 minutes, 4°C for ∞.

Conventional PCR for the human XBP1 transcript to confirm UPR activation was carried out on cDNA using 2x Go Taq master mix and with the following primers (Sigma):

XBP1 Fwd 5'GGGAATGAAGTGAGGCCAG3'

XBP1 Rev 5'TGAAGAGTCAATACCGCCCA3'

PCR cycle conditions include 94°C for 7s, then 30 cycles in 94 °C for 10s, 52 °C for 30 s, 72 °C for 30 s and 72 °C for 1 minute, 4 °C for ∞.

## **2-6. Real-Time Quantitative PCR (RT-qPCR)**

### **2-6-1. Real-time quantitative PCR assay for mRNAs**

RT-qPCR reactions were carried out in the final volumes of 10µl using an ABI 7500 Real-Time PCR System. The diluted cDNA is combined with the TaqMan Universal PCR master mix (Cat. No. 4440047, Life Technologies, Paisley, UK) and 20X Taqman gene expression assays (IDT, Iowa, USA) for each target gene and accurately dispensed into a MicroAmp 96-well plate (Applied Biosystems) in triplicate. Reactions consisted of the following:

IDT primer standard assay 20x	0.5 µl
Taqman 2x PCR master mix	5 µl
Nuclease-free water	1.5 µl
cDNA	3 µl

Standard thermal cycling conditions were applied consisting of 40 cycles at 95°C for 15 seconds and 60°C for 60 seconds. GAPDH was used as a reference gene to determine the relative expression level of target genes between treated and control samples using  $\Delta\Delta\text{Ct}$ /Livak method [341].

### **2-6-2. Real-time quantitative PCR assay for miRNAs**

Complementary DNA (cDNA) was analysed by qPCR using specific microRNA TaqMan probes (Life Technologies, Paisley, UK) and the TaqMan Universal PCR master mix (Cat. No. 4440047, Life Technologies, Paisley, UK) according to the manufacturers' instructions (10  $\mu\text{L}$  PCR master mix, 7.67  $\mu\text{L}$  nuclease-free water, 1.33  $\mu\text{L}$  cDNA and 1  $\mu\text{L}$  20X specific microRNA assay).

QPCR reactions were performed on an ABI 7500 Real-Time PCR System. The thermocycling conditions were 95°C for 10 min and followed by 40 cycles of 95°C for 15 seconds/60°C for 60 seconds. RNU6B was used as a reference gene to determine the relative expression level of miRNAs between treated and control samples using the  $\Delta\Delta\text{Ct}$ /Livak method [341]. All qPCR reactions were performed in triplicate, otherwise it is mentioned.

## **2-7. Plasmids**

### **2-7-1. PERK, ATF6 and XBP1 shRNA plasmids**

PLKO.1 puro, which is the third-generation lentiviral backbone, was used for expression of PERK, ATF and XBP1 shRNA (short hairpin RNA) sequences. The PERK shRNA plasmid was a gift from Dr. Piyush Gupta, MIT, Boston, USA. ATF6 TRC Lentiviral shRNA (Cat. No. RHS4533-EG22926) was purchased from Dharmacon GE Healthcare Life Sciences.

XBP1 Lentiviral shRNA (Cat. No. SHCLND-NM\_005080) was purchased from Sigma Aldrich. Packaging plasmid (psPAX2, Cat. No. #12260) and the envelope protein plasmid (VSVG, pMD2.G, Cat. No. #12259) were purchased from Addgene (Cambridge, MA, USA). The shRNA plasmids details are mentioned below;

- 1- Name: pLKO.1 puro (Empty backbone plasmid)  
Size: 7050 bp Vector type: Mammalian Expression, Lentiviral, RNAi  
Stable selection marker: Puromycin  
Cat Number: #8453  
Company: Addgene
- 2- Name: ATF6 TRC Lentiviral shRNA [Simple hairpin shRNAs in the pLKO.1 lentiviral vector designed by The RNAi Consortium (TRC)]  
Cat Number: RHS4533-EG22926  
Company: Dharmacon GE Healthcare Life Sciences
- 3- Name: PERK Lentiviral shRNA [Simple hairpin shRNAs in the pLKO.1 lentiviral vector  
Source: Gift from Dr. Piyush Gupta, MIT, Boston, USA.
- 4- Name: XBP1 Lentiviral shRNA [Simple hairpin shRNAs in the pLKO.1 lentiviral vector  
Cat Number: SHCLND-NM\_005080  
Company: Sigma Aldrich.

#### **2-7-2. miR-378, miR-616, XBP1s, VAV1 and c-MYC overexpressing plasmids**

miR-378 and miR-616 expressing plasmids were purchased from Genecopoeia (Maryland, USA). PCMV5-FLAG-XBP1s and PCDH-FLAG-c-MYC plasmids were purchased from Addgene (Cambridge, MA, USA) and were received as E. Coli colonies in a LB agar tube containing ampicillin. The PCDH-VAV1 plasmid was a gift from professor Youjia Cao, Nankai University School of Life Sciences, China. The overexpressing plasmids details are mentioned below:

- 1- Name: PCMV5-Flag-XBP1s  
Vector type: Mammalian Expression, Lentiviral  
Selectable markers: Puromycin  
Cat Number: #63680  
Company: Addgene
- 2- Name: PCDH-Flag- c-MYC  
Vector type: Mammalian Expression, Lentiviral  
Selectable markers: Puromycin  
Cat Number: #102626  
Company: Addgene
- 3- Name: PCDH-VAV1  
Source: Gift from professor Youjia Cao, Nankai university school of life sciences, China.
- 4- Name: Precursor miR-616  
Vector type: Homo sapiens miR-616 stem-loop  
Selectable markers: Puromycin  
Cat Number: HmiRQP0721, HmiRQP0722  
Company: Genecopoeia
- 5- Name: Precursor miR-378  
Vector type: Homo sapiens miR-378 stem-loop  
Selectable markers: Puromycin  
Cat Number: HmiR-AN0474, HmiR-AN3114  
Company: Genecopoeia

### **2-7-3. Transformation of plasmids**

Transformation is the process by which foreign DNA is introduced into a competent bacterial cell. DH5 $\alpha$  E. coli cells (Invitrogen, Ireland, Cat # C737303) were used to amplify all plasmids. 1  $\mu$ l (100 ng) of plasmid DNA was added and mixed with the E. coli cells by pipetting up and down and then incubated on ice for 30 min to permeabilise the cells. The vial was put in a 42°C water bath for 30s to heat shock the cells in order to draw the DNA plasmids into the cells. The vial was then placed on ice for 2 minutes and 250  $\mu$ l of LB broth media was added into the vial. E. coli cells were allowed to grow at 37°C for 1 hour and then were spread on a LB agar plate containing the antibiotic Ampicillin (100 mg/mL) or Kanamycin (50 mg/mL) and grown at 37 °C.

To prepare the LB liquid medium, 25 g of LB broth powder (ThermoFisher, Ireland, Cat # 12780029) was added into a 1 litre autoclave bottle and 1000 mL ultrapure water was added and mixed properly. The medium was then autoclaved (121 °C, 20 minutes). To prepare LB agar medium, 15 g of LB agar powder (ThermoFisher, Ireland, Cat # 22700041) was dissolved in 1 litre ultrapure water and was autoclaved (121 °C, 20 minutes). The medium was then poured into Petri dishes (~25 mL per 100 mm plate).

Bacteria from a single colony was inoculated into the LB broth containing antibiotic and was incubated for 18 hours at 37°C while shaking. The bacterial culture was then centrifuged at 5000 g for 20 min to make a pellet. Finally, plasmids were extracted from the bacterial pellet using the Qiagen Midi kit (Qiagen, Germany, Cat #12143). The quantity and quality of extracted plasmids were determined by UV spectrophotometry (NanoDrop, ThermoFisher, UK) and gel agarose electrophoresis.



#### **2-7-4. Transient transfection of spliced XBP1 in MCF7 cells**

Spliced XBP1 was overexpressed in the MCF7 cells by electroporation using the Nucleofector technology (AMAXA, Lonza, Switzerland). Briefly, Parental MCF7 cells were cultured in a T-25 flask and then trypsinised (0.05% trypsin/0.02% EDTA) at 75-80% confluency. MCF7 cells ( $1 \times 10^6$  cells) were centrifuged at  $90 \times g$  for 10 minutes in room temperature and the supernatant was removed. The cell pellet was resuspended by 4D Nucleofector™ Solution (100  $\mu$ l) at room temperature. The cells were then transferred into the Nucleo-cuvette™ and the nucleofection process was started by pressing “Start” on the display of the 4D-Nucleofector™ Core Unit. After completion of the run, the cells were resuspended with pre-warmed DMEM medium and then plated ( $2.5 \times 10^5$  cells) in 6 well plates and cultured for 24 and 48 hours. Protein samples were then prepared for further experiments.

#### **2-7-5. Transient transfection of miR-616, VAV1, and c-MYC in HEK 293T cells**

HEK 293T cells ( $250 \times 10^3$  cells) were plated in 6 well plates and transfected with JetPEI, according to the manufacturer’s instructions. Briefly, HEK 293T cells were either untransfected or transfected with plasmids containing ORFs of VAV1, c-MYC in absence and presence of miR-616 expressing plasmids. 48h post transfection whole cell lysates were analysed for the expression of VAV1 and c-MYC proteins by western blot assay.

## 2-8. Preparation of lentivirus

The jetPEI® (Polyplus-transfection®, France) reagent was used to transfect plasmids into 293T cells. The jetPEI® is a linear polyethylenimine that compacts DNA into positively charged particles to interact with anionic proteoglycans on the cell surface. These particles then enter the cytoplasm via endocytosis procedure. The jetPEI®/DNA complexes play a very important role in the success of transfection. This complex is known as the N/P ratio which is the number of nitrogen residues (N) in the jetPEI® per phosphate (P) of DNA and is calculated by the following formula:

$$\text{N/P ratio} = 7.5^* \times \mu\text{l of jetPEI}^\circledast / 3^\diamond \times \mu\text{g of DNA}$$

\* Concentration of nitrogen residues in jetPEI®                       $\diamond$  nmoles of phosphate per  $\mu\text{g}$  of DNA

For 10.5  $\mu\text{g}$  DNA, 63  $\mu\text{l}$  of JetPEI was added to get N/P ratio of 15.

On day one, the 293T cells ( $10 \times 10^6$  cells) were seeded in a T-175 flask containing DMEM with 10% heat-inactivated fetal bovine serum (FBS), 100 U/ml penicillin and 100  $\mu\text{g}/\text{ml}$  streptomycin.

On day two, the second-generation lentiviral plasmids (10.50  $\mu\text{g}$  DNA) were prepared. Briefly, 1 ml of 150mM NaCl solution was added into a 1.5 mL tube and lentiviral plasmids (10.50  $\mu\text{g}$  DNA) were then added. The lentiviral plasmids included;

- 1- Packaging plasmid (psPAX2) 3.50  $\mu\text{g}$ .
- 2- Envelope protein plasmid (VSVG, pMD2.G) 1.57  $\mu\text{g}$ .
- 3- Plasmid of interest (PERK, ATF6, and XBP1 shRNAs) 5.25  $\mu\text{g}$ .

Next, in a separate 1.5 ml tube, 63  $\mu$ l of the JetPEI solution were added into 1ml of 150mM NaCl. Both solutions were incubated at room temperature for 10 minutes and then the JetPEI solution was mixed with DNA solution and incubated for 20 minutes at room temperature. Then, 2 ml JetPEI/DNA solution mixture were added drop by drop into the 20 ml of DMEM and mixed by gently swirling the T-175 flask containing the HEK 293T cells. On day three, the medium was replaced with 20 ml of DMEM with 10% FBS, 100 U/ml penicillin, 100  $\mu$ g/ml streptomycin and 4 mM caffeine. On day four, syncytia of fused cells appeared and green fluorescent protein (GFP) reporter was detected under a fluorescence microscope. On day five, the culture supernatant containing the lentiviral particles was collected in a 50ml tube and centrifuged at 500 X g for 5 minutes at room temperature. The supernatant was then filtered with a 45 $\mu$ m filter and was aliquoted in two 15ml tubes and was applied for transduction or stored at -80°C until required.

## **2-9. Lentivirus transduction**

Lentivirus vectors were used to create stable overexpressing cell lines (for miR-378, miR-616, VAV1, and c-MYC) and knockdown cell lines for UPR genes (PERK, XBP1 and ATF6). MCF7 cells (1 X 10<sup>6</sup> cells), ZR-75-1 (1 X 10<sup>6</sup> cells), MDA-MB-231 (1 X 10<sup>6</sup> cells) and HCT116 cells (3 X 10<sup>6</sup> cells) were plated in a T-75 flask and after 24 hours, 10 ml of media containing lentivirus vectors were added into each flask. After 24 hours, the media was removed and replaced with fresh complete medium containing 1  $\mu$ g/ml of puromycin to select for transduced cells.

## 2-10. Protein extraction and western blotting

To prepare the protein sample, cells were washed with cold PBS and harvested by a scraper into a 15 ml tube. Cells were then centrifuged at 1500 rpm and 4°C for 5 min. The cell pellet was then lysed in a whole cell lysis buffer (Table 2-2).

Table 2-2. Recipes for cell lysis buffer.

<b>Solution</b>	<b>Volume</b>	<b>Final concentration</b>
HEPES pH 7.5	2 ml	20 mM
NaCl	17.5 ml	350 mM
Mgcl <sub>2</sub>	350 µl	1.0 mM
EDTA	250 µl	0.5 mM
EGTA	25 µl	0.1 mM
IGEPAL-630	5 ml	1%
H <sub>2</sub> O	24.7 ml	-----

Protein concentration was determined by Bradford assay and was adjusted with extra lysis buffer and Laemmli's SDS-PAGE buffer (Table 2-3) to get 1 microgram protein per microliter.

Table 2-3. Recipes for Laemmli's SDS-PAGE.

<b>Components</b>	<b>5X</b>
Tris (1M, pH 6.8)	3.1 ml
SDS	1 g
Glycerol	2 ml
Mercaptoethanol	2.5 ml
PMSF (100nM)	0.5 ml
Bromphenol blue (05 %)	1.0 ml
H <sub>2</sub> O	Up to 10 ml

The protein samples were boiled at 95°C for 5 minutes and then 20-30 µg/lane of protein samples were run on an SDS polyacrylamide gel (Table 2-4) using a running buffer (Table 2-5).

Table 2-4. Recipes for immunoblotting gels.

<b>Components</b>	<b>10 % Resolving Gel</b>	<b>8 % Resolving Gel</b>	<b>Stacking Gel</b>
Deionised H <sub>2</sub> O (ml)	8	9.2	6.8
30% Bis-acrylamide (ml)	6.8	5.2	1.7
1.5M Tris-HCl pH 8.8 (ml)	5.2	5.2	1.3
10 % SDS (ml)	0.2	0.2	0.1
10% ammonium persulfate (APS) (ml)	0.2	0.2	0.1
TEMED (ml)	0.008	0.012	0.01

Table 2-5. Recipes for running buffer.

<b>Components</b>	<b>1 X</b>	<b>10 X</b>
Tris base	3 g	30.35 g
Glycine	14.4 g	144 g
SDS	1 g	10 g
H <sub>2</sub> O	up to 1 litre	

The protein after gel run were transferred onto the nitrocellulose membrane by a semi-dry method using transfer buffer (Table 2-6) and protein transfer was confirmed by Ponceau stain (Sigma, Ireland). The nitrocellulose membranes were then blocked with the specific blocking solution for 2 hours at room temperature. The nitrocellulose membranes were then treated with specific primary antibodies (Table 2-7) at 4°C overnight and then after washing three times with PBS/0.05%Tween solution, the membranes were incubated with appropriate horseradish peroxidase-conjugated secondary antibody at room temperature for 2 hours.

Table 2-6. Recipes for transfer buffer.

<b>Components</b>	<b>10X</b>
Tris base	30.35 g
Glycine	144 g
SDS	2 g
H2O	up to 1 liter

1X transfer buffer

H2O	700 ml
10 X transfer buffer	100 ml
Methanol	200 ml

The membranes were then washed twice with PBS/0.05%Tween and once with PBS and finally the signals were detected using a Western Lightening chemiluminescent substrate (Perkin Elmer, Netherlands, Cat #NEL104001EA).

Table 2-7. Optimum conditions for different antibodies in western blotting.

<b>Antibody</b>	<b>Supplier</b>	<b>Source</b>	<b>Blocking Solution</b>	<b>Primary Incubation</b>	<b>Secondary Incubation</b>
PERK 8 % gel	Cell Signalling Technology #3192	Rabbit	5 % BSA in PBS/0.05 % Tween for 2 hours	1:2000 in 5 % BSA in PBS/0.05 % Tween for overnight at 4°C	Anti-Rabbit Ab (1:10000) in 5 % BSA in PBS/0.05 % Tween for 2 hours
PO4- PERK 8 % gel	Cell Signalling Technology #3179	Rabbit	5 % BSA in PBS/0.05 % Tween for 2 hours	1:1000 in 5 % BSA in PBS/0.05 % Tween for overnight at 4°C	Anti-Rabbit Ab (1:10000) in 5 % BSA in PBS/0.05 % Tween for 2 hours
XBP1 10 % gel	Bio Legend #619501	Rabbit	5 % milk in PBS/0.05 % Tween for 2 hours	1:1000 in 5 % Milk in PBS/0.05 % Tween for overnight at 4°C	Anti-Rabbit Ab (1:10000) in 5 % Milk in PBS/0.05 % Tween for 2 hours
ATF6 10 % gel	Abcam #ab122897	Mouse	5 % milk in PBS/0.05 % Tween for 2 hours	1:1000 in 5 % Milk in PBS/0.05 % Tween for overnight at 4°C	Anti-Mouse Ab (1:5000) in 5 % Milk in PBS/0.05 % Tween for 2 hours
$\beta$ -Actin 10 % gel	Sigma, # A-5060	Rabbit	5 % milk in PBS/0.05 % Tween for 2 hours	1:2000 in 5 % Milk in PBS/0.05 % Tween for overnight at 4°C	Anti-Rabbit Ab (1:10000) in 5 % Milk in PBS/0.05 % Tween for 2 hours

CHOP 10 % gel	Santa Cruz Biotechnology #sc-793	Rabbit	1 % milk in PBS/0.05 % Tween for 2 hours	1:800 in 1 % Milk in PBS/0.05 % Tween for 2 hours at room temperature	Anti-Rabbit Ab (1:5000) in 1 % Milk in PBS/0.05 % Tween for 2 hours
ATF4 10 % gel	Santa Cruz Biotechnology #sc-200	Rabbit	5 % milk in PBS/0.05 % Tween for 2 hours	1:1000 in 5 % Milk in PBS/0.05 % Tween for overnight at 4°C	Anti-Rabbit Ab (1:5000) in 5 % Milk in PBS/0.05 % Tween for 2 hours
VAV1 10 % gel	Santa Cruz Biotechnology #sc-8039	Mouse	5 % milk in TBS/0.1% Tween for 2 hours	1:1000 in 5 % milk in TBS/0.1%	Anti-Mouse Ab (1:5000) in 5 % Milk in TBS/0.1% Tween for 2 hours
c-MYC 10 % gel	Santa Cruz Biotechnology # sc-40	Mouse	2.5 % milk/2.5% BSA in TBS/0.1%	1:1000 in 2.5 % milk/2.5% BSA in TBS/0.1%	Anti-Mouse Ab (1:5000) in 5 % Milk in TBS/0.1% Tween for 2 hours

## 2-11. Colony formation assay

Colony formation assay is a technique that measures the ability of a single cell to grow into a colony [342]. For this experiment, cancer cells (1000 cells per well) were plated in 6 well plates and were grown for 14 days. Then, the cells were washed twice with PBS and fixed with 10% formaldehyde for 5 minutes and stained with 0.5 % crystal violet for 10 minutes. The number of colonies which have more than 50 cells was counted in 5 random view fields under a microscope and an average number of colonies were obtained. The Image J software was also applied to quantify the number and size of colonies.



## 2-12. Scratch wound healing assay

Scratch wound healing assay is a technique to measure cell migration *in vitro* by creating a scratch in a cell monolayer and imaging the scratch area at different time periods to measure the migration rate of the cells [343]. For conducting this experiment, cancer cells ( $3 \times 10^5$  cells/well) were plated in 6 well plates. After 24 hours of growth, when they reached 70-80% confluency, the cell monolayer was scratched with a sterile 0.2 ml pipette tip across the centre of the well. Each well was then washed twice with medium to remove the detached cells and then replaced with fresh medium. The scratched areas were then imaged at different time periods including 0 (after creating the scratch), 12, 24, 48 and 60 hours and were quantified by Image J software.

## 2-13. MTS cell proliferation assay

The MTS cell proliferation assay is a colourimetric, sensitive, technique that quantifies viable cells in proliferation and cytotoxicity assay [344]. In this method, viable cells use the MTS tetrazolium compound [3-(4,5-dimethylthiazol-2-yl)-5-(3-carboxymethoxyphenyl)-2-(4-sulfophenyl)-2H-tetrazolium, inner salt; MTS] and generate a coloured formazan product by NAD(P)H-dependent dehydrogenase enzymes. The formazan is a soluble in cell culture media and its absorbance can be detected with a multi-well spectrophotometer at OD=490-500 nm. cancer and control cells ( $2 \times 10^3$  cells/well) were plated in 96 well plates. After 24 hours of growth, for cytotoxicity assay, cells were treated with Tamoxifen (10 $\mu$ M) or Fulvestrant (100 $\mu$ M) for 0, 24, 48 and 72 hours. The 0.2 ml of the MTS solution from CellTiter 96® AQueous One Solution Cell Proliferation Assay kit (Promega, Cat #G3582) was directly added into each well and incubated at 37°C for 4 hours. The absorbance of each well was measured at OD=490 nm with a 96-well plate reader (Synergy™ HT, BIO-TEK, Vermont, USA).

## **2-14. Cell death analysis by Flow cytometry**

Control, miR-378 and miR-616 overexpressing MCF7 cells ( $2 \times 10^5$  cells/well) were plated in 6 well plates. After 24 hours of growth, cells were treated with Thapsigargin ( $1 \mu\text{M}$ ), Brefeldin A ( $0.05 \mu\text{g/ml}$ ) or Docetaxel ( $100 \text{ nM}$ ) for 48 hours for the cell death assay. Cells were then harvested and washed with ice-cold FACS Buffer (PBS, 0.5-1% BSA or 5-10% FBS and 0.1% sodium azide). Cell concentration was adjusted to  $1 \times 10^6$  cells/ml and  $1 \mu\text{L}$  of SYTOX Red dye (Invitrogen, UK, Cat#S34859) was added to each flow cytometry tube. SYTOX Red dye has a high affinity to stain nucleic acid and easily penetrates in dead cells. Cells were incubated for 15 minutes at  $4^\circ\text{C}$  and protected from the light. Then, the cells were analysed by a flow cytometry machine (BD Accuri™ C6 Plus, Biosciences, UK) using 635 nm for excitation and 660 nm for emission.

## **2-15. mRNA expression profiling by next-generation sequencing technology**

To find the miR-378 and miR-616 dependent genes, as a first step, NGS [345, 346] was performed to determine the mRNA expression profiles in miR-378 and miR-616 overexpressing MCF7 cells by BGI Tech solutions, Hong Kong. The total RNA (four replicates) was extracted from MCF7 cells including the control (A1, A2, A3, A4) and overexpressed miR-378 (B1, B2, B3, B4) and miR-616 (C1, C2, C3, C4) and sent to the BGI Company for further analysis. The quality of the RNA samples was assessed by UV spectrophotometry (NanoDrop, ThermoFisher, UK) and analysed by capillary electrophoresis (RNA 6000 NanoChip Kit Series II, Agilent Technologies, USA) to determine its integrity ( $\text{RIN} > 8$ ) (Table 2-8).

On average, 43,802,853 raw sequencing reads and then 43,749,166 clean reads after filtering low-quality signals, were generated for each sample. Clean reads were then mapped to the reference genome using HISAT [347] and Bowtie2 [348] tools. The average mapping ratio with the reference gene was 82.81% and the average genome mapping ratio was 95.95%. FPKM method was used to calculate the expression level, using the following formula:  $FPKM = 10^6 C / (NL/10^3)$ .

For the expression of a given gene A, C is the number of fragments that are aligned to gene A, N is the total number of fragments that are aligned to all genes, and L is the number of bases present in the gene A. We used NOISeq method to screen for differentially expressed genes between control and miRNA (miR-616 and miR-378) expressing groups. NOISeq uses sample's gene expression in each group to calculate log2fold change (M) and absolute different value (D) of control and miRNA (miR-616 and miR-378) expression group to build a noise distribution model. For any given gene A, NOISeq computes its average expression "Control\_avg" in control group and average expression "Treat\_avg" in the treatment group.

Next, the fold change and absolute different value were analysed using the following formula:

Fold change for gene A,  $MA = \log_2 [(Treat\_avg)/(Control\_avg)]$

Absolute different value for gene A,  $DA = |Control\_avg - Treat\_avg|$

If MA and DA diverge from the noise distribution model markedly, gene A will be defined as a differentially expressed gene (DEG). There is a probability value to assess how MA and DA both diverge from the noise distribution model. Finally, DEG was identified according to the following default criteria: Fold change  $\geq 2$  and diverge probability  $\geq 0.8$ .

Finally, the most deregulated genes with a log ratio of more than +2 (upregulated genes) and less than -2 (downregulated genes) were chosen for bioinformatic analysis.

## **2-16. Analysis of oncomine cancer gene microarray database**

To analyse the PPARGC1B expression profile in breast cancer tissues (GSE2109) the oncomine platform (Compendia Biosciences; Ann Arbor, MI, USA-<http://www.oncomine.org>) was used. The oncomine platform is a bioinformatics tool that collects and analyses microarray databases [349]. This platform has already found dysregulated genes and pathways by analysing more than 18000 cancer gene expression microarrays.

## **2-17. Preparation of conditioned media**

The conditioned media derived from the control and miR-378 expressing MCF7 cell were prepared as follows: The control and miR-378 expressing cells ( $1 \times 10^6$  cells) were cultured in a T25 flask with 5 ml of DMEM for 12 h. The medium was harvested and filter-sterilized using a 0.22- $\mu$ m Millex-HV syringe filter (Millipore, Ireland). Then, parental MCF7 cells ( $2 \times 10^3$  cells/well) were plated in 96 well plates and after 24 hours, the medium was replaced with the conditioned media derived from the control and miR-378 expressing MCF7 cell and MTS cell proliferation assay was performed at indicated time points.

## **2-18. Survival analysis for miR-378**

The prognostic value of the miR-378 in breast cancer was analysed using Kaplan-Meier Plotter (<http://kmplot.com/analysis/>), a database that integrates gene expression data and clinical data. We focused our analysis on ER-positive patients (IHC and Gene chip) and determined overall survival using the METABRIC dataset. The patient samples have been split into two groups. The two patient groups (higher and lower expression levels) were compared using a Kaplan-Meier survival plot. The hazard ratio with 95% confidence intervals and log-rank p-value was calculated.

## **2-19. Survival analysis for miR-378 signature**

We performed survival analysis using an aggregated compendium of gene expression profiles of 1809 breast cancer samples Kaplan-Meier Plotter (<http://kmplot.com/analysis/>) and GSE42568 and GSE2607 breast cancer datasets using PROGgene V2 prognostic database. We separated patients into two subgroups: one with higher and the other with a lower expression of the miR-378 signature. Patients were considered to have a higher miR-378 signature if they had average expression values of all the genes in the miR-378 signature above the median. Kaplan–Meier survival analysis was performed and the log-rank test was used to assess the statistical significance of survival difference between these two groups.

## **2-20. Statistical analysis of data**

The data were analysed using the software package SPSS 21.0 for windows and the two-tailed unpaired student's T-test was performed to determine any statistically significant differences between independent groups. All values are presented as the mean  $\pm$  standard deviation (SD). Results with a p-value less than 0.05 ( $p \leq 0.05$ ) were considered statistically significant. All experiments were performed in triplicates otherwise, it is mentioned.

## **Chapter 3**

**miRNA-378 is downregulated by XBP1 and  
inhibits growth and migration of luminal  
breast cancer cells**

## 3-0. Results chapter 1

### 3-1. Background

Signals that increase protein production and secretion can activate the UPR in the absence of detectable ER stress [350]. Estrogens, which stimulate cell proliferation through ER $\alpha$  in normal and breast tumour cells, stimulate UPR, and is known as an anticipatory mode of UPR activation [154]. In this mode, all three arms of UPR are activated without accumulation of unfolded or misfolded proteins in the ER lumen. In ER $\alpha$  + breast cancer cells, estrogen leads to an increase in the expression level of GRP78 and consequently it increases the protein production to promote cell proliferation [154]. It has been found that 17 $\beta$ -estradiol (E2) activates the phospholipase C  $\gamma$  (PLC $\gamma$ ) and leads to the opening of the IP3R calcium channels in the ER lumen. This causes calcium to translocate from the ER lumen to the cytosol and initiates UPR signalling pathway [154].

XBP1s is a key component of the UPR. Several studies suggest a crucial role of XBP1s in the development of highly secretory cells, such as exocrine pancreas, paneth cells, and antibody-producing plasma cells [351]. XBP1s also plays an important role in the homeostasis and function of non-secretory cells. For example, XBP1s is required for synthesis of fatty acid and sterol in the liver, development and survival of dendritic cells and optimal production of pro-inflammatory cytokines in macrophages [352, 353]. Several gene expression profiling studies have revealed that XBP1s induces the expression of a core group of genes involved in maintenance ER function in all cell types [351]. In addition, XBP1s can elicit a wide range of qualitatively and quantitatively distinct outputs that are determined by the physiological context [135, 352, 354].

The expression of XBP1 is upregulated upon E2-stimulation, which in turn, potentiates ER $\alpha$ -dependent transcriptional activity [151]. Ectopic expression of XBP1s in ER-positive breast cancer cells can lead to estrogen-independent growth and reduced sensitivity to anti-estrogens [145]. Downregulation of XBP1 reduces the survival of transformed human cells under hypoxic conditions and impairs their ability to grow as tumour xenografts in SCID mice [136]. Expression of XBP1s is significantly associated with clinical outcome of endocrine-treated breast cancer [146]. Targeting XBP1 expression by STF-083010 (small molecule inhibitor of IRE1) has been shown to restore endocrine sensitivity to tamoxifen-resistant MCF7 cells in a xenograft model [152]. XBP1s contributes to the development of endocrine-resistant breast cancer by upregulating the expression of BCL2, p65/RelA and NCOA3 [145, 153, 155]. It is likely that other, as yet unidentified, XBP1 regulated genes contribute to the ligand-independent growth and endocrine-resistant disease in ER-positive breast cancer.

The miR-378 gene is 65 base pair (bp) length and it is embedded within intron 1 of the Peroxisome proliferator-activated receptor  $\gamma$  coactivator-1 $\beta$  (PPARGC1B) gene at chromosome 5(5q32) (Figure 3-1).

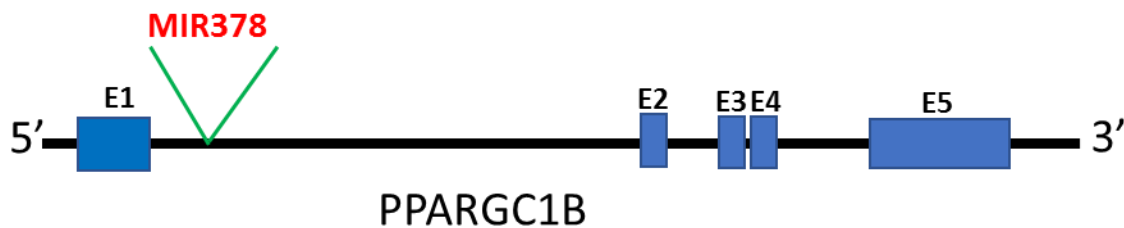


**Figure 3-1. Cytogenetic location of miR-378 in its host gene (PPARGC1B) sequence.** MiR-378 is located in intron number 1 of PPARGC1B gene in chromosome 5.



MiR-378 has been reported to play a key role in many types of cancers. Several studies have indicated that miR-378 is upregulated and acts as an oncomiR in: cervical cancer by targeting ST7L and ATG12 [282, 283]; lung cancer by inhibiting the expression of RBX1, HMOX1, TP53 and FOXG1 [284-286]; glioblastoma by inhibiting vimentin, Sufu, Fus and VEGFR2 [287-289]; nasopharyngeal carcinoma by targeting TOB2 [290]. However, miR-378 has been shown to play a tumour suppressor role in: colon cancer by inhibiting SDAD1, Vimentin, BRAF and CDC40 [269-272]; gastric cancer by inhibiting MAPK1, CDK6 and VEGF; prostate cancer by inhibiting MAPK1, KLK2 and KLK4 [273, 274]; pituitary adenoma by inhibiting RNF31 [275]; medulloblastoma by inhibiting UHRF1 [276] and myelodysplastic syndrome by inhibiting BCL-W and CDC40 [277]. These observations underscore the context-dependent behaviour of miR-378 in human cancers. Despite the wealth of knowledge about the function of miR-378 in human cancers, not much is known about the regulation of its expression.

Here we show that expression of miR-378 (and its host gene PPARGC1B) is downregulated during conditions of UPR in an XBP1-dependent manner. In addition, our results uncover a novel role for miR-378 in the UPR signalling, where miR-378 sensitizes the cells to UPR-induced cell death. Our results suggest that XBP1 modulates the proliferation of ER-positive breast cancer cells and resistance to anti-estrogens, in part by downregulation of miR-378. Our findings reveal a key function for the XBP1-miR-378 axis in luminal/ER-positive breast cancer and indicate that targeting this pathway may offer alternative treatment strategies for anti-estrogen resistant breast cancer.

### **3-2. Hypothesis**

Recently, miR-378 has been found to be downregulated in tamoxifen-resistant (TamR) and long-term estrogen-deprived (LTED) MCF-7 cells and its downregulation contributed to tamoxifen resistance [355]. The miR-378 was one of miRNA identified to be downregulated by UPR in the miRNA expression profiling experiment previously performed in our laboratory. We hypothesise that dysregulation of miR-378 expression by UPR may contribute to breast cancer progression and endocrine resistance.

### **3-3. Aims**

The aims of the experiments described in this chapter were: (i) to validate the microarray results showing downregulation of miR-378 during UPR, (ii) to determine the mechanisms of miR-378 downregulation during UPR, (iii) to evaluate the effect of miR-378 on cell growth, proliferation, migration and cell fate during UPR and finally and (iv) to identify the targets of miR-378.

## **3-4. Results**

### **3-4-1. MiR-378 is downregulated during conditions of EnR stress and UPR activation**

To determine the miRNA expression profile during conditions of EnR stress, HCT116 colorectal cancer cells were either untreated or treated with tunicamycin and Brefeldin A to induce EnR stress and UPR activation. Microarray analysis was carried out to generate the miRNA expression profile during conditions of EnR stress in HCT116 colorectal cancer cells. Microarray analysis showed that out of 875 miRNAs spotted per chip, an average of 238 miRNAs was detected. Furthermore, we found that expression of 79 miRNAs changed significantly during conditions of EnR stress. The expression of miR-663, miR-1908, miR-1915, miR-1469, miR-149\*, miR-638, miR-625\* and miR-483-5p were increased both by tunicamycin and Brefeldin A. The expression of miR-126, miR-200b\*, miR-342-3p, miR-221\*, miR-198, miR-1910, miR-629, miR-378 and miR-224 were reduced upon treatment with tunicamycin and Brefeldin A (Figure 3-4-1-1). This analysis was performed by Dr. Sanjeev Gupta and colleagues, in Prof. Afshin Samali's group at ARC, NUI Galway, and the results were available prior to my PhD work. These results are illustrated below to present the complete picture.

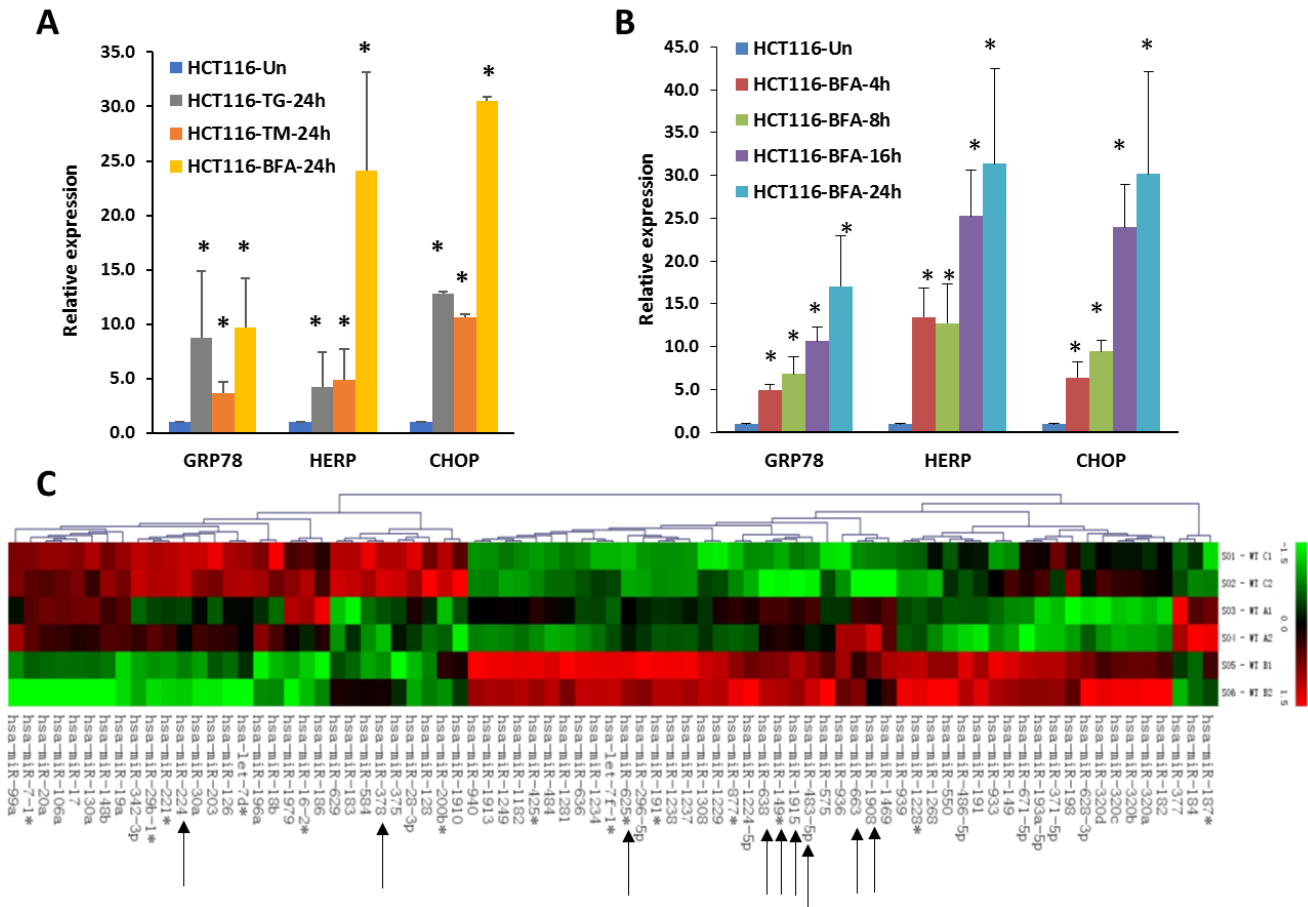


**Figure 3-4-1-1. MiRNA expression profiles in HCT116 cells during conditions of EnR stress.** HCT116 cells were either untreated or treated with (1 $\mu$ M) TG, (1.0  $\mu$ g/ml) TM and (0.5 $\mu$ g/ml) BFA for indicated time points. The expression level of (A, B) three UPR-target genes (GRP78, HERP, and CHOP) were determined. (C) Microarray heat map summarising the expression of miRNAs. Each column represents one of the samples and each row represents a differentially expressed miRNA at  $P < 0.05$ . Samples were grouped by treatments and miRNAs were arranged by unsupervised hierarchical clustering. Red and green indicate up and downregulation, respectively, relative to the overall mean for each miRNA. C1 and C2, untreated HCT116 cells; A1 and A2, tunicamycin treated HCT116 cells; B1 and B2, Brefeldin A treated HCT116 cells. The nine indicated miRNAs were selected to validate the microarray results qRT-PCR. Error bars represent mean  $\pm$  S.D. from three independent experiments performed in triplicate. \* $P < 0.05$ , two-tailed unpaired t-test as compared to the untreated control.

The nine most dysregulated miRNAs (fold change in expression) and affected by both tunicamycin and Brefeldin A treatments (miR-663a, miR-1908, miR-625\*, miR-1915, miR-149\*, miR-638, miR-483, miR-378 and miR-224) were chosen for validation by RT-qPCR assay. From the nine selected miRNAs, RT-qPCR assay showed that miR-1908 and miR-378 were downregulated during conditions of EnR stress (Figure 3-4-1-2).

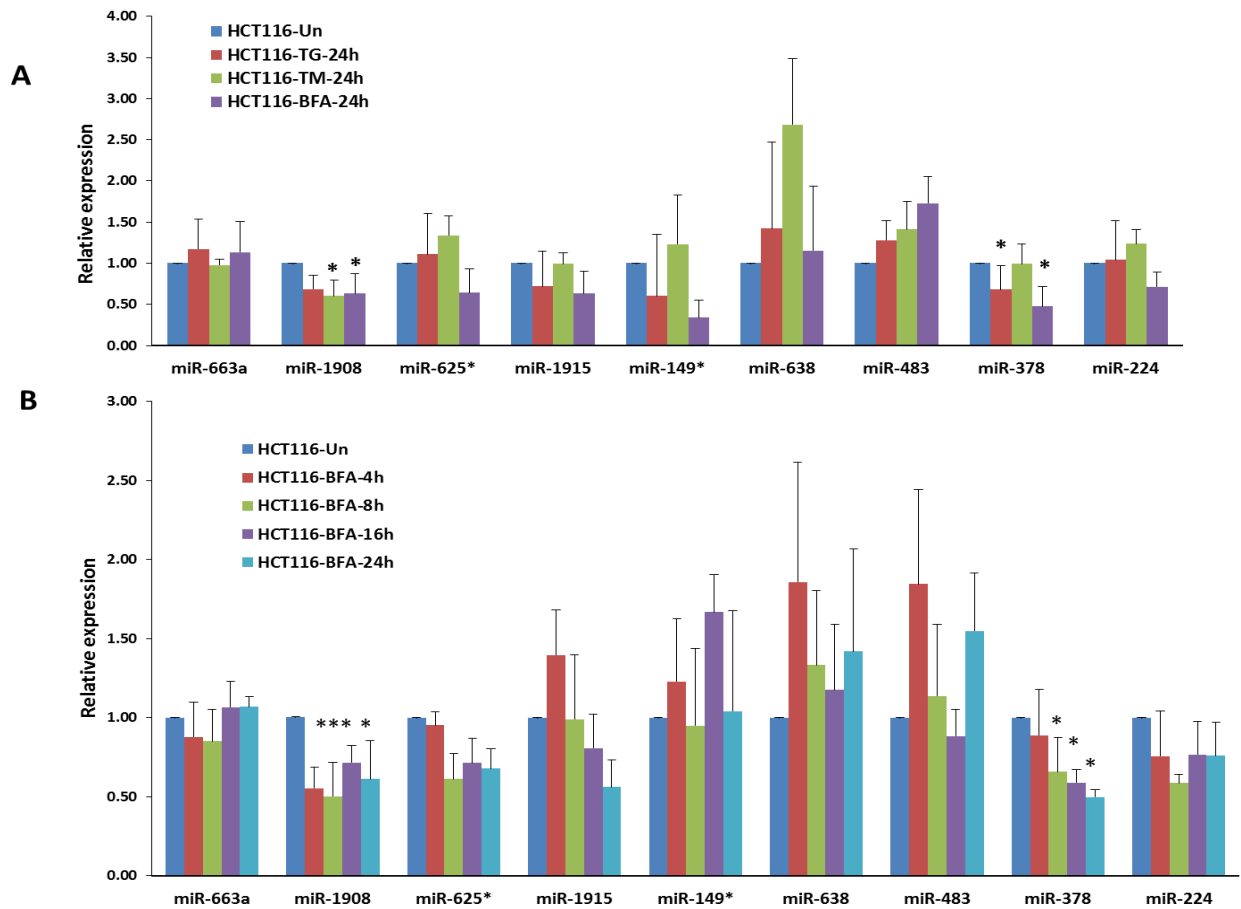


**Figure 3-4-1-2. MiR-378 and miR-1908 are downregulated in HCT116 cells during conditions of EnR stress.** The expression level of nine miRNAs was determined in HCT116 cells treated with (A) 1µM of TG, 1.0 µg/ml of TM and 0.5µg/ml of BFA for 24h and with (B) 0.5µg/ml of BFA for 0, 4, 8, 16 and 24h. Error bars represent mean ±S.D. from three independent experiments performed in triplicate. \*P < 0.05, two-tailed unpaired t-test as compared to the untreated control.

Since the results for miR-378 were concordant between microarray and qRT-PCR analysis, miR-378 was chosen for further analysis. The expression level of miR-378 was also determined in RKO colorectal cancer cells during conditions of EnR stress. RKO cells were either untreated or treated with 1 $\mu$ M of TG, 1.0  $\mu$ g/ml of TM, and 0.5  $\mu$ g/ml of BFA for 24 hours to induce EnR stress and UPR activation. MiR-378 was also found to be downregulated in RKO cells (Figure 3-4-1-3).

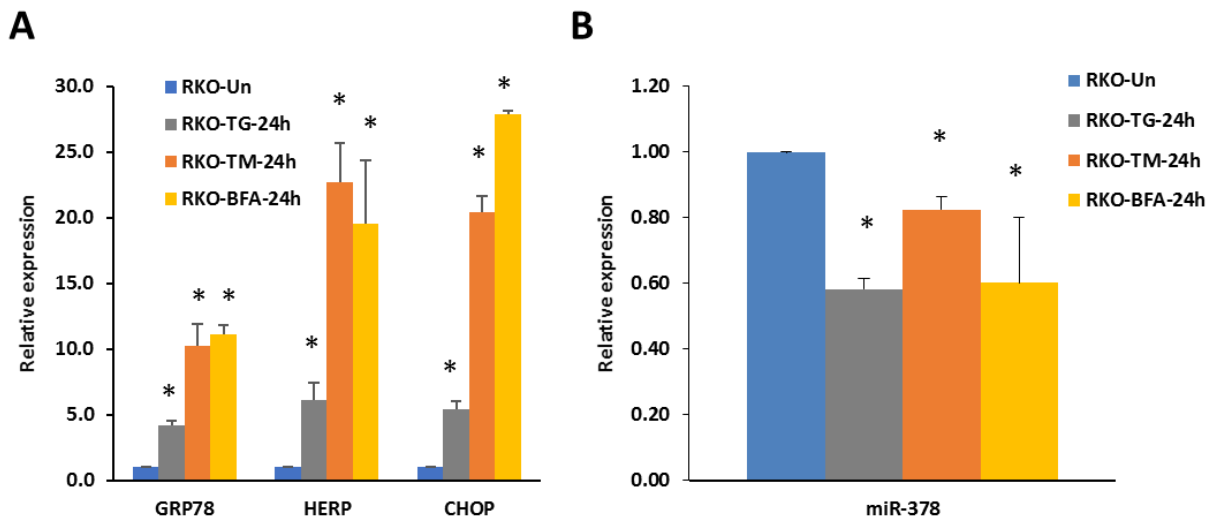


**Figure 3-4-1-3. MiR-378 is downregulated in RKO cells during conditions of EnR stress.** The expression level of (A) three UPR target genes (GRP78, HERP, and CHOP) and (B) miR-378 determined in RKO cells treated with 1 $\mu$ M of TG, 1.0  $\mu$ g/ml of TM, and 0.5  $\mu$ g/ml of BFA for 24h. Error bars represent mean  $\pm$ S.D. from three independent experiments performed in triplicate. \*P < 0.05, two-tailed unpaired t-test as compared to the untreated control.

### 3-4-2. MiR-378 is downregulated in MCF7 human breast cancer cells during conditions of EnR stress and UPR activation

To check if the downregulation of miR-378 during UPR is a cell type-specific or if it is a general effect, we also analysed the miR-378 expression in MCF7 breast cancer cells. MCF7 cells were treated with 1 $\mu$ M of TG, 1.0  $\mu$ g/ml of TM and 0.5  $\mu$ g/ml of BFA for 24 hours to induce EnR stress and UPR activation. Our results showed that the expression level of miR-378 is reduced in MCF7 cells in response to UPR activation (Figure 3-4-2).

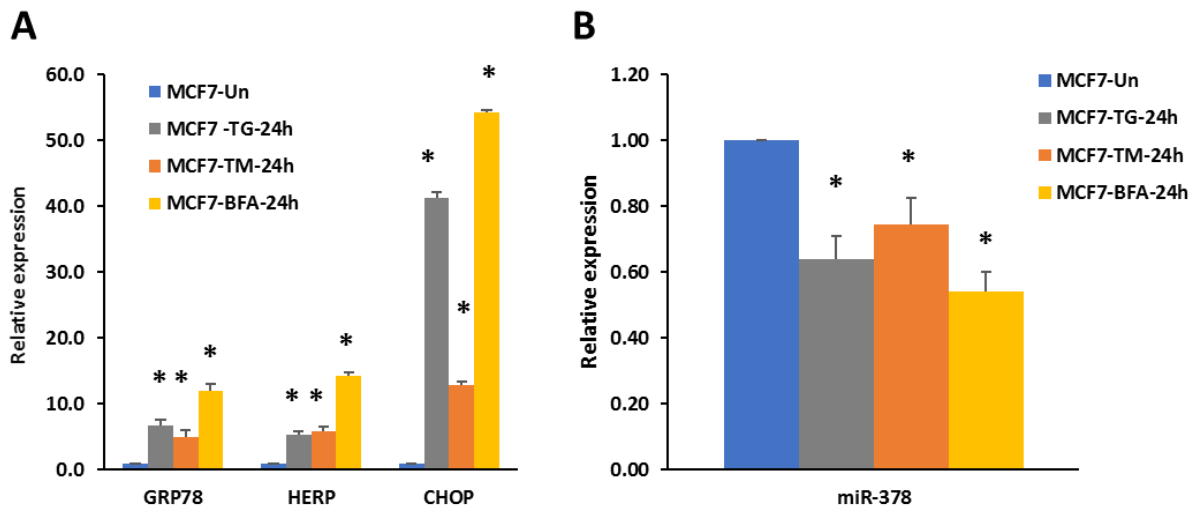


**Figure 3-4-2. MiR-378 is downregulated in MCF7 breast cancer cells during conditions of EnR stress.** The expression level of (A) three UPR-target genes (GRP78, HERP, and CHOP) and (B) miR-378 were determined in MCF7 cells treated with 1 $\mu$ M of TG, 1.0  $\mu$ g/ml of TM, and 0.5  $\mu$ g/ml of BFA for 24h. Error bars represent mean  $\pm$ S.D. from three independent experiments performed in triplicate. \*P < 0.05, two-tailed unpaired t-test as compared to untreated control.

### 3-4-3. MiR-378 host gene (PPARGC1B) is downregulated in colorectal and breast cancer cells during conditions of EnR stress and UPR activation

PPARGC1B stimulates the activity of several transcription factors and nuclear receptors such as nuclear respiratory factor 1, glucocorticoid receptor and ER $\alpha$  [356, 357]. It has been found that PPARGC1B plays an important role in energy homeostasis and metabolism [358] and it is downregulated in prediabetic and type 2 diabetes mellitus patients [356]. PPARGC1B gene has 127,609 base pair (bp) length and it is located at chromosome 5. The expression level of PPARGC1B transcript was determined in HCT116, RKO and MCF7 cells during conditions of EnR stress and UPR activation. We found that PPARGC1B was downregulated in all three cancer cell types (Figure 3-4-3) during UPR. Our results showed that the downregulation of PPARGC1B is not a cell type or stimulus specific.

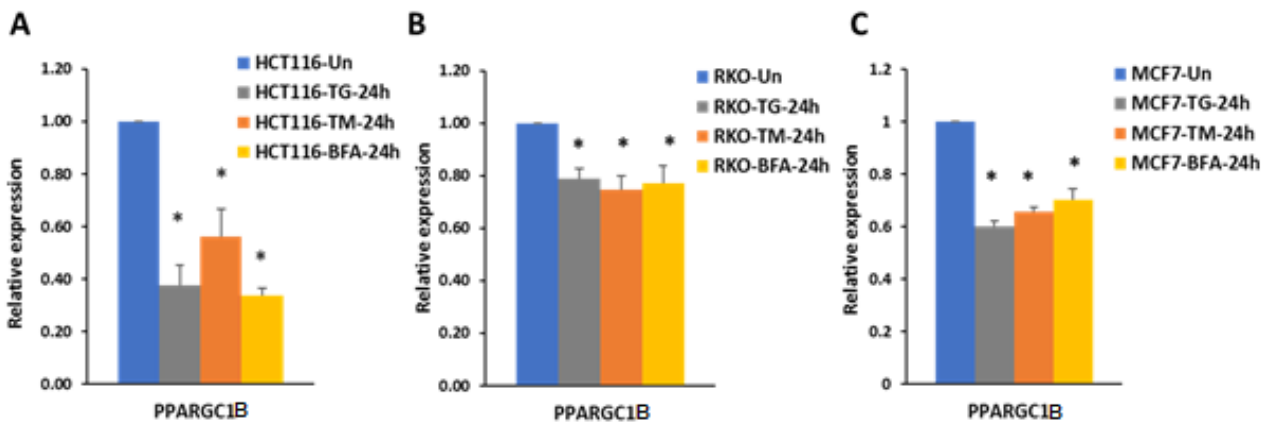


**Figure 3-4-3. PPARGC1B is downregulated in cancer cells during conditions of EnR stress.** The expression level of PPARGC1B was determined in A) HCT116, B) RKO and C) MCF7 cells treated with 1 $\mu$ M of TG, 1.0  $\mu$ g/ml of TM and 0.5  $\mu$ g/ml of BFA for 24h. Error bars represent mean  $\pm$ S.D. from three independent experiments performed in triplicate. \*P < 0.05, two-tailed unpaired t-test as compared to the untreated control.



### 3-4-4. The expression level of miR-378 and PPARGC1B are downregulated in breast cancer

We investigated the expression of the PPARGC1B gene in ductal breast carcinoma using the Oncomine database [359]. We found that upon separating the tumours by stage (Bittner dataset GSE2109) the expression of PPARGC1B showed a significant downregulation with increasing tumour stage (Figure 3-4-4A). The endogenous level of miR-378 was determined in several breast cancer cell lines including MCF7 and T47D (luminal A), BT474 (luminal B), MDA-MB-231 (triple negative) and SKBR3 (HER2 positive) cells. We found that an endogenous level of miR-378 was decreased in all these breast cancer cell lines (Figure 3-4-4B).

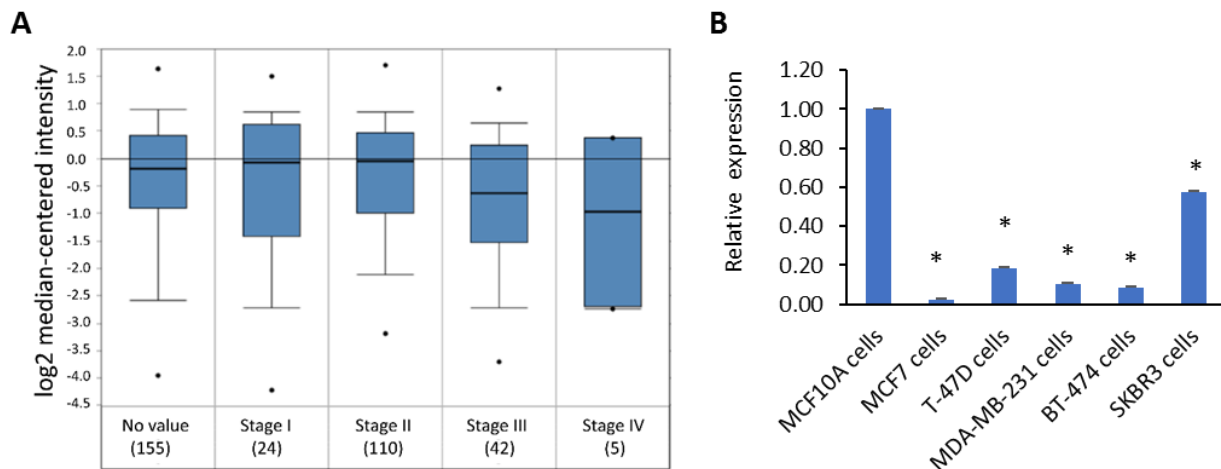
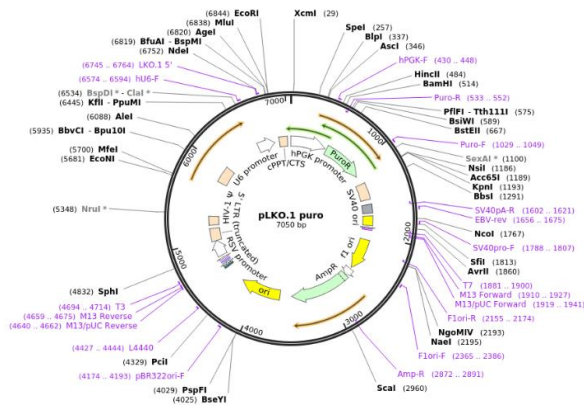


**Figure 3-4-4. Expression of miR-378 and PPARGC1B are downregulated in breast cancer.** (A) Box plots showing the expression of PPARGC1B gene in the indicated categories of ductal breast carcinoma are derived from the Oncomine database. (B) The expression level of miR-378 was determined in various breast cancer cells compared to the non-tumorigenic epithelial mammary gland cells (MCF10A). Error bars represent mean  $\pm$ S.D. from two independent experiments performed in triplicate. \*P < 0.05, two-tailed unpaired t-test as compared to the untreated control.

### **3-4-5. Generation of stable pools of human colorectal and breast cancer cells with knockdown of UPR sensors**

To study the effect of UPR sensors on the expression of miR-378 during conditions of EnR stress, stable pools of PERK, ATF6 and XBP1 knockdown genes were generated in HCT116 and MCF7 cells. For this purpose, lentivirus vectors (Figure 3-4-5-1) containing a short hairpin sequence of PERK, ATF6 and XBP1 genes were made in HEK 293T cells (Human embryonic kidney cells 293) and then generated lentivirus were transduced in HCT116 and MCF7 cells. Briefly, MCF7 ( $1 \times 10^6$  cells) and HCT116 cells ( $3 \times 10^6$  cells) were plated in T-75 flasks and after 24 hours, 10 ml of media containing lentivirus vectors were added into each flask. After 24 hours, the media was removed and replaced with fresh complete medium containing  $1 \mu\text{g/ml}$  of puromycin to enrich the cells containing knockdown genes (PERK, XBP1, and ATF6). Knockdown efficacy of lentivirus vector in HCT116 cells was confirmed by assessing the expression level of PERK, ATF6 and XBP1 at both protein and mRNA using western blot and RT-qPCR assays. HCT116 knockdown clones were either treated or untreated with  $0.5 \mu\text{g/ml}$  of BFA for 24h. Total RNA and protein samples were extracted and analysed by RT-qPCR and western blot. As expected, the expression level of PERK, ATF6 and XBP1 at both protein and mRNA levels were reduced in HCT116 knockdown clones (Figure3-4-5-2). The expression level of PERK, ATF6 and XBP1 were also confirmed in MCF7 knockdown clones. We found that the expression level of PERK, ATF6 and XBP1 at both protein and mRNA levels were reduced in MCF7 knockdown clones (Figure3-4-5-3). The ATF6, PERK and XBP1 knockdown sub-clones of MCF7 cells were generated by Mosaraf Hossain in the laboratory. These results are illustrated below to present the complete picture.

A



B

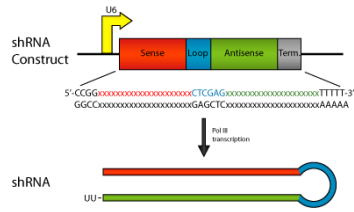


**Figure 3-4-5-1.** Schematic images of (A) lentiviral vector map and (B) shRNA construct for cloning of PERK, ATF6, and XBPI by short hairpin RNA.

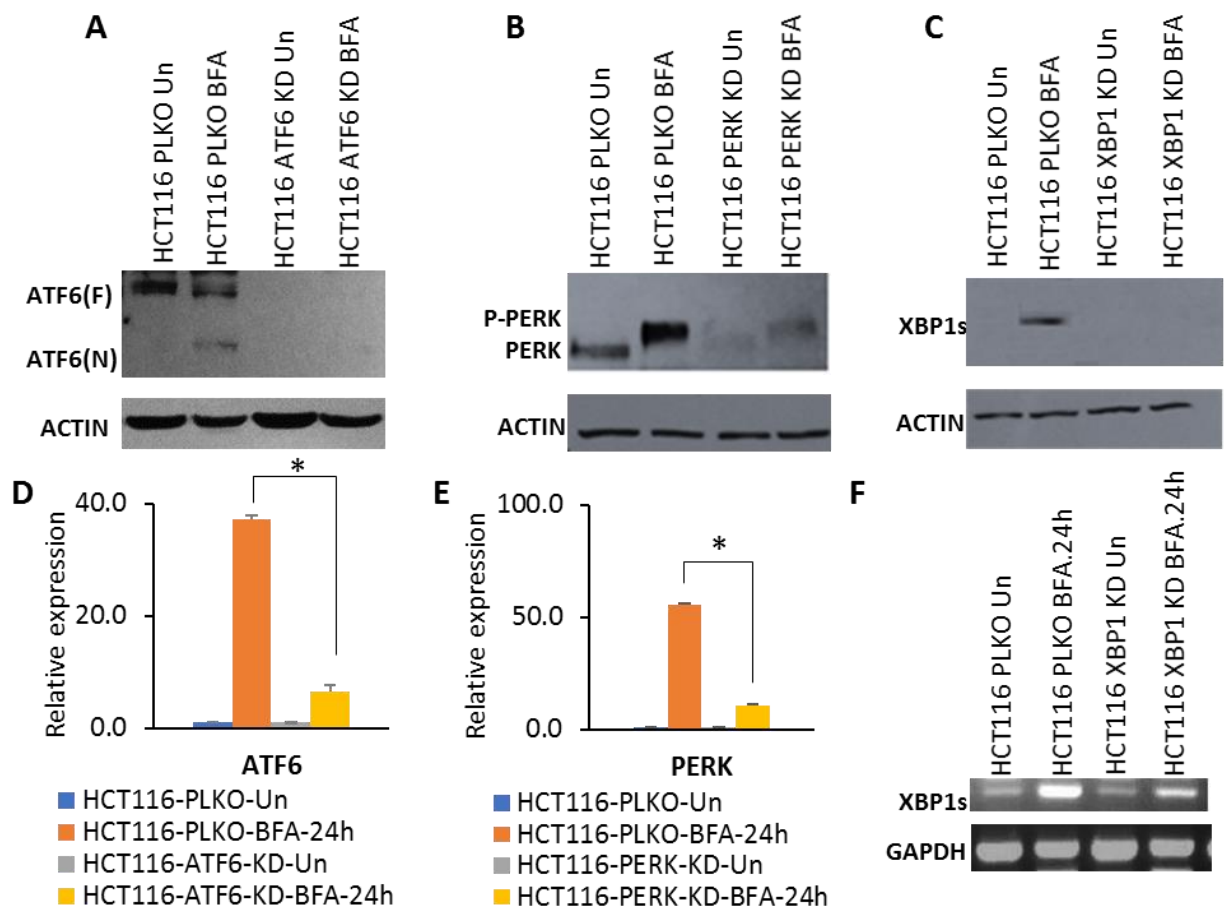


**Figure 3-4-5-2. PERK, ATF6, and XBP1 expression were reduced in HCT116 knockdown pools.** HCT116 knockdown pools were either untreated or treated with (0.5µg/ml) BFA for 24 hours. The expression levels of (A) ATF6, (B) PERK and (C) XBP1s proteins were quantified by western blot assay using antibodies against ATF6 (size: 90 K da), PERK (size:110 K.da), XBP1s (size:55 K.da) and β-actin (size: 42 K.da). The change in expression level of (D) ATF6, (E) PERK and (F) XBP1 transcripts was quantified by RT-qPCR and conventional PCR assays. Error bars represent mean ±S.D. from three independent experiments performed in triplicate. \*P < 0.05, two-tailed unpaired t-test as compared to the untreated control. K.da; Kilodaltons.

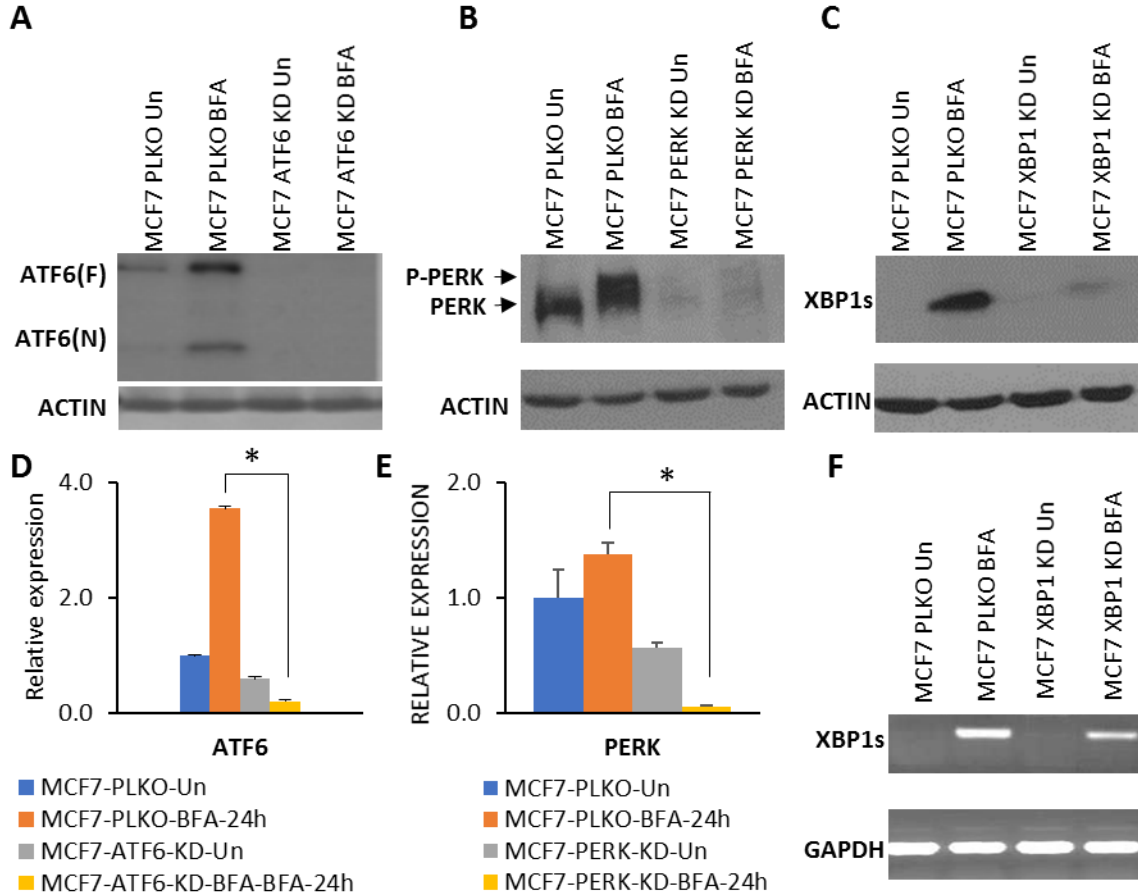


**Figure 3-4-5-3. PERK, ATF6, and XBP1 expression were reduced in MCF7 knockdown pools.** MCF7 knockdown pools were either untreated or treated with (0.5µg/ml) BFA for 24 hours. The expression levels of (A) XBP1s, (B) PERK and (C) ATF6 proteins were quantified by western blot assay using antibodies against ATF6, PERK, XBP1s and β-actin. The change in expression levels of (D) ATF6, (E) PERK and (F) XBP1 transcripts were quantified by RT-qPCR and conventional PCR assays. Error bars represent mean ±S.D. from three independent experiments performed in triplicate. \*P < 0.05, two-tailed unpaired t-test as compared to the untreated control. The ATF6, PERK and XBP1 knockdown sub-clones of MCF7 cells were generated by Mosaraf Hossain in the laboratory.

### 3-4-6. XBP1 is required for downregulation of miR-378 and its host gene (PPARGC1B) during UPR.

To understand the role of UPR signalling pathway in the regulation of miR-378, the expression level of miR-378 was determined in XBP1-knockdown, PERK-knockdown and ATF6-knockdown pools. HCT116 and MCF7 cells (XBP1-knockdown, PERK-knockdown and ATF6-knockdown) were either untreated or treated with 0.5 µg/ml of BFA and 1µM of TG for 24 hours respectively. Our results showed that the expression level of miR-378 was not downregulated by BFA treatment in XBP1 knockdown pools compared to the control cells while it was downregulated in PERK and ATF6 knockdown pools during UPR activation (Figure 3-4-6-1).

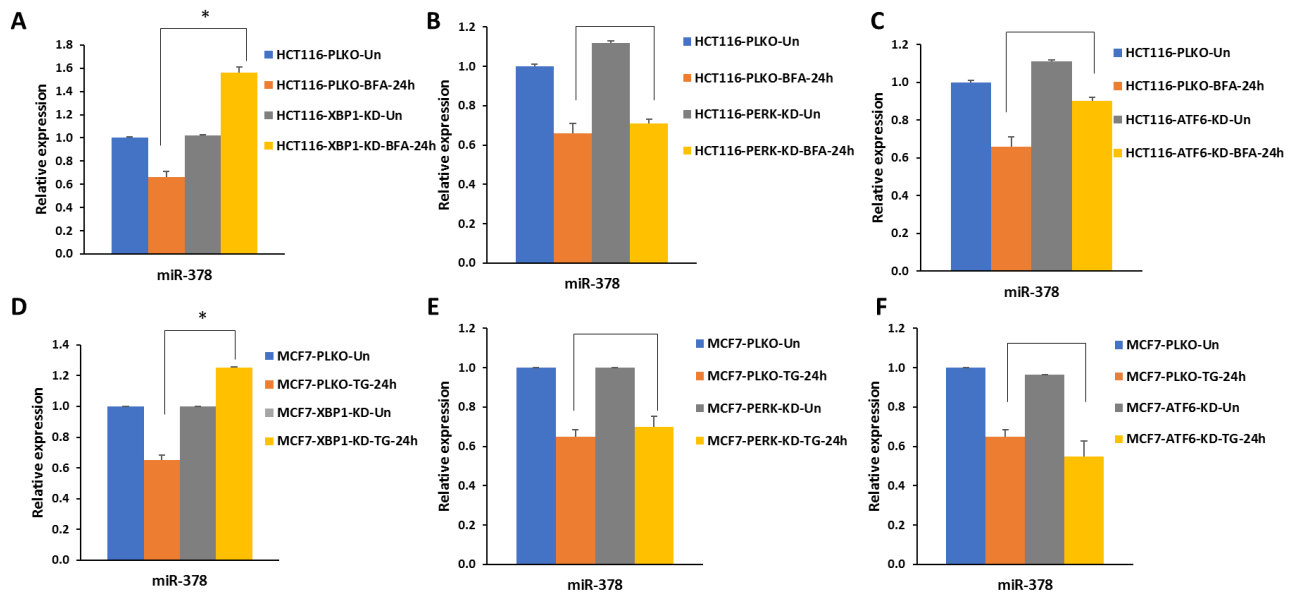


**Figure 3-4-6-1. XBP1 is required for downregulation of miR-378 during UPR.** HCT116 and MCF7 knockdown cells were either untreated or treated with 0.5 µg/ml of BFA and 1µM of TG for 24 hours respectively. The expression level of miR-378 was determined in HCT116 knockdown cells of (A) XBP1, (B) PERK, (C) ATF6 and MCF7 knockdown cells of (D) XBP1, (E) PERK, (F) ATF6. Error bars represent mean ±S.D. from three independent experiments performed in triplicate. \*P < 0.05, two-tailed unpaired t-test as compared to the untreated control.

To confirm the role of XBP1 in the regulation of miR-378 and PPARGC1B during conditions of EnR stress, IRE1 and PERK inhibitors were applied in parental MCF7 cells. Parental MCF7 cells were either untreated or treated with 0.5  $\mu\text{g/ml}$  BFA, 10  $\mu\text{M}$  IRE1 inhibitor (4 $\mu\text{8c}$ ) and 100 nM GSK PERK inhibitor (2606144) for 24 hours. The efficiency of IRE1 and PERK inhibitor compounds were confirmed by measuring the expression level of IRE1, XBP1, PERK, ATF4 and CHOP transcripts. We found that the downregulation of miR-378 and its host gene (PPARGC1B) was compromised when the IRE1 arm was inhibited while their expression was downregulated upon inhibition of the PERK arm (Figure 3-4-6-2).

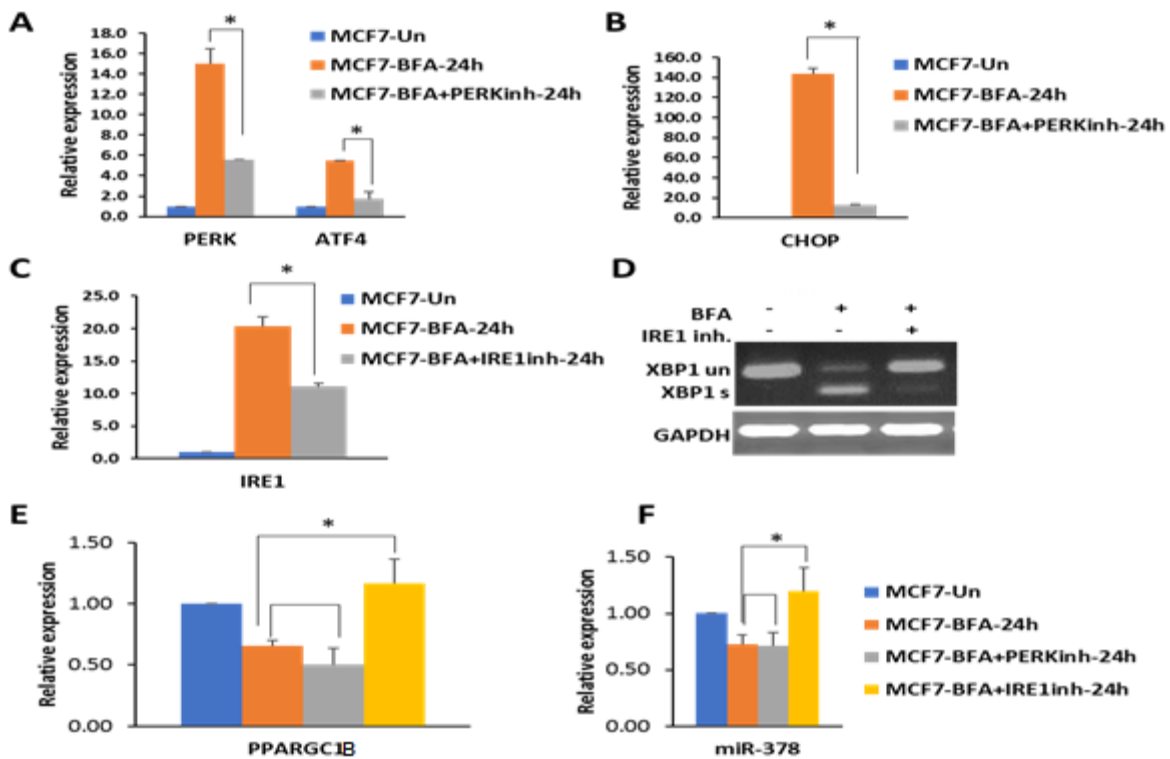


**Figure 3-4-6-2. Downregulation of miR-378 and its host gene (PPARGC1B) is dependent on the IRE1-XBP1 axis during conditions of EnR stress.** MCF7 cells were either untreated or treated with (0.5  $\mu\text{g/ml}$ ) BFA, (10  $\mu\text{M}$ ) IRE1 inhibitor (4 $\mu\text{8c}$ ) and (100 nM) GSK PERK inhibitor (2606144) for 24 hours. The change in expression levels of (A) ATF4 and PERK, (B) CHOP, (C) IRE1, (D) XBP1, (E) PPARGC1B and (F) miR-378 were quantified by RT-qPCR and conventional PCR assay. Error bars represent mean  $\pm$  S.D. from three independent experiments performed in triplicate. \* $P < 0.05$ , two-tailed unpaired t-test as compared to the untreated control.

To further investigate the IRE1-XBP1 axis role in the regulation of miR-378 and its host gene (PPARGC1B), we carried out a transient transfection experiment. Parental MCF7 cells ( $2 \times 10^6$  cells) were transfected with spliced XBP1 vector by electroporation using the Nucleofector technology. Overexpression of spliced XBP1 was confirmed by western blot assay. Then, the expression level of miR-378 and PPARGC1B were assessed by RT-qPCR assay. Our results showed that overexpression of spliced XBP1 significantly reduced the expression level of both miR-378 and its host gene (PPARGC1B) in the absence of UPR activation (Figure 3-4-6-3).

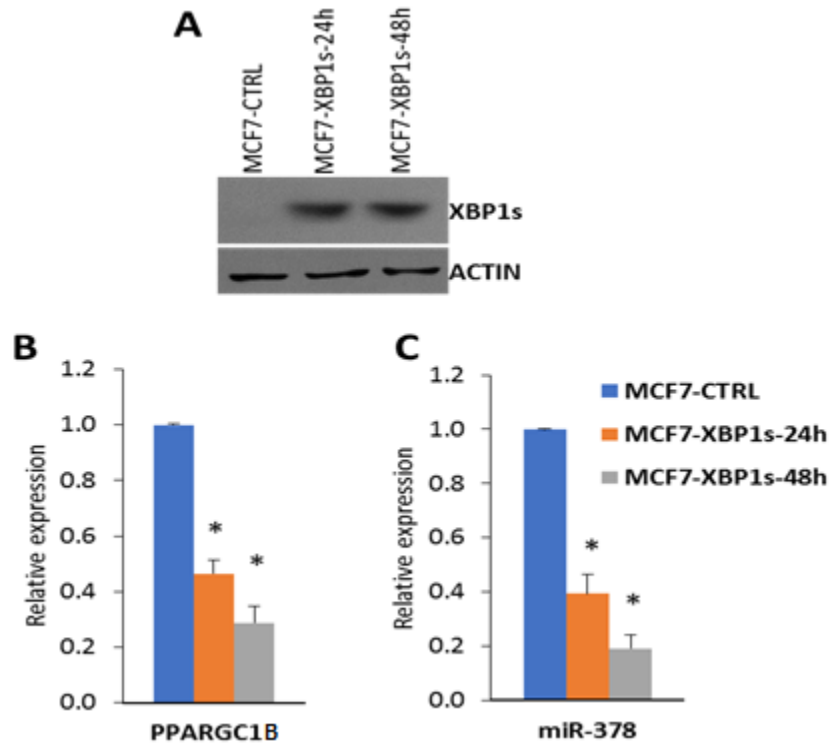


**Figure 3-4-6-3. Downregulation of miR-378 and its host gene (PPARGC1B) is dependent on spliced XBP1.** Overexpressing spliced XBP1 MCF7 cells ( $2 \times 10^6$  cells) were cultured for 24 and 48 hours. (A) The expression levels of XBP1s was quantified by western blot assay using antibodies against XBP1s (size:55 K.da) and  $\beta$ -actin (size:42 K.da). The change in expression level of (B) PPARGC1B and (C) miR-378 was quantified by RT-qPCR. Error bars represent mean  $\pm$ S.D. from two independent experiments performed in triplicate. \* $P < 0.05$ , two-tailed unpaired t-test as compared to the untreated control.



**3-4-7. The expression of XBP1 and PPARGC1B has a negative correlation in breast cancer patients.**

To evaluate if there were any correlations between the expression of XBP1 and PPARGC1B, we analysed the Cancer Genome Atlas Breast Invasive Carcinoma (TCGA-BRCA) data. We found that expression of XBP1 mRNA levels have a negative relationship with the transcript levels of PPARGC1B (Significance of correlation: R-value = -0.418, p-value = 9.9e-48, T-value = -15.245, degrees of freedom = 1095) in TCGA- BRCA datasets of breast cancer patients (Figure 3-4-7).

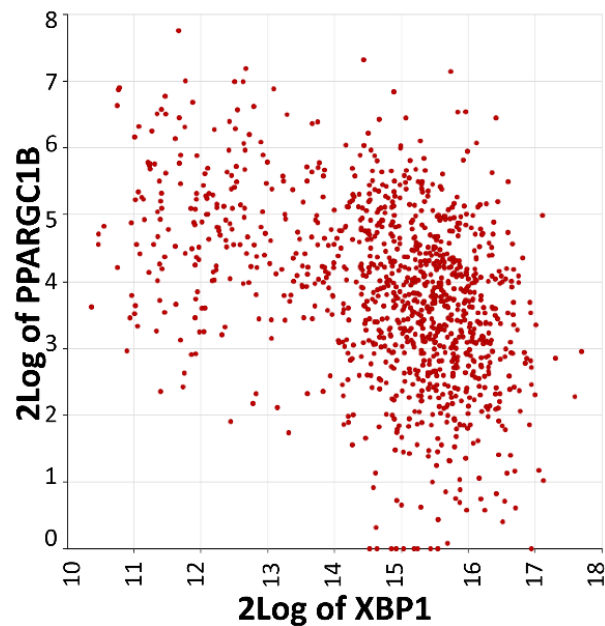


**Figure 3-4-7. The negative relationship between XBP1 and PPARGC1B expression in breast cancer patients.** The dot plot of log<sub>2</sub> transformed values for co-expression of PPARGC1B and XBP1 as determined by R<sup>2</sup> is shown. R-value: -0.418, P-value: 9.9e-48, T-value: -15.245.

### 3-4-8. Generation of stable overexpressing miR-378 clones in colorectal and breast cancer cells

To study the effect of miR-378 in cancer cells, precursor miR-378 was stably expressed in colorectal (HCT116) and breast cancer (MCF7, ZR-75-1 and MDA-MB-231) cells using a lentivirus vector (Figure 3-4-8-1). Overexpression of miR-378 was confirmed by fluorescence microscopy imaging and RT-qPCR to check the expression of GFP and miR-378 respectively (Figure 3-4-8-2).

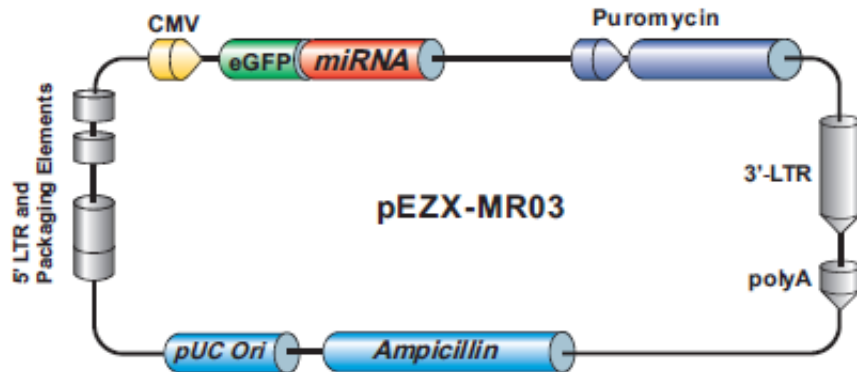


**Figure 3-4-8-1.** Schematic image of lentivirus vector map for cloning and expression of precursor miR-378 in colorectal and breast cancer cells.

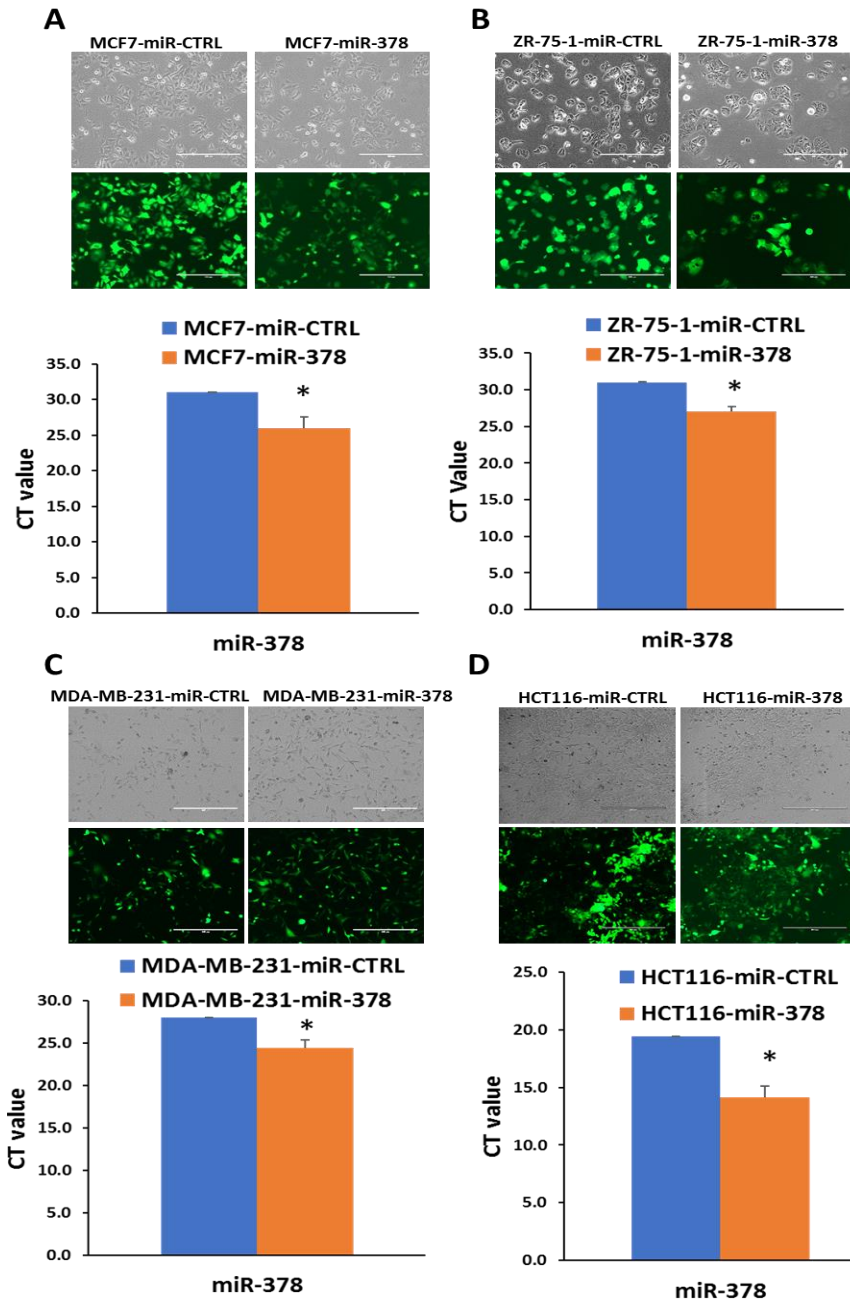


**Figure 3-4-8-2. Generation of stable overexpressing miR-378 pools in colorectal and breast cancer cells.** Precursor miR-378 was transduced in cancer cells using GFP expressing lentivirus vector. The expression level of miR-378 was assessed by fluorescence microscopy imaging (for GFP expression) and RT-qPCR assay (CT values) in (A) MCF7, (B) ZR-75-1, (C) MDA-MB-231 and (D) HCT116 cells. RNU6B was used as a reference gene to normalise the CT values. Error bars represent mean  $\pm$ S.D. from three independent experiments performed in triplicate. \*P < 0.05, two-tailed unpaired t-test as compared to the control.

### 3-4-9. MiR-378 reduced proliferation of luminal breast cancer cells

To study the effect of miR-378 on cancer cell growth, MTS cell proliferation assay was performed on HCT116 (colorectal), MCF7, ZR-75-1 (luminal A) and MDA-MB-231 (triple negative) cells. Our results showed that miR-378 significantly reduced the cell proliferation of MCF7 and ZR-75-1 cells whereas it had no effect on cell proliferation of HCT116 and MDA-MB-231 cells (Figure 3-4-9).

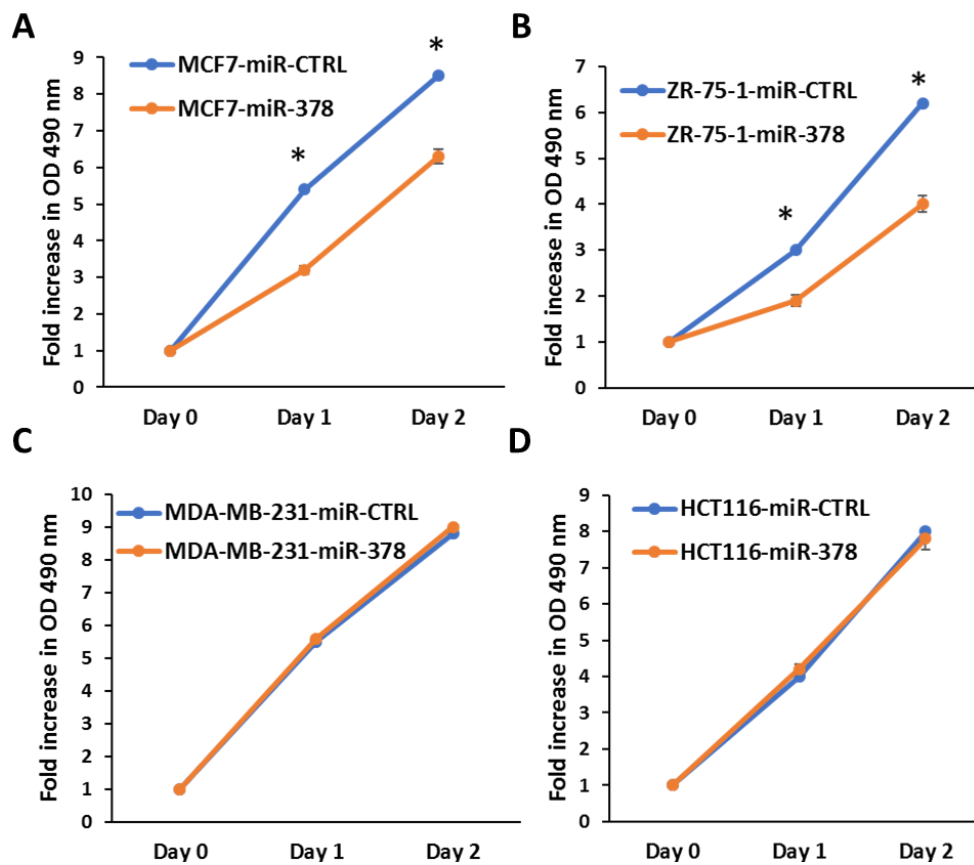


**Figure 3-4-9. The effect of miR-378 on colorectal and breast cancer cells proliferation.** Cancer cells ( $2 \times 10^3$  cells/well) were plated in 96 well plates and cell proliferation was assessed by MTS assay in (A) MCF7, (B) ZR-75-1, (C) MDA-MB-231 and (D) HCT116 cells at indicated time points. Error bars represent mean  $\pm$ S.D. from three independent experiments performed in triplicate. \*P < 0.05, two-tailed unpaired t-test as compared to the control.

### 3-4-10. MiR-378 reduced colony formation of luminal breast cancer cells

The capacity of overexpressing miR-378 cancer cells to form a colony of 50 or more cells from single cells was assessed by colony formation assay. In this experiment, HCT116 (colorectal), MCF7, ZR-75-1 (luminal A) and MDA-MB-231 (triple negative) cells ( $1 \times 10^3$  cells/well) were plated in 6 well plates and were cultured for 14 days. Then, cells were fixed (10% formaldehyde) and stained with 0.5 % crystal violet (Figure 3-4-10-1). The number of colonies was counted in five random view fields under a microscope and an average number of colonies was achieved. The colony sizes and numbers were also quantified by Image J software to obtain more quantitative results (Figure 3-4-10-2). We found that miR-378 significantly reduced colony formation in MCF7 and ZR-75-1 cells but it did not have any effect on colony formation of HCT116 and MDA-MB-231 cells.

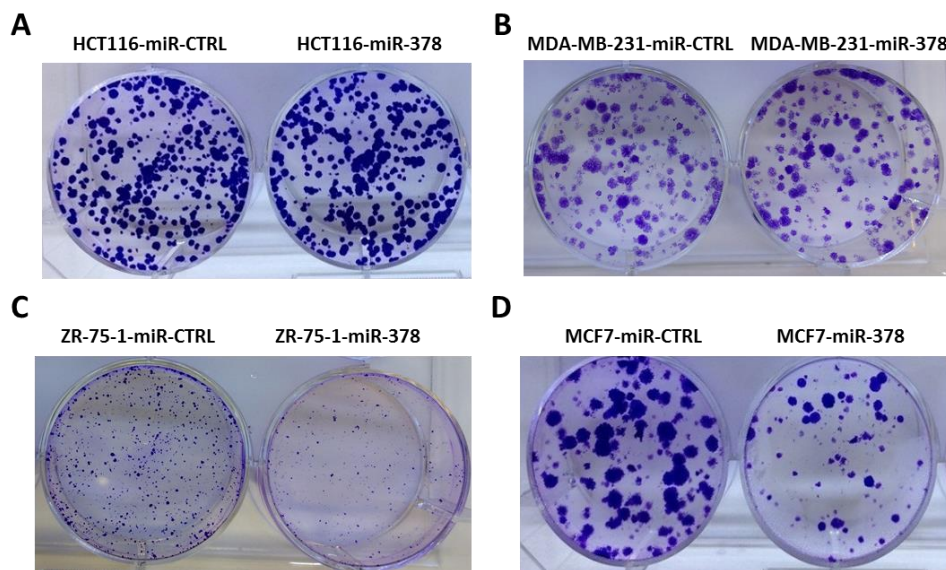


**Figure 3-4-10-1. The effect of miR-378 in colony formation of colorectal and breast cancer cells.** Cancer cells ( $1 \times 10^3$  cells/well) were plated in 6 well plates and were cultured for 14 days. Cells were fixed (10% formaldehyde) and stained with 0.5 % crystal violet. Colony formation was assessed by imaging of colonies in (A) HCT116, (B) MDA-MB-231, (C) ZR-75-1, and (D) MCF7 cells.

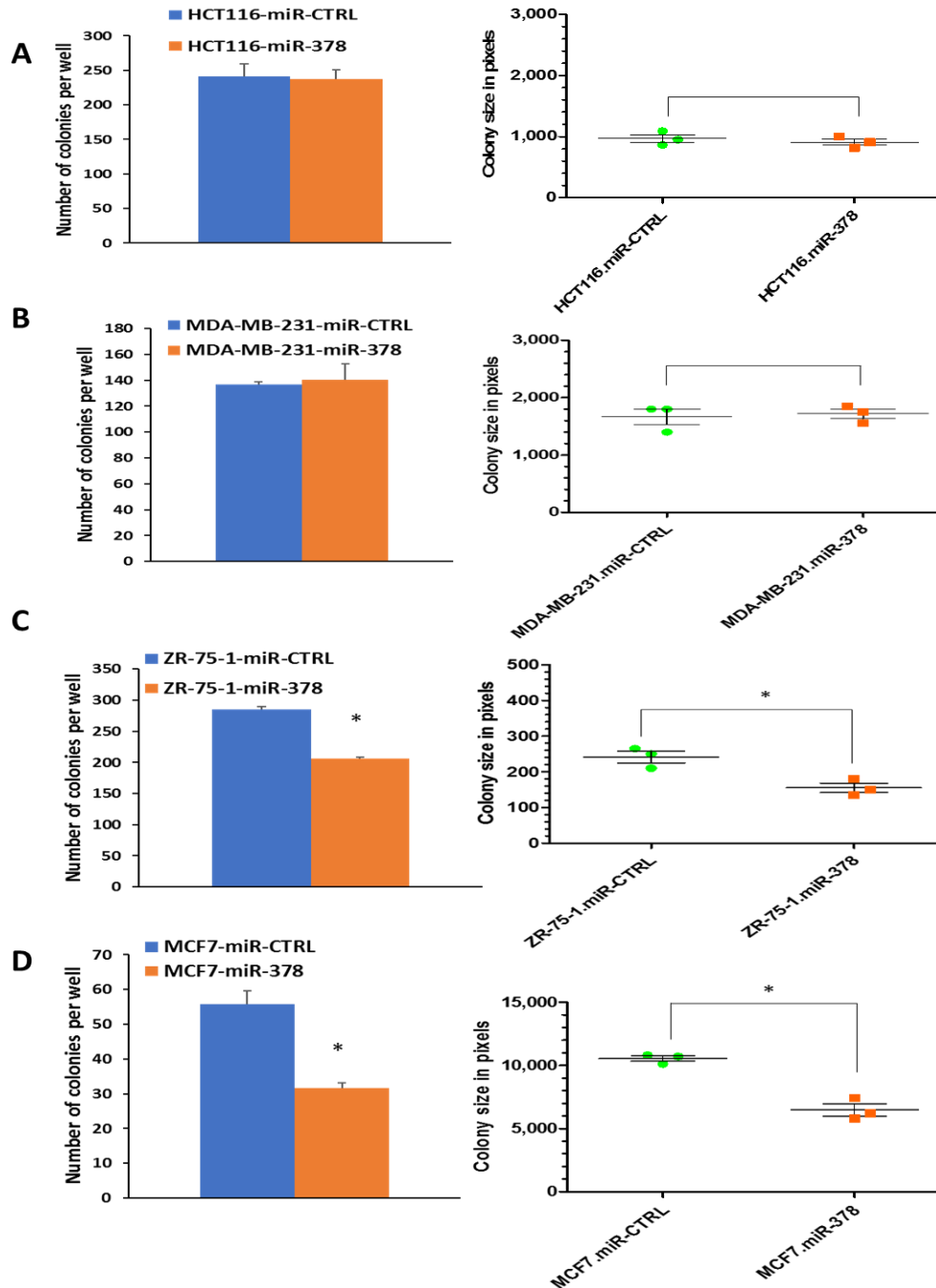


**Figure 3-4-10-2. The effect of miR-378 on size and number of colorectal and breast cancer cells.** Average of colony numbers and colony sizes from colony formation assay were determined in (A) HCT116, (B) MDA-MB-231, (C) ZR-75-1, and (D) MCF7 cells using Image J software. Error bars represent mean  $\pm$ S.D. from three independent experiments performed in triplicate. \*P < 0.05, two-tailed unpaired t-test as compared to the control.

### **3-4-11. MiR-378 reduced migration of luminal breast cancer cells**

To study the effect of miR-378 on cancer cell migration, a scratch wound healing assay was performed. MCF7, ZR-75-1 (luminal A) and MDA-MB-231 (triple negative) cells ( $3 \times 10^5$  cells/well) were plated in 6 well plates. After 24 hours of growth, when the cells reached 70-80% confluency, the cell monolayer was scratched with a sterile 0.2 ml pipette tip across the centre of the well. The scratched areas were then imaged at the indicated time point and were quantified by Image J software. Our results showed that miR-378 reduced cell migration in MCF7 and ZR-75-1 cells while it increased the migration of MDA-MB-231 cells (Figure 3-4-11).

As per the ATCC (American Type Culture Collection) the population doubling time of MCF7 and ZR-75-1 cells is 29h and 80h, respectively. Considering these doubling times, it was concluded that observed differences in the healing of a wound in miR-378 expressing MCF7 and ZR-75-1 cells at early time points were mainly due to migration, whereas at later time points this effect was the combination of both migration and proliferation.



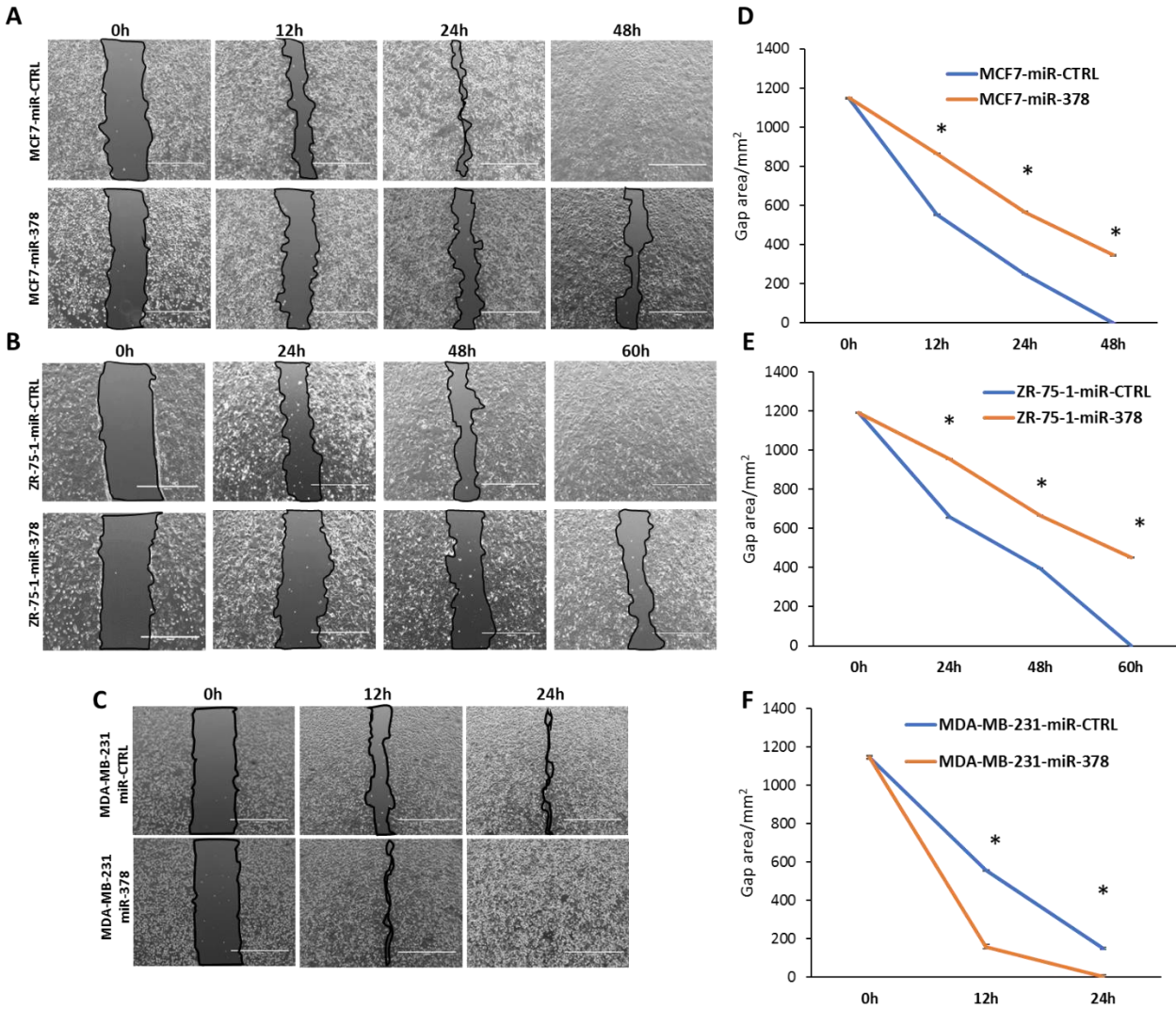


**Figure 3-4-11. The effect of miR-378 on breast cancer cell migration.** Control and overexpressing miR-378 cells ( $3 \times 10^5$  cells/well) were plated in 6 well plates. Scratch was done in some confluent monolayer cells by 0.2 ml pipette tip and migration of cells into the wound was observed after indicated time points. Representative images showing the scratch in (A) MCF7, (B) ZR-75-1 and (C) MDA-MB-231 cells at indicated time points. The graphs show the gap area ( $\text{mm}^2$ ) in (D) MCF7, (E) ZR-75-1 and (F) MDA-MB-231 cells. Error bars represent mean  $\pm$ S.D. from three independent experiments performed in triplicate. \* $P < 0.05$ , two-tailed unpaired t-test as compared to the control.



### 3-4-12. MiR-378 enhanced the sensitivity of MCF7 cells toward the anti-estrogen compounds

To study the effect of miR-378 on MCF7 cells response to the anti-estrogen compounds, MTS assay was carried out in these cells. Control and miR-378 expressing MCF7 cells ( $2 \times 10^3$  cells/well) were plated in 96 well plates and after 24 hours they were either untreated or treated with 10 $\mu$ M tamoxifen and 100 $\mu$ M fulvestrant for 24, 48 and 72 hours. After the indicated time point, 0.02 ml of the MTS solution was directly added to each well and incubated at 37°C for 4 hours. The absorbance of each well was measured at OD=490 nm with a 96-well plate reader. Our results showed that miR-378 enhanced the sensitivity of MCF7 cells towards the anti-estrogen compounds (Figure 3-4-12).

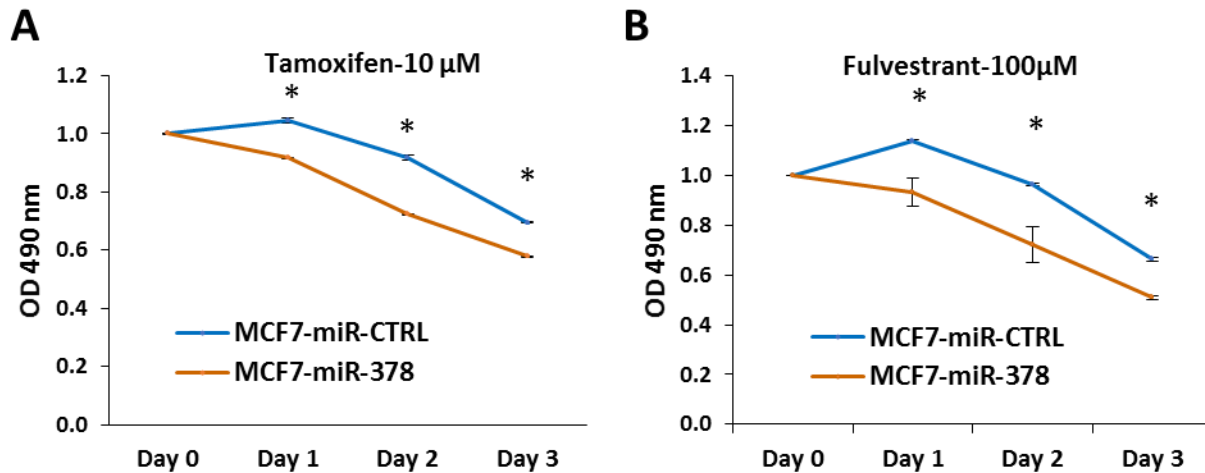


**Figure 3-4-12. The effect of miR-378 on MCF7 cells response to the anti-estrogen compounds.** Control and miR-378 expressing MCF7 cells ( $2 \times 10^3$  cells/well) were plated in 96 well plates and after 24 hours they were either untreated or treated with (A) 10 $\mu$ M Tamoxifen and (B) 100 $\mu$ M Fulvestrant for 24, 48 and 72 hours. Cell proliferation was assessed by MTS assay at indicated time points. Error bars represent mean  $\pm$ S.D. from three independent experiments performed in triplicate. \*P < 0.05, two-tailed unpaired t-test as compared to the control.

### **3-4-13. MiR-378 enhanced the sensitivity of MCF7 cells toward the EnR stress-inducing compounds**

To study the effect of miR-378 on MCF7 cells response to the EnR stress-inducing compounds, cell death assay was carried out by flow cytometry analysis. Control and miR-378 expressing MCF7 cells ( $2 \times 10^5$  cells/well) were plated in 6 well plates. After 24 hours, cells were either treated or untreated with (0.1 mM) TG, (0.5 $\mu$ g/ml) BFA and (100 nM) DTX (docetaxel) for 48 hours. Cells were then stained with SYTOX Red and the percentage of the dead cells were assessed by flow cytometry. Our results showed that miR-378 increased the MCF7 cells sensitivity towards the EnR stress-inducing compounds. On the other hand, miR-378 decreased MCF7 cells sensitivity towards the chemotherapeutic compound, docetaxel (Figure 3-4-13).

### **3-4-14. MiR-378 does not have any effect on UPR sensors during conditions of EnR stress and UPR activation**

To study the effect of miR-378 on UPR signalling pathway, the expression levels of four bona fide UPR genes were quantified in HCT116 and MCF7 cells during conditions of EnR stress. Control and miR-378 expressing HCT116 and MCF7 cells were either untreated or treated with 0.5  $\mu$ g/ml of BFA for 8 and 24 hours and the expression level of GRP78, HERP, CHOP and XBP1 transcripts were quantified by real-time and conventional PCR assay. Our results showed that miR-378 did not have any effect on the UPR signalling pathway during conditions of EnR stress (Figure 3-4-14).

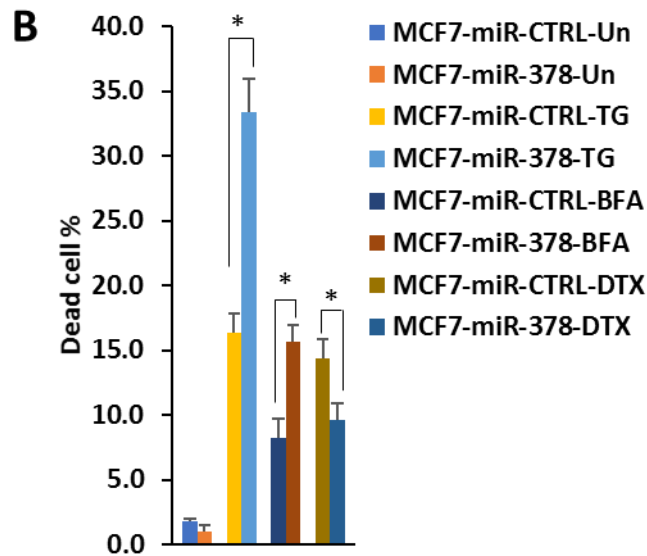
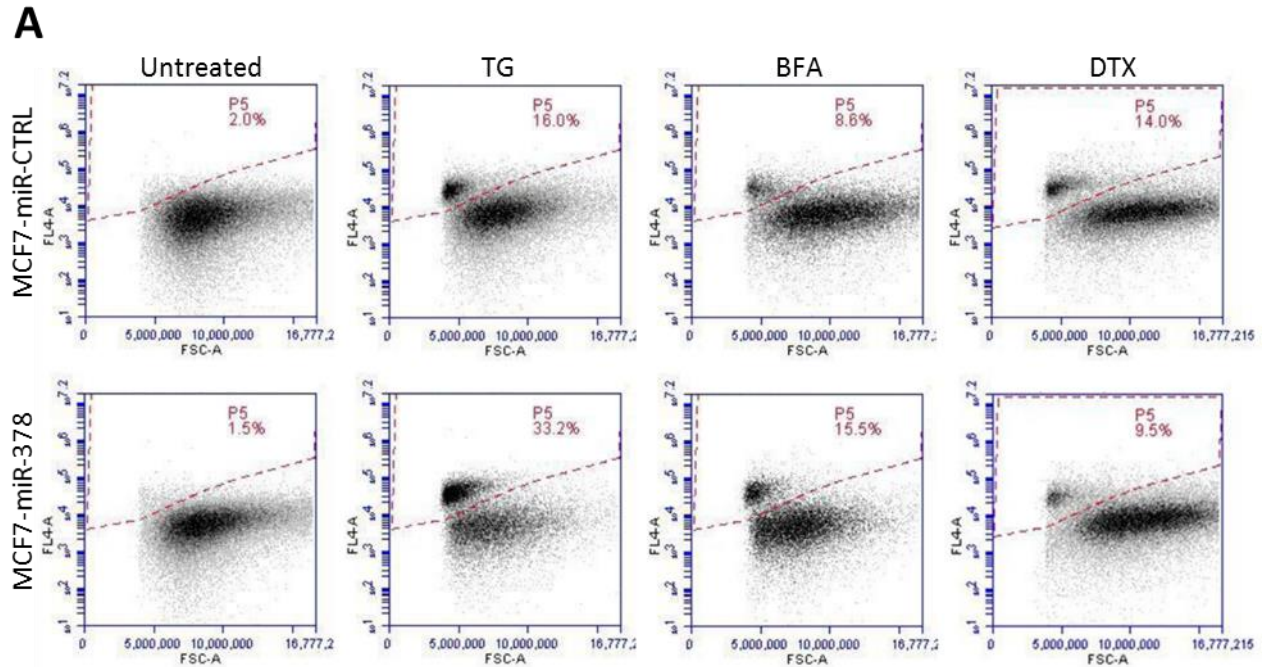


**Figure 3-4-13. The effect of miR-378 on MCF7 cells response to the EnR stress-inducing compounds.** Control and miR-378 expressing MCF7 cells were either untreated or treated with (1 $\mu$ M) TG, (0.5 $\mu$ g/ml) BFA and (100nM) DTX for 48 hours. Representative dot plot (A) and a bar graph (B) of the dead cell percentage of control and miR-378 expressing MCF7 cells, stained by SYTOX Red dye, are shown. Error bars represent mean  $\pm$ S.D. from three independent experiments. \*P < 0.05, two-tailed unpaired t-test as compared to the untreated control.

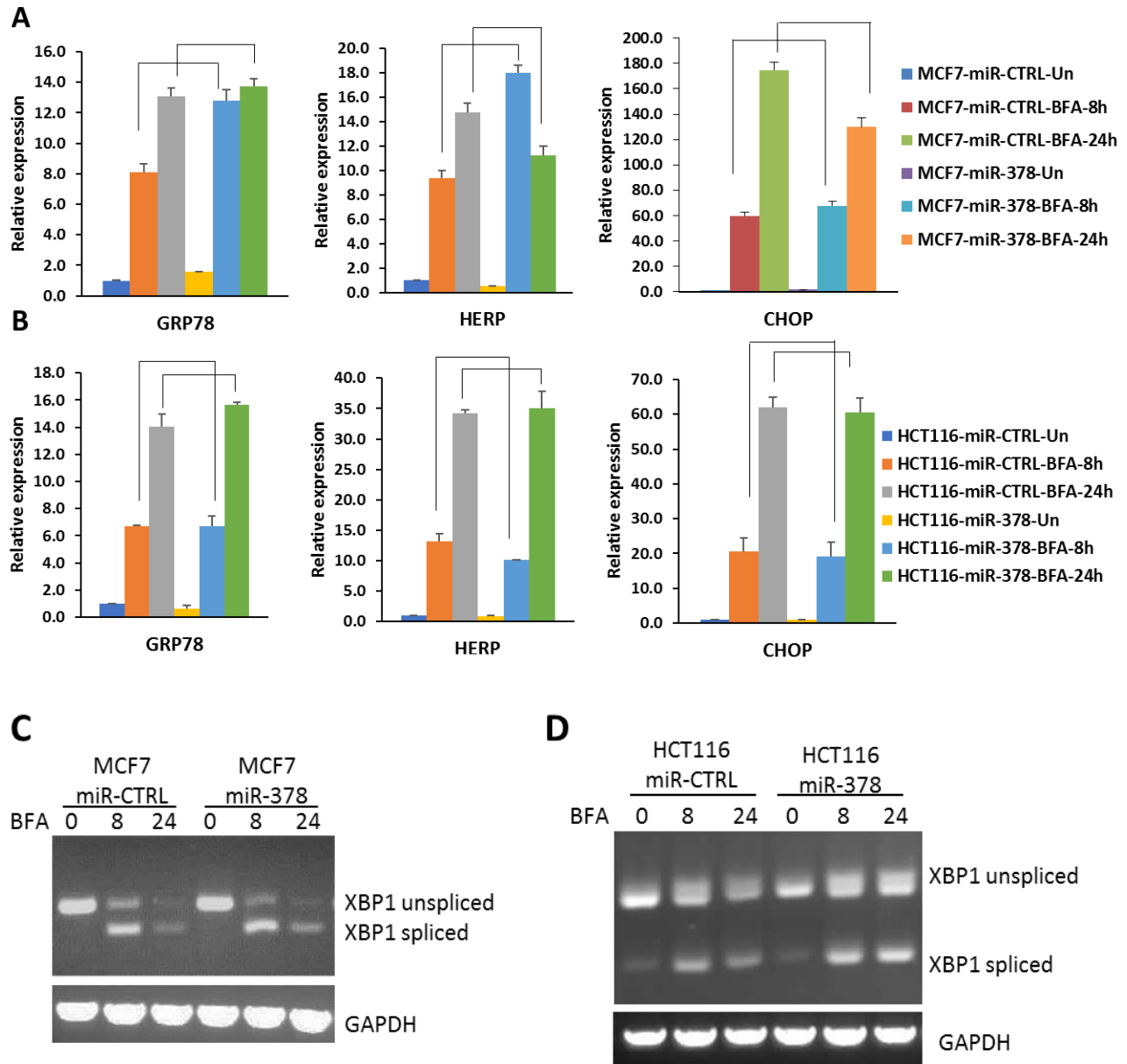


**Figure 3-4-14. MiR-378 has no effect on UPR sensors during conditions of EnR stress.** Control and miR-378 expressing HCT116 and MCF7 cells were either untreated or treated with (0.5 $\mu$ g/ml) BFA for 8 and 24 hours. The change in expression levels of EnR stress markers (GRP78, HERP, and CHOP) in (A) MCF7 and (B) HCT116 cells were quantified by RT-qPCR assay. The expression level of unspliced and spliced XBP1 was measured in (C) MCF7 and (D) HCT116 cells by conventional PCR assay. Error bars represent mean  $\pm$  S.D. from three independent experiments performed in triplicate. Two-tailed unpaired t-test as compared to the untreated control.

### **3-4-15. MiR-378 dependent gene signature was identified by the transcriptomic and bioinformatic analysis**

To investigate the mechanism of action for miR-378 on breast cancer cells, miR-378 regulated genes were identified by whole-genome sequencing transcriptomic analysis. For this experiment, the total RNA samples from control and miR-378 expressing MCF7 cells (four replicates) were sent to the BGI company for whole-genome sequencing.

We generated an average of 43 million clean reads per sample. The gene expression level was quantified by RSEM (RNA-Seq by Expectation Maximization). The most deregulated genes with log ratio of more than +2 (upregulated genes) and less than -2 (downregulated genes) were chosen for bioinformatic analysis. The Venn diagram tool was applied to select the common up and downregulated genes from four replicates [360]. We found that 53 genes were expressed at a significantly lower level and 254 genes were expressed at a higher level in miR-378 expressing MCF7 cells (Figure 3-4-15A-B, Appendix 6-8 and 6-9).

Based on fold change in expression, function and novelty, eight short-listed genes were chosen for validation by RT-qPCR assay including four upregulated (IFIT1, IFT2, DDX58 and PLA2G4B) and four downregulated genes (GBX2, GAL, GALNT13 and H19) (Figure-3-4-15C-D).

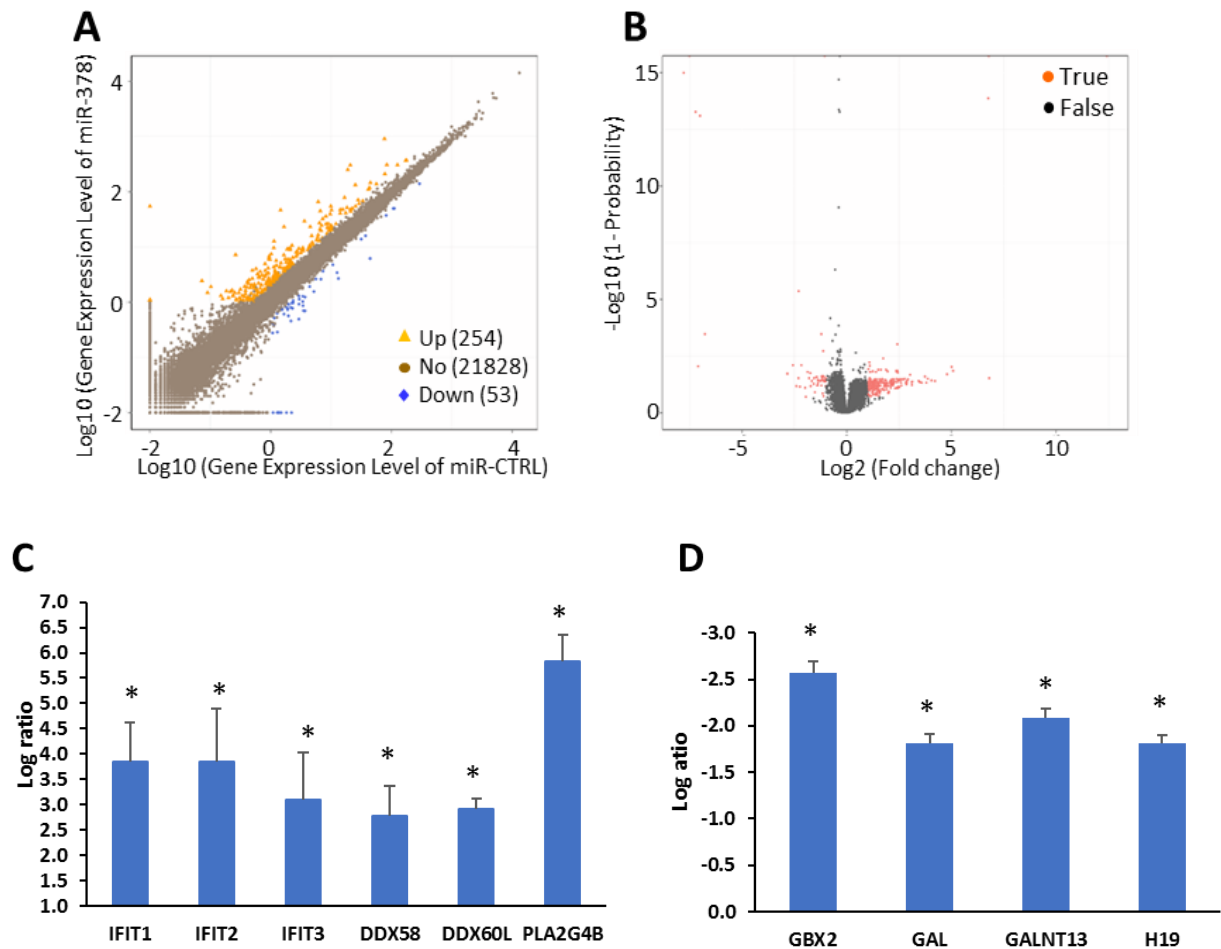


**Figure 3-4-15. Identification of miR-378 regulated genes.** (A) Scatter plot of expressed genes in control and miR-378 expressing MCF7 cells as determined by NOISEq method. The x-axis and Y-axis present log<sub>10</sub> value of gene expression in control and miR-378 expressing cells. (B) Volcano plot of differentially expressed genes in control and miR-378 expressing MCF7 cells. The x-axis represents the fold change and Y-axis represents threshold value. Each dot is a differentially expressed gene. Dots in red mean significant differentially expressed genes which passed the screening threshold and black dots are non-significant differentially expressed genes. The log ratio of selected (C) upregulated and (D) downregulated dependent genes of miR-378 which is determined by transcriptomic and bioinformatic analysis. Error bars represent mean  $\pm$ S.D. from four independent experiments performed in triplicates. \*P < 0.05, two-tailed unpaired t-test as compared to the control.

### 3-4-16. Confirmation of selected miR-378 dependent genes expression by RT-qPCR assay

To validate the transcriptomic analysis results, the expression level of selected deregulated genes by miR-378 was confirmed in miR-378 expressing MCF7 cells (from the same RNA samples that were sent for transcriptomic analysis) by RT-qPCR assay. Our RT-qPCR results confirmed upregulation of three genes including IFIT1, IFIT2 and DDX58. We also quantified the expression level of these selected miR-378 dependent genes in ZR-75-1 and MDA-MB-231 cells. Our results confirmed that IFIT1, IFIT2 and DDX58 transcripts were upregulated in ZR-75-1 cells. There was not any significant difference in the expression of these upregulated genes in MDA-MB-231 cells (Figure 3-4-16-1).

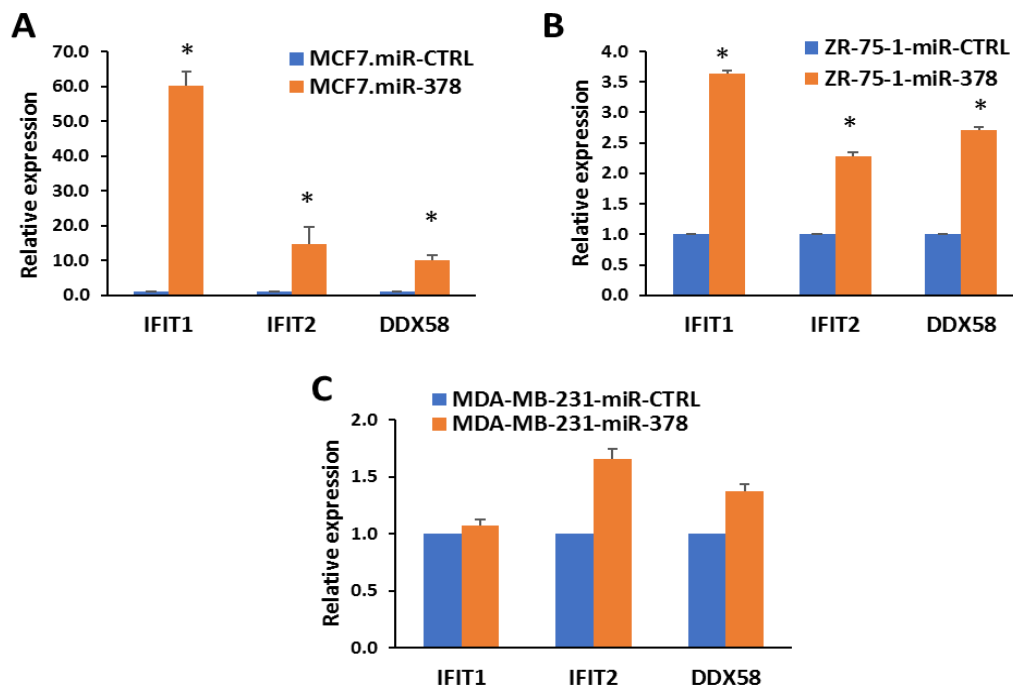


**Figure 3-4-16-1. Confirmation of miR-378 upregulated dependent genes by RT-qPCR assay.** The expression level of selected upregulated miR-378 dependent genes were quantified by RT-qPCR assay in (A) MCF7, (B) ZR-75-1 and (C) MDA-MB-231 cells. Error bars represent mean  $\pm$ S.D. from three independent experiments performed in triplicate. \* $P < 0.05$ , two-tailed unpaired t-test as compared to the control.

The relative expression of selected downregulated miR-378 dependent genes was also quantified by RT-qPCR assay. Our results confirmed downregulation of two (GAL and GALNT13) and three (GAL, GALNT13 and GBX2) genes in MCF7 and ZR75-1 cells respectively. The RT-qPCR assay could not confirm the downregulation of these genes in miR-378 expressing MDA-MB-231 cells (Figure 3-4-16-2). Several studies have demonstrated the role of these downregulated genes in human cancers;

**GAL** gene encodes galanin protein, which is a neuropeptide and is expressed in several tissues including gut, spinal cord and brain [361]. It has been reported that galanin plays a crucial role in tumour metastasis and it is associated with poor prognosis in colorectal cancer [362].

**GALNT13** gene encodes an enzyme named Polypeptide N-acetyl-galactosaminyl-transferase 13 which plays a role in glycosylation [363]. Nogimori and colleagues showed that GALNT13 is upregulated in human lung cancer cells and can be used as a prognostic biomarker in lung cancers [364].

**H19** is a long non-coding RNA that plays a pivotal role in breast cancer development [365]. Overexpression of H19 has been reported in 73% of breast tumours and its expression is highly associated with ER+ breast cancer [366]. Moreover, it has been found that H19 promotes cell cycle transition G1/S in breast cancer cells and knockdown of this gene significantly suppresses cancer cell growth [367].

**GBX2** (Gastrulation Brain Homeobox 2) is a transcription factor that plays a role in cell identity and differentiation [368] and overexpression of GBX2 have shown to increase the growth of PC3 prostate cancer cells through Interleukin 6 (IL-6) [369].



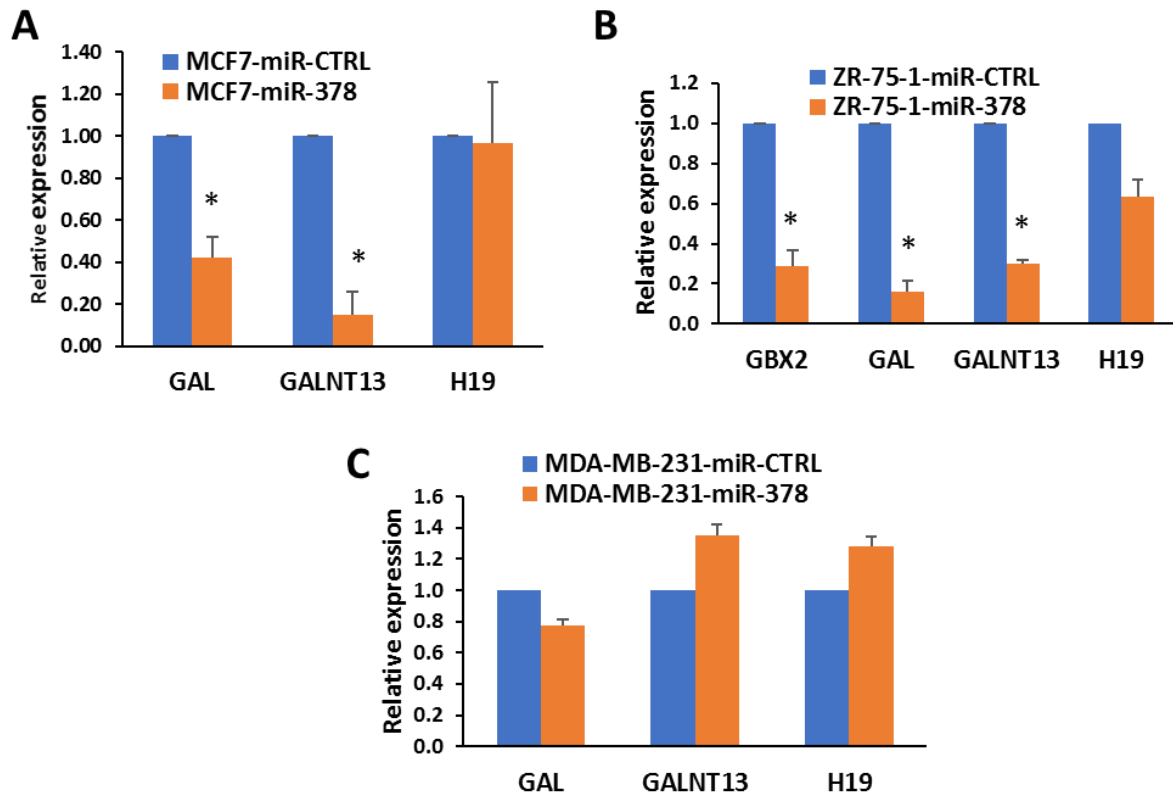


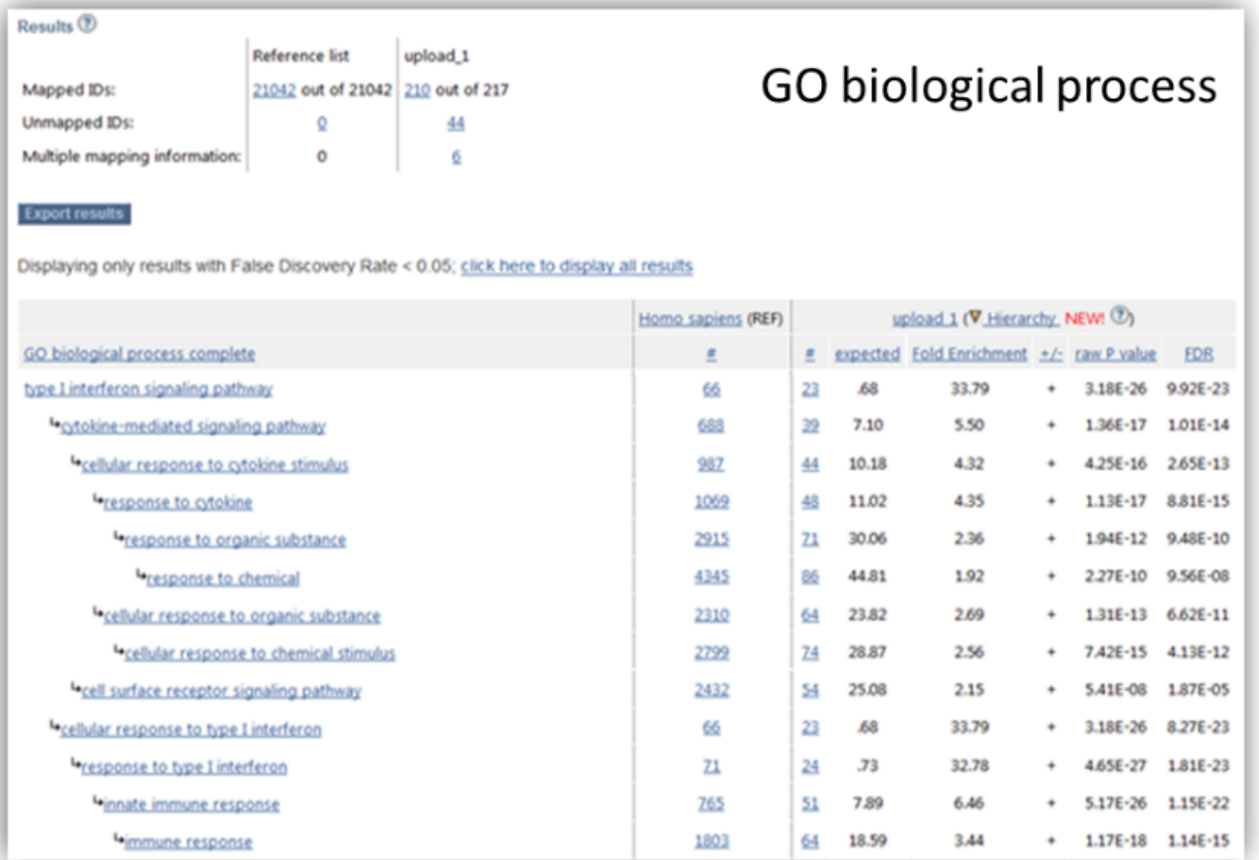
**Figure 3-4-16-2. Confirmation of miR-378 downregulated dependent genes by RT-qPCR assay.** The expression level of selected miR-378 dependent genes were quantified by RT-qPCR assay in (A) MCF7, (B) ZR-75-1 and (C) MDA-MB-231 cells. Error bars represent mean  $\pm$ S.D. from three independent experiments performed in triplicate. \* $P < 0.05$ , two-tailed unpaired t-test as compared to the control.

### **3-4-17. Type I interferon signalling pathway plays a role to reduce MCF7 cell proliferation through miR-378**

To analyse the differentially expressed genes at a functional level, GO enrichment analysis was performed (<http://www.geneontology.org/>). Gene set enrichment analysis of upregulated genes identified significant enrichment of type I interferon signalling pathway genes, while analysis of downregulated genes showed no significant enrichment (Figure 3-4-17A).

Our transcriptomic and bioinformatic analysis identified 23 upregulated genes in miR-378 expressing MCF7 cells which belonged to the type I interferon signalling pathway. Interferons are cytokines that are secreted by cells and have antiproliferative, antiviral and immunomodulatory effects [370]. We reasoned that miR-378 expressing cells may secrete growth suppressing cytokines due to the upregulated type I interferon signalling. Next, we evaluated the effect of miR-378 conditioned-medium on proliferation of parental MCF7 cells. For this purpose, control and miR-378 expressing MCF7 cells were cultured for 12 hours and the supernatant medium was then collected and added to the parental MCF7 cells and finally, cell growth was assessed by MTS assay. We found that the conditioned medium from miR-378 expressing MCF7 cells reduced the growth of parental MCF7 cells (Figure 3-4-17B) as compared to conditioned-medium from the control cells. These observations suggest that miR-378 may regulate cell growth via the secretion of growth inhibitory factors as transcriptomic analysis showed upregulation of type I interferon signalling genes.

A



B

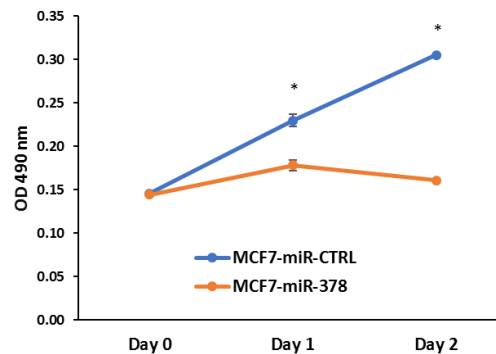


**Figure 3-4-17. Type I interferon signalling pathway regulates MCF7 cell proliferation through miR-378.** (A) PANTHER overrepresentation Test (Released 20171205) using GO biological process complete annotation data set at FDR < 0.05. (B) MCF7 cells were incubated with control or miR-378 conditioned medium in 96-well plate (2,000 cells/well). Cell proliferation was assessed by MTS assay. Line graphs show the absorbance in cells at the indicated time points. Error bars represent mean  $\pm$  S.D. from two independent experiments performed in triplicate. \*P < 0.05.

### **3-4-18. High expression of miR-378 has a good outcome in ER-positive breast cancer patients**

To find the association between the expression of miR-378 and overall survival rate of breast cancer patients, we used a web-based analysis tool, Kaplan-Meier plotter. The KM estimator is a nonparametric statistic tool that can estimate the cancer patient survival time. Using Kaplan-Meier estimator, we found that the high expression of miR-378 has a good outcome in breast cancer patients. We found that in ER-positive breast cancer, higher miR-378 expression was associated with increased overall survival (OS) as determined by Kaplan-Meier estimates ( $p = 0.038$ , log-rank test) (Figure 3-4-18A).

We further analysed the relationship between miR-378 expression and response to endocrine therapy by comparing the survival curves of patients with above or below median miR-378 expression levels who either received endocrine therapy or did not receive endocrine therapy. We observed that higher miR-378 expression was a significant predictor of better survival in the ‘no systemic therapy’ group as well as ‘endocrine therapy treatment’ group (Figure 3-4-18B-D and Appendix 6-10).

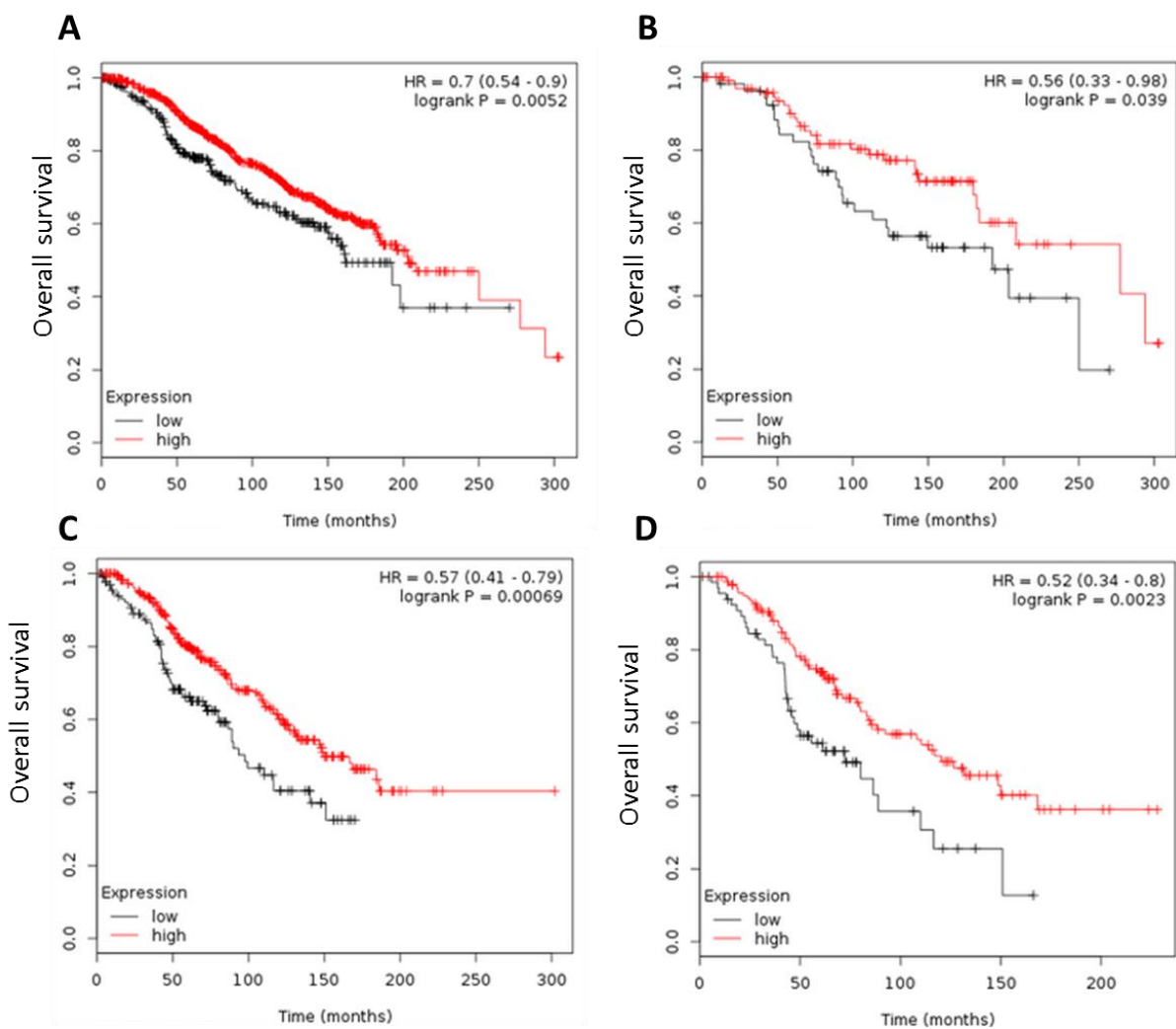
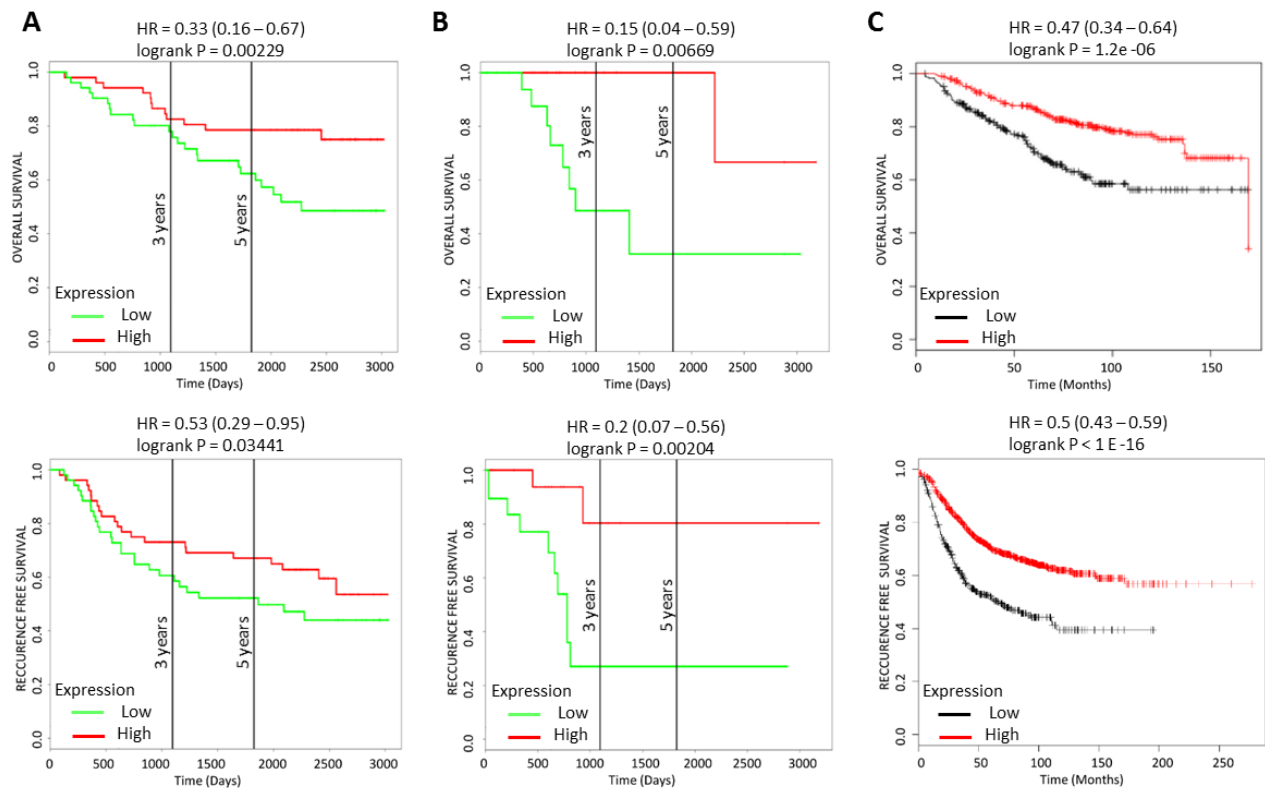


**Figure 3-4-18. High expression of miR-378 is associated with better overall survival in ER-positive breast cancer.** Kaplan-Meier plots showing overall survival in ER-positive breast cancer from the METABRIC dataset. (A) ER-positive patients (n=944). (B) ER-positive patients with no systemic treatment (n=146). (C) ER-positive and node-positive patients who received only endocrine therapy (n=318). (D) ER-positive, grade 3 and node-positive patients who received endocrine therapy (n=134). In red: patients with expression above the median and in black, patients with expressions below the median.

### 3-4-19. MiR-378 dependent gene signature is associated with good outcome in breast cancer

The integration of miR-378 dependent gene expression profiles and GO enrichment analysis identified eight genes upregulated by miR-378 (Appendix 6-11). This gene set was defined as the miR-378 signature. Survival analysis using breast cancer datasets (GSE42568 and GSE2607) and using PROGgene V2 demonstrated that tumours with an elevated miR-378 gene signature displayed longer overall and relapse-free survival (Figure 3-4-19A-B). These findings were validated in another dataset of breast cancer patients using KM plotter (Figure 3-4-19C).



**3-4-19. MiR-378 gene signature is associated with prognosis in breast cancer.** (A-B) Kaplan-Meier graphs demonstrating a significant association of elevated expression of the miR-378 gene signature (red line) with increased overall survival and recurrence-free survival in two cohorts of breast cancer patients using PROGgene V2. (C) Kaplan-Meier graphs demonstrating a significant association between elevated expression of the miR-378 signature (red line) and longer relapse-free survival in 1809 patients using KM plotter.

## **Chapter 4**

# **CHOP-intronic miR-616 inhibits cell growth and migration by targeting c-MYC and VAV1**

## 4-0. Results Chapter 2

### 4-1. Background

DDIT3 or CHOP (host gene of miR-616) is a transcription factor and a downstream target of the PERK signalling pathway. PERK has been shown to act as a haploinsufficient tumour suppressor, where it can function both as a tumour suppressor and a tumour promoter, and the nature of its function is determined by gene dose [371]. Transient pause in protein synthesis, due to eIF2 $\alpha$  phosphorylation by PERK, is beneficial by reducing secretory load in the ER [372]. Phosphorylation of NRF2 by PERK attenuates Keap1-mediated degradation of NRF2 and promotes expression of anti-oxidant enzymes through the antioxidant response elements (ARE) [372]. PERK hyperactivation can upregulate the CHOP/GADD153 transcription factor. It has been reported that CHOP downregulates the expression of anti-apoptotic BCL2 family proteins to induce cell death [33]. CHOP also increases the expression level of pro-apoptotic BCL2 family proteins such as BIM and PUMA to promote apoptosis [34-36]. Studies in both cellular and animal models with CHOP gene deficiency have shed light on the pro-apoptotic role of CHOP during cellular stress [373, 374]. Furthermore, ectopic expression of CHOP was reported to induce a G1 cell cycle arrest. CHOP maintains the integrity of the human hematopoietic stem cell (HSC) pool by eliminating of HSCs which harbours oncogenic mutations, and decreases the risk of leukaemia [374].

CHOP induction triggers apoptosis of premalignant cells to prevent malignant progression in a mouse lung cancer model [374]. Hepatocyte-specific CHOP ablation increased tumourigenesis in high fat diet-induced steatohepatitis and hepatocellular carcinoma [374]. CHOP has been shown to promote cancer progression, when fused with FUS/TLS or EWS protein by genomic rearrangement [373, 374].



The FUS-CHOP oncoprotein has been shown to induce metastasis in *in vivo* model of sarcoma [374]. Accumulating data suggests that CHOP impinges upon several aspects of cancer including initiation as well as progression of tumours [373-375].

Furthermore, several studies have shown the role of PERK-regulated miRNAs in human cancer. Chitnis and colleagues reported that miR-211 directly targets the CHOP promoter in mouse embryonic fibroblasts (MEFs), leading to CHOP downregulation [318]. In another published study, it was shown miR-204 targets the 3'UTR of the PERK transcript and downregulates ATF4 and CHOP expression, consequently increasing ER stress-induced  $\beta$ -cell apoptosis [376]. Moreover, Yang and colleagues found that miR-122 inhibits the UPR chaperon activity in hepatocarcinoma cells (HCC). They showed that downregulation of miR-122 activates the CDK4-PSMD10-UPR pathway and reduces the tumour cell anticancer drug-mediated apoptosis [312].

Several studies have shown that miR-616 acts as a tumour promoting miRNA in human cancers [291-295]. The expression of miR-616 has been shown to be upregulated in androgen-independent prostate cancer, gastric cancer, non-small cell lung cancer (NSCLC), hepatocellular carcinoma (HCC) and gliomas. MiR-616 targets tissue factor pathway inhibitor (TFPI-2) in prostate cancer [291] ; PTEN in HCC and gastric cancer [292] ; SOX7 in glioma [293] and NSCLC [294]. This chapter, investigates the role of miR-616 during conditions of ER stress and UPR activation in colorectal and breast cancer cells. MiR-616 was chosen in this study as it is located in intron 1 of DDIT3 (CHOP) gene at chromosome 12 (12q13.3) (Figure 4-1) and CHOP is a downstream gene of one of the three major UPR sensors, PERK.

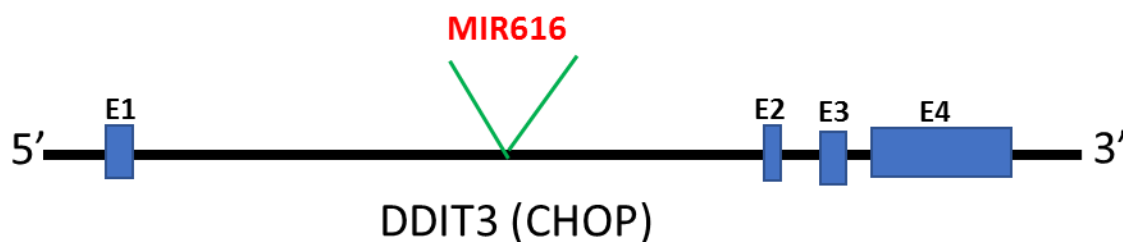


**Figure 4-1. Cytogetic location of miR-616 in its host gene (DDIT3) sequence.** The miR-616 gene is located in intron number 1 of DDIT3 (CHOP) gene at chromosome 12.

In this study, we report that expression of miR-616 and CHOP (host gene of miR-616) is increased during UPR. We report that miR-616 significantly suppressed cell proliferation, colony formation and migration of cancer cells. Furthermore, we show that miR-616 exerts the growth inhibitory effect on MCF7 cells through suppressing the expression of c-MYC and VAV1. Our results establish a new and unexpected role for the CHOP locus by providing evidence that miR-616 can inhibit cell proliferation by targeting c-MYC and VAV1. In summary, our results suggest that the CHOP locus generates two gene products, where CHOP protein and miR-616 can act together to inhibit cancer progression.

## **4-2. Hypothesis**

The presence of miRNA gene within the introns of protein-coding genes suggests a possible functional relationship between intronic miRNA and its host gene. Potentially, miRNAs can affect their hosts' function in multiple ways – (i) an intronic miRNA can post-transcriptionally autoregulate its host by targeting the host gene's transcript, and (ii) miRNAs may be associated with their host function by targeting genes involved in pathways in which the host gene is involved. Therefore, we hypothesise that miR-616 (originating from CHOP locus) may influence the cellular response during conditions of EnR stress, and dysregulation of miR-616 may contribute to cancer progression.

## **4-3. Aims**

The aims of the experiments described in this chapter were: (i) to elucidate the mechanism of EnR stress-induced expression of miR-616, (ii) to evaluate the effect of miR-616 on cell growth, proliferation and migration, (iii) to understand regulation of cell fate during UPR and (iv) to identify functionally relevant miR-616 target mRNAs.

## **4-4. Results**

### **4-4-1. MiR-616 is upregulated during conditions of EnR stress in colorectal and breast cancer cells**

To evaluate the expression level of miR-616 during conditions of EnR stress, HCT116, RKO and MCF7 cells were either treated or untreated with 1 $\mu$ M of TG, 1.0  $\mu$ g/ml of TM and 0.5 $\mu$ g/ml of BFA for different time points. First, the UPR signalling pathway activation was confirmed by quantifying bonafide UPR genes using RT-qPCR assay (Figure 3-4-1-1A, B, and 3-4-1-3A).

Then, the expression level of miR-616 was determined by RT-qPCR assay. Our results showed that miR-616 is upregulated during conditions of EnR stress in colorectal and breast cancer cells (Figure 4-4-1).

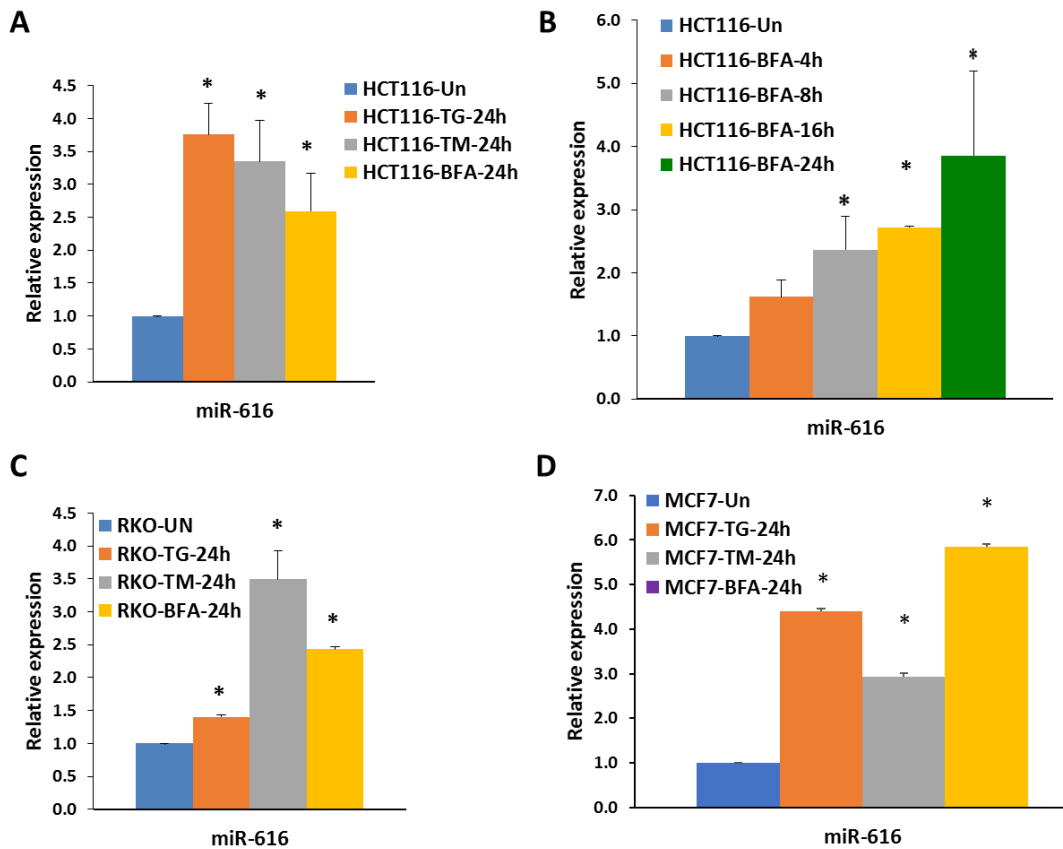


**Figure 4-4-1. MiR-616 is upregulated in colorectal and breast cancer cells during conditions of EnR stress.** The expression level of miR-616 was determined in (A) HCT116, (C) RKO and (D) MCF7 cells either untreated or treated with 1 $\mu$ M of TG, 1.0  $\mu$ g/ml of TM and 0.5 $\mu$ g/ml of BFA for 24h. (B) HCT116 cells either untreated or treated with 0.5  $\mu$ g/ml of BFA for 4, 8, 16 and 24h. Error bars represent mean  $\pm$ S.D. from three independent experiments performed in triplicate. \*P < 0.05, two-tailed unpaired t-test as compared to the untreated control.

#### 4-4-2. MiR-616 host gene (CHOP) is upregulated during conditions of EnR stress in colorectal and breast cancer cells

The CHOP is a downstream gene of the PERK arm that is located on chromosome 12 and is the host gene for miR-616. HCT116, RKO and MCF7 cells were either treated or untreated with 1 $\mu$ M of TG, 1.0  $\mu$ g/ml of TM and 0.5 $\mu$ g/ml of BFA for different time points and CHOP expression was determined by RT-qPCR assay. As expected, the expression level of CHOP transcript was also upregulated during conditions of EnR stress (Figure 4-4-2).

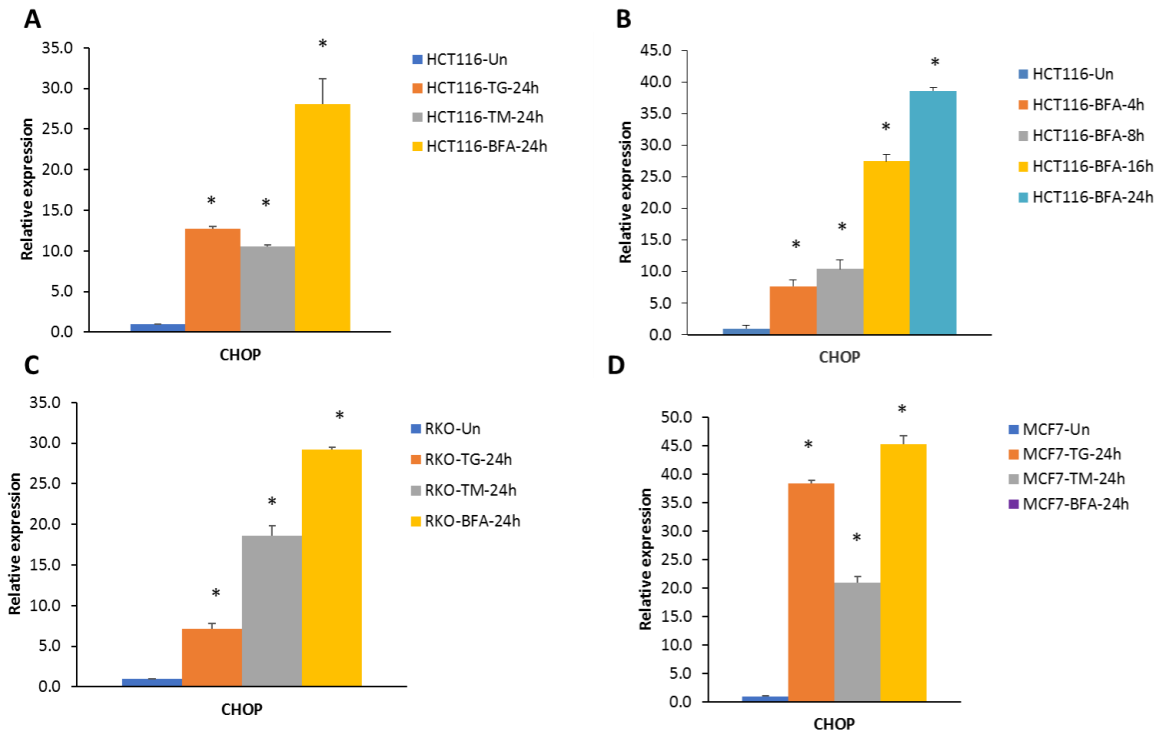


**Figure 4-4-2. CHOP (miR-616 host gene) is upregulated in colorectal and breast cancer cells during conditions of EnR stress.** The expression level of CHOP was determined in (A) HCT116, (C) RKO and (D) MCF7 cells either untreated or treated with 1 $\mu$ M of TG, 1.0  $\mu$ g/ml of TM and 0.5 $\mu$ g/ml of BFA for 24h. (B) HCT116 cells either untreated or treated with 0.5 $\mu$ g/ml of BFA for 4, 8, 16 and 24h. Error bars represent mean  $\pm$ S.D. from two independent experiments performed in triplicate. \*P < 0.05, two-tailed unpaired t-test as compared to the untreated control.

#### 4-4-3. Expression level of miR-616 in breast cancer cell lines

An endogenous level of miR-616 was determined in various breast cancer cell lines including luminal A (MCF7 and T47D), luminal B (BT474), triple negative (MDA-MB-231) and HER2 positive (SKBR3). Our results showed that the endogenous level of miR-616 is lower in MCF7, T-47D, MDA-MB-231 and SKBR3 cells compared to the MCF10 A cells. There was no significant difference in miR-616 expression in BT-474 cells compared to the MCF10 A cells (Figure 4-4-3).

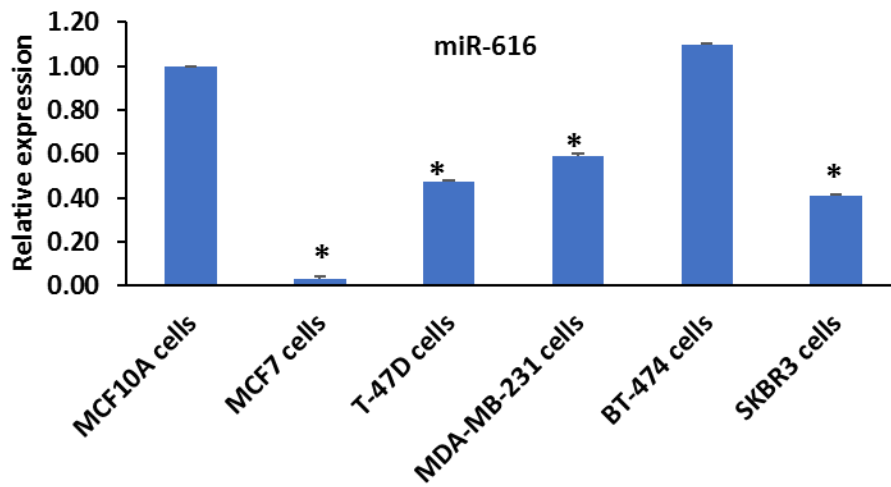


**Figure 4-4-3. Endogenous level of miR-616 in breast cancer cell lines.** The expression level of miR-616 was determined in various breast cancer cells compared to non-tumorigenic epithelial mammary gland cells (MCF10A). Error bars represent mean  $\pm$ S.D. from two independent experiments performed in triplicate. \*P < 0.05, two-tailed unpaired t-test as compared to the control.

#### 4-4-4. PERK is required for regulation of primary miR-616 during conditions of EnR stress

To check the role of UPR arms in the regulation of miR-616, the expression level of miR-616 was quantified in HCT116 knockdown cells (HCT116-ATF6-KD, -PERK-KD and -XBP1-KD) during conditions of EnR stress. HCT116 knockdown cells were either untreated or treated with 0.5µg/ml of BFA for 24 hours. Our RT-qPCR assay results showed that the UPR arms do not have any effect on mature miR-616 expression while the expression of primary miR-616 was reduced in HCT116 PERK knockdown cells compared to the control cells (Figure 4-4-4-1).

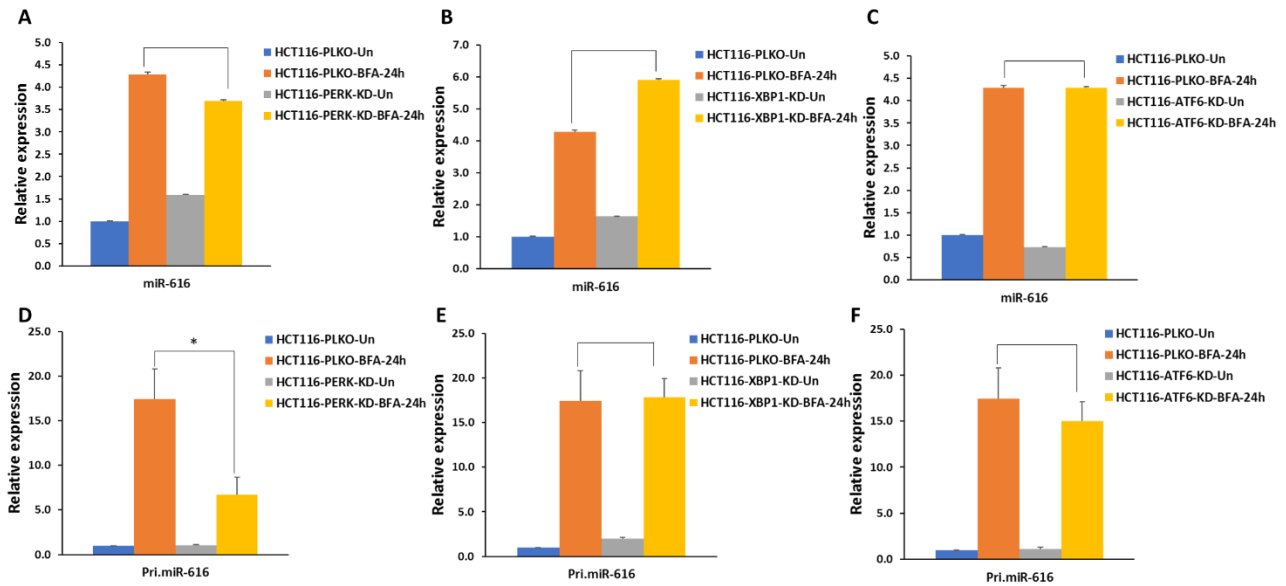


**Figure 4-4-4-1. PERK is required for regulation of primary miR-616.** HCT116 knockdown cells were either untreated or treated with 0.5µg/ml of BFA for 24h. The expression level of miR-616 was determined in HCT116 knockdown cells of (A) PERK, (B) XBP1 and (C) ATF6. The expression level of primary miR-616 was also determined in HCT116 knockdown cells of (D) PERK, (E) XBP1 and (F) ATF6. Error bars represent mean ±S.D. from three independent experiments performed in triplicate. \*P < 0.05, two-tailed unpaired t-test as compared to the untreated control.

To further investigate the role of PERK in the regulation of primary miR-616, the expression level of mature miR-616 and primary miR-616 were also quantified in the presence of PERK inhibitor during a UPR activation. HCT116 cells were either untreated or treated with 0.5µg/ml of BFA, 100nM and 300 nM of PERK inhibitor for 24 hours. First, the efficacy of PERK inhibitor compound was confirmed by measuring the expression level of PERK, ATF4, CHOP and GRP78. Then the expression level of primary and mature miR-616 was determined in these cells. Our results showed that the expression level of primary miR-616 reduced in BFA + PERK inhibitor-treated cells compared to the BFA treated cells whereas the expression level of mature miR-616 stayed high in both BFA and PERK inhibitor-treated cells (Figure 4-4-4-2).

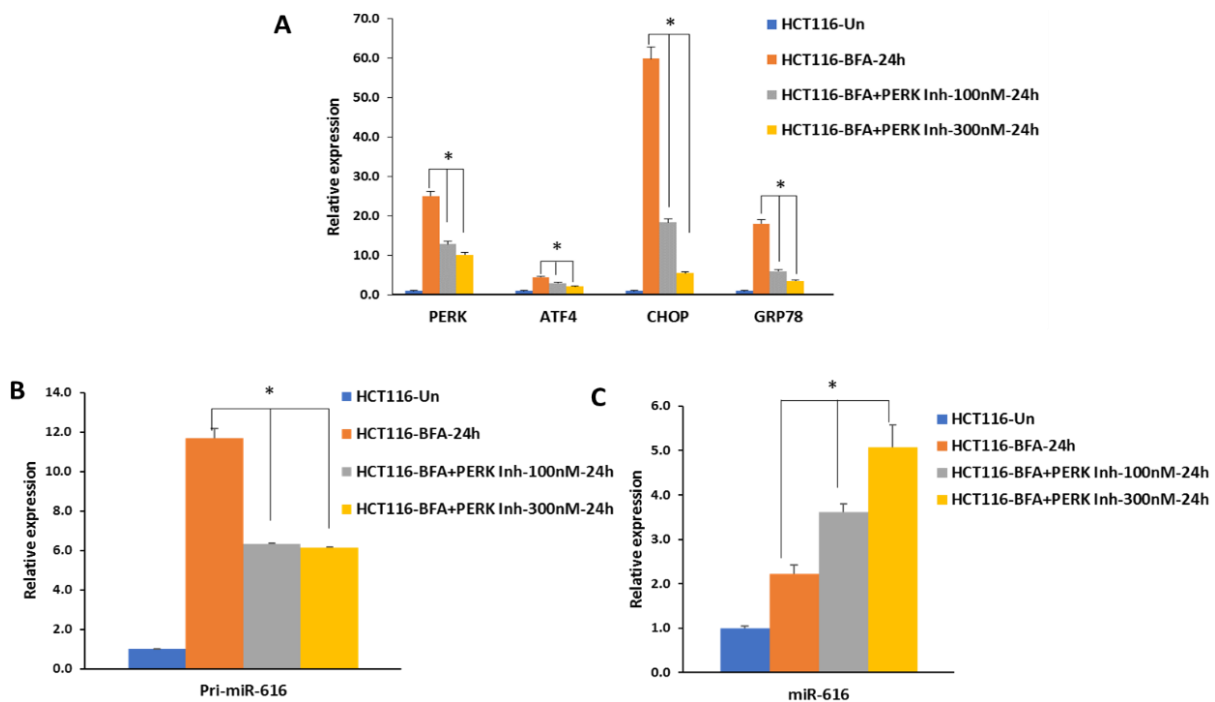


**Figure 4-4-4-2. PERK is required for regulation of primary miR-616 but not for miR-616 during conditions of EnR stress.** HCT116 cells were either untreated or treated with 0.5µg/ml of BFA, 100nM and 300 nM of PERK inhibitor for 24 hours. The expression level of (A) four UPR-target genes (PERK, ATF4, CHOP and GRP78), (B) primary miR-616 and (C) miR-616 was quantified by RT-qPCR assay. Error bars represent mean  $\pm$ S.D. from three independent experiments performed in triplicate. \*P < 0.05, two-tailed unpaired t-test as compared to the untreated control.



#### 4-4-5. Generation of stable overexpressing miR-616 pools in colorectal and breast cancer cells

To study the effect of miR-616 on cancer cells, precursor miR-616 was stably expressed in colorectal (HCT116) and breast cancer (MCF7, ZR-75-1 and MDA-MB-231) cells using a lentivirus vector (Figure 4-4-5-1). Overexpression of miR-616 was confirmed by fluorescence microscopy imaging and RT-qPCR assay to check the expression of GFP and the CT value of miR-616, respectively (Figure 4-4-5-2).

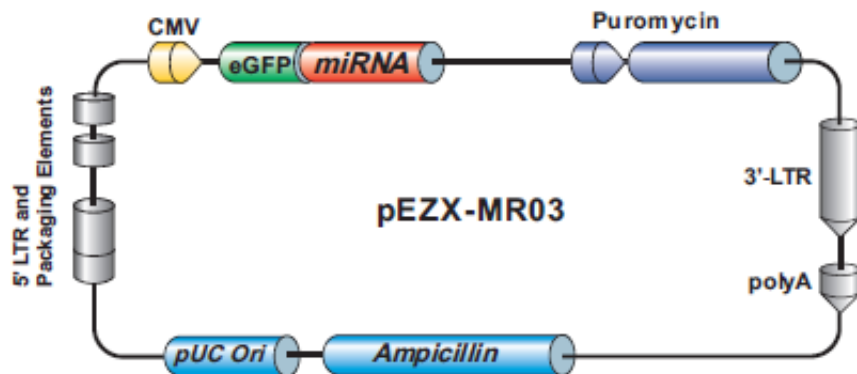


**Figure 4-4-5-1.** Schematic image of the lentivirus vector map for cloning and expression of precursor miR-616 in colorectal and breast cancer cells.

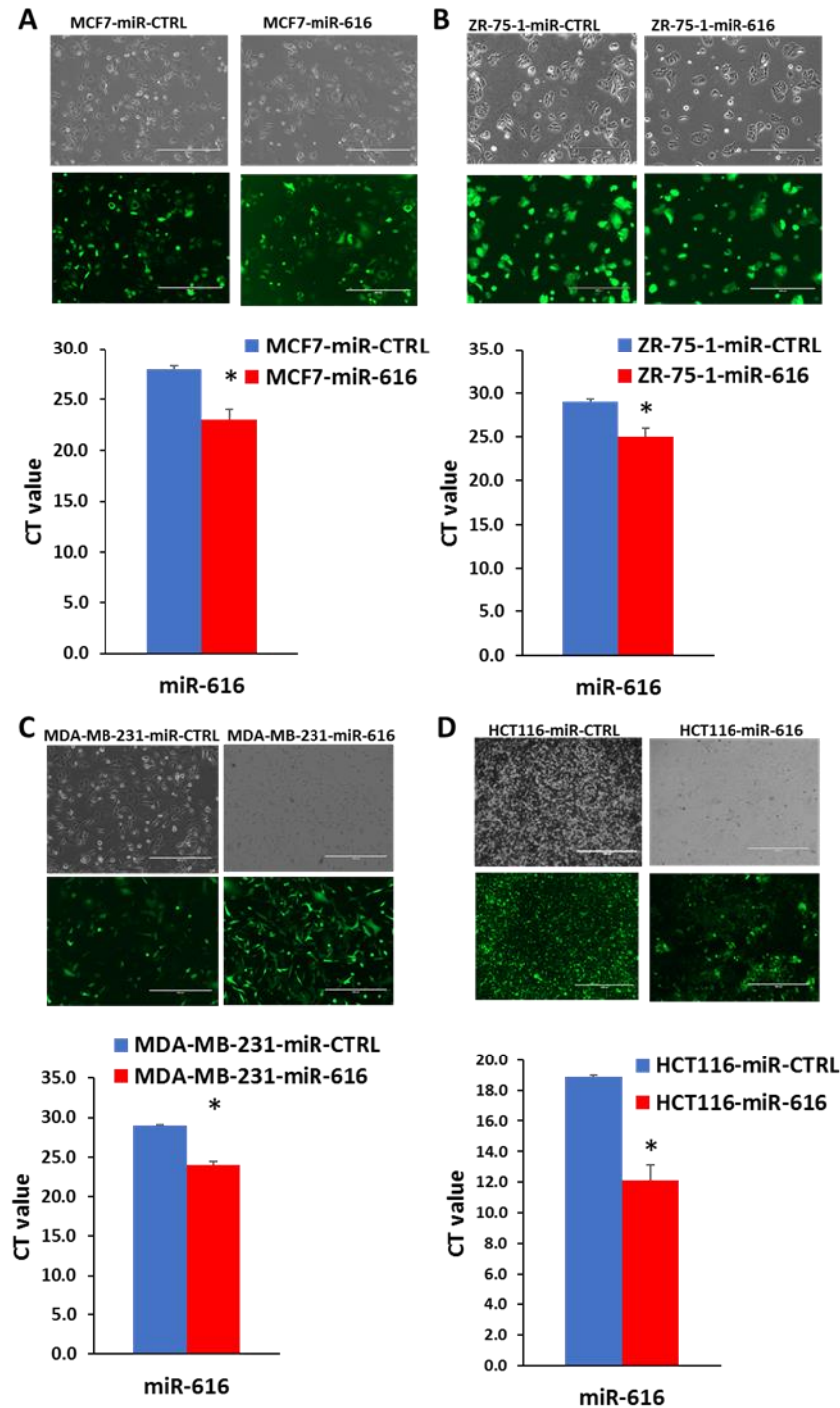


**Figure 4-4-5-2. Generation of stable overexpressing miR-616 pools in colorectal and breast cancer cells.** Precursor miR-616 was transduced in cancer cells using the lentivirus vector. The expression of miR-616 was determined by fluorescence microscopy imaging (for GFP expression) and RT-qPCR assay (CT values) in (A) MCF7, (B) ZR-75-1, (C) MDA-MB-231, and (D) HCT116 cells. RNU6B was used as a reference gene to normalise the CT values. Error bars represent mean  $\pm$ S.D. from two independent experiments performed in triplicate. \* $P < 0.05$ , two-tailed unpaired t-test as compared to the control.

#### 4-4-6. MiR-616 reduced proliferation of colorectal and luminal breast cancer cells

To determine the effect of miR-616 on cancer cell growth, HCT116 (colorectal), MCF7, ZR-75-1 and MDA-MB-231 cells ( $2 \times 10^3$  cells/well) were plated in 96 well plates and MTS cell proliferation assay was performed. We showed that miR-616 significantly decreased the cell proliferation of HCT116, MCF7 and ZR-75-1 cells. However, it had no effect on MDA-MB-231 cell growth (Figure 4-4-6).

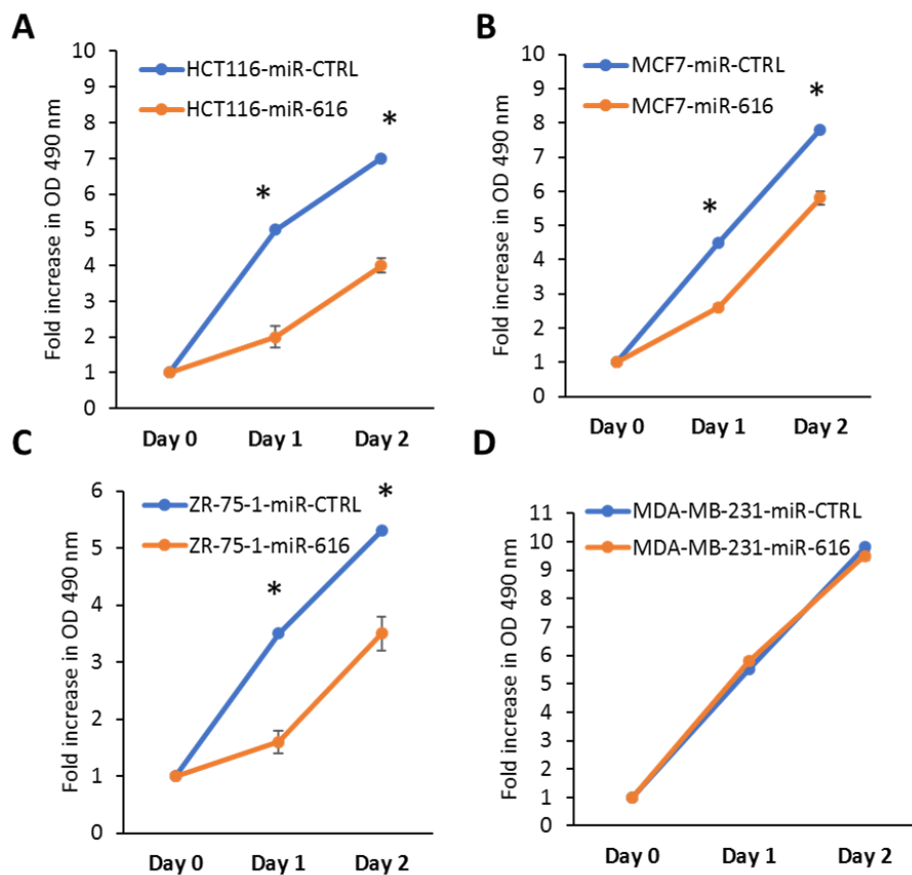


**Figure 4-4-6. The effect of miR-616 on cell proliferation of colorectal and breast cancer cells.** (A) HCT116, (B) MCF7, (C) ZR-75-1 and (D) MDA-MB-231 cells ( $2 \times 10^3$  cells/well) were plated in 96 well plates. Cell proliferation was assessed by MTS assay at indicated time points. Error bars represent mean  $\pm$ S.D. from two independent experiments performed in triplicate. \*P < 0.05, two-tailed unpaired t-test as compared to the control.

#### 4-4-7. MiR-616 reduced colony formation of colorectal and luminal breast cancer cells

The capacity of overexpressed miR-616 cancer cells to form a colony of 50 or more cells from single cells was assessed by colony formation assay. In this experiment, HCT116 (colorectal), MCF7, ZR-75-1 (luminal A) and MDA-MB-231 (triple negative) cells ( $1 \times 10^3$  cells/well) were plated in 6 well plates and cultured for 14 days. Then, cells were fixed (10% formaldehyde) and stained with 0.5 % crystal violet (Figure 4-4-7-1). The number of colonies was counted in five random view fields under a microscope and an average number of colonies was achieved. The colony sizes and numbers were also quantified by Image J software. We found that miR-616 reduced colony formation in HCT116, MCF7 and ZR-75-1 cells but it did not change colony formation of MDA-MB-231 cells (Figure 4-4-7-2).

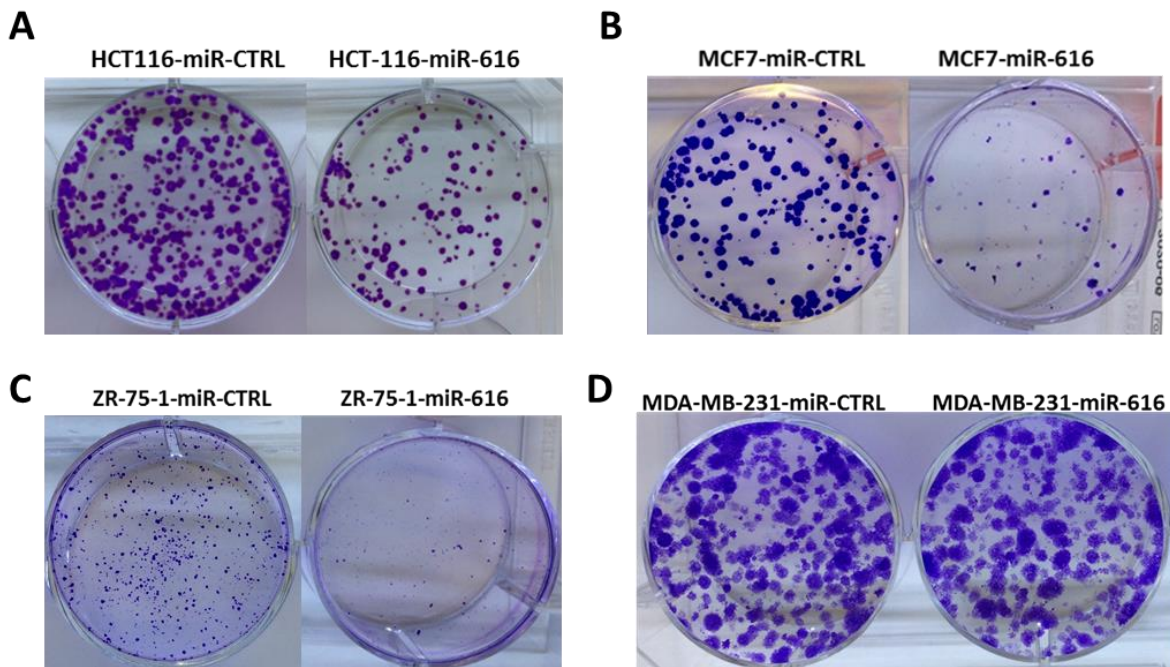


**Figure 4-4-7-1. The effect of miR-616 on colony formation of colorectal and breast cancer cells.** Cancer cells ( $1 \times 10^3$  cells/well) were plated in 6 well plates and cultured for 14 days. Cells were fixed (10% formaldehyde) and stained with 0.5 % crystal violet. Colony formation was assessed by imaging of colonies in (A) HCT116, (B) MCF7, (C) ZR-75-1 and (D) MDA-MB-231 cells.

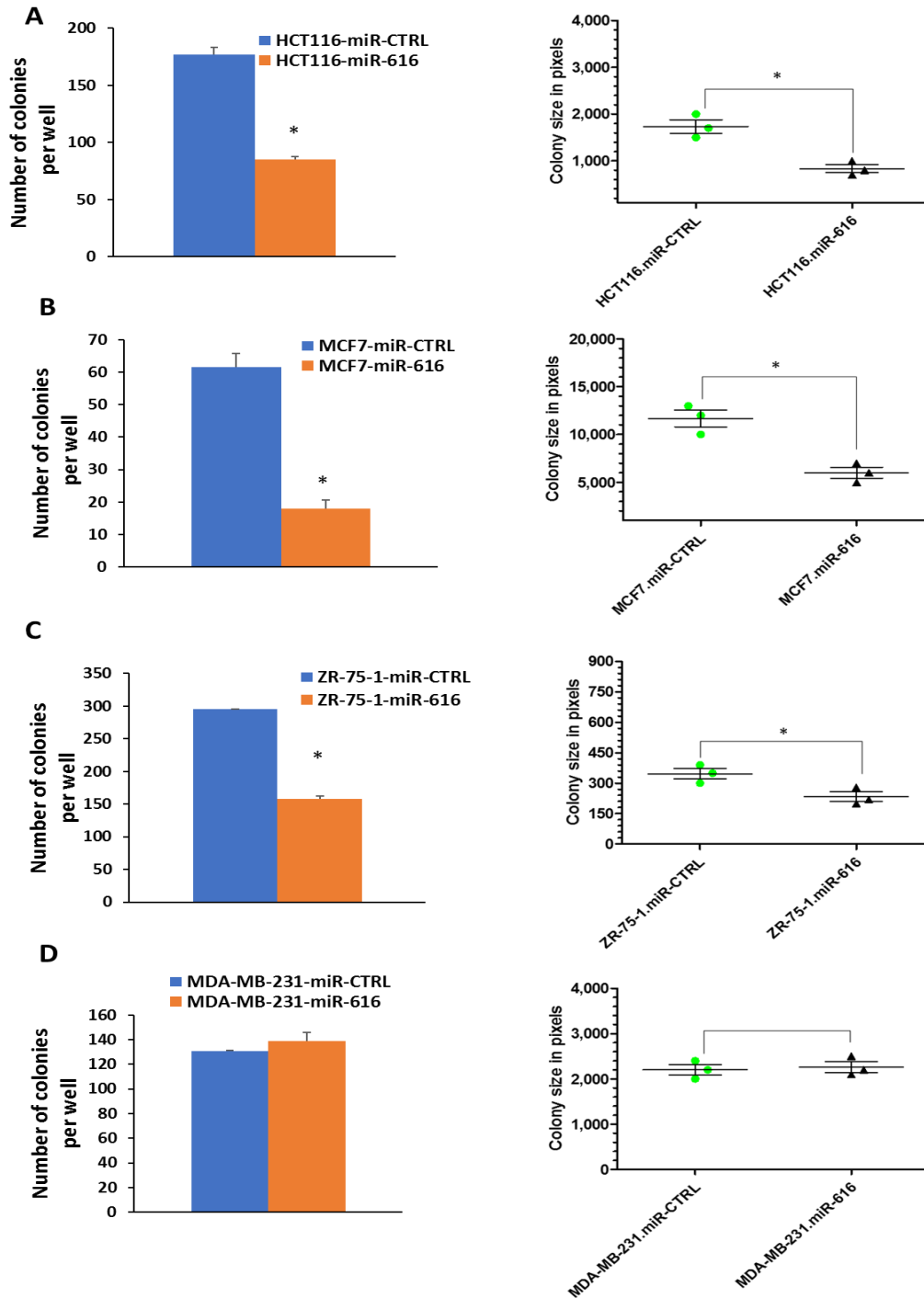


**Figure 4-4-7-2. The effect of miR-616 on the size and number of colorectal and breast cancer cells.** Average of colony numbers and colony sizes from the colony formation assay were determined in (A) HCT116, (B) MCF7, (C) ZR-75-1 and (D) MDA-MB-231 cells using Image J software. Error bars represent mean  $\pm$ S.D. from two independent experiments performed in triplicate. \* $P < 0.05$ , two-tailed unpaired t-test as compared to the control.

#### **4-4-8. MiR-616 reduced migration of colorectal and luminal breast cancer cells**

To study the effect of miR-616 on cancer cell migration, a scratch wound healing assay was performed. HCT116 (colorectal), MCF7, ZR-75-1 (luminal A) and MDA-MB-231 (triple negative) cells ( $3 \times 10^5$  cells/well) were plated in 6 well plates. After 24 hours of growth, when the cells reached 70-80% confluency, the cell monolayer was scratched with a sterile 0.2 ml pipette tip across the centre of the well. The scratch areas were then imaged at the indicated time point and quantified by Image J software. Our results showed that miR-616 decreased cell migration of HCT116, MCF7 and ZR-75-1 cells while it increased migration of the MDA-MB-231 cells (Figure 4-4-8).

Population doubling time (PDT) for MCF7, HCT116, ZR-75-1 and MDA-MB-231 cells is approximately 29 h, 22 h, 80 h and 25-30 h respectively. Considering these doubling times, it was concluded that healing of the wound in these miR-616 expressing MCF7, HCT116 and ZR-75-1 cells at early time points were mainly due to migration whereas at later time points this effect was the combination of both migration and proliferation.



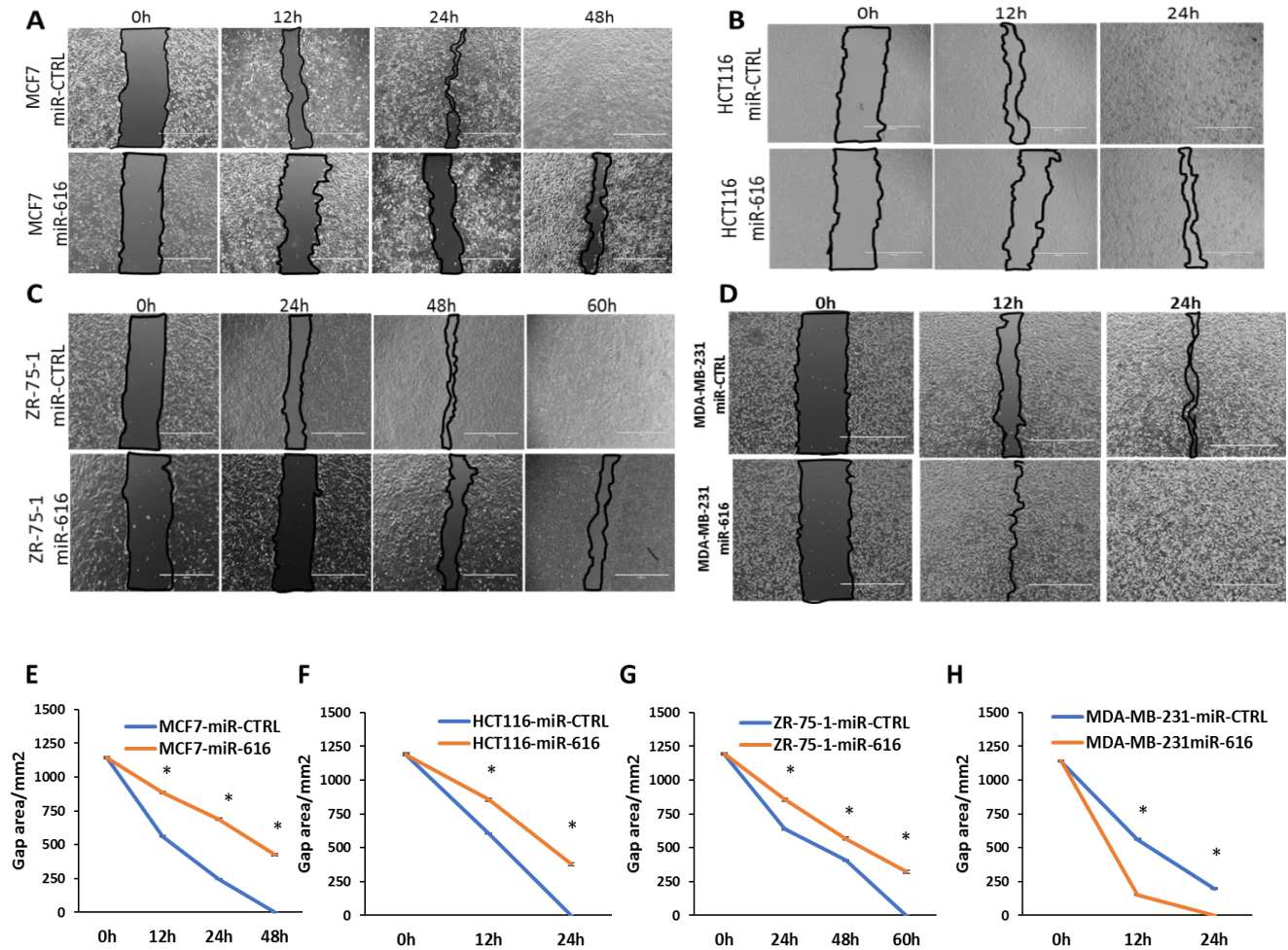


**Figure 4-4-8. The effect of miR-616 on migration of colorectal and breast cancer cells.** Control and overexpressing miR-616 cells ( $3 \times 10^5$  cells/well) were plated in 6 well plates. Confluent monolayer of cells were scratched by a 0.2 ml pipette tip and migration of cells into the wound was observed at the indicated time points. Representative images show the scratch in (A) MCF7, (B) HCT116, (C) ZR-75-1 and (D) MDA-MB-231 cells at indicated time points. The graphs show the gap area ( $\text{mm}^2$ ) in (E) MCF7, (F) HCT116, (G) ZR-75-1 and (H) MDA-MB-231 cells. Error bars represent mean  $\pm$  S.D. from two independent experiments performed in triplicate. \* $P < 0.05$ , two-tailed unpaired t-test as compared to the control.

#### 4-4-9. MiR-616 enhanced the sensitivity of MCF7 cells towards the anti-estrogen compounds

Next, we determined the role of miR-616 in response to anti-estrogens. For this we tested the effect of miR-616 on the sensitivity against (tamoxifen) SERMs and (fulvestrant) SERDs. Control and miR-616 expressing MCF7 cells ( $2 \times 10^3$  cells/well) were plated in 96 well plates and after 24 hours were either untreated or treated with 10 $\mu$ M tamoxifen and 100 $\mu$ M fulvestrant for 24, 48 and 72 hours. After the indicated time point, 0.02 ml of the MTS solution was directly added to each well and incubated at 37°C for 4 hours. The absorbance of each well was measured at OD=490 nm with a 96-well plate reader. A cell viability assay showed that tamoxifen and fulvestrant treatment significantly repressed the growth of miR-616 expressing MCF7 cells as compared to the control cells (Figure 4-4-9).

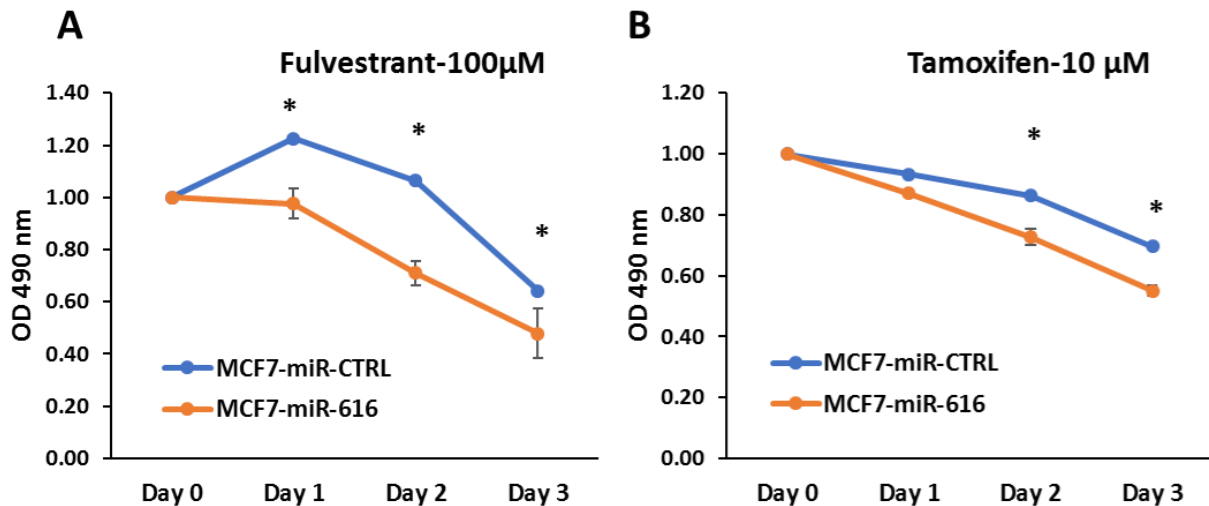


**Figure 4-4-9. The effect of miR-616 on MCF7 cells response to the anti-estrogen compounds.** Control and miR-616 expressing MCF7 cells ( $2 \times 10^3$  cells/well) were plated in 96 well plates and after 24 hours were either untreated or treated with (A) 100 $\mu$ M fulvestrant and (B) 10 $\mu$ M tamoxifen for 24, 48 and 72 hours. Cell proliferation was assessed by MTS assay at indicated time points. Error bars represent mean  $\pm$ S.D. from two independent experiments performed in triplicate. \*P < 0.05, two-tailed unpaired t-test as compared to the control.



#### **4-4-10. MiR-616 did not have any effect on the sensitivity of MCF7 cells towards the EnR stress-inducing compounds**

To study the effect of miR-616 on MCF7 cells response to the EnR stress-inducing compounds, a cell death assay was carried out by flow cytometry analysis. Control and miR-616 expressing MCF7 cells ( $2 \times 10^5$  cells/well) were plated in 6 well plates. After 24 hours of growth, cells were either treated or untreated with thapsigargin ( $1 \mu\text{M}$ ), brefeldin A ( $0.5\mu\text{g/ml}$ ) and docetaxel ( $100 \text{ nM}$ ) for 48 hours. Cells were stained with SYTOX Red and the percentage of dead cells was assessed by flow cytometry. We found that miR-616 did not have any effect on MCF7 cells sensitivity towards the EnR stress-inducing compounds. Moreover, our results showed that miR-616 decreased the MCF7 cell death towards the chemotherapeutic compound, docetaxel (Figure 4-4-10).

#### **4-4-11. MiR-616 reduced CHOP expression during conditions of EnR stress**

To determine the effect of miR-616 on UPR signalling pathway, the expression levels of four UPR target genes were quantified in HCT116 and MCF7 cells during conditions of EnR stress. Control and miR-616 expressing HCT116 and MCF7 cells were either untreated or treated with  $0.5\mu\text{g/ml}$  of BFA for 8 and 24 hours and the expression levels of GRP78, HERP, CHOP and XBP1 transcripts were quantified by real-time and conventional PCR. Our results showed that miR-616 reduced the CHOP expression in both HCT116 and MCF7 cells compared to the control cells in the context of UPR activation (Figure 4-4-11).

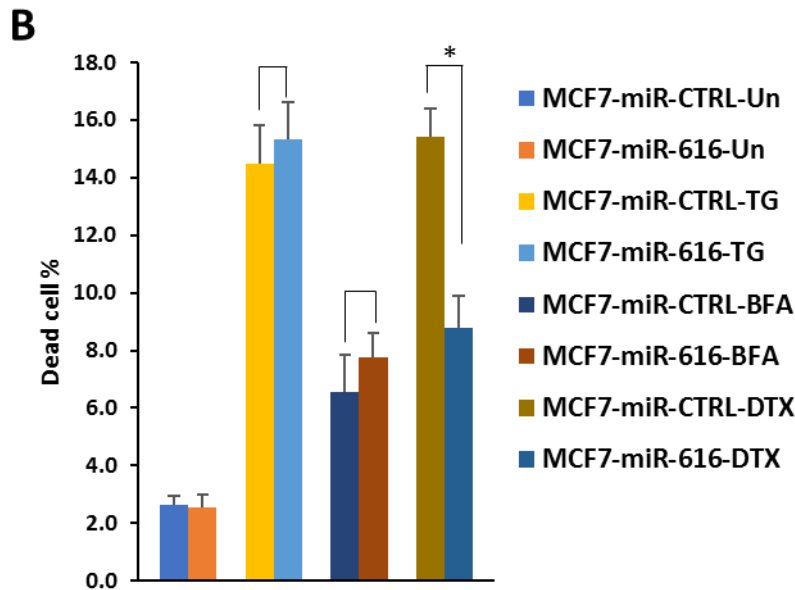
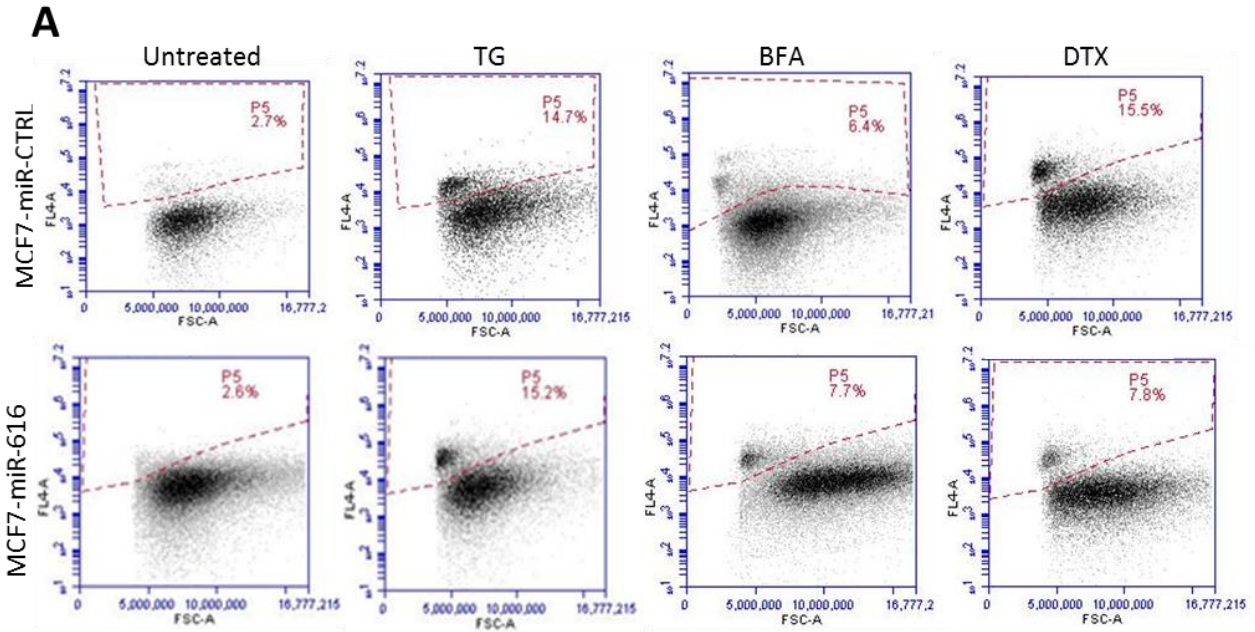


**Figure 4-4-10. The effect of miR-616 on MCF7 cells response to the EnR stress-inducing compounds.** Control and miR-616 expressing MCF7 cells were either untreated or treated with (1 $\mu$ M) TG, (0.5 $\mu$ g/ml) BFA and (100nM) DTX for 48 hours. Representative dot plot (A) and a bar graph (B) of dead cell percentage of control and miR-616 expressing MCF7 cells, stained by SYTOX Red dye, are shown. Error bars represent mean  $\pm$ S.D. from two independent experiments. \*P < 0.05, two-tailed unpaired t-test as compared to the untreated control.

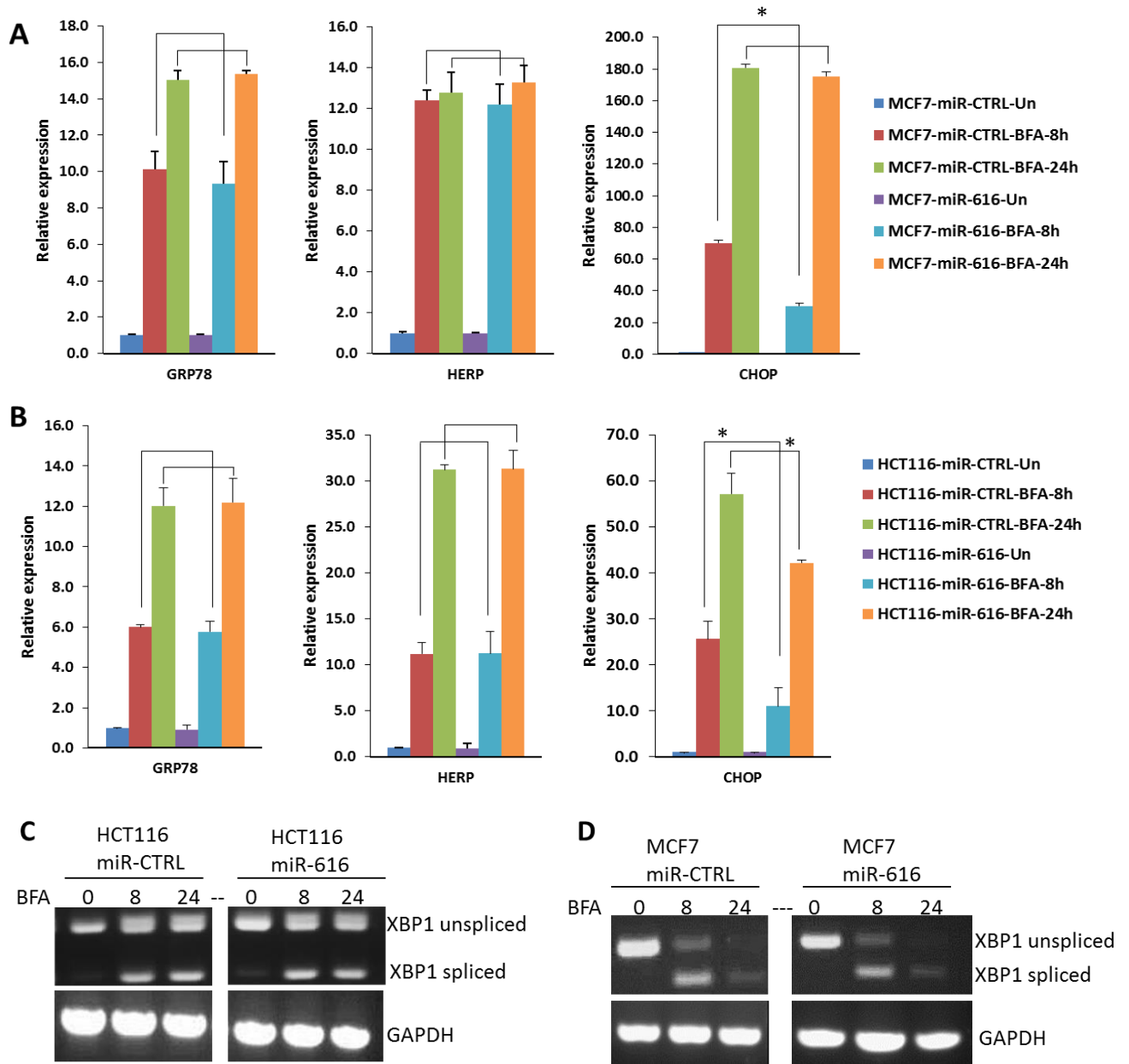


**Figure 4-4-11. MiR-616 reduced the CHOP expression during conditions of EnR stress.** Control and miR-616 expressing HCT116 and MCF7 cells were either untreated or treated with (0.5 $\mu$ g/ml) BFA for 8 and 24 hours. The change in expression levels of EnR stress markers (GRP78, HERP, and CHOP) in (A) MCF7 and (B) HCT116 cells was quantified by RT-qPCR assay. Error bars represent mean  $\pm$ S.D. from two independent experiments performed in triplicate. \* $P < 0.05$ , two-tailed unpaired t-test as compared to the untreated control. The expression level of XBP1u and XBP1s were measured in (C) HCT116 and (D) MCF7 cells by conventional PCR assay. These samples were run on a same gel, but few lanes were cropped as there were other non-relevant samples between the control and miR-616 expressing cells samples.

#### **4-4-12. MiR-616 dependent gene signature was identified by the transcriptomic and bioinformatic analysis**

To understand the mechanism of action for miR-616 on breast cancer cells, we profiled the differential transcriptome induced by miR-616 expression in MCF7 cells. For this experiment, the total RNA samples from the control and miR-616 expressing MCF7 cells (four replicates) were sent to the BGI Company for whole-genome sequencing. The most deregulated genes with log ratio more than +2 (upregulated genes) and less than -2 (downregulated genes) were chosen for bioinformatic analysis. We found that 276 genes were expressed at a significantly lower level and 610 were expressed at a significantly higher level in miR-616 expressing cells (Figure 4-4-12A-B).

On the other hand, the dependent target genes of miR-616 were predicted using MiRWalk database [377]. The selected deregulated dependent genes (obtained from transcriptomic analysis) were compared to the target genes predicted by MiRWalk database. Based on fold change in expression, function and novelty the ten short-listed genes were chosen for confirmation by RT-qPCR assay including six downregulated genes (SUSD3, GALNT14, BCL2, VAV1, MYC and LIN00052) and four upregulated genes (ALCAM, ID4, RAB6C, and SOCS2) (Figure-4-4-12 C-D and Appendix 6-12/6-13).

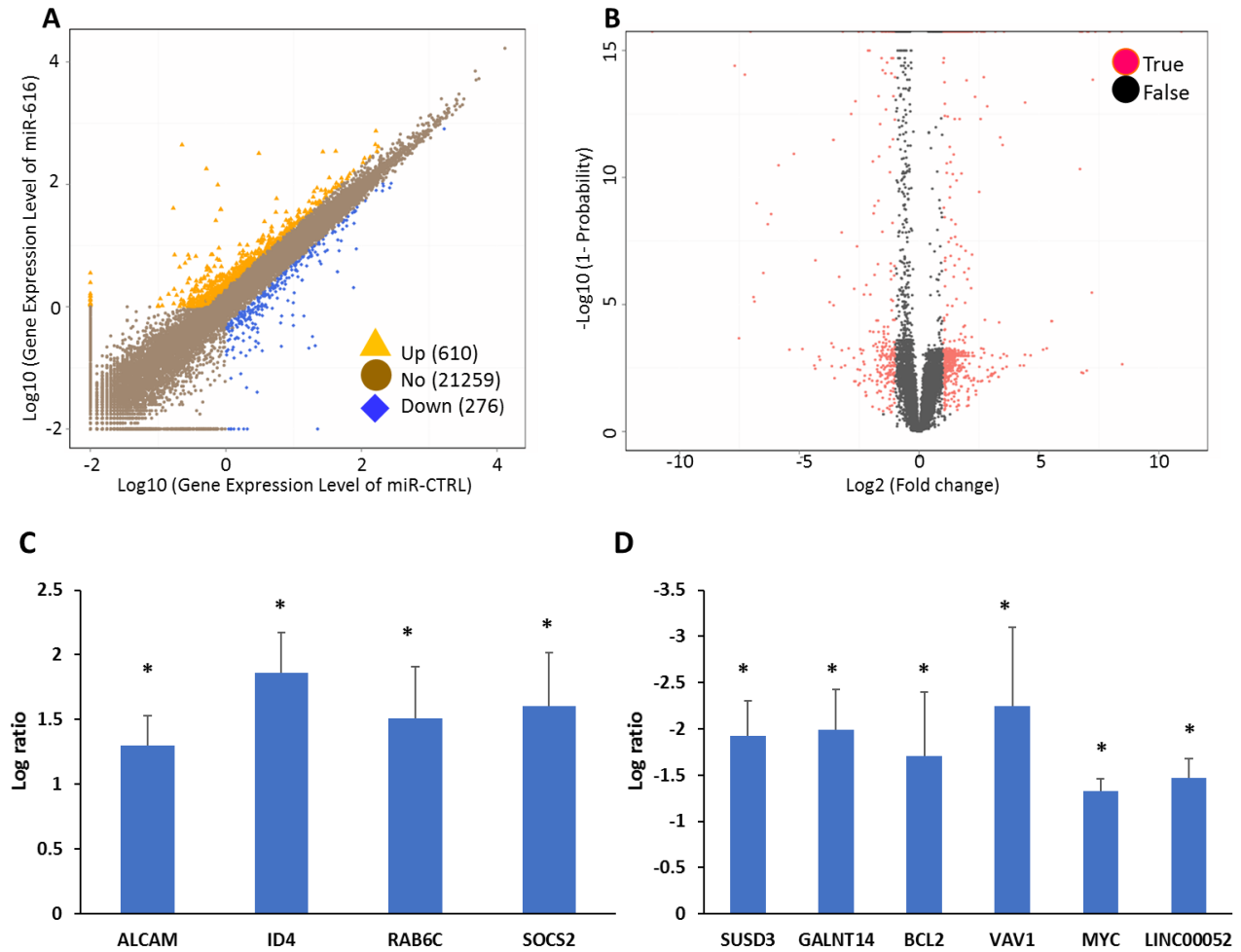


**Figure 4-4-12. Identification of miR-616 dependent gene signature.** (A) Scatter plot of expressed genes in control and miR-616 expressing MCF7 cells as determined by NOISeq method. X-axis and Y-axis present log2 value of gene expression in control and miR-616 expressing cells. (B) Volcano plot of differentially expressed genes in control and miR-616 expressing MCF7 cells. The X-axis represents the fold change and the Y-axis represents threshold value. Each dot is a differentially expressed gene. Dots in red represent significant differentially expressed genes which passed screening threshold and black dots are non-significant differentially expressed genes. The log ratio of (C) four upregulated and (D) six downregulated dependent genes of miR-616 are shown. Error bars represent mean  $\pm$  S.D. from four independent experiments performed in triplicates. \* $P < 0.05$ , two-tailed unpaired t-test as compared to the control.

#### **4-4-13. Confirmation of selected miR-616 dependent genes expression by RT-qPCR assay**

To confirm the results obtained from transcriptomic analysis, the expression levels of selected miR-616 dependent genes were confirmed in MCF7 cells (from the same RNA samples that were sent for transcriptomic analysis) by RT-qPCR assay. Our RT-qPCR result confirmed downregulation of five miR-616 regulated genes including GALNT14, BCL2, VAV1, MYC and LINC00052. We also quantified the expression level of these selected miR-616 dependent genes in ZR-75-1, MDA-MB-231 and HCT116 cells. We found that GALNT14, BCL2, VAV1, MYC and LINC00052 were downregulated in ZR-75-1 cells and BCL2, VAV1 and MYC were downregulated in HCT116 cells. There were no significant differences in the expression of these downregulated genes in MDA-MB-231 cells (Figure 4-4-13-1).

**BCL2** (B-cell lymphoma 2) is a member of the BCL family proteins that plays a key role in cell fate by inducing or inhibiting apoptosis [378]. Many published studies have investigated the role of BCL2 in cancers including breast cancer [379].

**GALNT14** (polypeptide N-acetyl-galactos-aminyl-transferase 14) is a Golgi protein that play a role in N-acetyl-D-galactosamine (GalNAc) transportation [380]. It has been reported that GALNT14 is upregulated in breast cancers and plays a crucial role in cell metastasis and proliferation [381].

**LINC00052** (long intergenic non-protein coding RNA 52) is a long non- coding RNA (lncRNA). Dysregulation of LINC00052 has been seen in several cancers including breast, gastric and hepatocellular carcinoma[382-384] .

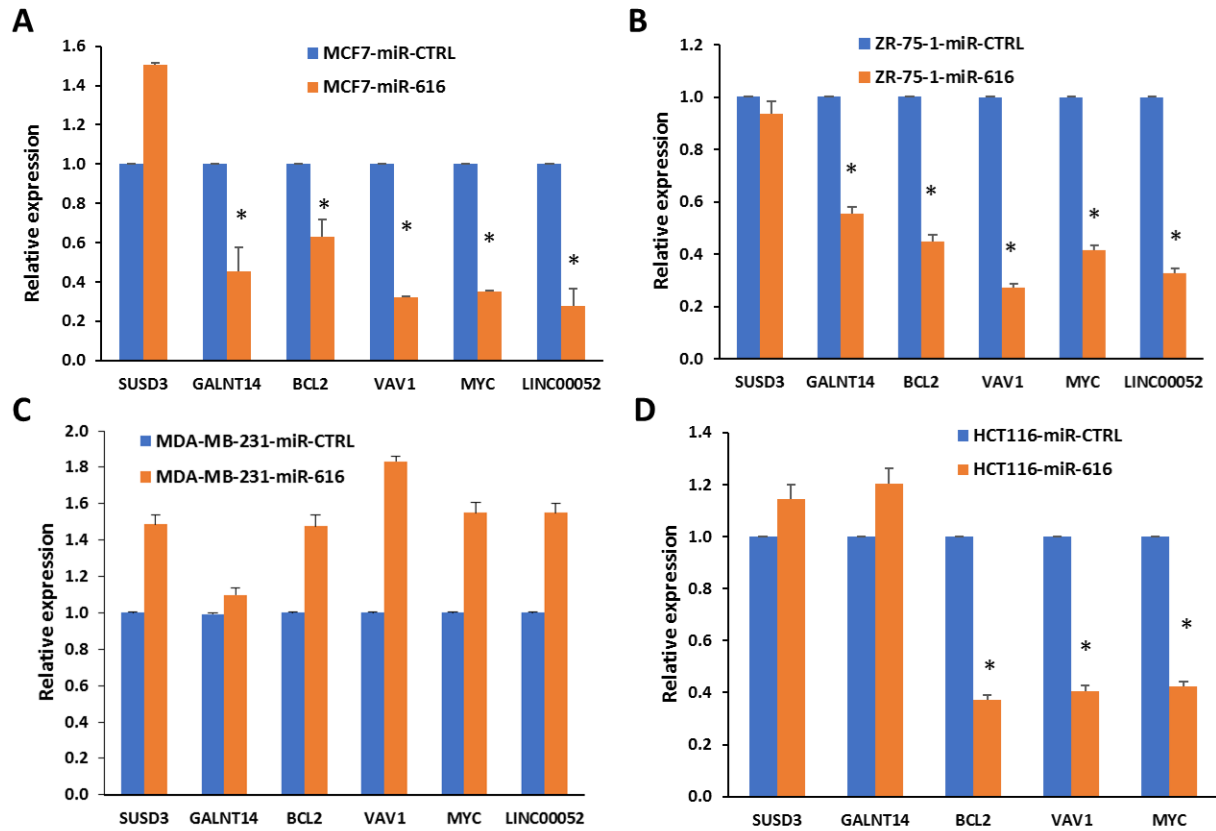


**Figure 4-4-13-1. Confirmation of downregulated miR-616 dependent genes by RT-qPCR assay.** The expression level of selected miR-616 dependent genes were quantified by RT-qPCR assay in (A) MCF7, (B) ZR-75-1, (C) MDA-MB-231 and (D) HCT116 cells. Error bars represent mean  $\pm$ S.D. from two independent experiments performed in triplicate. \* $P < 0.05$ , two-tailed unpaired t-test as compared to the control.

The expression level of two downregulated genes including VAV1 and c-MYC were determined in the control and overexpressed miR-616 cells (HCT116 and MCF7 cells) by western blot assay. Our result confirmed the downregulation of VAV1 and c-MYC proteins in these cells (Figure 4-4-13-2).

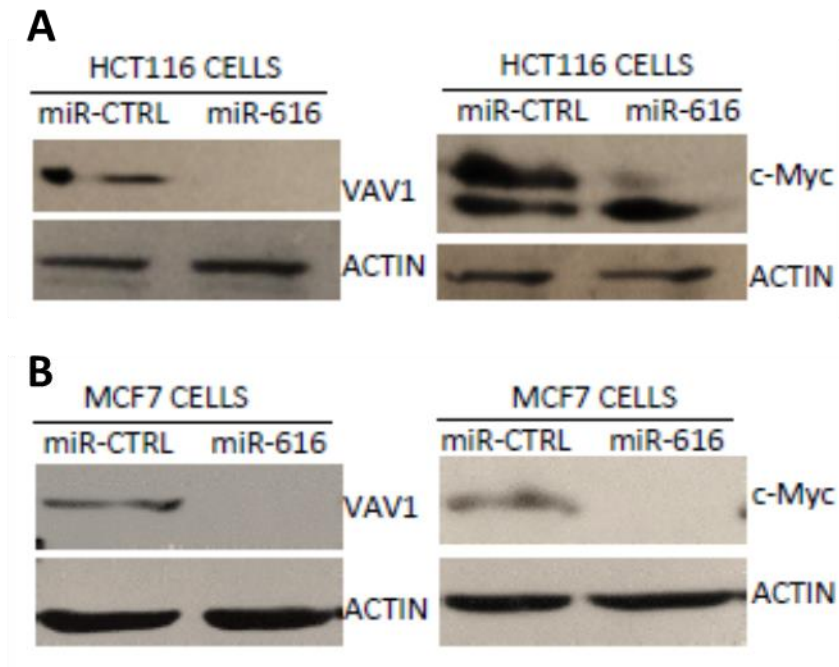


**Figure 4-4-13-2. VAV1 and c-MYC proteins are reduced in miR-616 expressing HCT116 and MCF7 cells.** The expression levels of VAV1 and c-MYC proteins were quantified by western blot assay in control and miR-616 expressing (A) HCT116 and (B) MCF7 cells using antibodies against VAV1 (size:95 K.da), c-MYC (size:67 K.da) and  $\beta$ -actin (size:42 K.da).



Moreover, the upregulated miR-616 dependent genes (ALCAM, ID4, RAB6C and SOCS2) were quantified by RT-qPCR assay. The RT-qPCR could not confirm the upregulation of these dependent genes in overexpressing miR-616 cells (MCF7, ZR-75-1, MDA-MB-231 and HCT116 cells) (Figure 4-4-13-3).

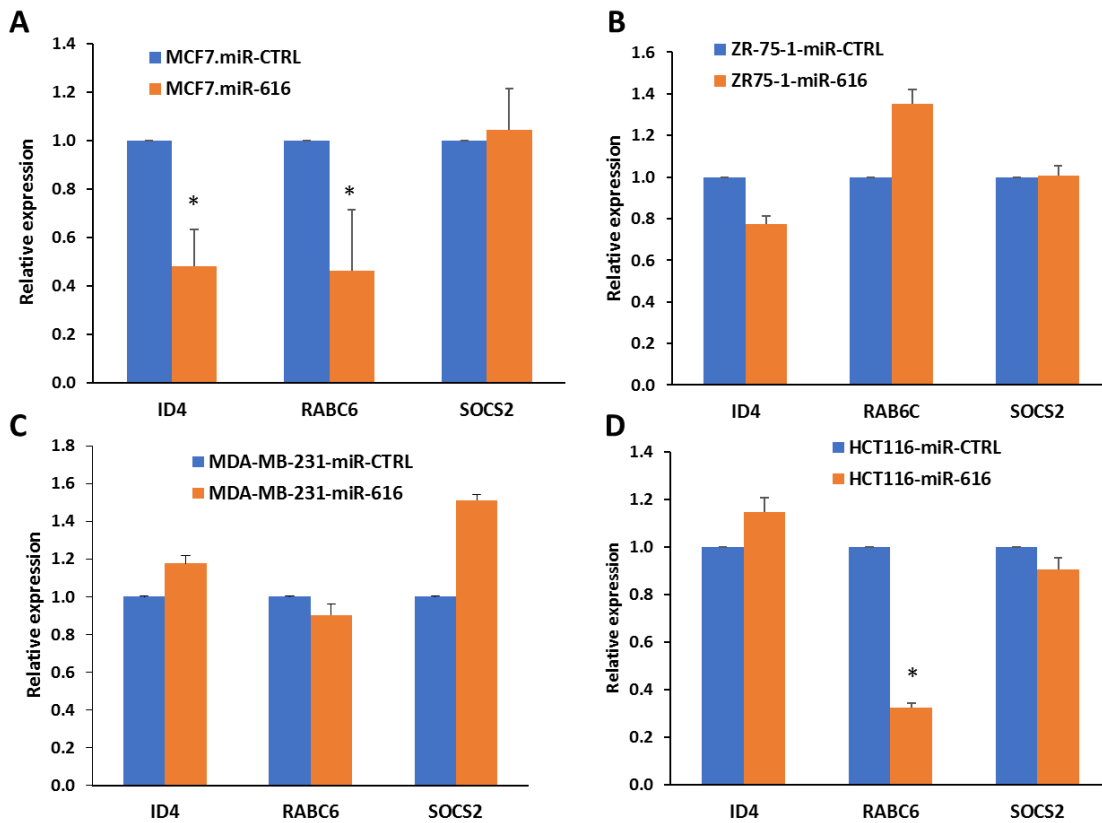


**Figure 4-4-13-3. Confirmation of upregulated miR-616 dependent genes by RT-qPCR assay.** The expression level of selected upregulated miR-616 dependent genes were quantified by RT-qPCR assay in (A) MCF7, (B) ZR-75-1, (C) MDA-MB-231 and (D) HCT116 cells. Error bars represent mean ±S.D. from three independent experiments performed in triplicate. \*P < 0.05, two-tailed unpaired t-test as compared to the control.

#### 4-4-14. MiR-616 targets the coding sequence region (CDS) of VAV1 and c-MYC transcripts

To investigate if miR-616 directly targets the 3'UTR of VAV1 and c-MYC transcripts, two algorithms including RNAHybrid (<https://bibiserv2.cebitec.uni-bielefeld.de/rnahybrid>) and TargetScan ([http://www.targetscan.org/vert\\_72/](http://www.targetscan.org/vert_72/)) were used. TargetScan did not find any binding sites in the 3'UTR of VAV1 and c-MYC transcripts. Our analysis by RNAHybrid algorithm showed that miR-616 has matching sequences in VAV1 and c-MYC transcripts but they are not located in the 3'UTR (Figure 4-4-14-1) and it seems that miR-616 targets an area which is located in the coding region (CDS).

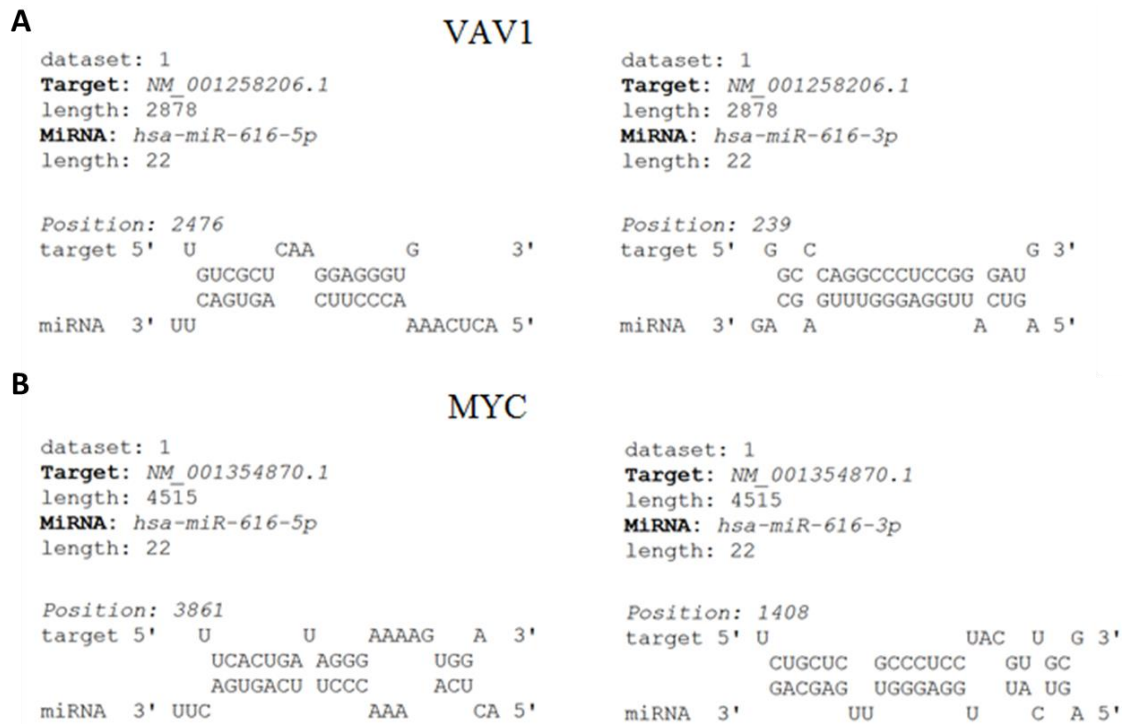


**Figure 4-4-14-1. Identification of a potential miR-616 binding site in VAV1 and c-MYC transcripts.** The RNAhybrid database was applied to identify the potential miR-616 binding site in (A) VAV1 and (B) c-MYC transcripts.

Furthermore, to determine whether miR-616 regulated the expression of c-MYC and VAV1 via the identified sites in the coding region, we co-transfected human embryonic kidney (HEK) 293T cells with an expression vector containing the coding sequence of c-MYC or VAV1 (without its 3' UTR and 5' UTR) and miR-616 plasmid. HEK 293T cells ( $2.5 \times 10^5$  cells) were plated in 6 well plates and transfected with JetPEI transfection reagent. Briefly, HEK 293T cells were either untransfected or transfected with plasmids containing VAV1 and c-MYC in the absence and presence of miR-616 expressing plasmids. 48 hours post transfection, whole cell lysates were analysed for the expression of VAV1 and c-MYC proteins by western blot assay. Our results showed that ectopic expression of c-MYC and VAV1 were strongly downregulated by co-expression of miR-616 (Figure 4-4-14-2).

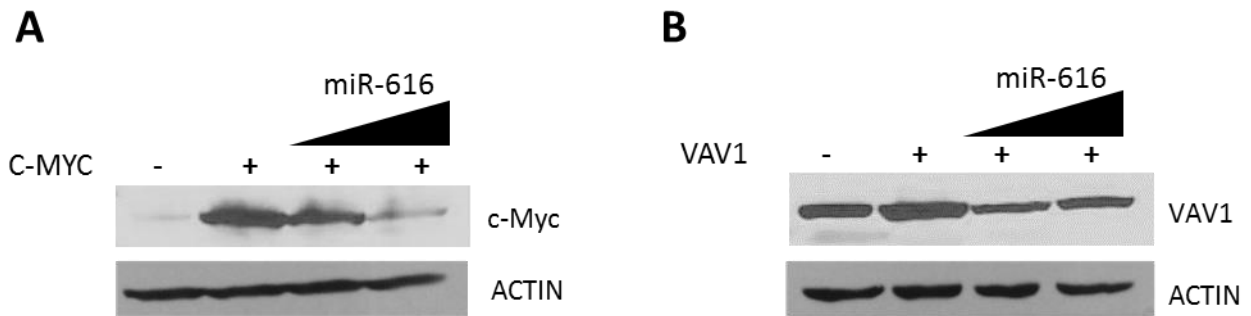


**Figure 4-4-14-2. MiR-616 targets the coding sequence region (CDS) of VAV1 and c-MYC transcripts.** HEK 293T cells ( $2.5 \times 10^5$  cells) were plated in 6 well plates and after 24 hours, cells were transfected with plasmid containing (A) c-MYC and (B) VAV1 in absence and presence of miR-616 plasmid. The expression levels of c-MYC and VAV1 proteins were quantified by western blot assay using antibodies against c-MYC (size:67 K.da), VAV1 (size:95 K.da), and  $\beta$ -actin (size:42 K.da).

#### **4-4-15. Generation of stable overexpressing VAV1 and c-MYC clones in overexpressing miR-616 MCF7 cells**

Vav guanine nucleotide exchange factor 1 (VAV1) is a member of the VAV proto-oncogene family. It is a hematopoietic guanine exchange factor for GTPase that activate some pathways causing the actin cytoskeletal rearrangements [385]. It has been found that downregulation of VAV1 in breast, lung and pancreatic cancer cells can decrease cell proliferation and reduce tumour size in mice [386-388]. MYC or BHLH transcription factor is a proto-oncogene that plays a critical role in several cellular processes such as cell cycle progression, differentiation, apoptosis and cellular transformation [389]. It has been reported that the expression of c-MYC is dysregulated in different cancer types including breast cancer [390]. In light of our results, we reasoned that c-MYC and VAV1 could be the potential functionally relevant targets that mediate tumour-suppressive effects of miR-616. If suppression of c-MYC and VAV1 by miR-616 is indeed crucial for tumour-suppressive effects of miR-616, overexpression of these proteins should rescue the effect of miR-616 on cell growth. To test this hypothesis, we transduced miR-616 expressing MCF7 cells with lentivirus that express either c-MYC and/or VAV1. Overexpression of VAV1 and/or c-MYC were confirmed by RT-qPCR assay. Our results showed the successful stable expression of VAV1 and c-MYC transcripts in these cells (Figure 4-4-15).

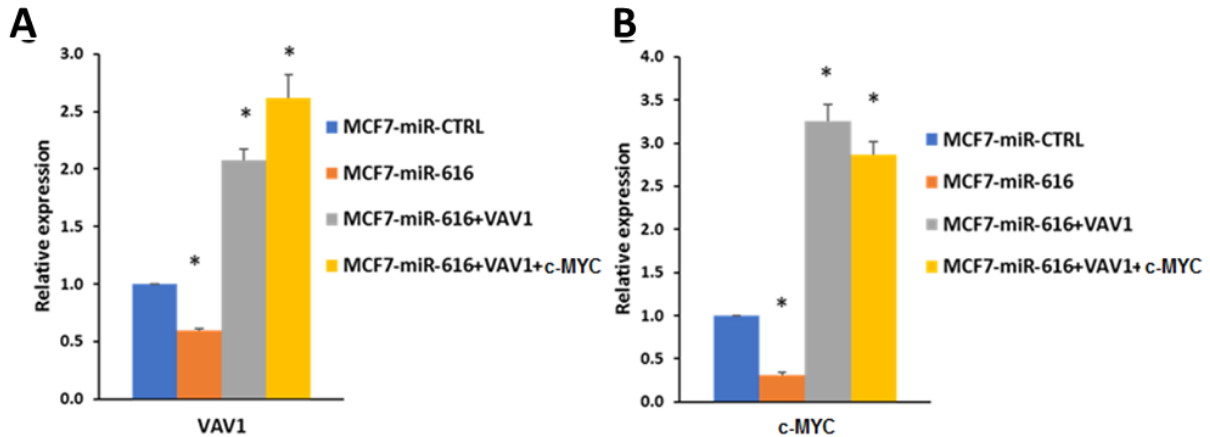


**Figure 4-4-15. Generation of stable clones expressing VAV1 and c-MYC in MCF7-miR-616 cells.** VAV1 and c-MYC transcripts were transduced in overexpressing miR-616 MCF7 clones by a lentivirus vector. The expression levels of (A) VAV1 and (B) c-MYC transcripts were quantified by RT-qPCR assay. Error bars represent mean  $\pm$ S.D. from two independent experiments performed in triplicate. \* $P < 0.05$ , two-tailed unpaired t-test as compared to the control.

#### 4-4-16. VAV1 and c-MYC reversed the growth inhibition effect of miR-616 in MCF7-miR-616 cells

To study whether VAV1 or c-MYC play a role to regulate cell growth, the MTS proliferation assay was carried out using MCF7-miR-616 clones overexpressing VAV1 and/or c-MYC. Control and MCF7-miR-616 overexpressing VAV1, c-MYC and both VAV1+ c-MYC cells ( $2 \times 10^3$  cells/well) were plated in 96 well plates. After the indicated time point, the absorbance of each well was measured at OD=490 nm with a 96-well plate reader. Our results showed that both VAV1 and/or c-MYC expression increased the proliferation of MCF7-miR-616 cells similar to the MCF7-miR-control cells (Figure 4-4-16).

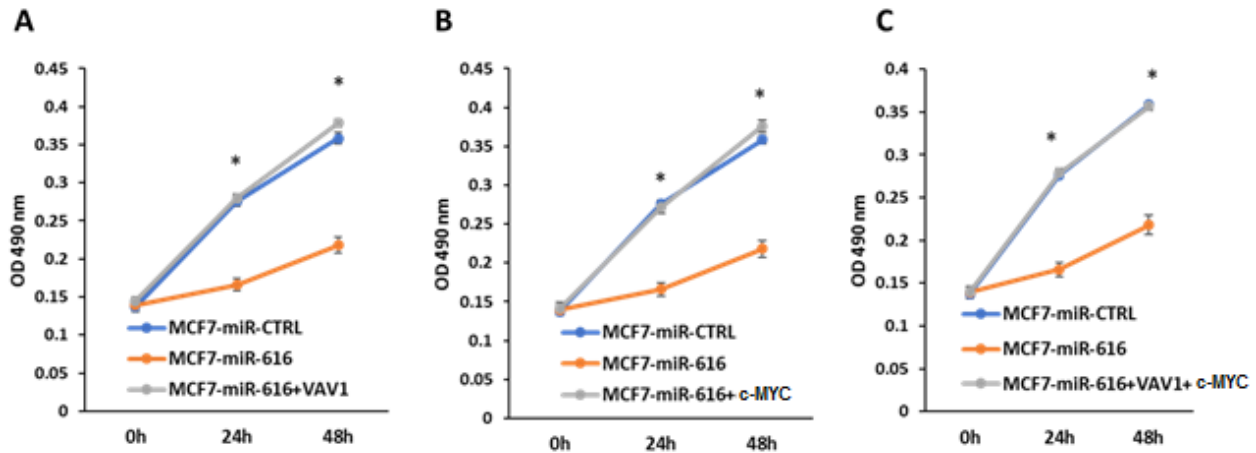


**Figure 4-4-16. The effect of VAV1 and c-MYC on miR-616 expressing MCF7 cells proliferation.** An MTS cell proliferation assay was performed in control and MCF7-miR-616 overexpressing (A) VAV1, (B) c-MYC and (C) VAV1+ c-MYC clones at indicated time points. Error bars represent mean  $\pm$ S.D. from three independent experiments performed in triplicate. \* $P < 0.05$ , two-tailed unpaired t-test as compared to the MCF7-miR-616 cells.

#### 4-4-17. VAV1 and c-MYC reversed miR-616 effect in colony formation on MCF7-miR-616 cells

To study whether suppression of c-MYC and VAV1 by miR-616 is indeed crucial for tumour-suppressive effects of miR-616, a colony formation assay was performed in MCF7-miR-616 clones overexpressing VAV1 and/or c-MYC. Control and MCF7-miR-616 overexpressing VAV1, c-MYC and both VAV1+ c-MYC cells ( $1 \times 10^3$  cells/well) were plated in 6 well plates and were cultured for 14 days. Then, cells were fixed (10% formaldehyde) and stained with 0.5 % crystal violet. The number of colonies were counted in each well and an average number of colonies were achieved from three independent experiments. The colony sizes and numbers were also determined by Image J software to quantify the results. We found that VAV1 and/or c-MYC expression increased the colony formation of MCF7-miR-616 cells, similar to the MCF7-miR-control cells (Figure 4-4-17).

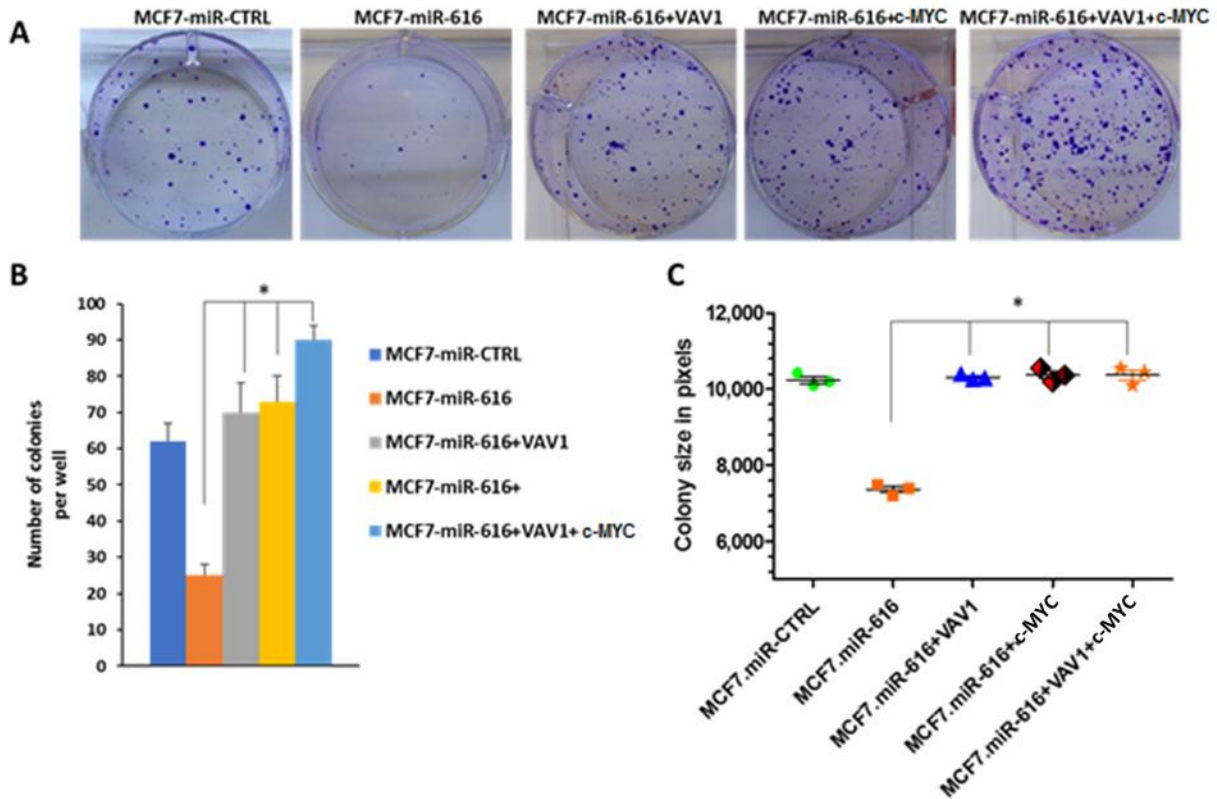


**Figure 4-4-17. The effect of VAV1 and c-MYC on MCF7-miR-616 cells colony formation.** Control and MCF7-miR-616 overexpressing VAV1, c-MYC and VAV1+ c-MYC cells ( $1 \times 10^3$  cells/well) were plated in 6 well plates and cultured for 14 days. Colony formation was assessed by (A) imaging of colonies, (B) average of colony numbers and (C) colony sizes by Image J software. Error bars represent mean  $\pm$  S.D. from three independent experiments performed in triplicate. \* $P < 0.05$ , two-tailed unpaired t-test as compared to the MCF7-miR-616 cells.

#### 4-4-18. VAV1 and c-MYC reversed miR-616 effect in migration on MCF7-miR-616 cells

To evaluate the effect of VAV1 and c-MYC on cell migration in MCF7-miR-616, a scratch wound healing assay was performed in MCF7-miR-616 clones overexpressing VAV1 and/or c-MYC. Control and MCF7-miR-616 overexpressing VAV1, c-MYC and both VAV1+ c-MYC cells ( $3 \times 10^5$  cells/well) were plated in 6 well plates. After 24 hours of growth, when the cells reached 70-80% confluency, the cell monolayer was scratched with a sterile 0.2 ml pipette tip across the centre of the well. The scratched areas were then imaged at the indicated time point and quantified by Image J software. Our results showed that VAV1 and c-MYC expression increased the cell migration of MCF7-miR-616 cells similar to the MCF7-miR-control cells (Figure 4-4-18).

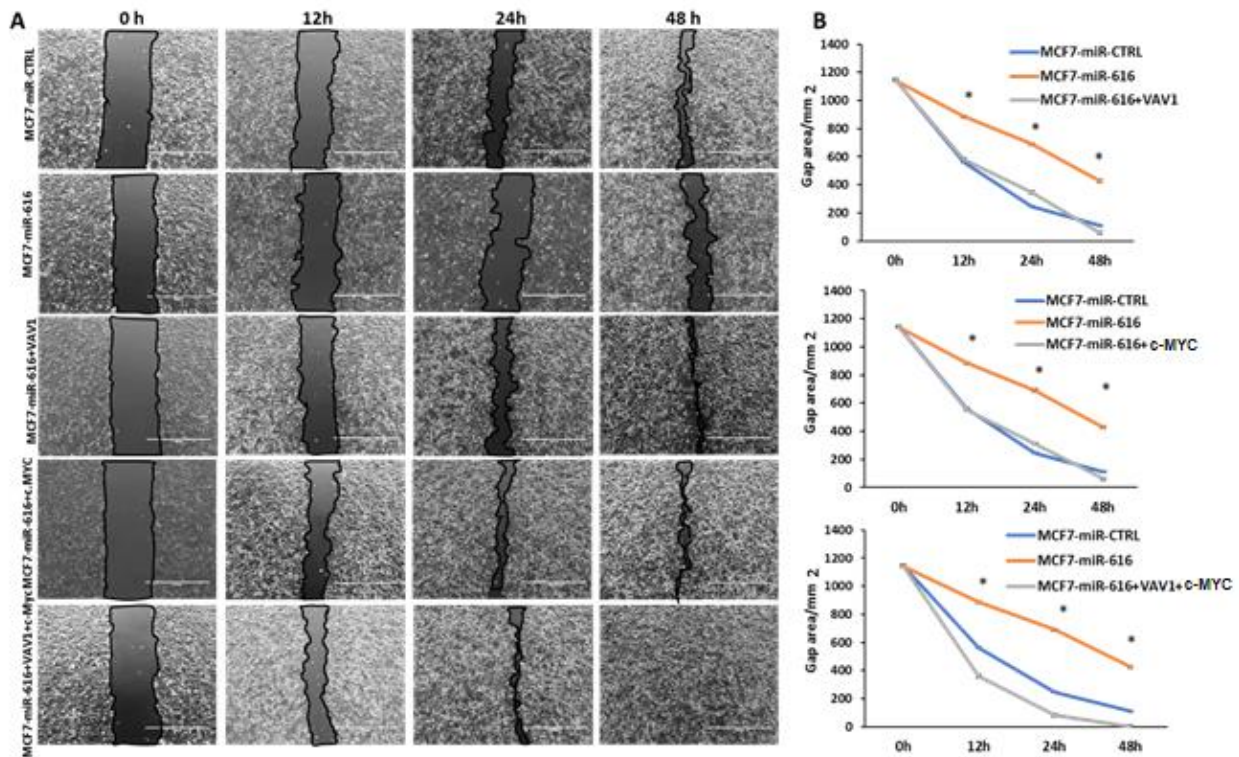


**Figure 4-4-18. The effect of VAV1 and c-MYC on MCF7-miR-616 cells migration.** control and MCF7-miR-616 overexpressing VAV1, c-MYC and VAV1+ c-MYC cells ( $3 \times 10^5$  cells/well) were plated in 6 well plates. Some confluent monolayer cells were scratched by a 0.2 ml pipette tip and migration of cells into the wound was observed after indicated time points. (A) Representative images showing the scratch at indicated time points. (B) The graphs show the gap area (mm<sup>2</sup>) in overexpressed VAV1 and c-MYC clones compared to the MCF7-miR-616 cells. Error bars represent mean  $\pm$ S.D. from three independent experiments performed in triplicate. \*P < 0.05, two-tailed unpaired t-test as compared to the control.



#### 4-4-19. Generation of stable overexpressing VAV1 and c-MYC pools in parental MCF7 cells

As a next experiment, VAV1 and c-MYC were overexpressed in parental MCF7 cells to study the effect on cell growth and proliferation. Western blot and RT-qPCR assay results confirmed stable expression of VAV1 and c-MYC in parental MCF7 cells (Figure 4-4-19). Subsequently the following functional studies were performed in these MCF7 cells overexpressing VAV1 and/or c-MYC: MTS cell proliferation, colony formation and migration assays.

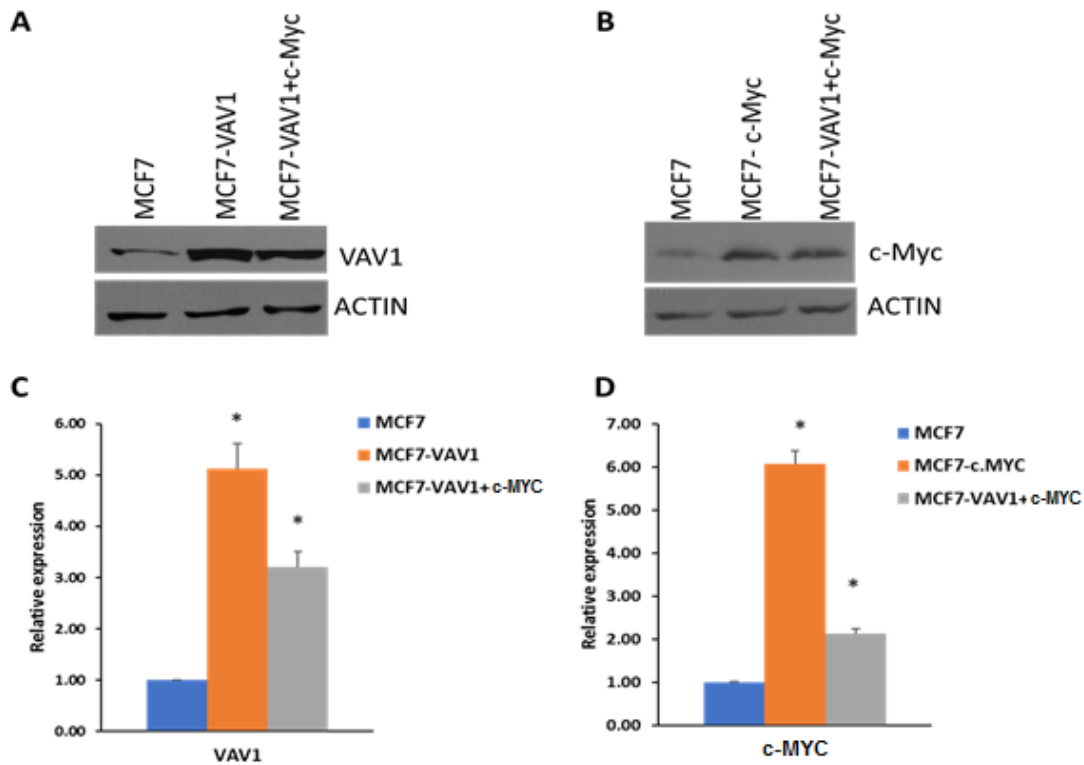


**Figure 4-4-19. Generation of stable overexpressing VAV1 and c-MYC clones in parental MCF7 cells.** VAV1 and c-MYC genes were transduced in parental MCF7 cells by lentivirus vector. The expression levels of (A) VAV1 and (B) c-MYC proteins were quantified by western blot assay using antibodies against VAV1 (size:95 K.da), c-MYC (size:67 K.da) and  $\beta$ -actin (size:42 K.da). The change in expression levels of (C) VAV1 and (D) c-MYC transcripts were quantified by RT-qPCR assay. Error bars represent mean  $\pm$ S.D. from two independent experiments performed in triplicate. \*P < 0.05, two-tailed unpaired t-test as compared to the untreated control.

#### 4-4-20. VAV1 and c-MYC increased the proliferation of parental MCF7 cells

To study the effect of VAV1 and c-MYC on MCF7 cells proliferation, an MTS assay was carried out in MCF7 cells overexpressing VAV1 and/or c-MYC. Our results showed that both VAV1 and c-MYC increased cell proliferation of parental MCF7 cells as compared to the control cells (Figure 4-4-20).

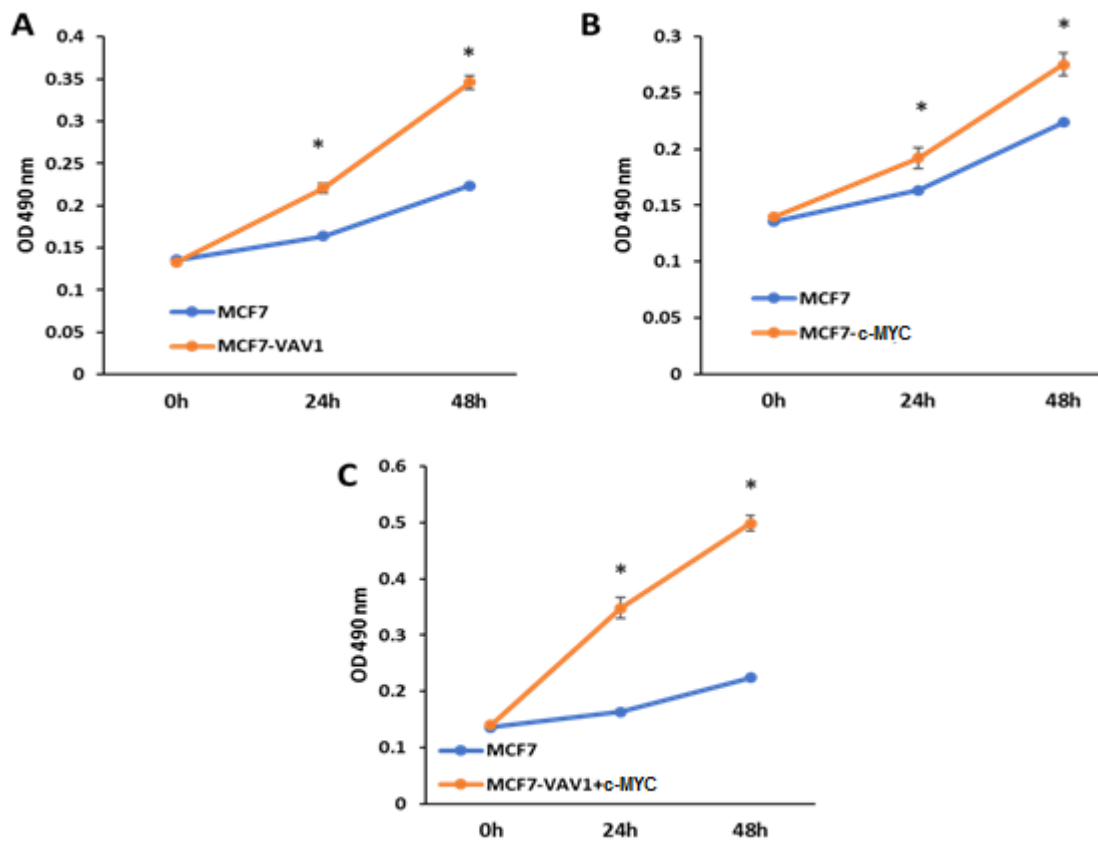


**Figure 4-4-20. The effect of VAV1 and c-MYC on parental MCF7 cells proliferation.** An MTS cell proliferation assay was performed in control and parental MCF7 cells with overexpressed (A) VAV1, (B) c-MYC and (C) VAV1+ c-MYC clones at indicated time points. Error bars represent mean  $\pm$ S.D. from three independent experiments performed in triplicate. \*P < 0.05, two-tailed unpaired t-test as compared to the MCF7-miR-616 cells.

#### 4-4-21. VAV1 and c-MYC increased colony formation of parental MCF7 cells

A colony formation assay was also performed to see the effect of VAV1 and c-MYC in parental MCF7 cells. Control and MCF7 cells overexpressing VAV1 and/or c-MYC ( $1 \times 10^3$  cells/well) were plated in 6 well plates and were cultured for 14 days. Then, cells were fixed (10% formaldehyde) and stained with 0.5 % crystal violet. The number of colonies were counted in each well and an average number of colonies was derived from three independent experiments. The colony sizes and numbers were also determined by Image J software to quantify the results. Our results showed that both VAV1 and c-MYC expression significantly increased colony formation of parental MCF7 cells (Figure 4-4-21).

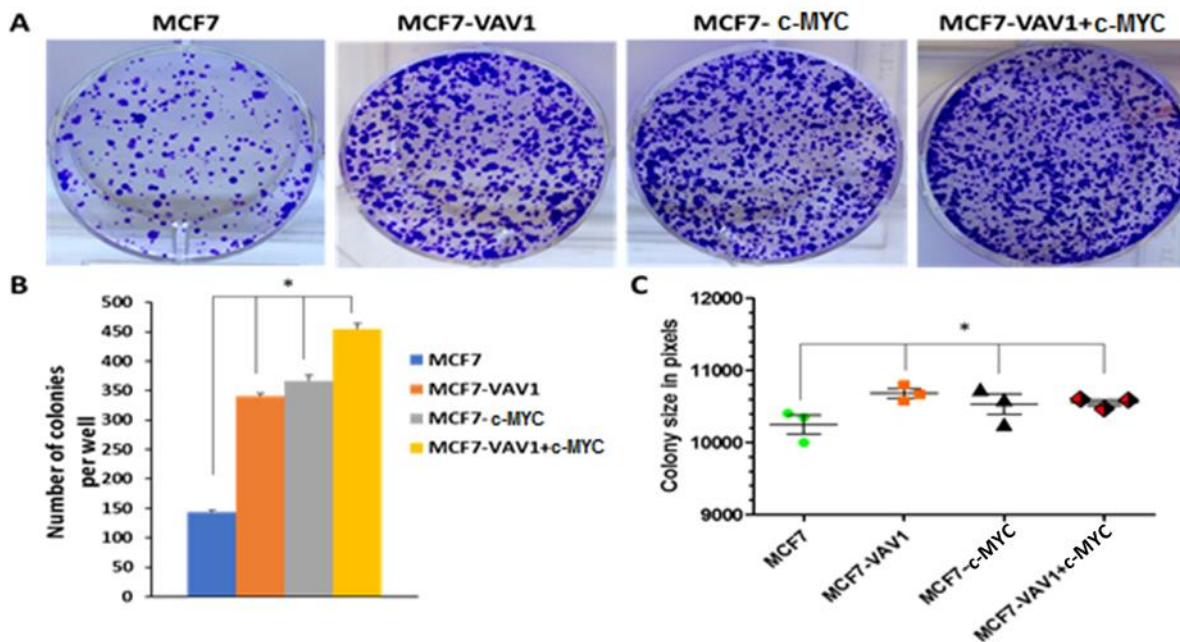


**Figure 4-4-21. The effect of VAV1 and c-MYC on parental MCF7 cells colony formation.** Control and MCF7 overexpressing VAV1, c-MYC and VAV1+ c-MYC cells ( $1 \times 10^3$  cells/well) were plated in 6 well plates and cultured for 14 days. Colony formation was assessed by (A) imaging of colonies, (B) average of colony numbers and (C) colony sizes by Image J software. Error bars represent mean  $\pm$ S.D. from three independent experiments performed in triplicate. \* $P < 0.05$ , two-tailed unpaired t-test as compared to the MCF7-miR-616 cells.

#### **4-4-22. VAV1 and c-MYC increased migration of parental MCF7 cells**

To determine the effect of VAV1 and c-MYC on cell migration of parental MCF7 cells, scratch wound healing assay was performed using MCF7 cells overexpressing VAV1 and/or c-MYC. Control and MCF7 overexpressing VAV1, c-MYC and both VAV1+ c-MYC cells ( $3 \times 10^5$  cells/well) were plated in 6 well plates. After 24 hours of growth, when the cells reached 70-80% confluency, the cell monolayer was scratched with a sterile 0.2 ml pipette tip across the centre of the well. The scratched areas were then imaged at the indicated time points and quantified by Image J software. Our results show that VAV1 and c-MYC overexpression increased cell migration in parental MCF7 cells as compared to the control cells (Figure 4-4-22).

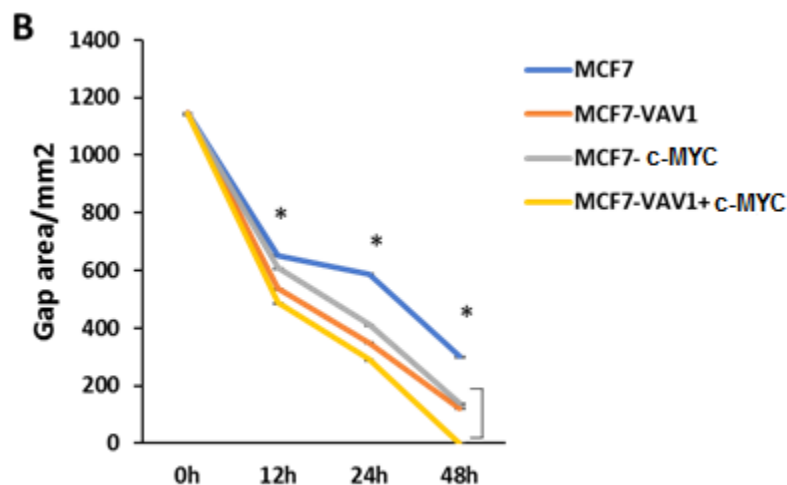
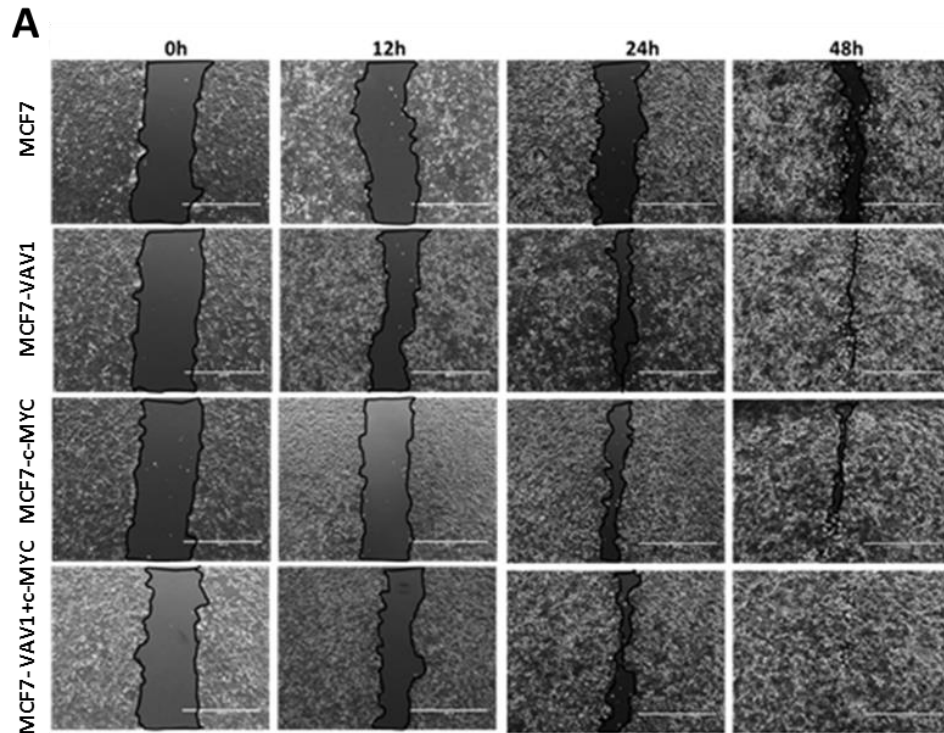


**Figure 4-4-22. The effect of VAV1 and c-MYC on parental MCF7 cells migration.** Control and MCF7 overexpressing VAV1, c-MYC and VAV1+ c-MYC cells ( $3 \times 10^5$  cells/well) were plated in 6 well plates. Confluent monolayers of cells were scratched by P-200 tip and migration of cells into the wound was observed after indicated time points. (A) Representative images show the scratch at indicated time points. (B) The graph shows the gap area (mm<sup>2</sup>) in overexpressed VAV1 and c-MYC clones compared to the control cells. Error bars represent mean  $\pm$ S.D. from three independent experiments performed in triplicate. \*P < 0.05, two-tailed unpaired t-test as compared to the control.

# Chapter 5

## **5-0. Discussion**

The work in this thesis revealed the role of two UPR-regulated miRNAs including miR-378 and miR-616 in breast cancer and during conditions of EnR stress. The first work, which is described in chapter three, showed the role of XBP1-regulated miR-378 in the regulation of breast cancer cell fate during EnR stress and UPR activation. The second work, that is explained in chapter four, found the mechanism of action of miR-616 to regulate breast cancer cells during EnR stress and UPR activation.

### **5-1. MiRNA-378 is downregulated by XBP1 and inhibits growth and migration of luminal breast cancer cells**

This study confirmed that XBP1 plays a significant role in downregulation of miR-378 and its host gene (PPARGC1B) during conditions of EnR stress. EnR stress and UPR activation play pivotal roles in the development and progression of human diseases, including neurodegenerative disorders, diabetes, obesity, cancer and cardiovascular disease [391]. XBP1 is a member of the activated transcription factor (ATF) family and a key component of the UPR [392]. Our results, showing the repression of miR-378 by XBP1, provide a mechanism for reduced expression of miR-378 in physiological and pathological conditions leading to UPR. The stressful conditions in the tumour microenvironment including low oxygen supply, nutrient deprivation, and pH changes activate a range of cellular stress-response pathways including activation of the UPR [5].

From the several dysregulated miRNAs identified by microarray during EnR stress in HCT116 colorectal cells (Figure 3-4-1-1), the nine most dysregulated miRNAs were chosen to confirm their expression by RT-qPCR assay. We confirmed that two miRNAs including miR-378 and miR-1908 are downregulated in HCT116 cancer cells upon EnR stress (Figure 3-4-1-2). We chose miR-378 for further analysis, as both microarray and RT-qPCR assays show that miR-378 is downregulated while microarray analysis shows that miR-1908 is upregulated. We found that expression of miR-378 was reduced upon treatment with three different EnR stress-inducing compounds and in multiple cancer cell lines (Figure 3-4-1-3 and 3-4-2). We concluded that downregulation of miR-378 is not cell or stimulus specific, but rather a general effect.

The pharmacological EnR stress inducers such as thapsigargin, tunicamycin and brefeldin A activate UPR through various mechanisms (Method section 2-2). The common effect of these inducers is increasing unfolded or misfolded proteins in the EnR lumen. This leads to dissociation of GRP78 from luminal domain of IRE1, PERK and ATF6 arms, resulting in activation of these three UPR arms. Physiological inducers such as hypoxia and glucose deprivation also cause accumulation of unfolded or misfolded proteins in the EnR lumen. For example, both hypoxia and glucose deprivation are commonly seen in the tumour microenvironment because of disorganised vascular formation and increased cell proliferation. The lack of glucose and oxygen increase the production of reactive oxygen species (ROS) dramatically and lead to EnR stress. It has also been reported that hypoxia activates the PERK arm through hypoxia inducible factor (HIF) independent pathways [393]. Although pharmacological and physiological inducers have different mechanisms of action to initiate EnR stress, directly or indirectly, eventually both inducers cause accumulation of unfolded or misfolded proteins in the EnR lumen and activate all three UPR branches.



We also quantified the endogenous level of miR-378 in several breast cancer cells and found that it is reduced in all breast cancer cell subtypes including luminal A (MCF7 and T-47D), triple negative (MDA-MB-231) and HER2 positive (SKBR3) cells (Figure 4-4-3). Dysregulation of miR-378 has been reported in various cancers. For instance, Megiorni and colleagues found that miR-378 family members were significantly reduced in rhabdomyosarcoma tumour tissue and cell lines [394]. In another study, Li *et al.* found that miR-378 was downregulated in glioblastoma and it increased the growth inhibitory effect of curcumin [395]. During ischemia, oxygen and glucose deprivation causes a significant lack of energy, which results in defective protein-folding processes and triggers EnR stress responses [37, 391]. In agreement with our findings, the expression of miR-378 has been reported to be downregulated in ischemia/reperfusion injury of intestinal mucosa and brain [396, 397].

Furthermore, we quantified the expression level of the miR-378 host gene (PPARGC1B) during conditions of EnR stress in these cell lines and showed that the expression level of PPARGC1B is reduced (Figure 3-4-3). It has been shown that miRNAs, which are located within introns, are usually co-transcribed with their host genes [398]. PPAR $\gamma$  coactivator 1 alpha and beta (PPARGC1 A, B) are transcriptional coactivators that regulate energy metabolism, thermogenesis and mitochondrial biogenesis through stimulation of nuclear hormone receptors and other transcription factors [358]. It has been reported that PPARGC1 A and B play crucial roles in the ER signalling pathway [357]. It is also reported that the expression of PPARGC1B and miR-378 is increased in the liver during fasting [399, 400].

Deficiency of miR-378 renders mice resistant to high-fat-diet-induced obesity and enhanced mitochondrial fatty acid metabolism, suggesting that miR-378 is involved in the regulation of mitochondrial metabolism and systemic energy homeostasis [401]. XBP1s is a crucial regulator of glucose homeostasis in obesity [352, 402]. Liver-specific deletion of IRE1 $\alpha$ , which abrogates XBP1s activity, shows enhanced development of fatty liver [353]. Loss of XBP1 leads to the development of glucose intolerance and insulin resistance in HFD-fed BALB/c mice, a strain that is otherwise resistant to diet-induced insulin resistance [353, 402]. The function of XBP1s is severely impaired in mouse models of obesity [353]. Considering our results showing XBP1s dependent downregulation of PPARGC1B and miR-378 during UPR and ample overlap with human diseases where a role for miR-378 and UPR has been implicated, we posit that UPR-mediated repression of miR-378 may play a role in the coordination of energy metabolism in accordance with metabolic demand.

To study the effect of miR-378 on cell growth and proliferation, we generated stable pools of overexpressing miR-378 in colorectal (HCT116) and breast cancer (MCF7, ZR-75-1 and MDA-MB-231) cells. Our results showed that miR-378 expression reduced cell growth and migration of luminal breast cancer cells (MCF7 and ZR-75-1) (Figures 3-4-9,10,11). In agreement with our results, inhibition of miR-378 function has been reported to increase the migration of MCF7 cells [355]. Moreover, we showed that miR-378 increased the migration of MDA-MB-231 cells but it had no effect on cell proliferation. In a study by Browne and colleagues, miR-378 has been shown to increase migration and invasion without having any effect on proliferation of MDA-MB-231 cells [403]. Furthermore, miR-378 was reported to decrease cell proliferation in HCT116 cells but we did not observe any effect of miR-378 on the growth of HCT116 cells [271].

This may be due to differences in the approaches used to express the ectopic miR-378. We have used a plasmid-based method for stable expression of miR-378 which will increase the levels of both miR-378 and miR-378\* while Browne *et al.* and Wang *et al.* have used transient transfection of miR-378 mimics [271, 403].

Next, we investigated the effect of miR-378 on MCF7 cell death in the presence of EnR stress-inducing or anti-estrogens. Our results uncovered a novel role for miR-378 in UPR signalling, where miR-378 sensitises the cells to EnR stress-induced cell death but provides resistance to docetaxel (Figure 3-4-13). Such miR-378 overexpression has been reported to cause suppression of Aurora B kinase activity and insensitivity of cells to taxol [404]. In addition, miR-378 also sensitises the cells to anti-estrogens (Figure 3-4-12). Acquired resistance of ER-positive breast cancer to anti-estrogen compounds have been reported in one-third of ER-positive breast cancer patients [405]. The expression of miR-378 has been found to be downregulated in endocrine-resistant models (TamR and LTED cells) of breast cancer and breast cancer tissues [355]. Knockdown of miR-378 has been shown to reverse tamoxifen-dependent suppression of cell growth in MCF-7 cells [355].

PPARGC1B is a transcriptional coactivator that potentiates the ligand-dependent activity of the ER $\alpha$  while having only weak effects on similar steroid hormone receptors, such as ER- $\beta$  or the glucocorticoid receptor [406]. Tamoxifen can induce changes in the ligand-binding domain of ER $\alpha$  to promote interactions with PPARGC1B, which then cooperates with SRC-1 to enhance the ESR1-mediated agonistic activity of tamoxifen [406]. Thus, downregulation of miR-378 and PPARGC1B by XBP1 may modulate endocrine resistance by multiple mechanisms.

Several studies have demonstrated that miR-378 plays an oncogenic role in some cancers but suppresses tumour formation in other cancers. In breast cancer samples miR-378 expression has been reported to be downregulated and reduced expression levels of miR-378a-3p were associated with poor prognosis for tamoxifen-treated patients with breast cancer [355]. Our data showed that expression of miR-378 was reduced in breast cancer cell lines compared to the non-tumourigenic control MCF10A cells (Figure 4-4-3). Expression of miR-378 was significantly associated with better overall survival in the treatment of the ‘no systemic therapy’ group as well as the ‘endocrine therapy treatment’ group of ER-positive breast cancer (Figure 3-4-18).

Furthermore, we carried out a transcriptomic analysis to find miR-378 dependent genes signature in overexpressing miR-378 MCF7 cells. Our results revealed that 53 genes were expressed at a significantly lower level and 254 were expressed at a significantly higher level in miR-378 expressing cells (Figure 3-4-15). Our findings suggest that miR-378 is a positive regulator of type I interferon signalling and miR-378 expressing cells may secrete growth suppressing cytokines (Figure 3-4-17). Interestingly, expression of miR-378 was shown to be downregulated in IFN- $\alpha$  activated NK cells where miR-378 modulates the cytotoxicity of human NK cells by targeting cytolytic molecules granzyme B and perforin [407]. PPARGC1B has been shown to be a downstream target of IFN- $\gamma$ , and it acts in conjunction with ERR $\alpha$  as a key effector of IFN- $\gamma$  induced mitochondrial ROS production and host defence [408]. Furthermore, we found that patients with an elevated miR-378 signature (8 genes upregulated by miR-378) displayed longer overall and relapse-free survival (Figure 3-4-19).

Collectively, here we reported that XBP1s downregulated the expression of miR-378 and PARGC1B (host gene of miR-378) and we observed an inverse correlation between the expression of XBP1 and PPARGC1B in the TCGA breast cancer dataset. Higher expression of miR-378 was associated with better overall survival in ER-positive breast cancer. The ectopic expression of miR-378 significantly suppressed cell proliferation, colony formation and migration of ER-positive breast cancer cells. Furthermore, miR-378 expression sensitised MCF7 cells to UPR-induced cell death and anti-estrogens.

We propose that miR-378 expressing cells may secrete growth suppressive cytokines, which is required for miR-378 mediated growth inhibition. Further experiments are required to elucidate the mechanism of miR-378 mediated growth inhibition. Analysis of independent cohorts of patients revealed that specific gene-signature derived from miR-378 upregulated genes showed a strong association with improved overall and recurrence-free survival in breast cancer. Our data suggests that miR-378 might play a vital role in the carcinogenesis of ER-positive breast cancer (Figure 5-1). To the best of our knowledge this is the first report of identification and characterization of functionally relevant miRNA regulated by XBP1 in the context of luminal breast cancer.

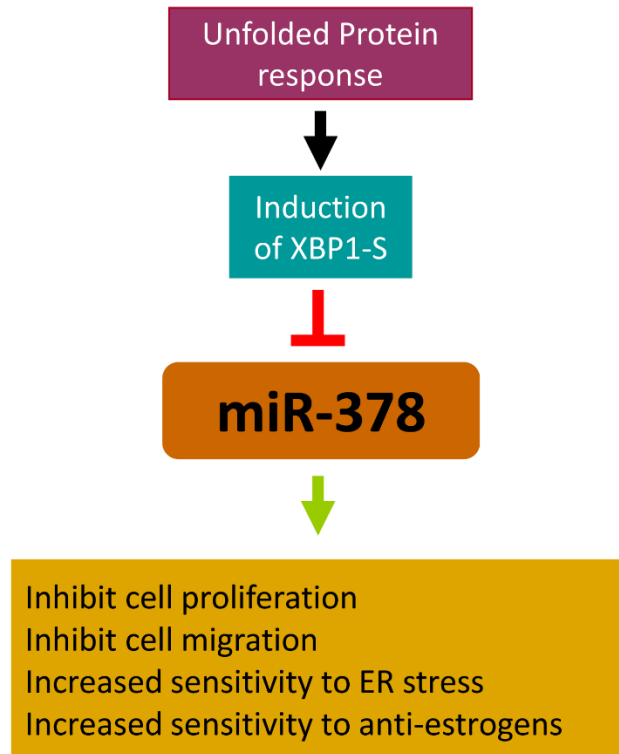


**Figure 5-1. Graphical abstract of UPR regulated miR-378.** Stressful conditions of the tumour microenvironment activate an adaptive mechanism called the unfolded protein response (UPR). X-box binding protein-1 (XBP1) is a critical transcriptional activator that is induced by the UPR. In ER-positive breast cancer cells XBP1 is rapidly induced in response to E2-stimulation. In luminal breast cancers, estrogen signalling and UPR induce the expression of XBP1s. Here we show that XBP1s downregulates the expression of PPARGC1B and miR-378 during UPR. Our results suggest that XBP1s regulates growth and migration of ER-positive breast cancer cells, sensitivity to anti-estrogens in part, by downregulation of miR-378.

## **5-2. CHOP-intronic miR-616 inhibits cell growth and migration by targeting c-MYC and VAV1**

The expression level of miR-616 was quantified in colorectal (HCT116 and RKO) and breast (MCF7) cancer cells during conditions of EnR stress and UPR activation. Our results illustrated that the expression level of miR-616 was increased in all these cancer cells during UPR activation (Figure 4-4-1) which means that the upregulation of miR-616 is not cell-type or stimulus specific. Furthermore, we quantified the expression level of miR-616 host gene (CHOP) during conditions of EnR stress in these cell lines, and as expected the expression level of CHOP was increased (Figure 4-4-2).

We also quantified the endogenous level of miR-616 in several breast cancer cells and we found that it is lower in luminal A (MCF7, T-47D), triple negative (MDA-MB-231) and HER2 positive (SKBR3) breast cancer subtypes compared to non-tumourigenic MCF10A cells (Figure 4-4-3). There was no difference in expression of miR-616 in BT-474 cells compared to MCF10A control cells. This observation may relate to the breast cancer cell hormone status as BT-474 cells (luminal B) are positive for all three hormone receptors including ER, PR and HER2, but other subtypes have different patterns (positive or negative) in terms of hormone receptor expression.

To investigate the role of PERK, IRE1, and ATF6 in the regulation of miR-616, we quantified the expression of miR-616 in our HCT116 and MCF7 knockdown pools during conditions of EnR stress. Our results suggest that miR-616 is co-transcribed with the CHOP transcript during UPR as attenuated PERK signalling compromised the induction of both CHOP mRNA and primary miR-616.

However discordant expression of the primary miR-616 and the mature miR-616 suggests additional regulation at the level of processing of miR-616 precursors and/or miR-616 turnover.

Overall, the levels of miRNAs in the cell are the result of both biogenesis and decay processes.

The expression of miRNAs starts with the transcription of a primary RNA (called pri-miRNA, a long transcript that contains a stem-loop region for each encoded miRNA) and is dependent on the same transcriptional machinery and regulatory mechanisms as used by protein coding genes [202]. This pri-miRNA is usually short-lived and generates mature miRNA molecules through two sequential processing events. The first processing event occurs in the nucleus and is mediated by the microprocessor complex (DROSHA/DGCR8), which generates a precursor miRNA (pre-miRNA) [202].

The pre-miRNA is then exported to the cytosol where the second cleavage event occurs, mediated by the DICER1/TRBP complex, producing a miRNA duplex. MiRNA processing is followed by loading of the miRNA duplex onto argonaute proteins (AGO). Once loaded onto the AGO-based complexes, miRNAs are stabilized and have long half-lives [202, 409]. The degradation dynamics of miRNAs and the mechanisms involved are not well defined, but are mediated by the enzymatic activities which are able to modify miRNA ends by adding or removing nucleotides[202, 410]. Further work is required to determine the mechanism behind the observed discrepancy in the expression of the primary and mature miR-616.



To understand the effects of miR-616 in cell growth and proliferation, firstly we successfully overexpressed miR-616 in different cancer cell types including HCT116 (colorectal), MCF7/ZR-75-1 (luminal A) and MDA-MB-231 (triple negative) cells (Figure 4-4-5). Our results from MTS cell proliferation (Figure 4-4-6) and colony formation (Figure 4-4-7-1,2) assays showed that miR-616 reduced the growth rate of luminal breast (MCF7 and ZR-75-1) and colorectal (HCT116) cancer cells, while it had no effect on the growth of triple negative breast cancer (MDA-MB-231) cells. Our results also illustrated that miR-616 inhibits cell migration of luminal breast (MCF7 and ZR-75-1) and colorectal (HCT116) cancer cells (Figure 4-4-8). However, it increased the migration of triple negative breast cancer (MDA-MB-231) cells. These observations indicated the presence of context-dependent pro- and anti-cancer effects of miR-616 in cancer cells. Indeed, context dependent oncogenic and tumour suppressor roles have been documented for several miRNAs including the miR-17-92 cluster. This cluster maps to human chromosome 13q31, a region amplified in Burkitt's lymphoma, diffuse large B-cell lymphoma, follicular lymphoma, mantle cell lymphoma and lung cancer [278, 279]. Although the majority of studies have characterised the oncogenic activities of miR-17-92, loss of heterozygosity at the 13q31, a locus that harbours human miR-17-92 has been reported [279, 297]. For example, miR-17-92 was deleted in 21.9% of breast cancers, and 20.0% of melanomas [297]. The expression of miR-17-92 is reduced in prostate cancer and restoration of its expression showed a therapeutic benefit [298]. The transgenic miR-17-92 expression in intestinal epithelial cells inhibited colon cancer progression by suppressing tumour angiogenesis [411].

Furthermore, we investigated the effects of miR-616 on sensitivity of MCF7 cells against anti-estrogen, chemotherapeutic and ER stress-inducing compounds. We found that miR-616 increases the sensitivity of MCF7 cells towards anti-estrogen (Tamoxifen and Fulvestrant) compounds (Figure 4-4-9). Moreover, miR-616 expressing MCF7 cells show resistance to docetaxel while our results showed that miR-616 expression had no effect on ER induced cell death (Figure 4-4-10). The mechanism of action of pharmacological compounds are different. docetaxel inhibits depolymerisation of microtubules by binding to stabilized microtubules and causes the failure of chromosomes to segregate to the daughter cells, while TG and BFA induce UPR. Thus, observed differences in the effects of miR-616 expression on the viability of MCF7 cells may be related to the mechanism of action of these compounds. Further work is required to determine the mechanism behind the observed differential effects of miR-616 towards antiestrogens and docetaxel.

Transcriptomic analysis identified VAV1 and c-MYC as miR-616 regulated genes. The expression of c-MYC and VAV1 were downregulated in MCF7, ZR-75-1 and HCT116 cells but not in MDA-MB-231 cells. We found that both c-MYC and VAV1 have non-canonical binding sites for miR-616 in the protein coding region of the transcript. Most of the studies show that miRNAs regulate gene expression by targeting the 3'UTR. But in recent years, increasing evidence has elucidated that miRNAs can also target the coding region (CDS) of genes and inhibit translation [412, 413]. Several studies have reported the presence of miRNA binding sites in the protein coding sequence of the genes.

Indeed miRNAs have been shown play a role in regulation of embryonic stem cell differentiation [414], DNA methylation [415], regulation of apoptosis [416], aortic development [417], and tumour suppression [418] via the functional miRNA binding sites in the protein coding sequence of the target genes. Studies on target recognition by miRNAs have shown that complementarity at the 5' end of the miRNA, the so-called "seed region" at positions 2 to 7, is a primary determinant of target specificity [419]. However, a perfect seed match by itself is not a good predictor for miRNA regulation, and a number of studies have shown that some target sites with a mismatch or a G:U wobble in the seed region can exhibit a noticeable regulation [419, 420]. Furthermore, a study using a cross-linking and immunoprecipitation (CLIP) method to study in vivo microRNA targets found a significant number of non-canonical sites [420]. Therefore, perfect seed complementarity is neither necessary nor sufficient for microRNA regulation. In addition, target sites for endogenous miRNAs have been identified in ORFs and 5' UTRs, but they are less frequent than those in the 3' UTR.

To understand the role of VAV1 and c-MYC in mediating the tumour suppressive effects of miR-616 in MCF7 cells, we restored the expression of VAV1 and c-MYC in miR-616 expressing MCF7 cells (Figure 4-4-15). Our results showed that ectopic expression of VAV1 and c-MYC reversed inhibitory effects of miR-616 on cell growth and migration on MCF7 cells. Furthermore, we showed that VAV1 and c-MYC increased the cell growth and migration (Figure 4-4-19, 20, 21 and 22) of parental MCF7 cells which have the basal level of miR-616 expression. From these experiments, it is clear that miR-616 may play a role as a tumour suppressor by targeting both VAV1 and c-MYC transcripts and suppressing their expression. Several studies have reported the upregulation of VAV1 and c-MYC in different cancer cells and tumours such as neuroblastomas, lung and breast cancer [386, 421-424].

It has been shown that downregulation of VAV1 in lung and pancreatic cancer cells can decrease cell proliferation and reduce tumour size in mice [386, 387]. Moreover, VAV1 has oncogenic activities in various cancer types including breast cancer. Lane and colleagues found that high expression of VAV1 is associated with poor prognosis in breast tumours [425]. Sebban and colleagues analysed 65 primary human breast tumours by Immunohistochemical staining and found the high expression of VAV1 in 62 % of these tumours which have a positive correlation with ER expression [426]. In another study, Du *et al.* found that the expression level of VAV1 was upregulated in two ER-positive cell lines (MCF7 and T47D cells) and its expression was induced by 17 $\beta$ -estradiol (E2). They also showed that high expression of VAV1 increased the expression level of Cyclin D1 and consequently the cell cycle progression [422]. Yet another published study reported the upregulation of VAV1 and some other genes (CDC25A, TP73, BRCA1 and ZAP70) in colorectal HCT116 cancer cells, and these genes are highly correlated with poor prognosis in colorectal cancer patients [427]. Although we did not investigate the role of VAV1 in HCT116 cells, we showed that the expression level of VAV1 (at both mRNA and protein levels) was significantly reduced in HCT116 cells with overexpressed miR-616. Moreover, our functional analysis found that when the expression level of VAV1 is downregulated, the proliferation, colony formation and migration of HCT116 cells are reduced.

It has been shown that c-MYC plays a key role in cell cycle progression. c-MYC acts through binding to MYC associated factor X (MAX) and this complex then regulates cell proliferation through the cyclin-dependent kinases in G1 phase [390]. In addition, c-MYC has an important function in survival of cancer cells through multiple cellular pathways [423]. Studies have reported the dysregulation of c-MYC in different cancer cells and tumours.

The c-MYC mutation was first discovered in Burkitt Lymphoma as a chromosomal translocation in 1982 [424, 428]. Enhanced transcriptional activation of c-MYC was reported in colorectal cancer that causes some defects in the Wnt-APC pathway [429]. It has also been reported that c-MYC is upregulated in 30-50% of high-grade breast tumours [430, 431]. Moreover, several studies have shown that c-MYC mRNA expression is affected by miRNAs which leads to the translational modulation in different cancer types including breast cancer. For example, it has been reported that following DNA damage, miR-34a represses c-MYC expression through the MAPK/MK2 signalling pathway and leads to the inhibition of DNA replication in S phase [432]. Recently, Wang *et al.* found that c-MYC and BCL2 are direct targets of miR-184, which inhibits proliferation and promotes apoptosis of HCT116 and SW40 cells [433]. There are also several studies that investigated the role of miRNAs and dysregulation of c-MYC in breast cancer. In a recently published study, miR-20a was found to target and downregulate the expression level of c-MYC and sensitised MCF7 cells to the chemotherapeutic compounds and reduced cell proliferation [434].

Although endocrine therapy is a successful treatment option in most of the ER+ tumours, it has been shown that 30% of all ER+ breast cancer develop resistance to the endocrine therapy [435]. The exact mechanism of endocrine therapy resistance is still unknown but studies are suggesting that c-MYC overexpression may play a role to gain resistance in ER+ breast cancer cells. It has been reported that c-MYC is overexpressed in ER+ breast cancer cells (MCF7) and tumours [436] and its overexpression has been linked to endocrine therapy resistance [437, 438]. Moreover, it has been reported that ER stress and UPR signalling pathway are activated in endocrine resistance breast cancer cells [439].

Our results in this chapter showed that c-MYC expression was downregulated by miR-616. On the other hand, the expression level of miR-616 was upregulated during EnR stress and UPR. To our knowledge, this is the first study that shows the role of miR-616 in the inhibition of cell growth and migration of ER+ breast cancer cells by suppressing two well-known oncogenes VAV1 and c-MYC.

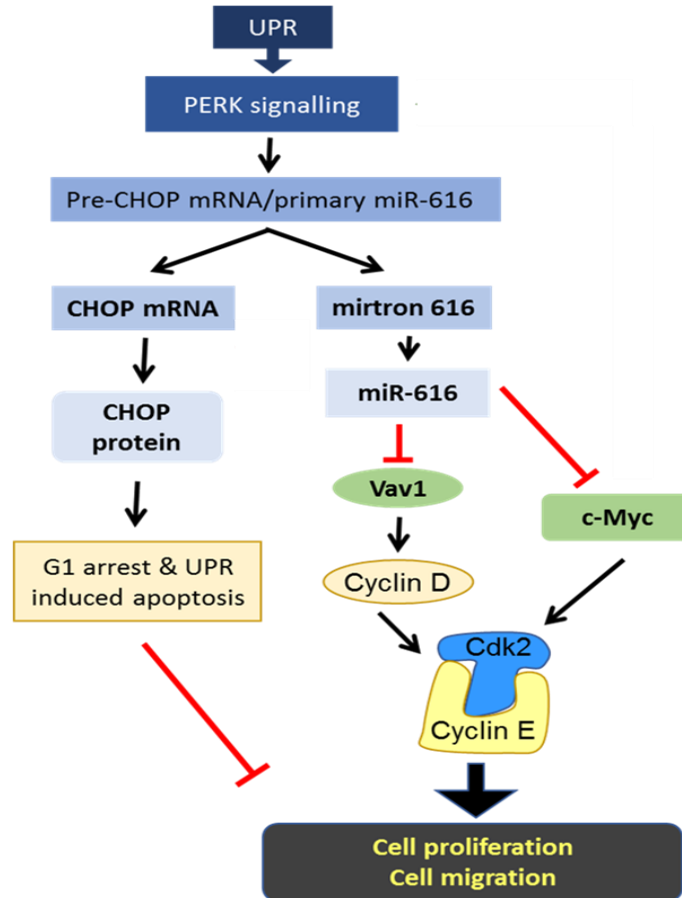


**Figure 5-2. Graphical abstract of UPR regulated miR-616.** Stressful conditions of the tumour microenvironment activate the unfolded protein response (UPR) signalling pathway including PERK sensor. PERK sensor increases the expression level of miR-616 and CHOP. CHOP, as a pro-apoptotic protein, induced cell apoptosis through cell cycle arrest and UPR. On the other hand, expression of miR-616 reduced cell proliferation and migration through suppressing two well-known oncogenes including VAV1 and c-MYC.

In this study, we report that expression of miR-616 and CHOP (host gene of miR-616) is increased during UPR (Figure 5-2). We report that miR-616 significantly suppressed cell proliferation, colony formation and migration of cancer cells. Furthermore, we show that miR-616 exerts the growth inhibitory effect on MCF7 cells through suppressing the expression of c-MYC and VAV1. Our results establish a new and unexpected role for the CHOP locus by providing evidence that miR-616 can inhibit cell proliferation by targeting c-MYC and VAV1 (Figure 5-2). In summary, our results suggest that the CHOP locus generates two gene products, where CHOP protein and miR-616 can act together to inhibit cancer progression

Depending on the cellular context, the UPR plays pro-survival and pro-death roles in determining cell fate. Cancer cells recruit UPR signalling pathway (pro-survival role) to cope with the stressful conditions in a tumour microenvironment. IRE1 arm of UPR play a pro-survival role in cancer through splicing of XBP1 and activation of its downstream genes (Figure 1-6). On the other hand, prolonged ER stress switches activation of the PERK arm from pro-survival to pro-death phase through activation of its downstream target CHOP (Figure 1-6). Here we showed that IRE1-XBP1 axis is required for downregulation of miR-378 during UPR whereas miR-616 and its host gene (CHOP) are upregulated during conditions of UPR in PERK-dependent manner. Our results suggest the expression of miR-378 and miR-616 will be lower during the adaptive phase of UPR and higher during the pro-death phase of UPR.

### **5-3. Limitations of the study and future directions**

#### **5-3-1. Limitations of the study**

In this study, we found dysregulation of both miR-378 and miR-616 during conditions of EnR stress in various cancer cell lines. To induce EnR stress, we applied three chemical EnR-stress inducing compounds. To investigate the significance of these findings further it would be useful to examine the miR-378 and miR-616 expression by inducing the physiological EnR-stress (e.g., hypoxia induction and glucose deprivation). Hypoxia is one of the hallmarks of the tumour microenvironment that adversely influences tumour phenotype and treatment response [440]. It is the result of insufficient blood supply to support proliferating tumour cells. A modular incubator chamber (hypoxia chamber) is used to induce hypoxia in cancer cells which provides a hypoxic environment containing a 1% O<sub>2</sub> gas mixture for cancer cells. For glucose deprivation, it is possible to grow cancer cells in a glucose free medium.

We investigated the effect of miR-378 and miR-616 on cancer cell growth and proliferation by overexpressing these miRNAs using a gain-of-function approach. To complement the existing data, it would be interesting to perform similar experiments using a loss-of-function approach by suppressing the miR-378 and miR-616 expression in these cancer cells. For this purpose, it is possible to suppress the expression of miR-378 and miR-616 using miRNA inhibitor and perform similar functional analysis. One would expect that effect of inhibitors of miR-378 and/or miR-616 on cell growth and proliferation would be opposite to effect of overexpression of miR-378 and/or miR-616. If this is indeed the case, than I would expect increased expression of VAV1 and c-MYC in cells expressing inhibitors of miR-616.



Moreover, a gain-of-function study was also carried out to evaluate the effects of VAV1 and c-MYC by overexpressing these two oncogenes in MCF7 cells. To complement the existing data, it would be interesting to perform a loss-of-function study by suppressing VAV1 and c-MYC transcripts by short hairpin RNA (ShRNA) in these cancer cells. If VAV1 and c-MYV are the key functional targets of miR-616 than one would expect that overexpression of miR-616 will not show any effect in VAV1 and c-MYC knockdown cells.

### **5-3-2. Future directions of the study**

In this study, we investigated the role of two UPR-regulated miRNAs in various breast and colorectal cancer cells. We found that the during conditions of UPR expression level of miR-378 was downregulated and miR-616 was upregulated. It would be interesting to investigate the association between the expression level of miR-378 and miR-616 and outcome using patient samples from colon cancer and breast cancer subtypes such as luminal A, luminal B, HER2 overexpressed and triple negative.

We found that both miR-378 and miR-616 play a tumour suppressor role in cancer cells by performing functional analysis such as colony formation and migration assays. To validate the tumour suppressor function of these two miRNAs, it would be interesting to investigate these miRNAs in more clinically relevant xenograft models. For instance, one could inject miR-378 or miR-616 overexpressing MCF7/ZR-75-1 cells in to nude mice and then evaluate tumour formation.

Our results suggest that miR-378 is a positive regulator of type I interferon signalling pathway and regulates cell growth via the secretion of growth inhibitory factors. It may be important to elucidate mechanisms by which miR-378 upregulates the type I interferon signalling pathway and identify the key growth inhibitory molecules secreted by miR-378 expressing cells. For this purpose, one possibility would be to determine the expression level of secreted proteins by mass spectrometry analysis or cytokine array in the culture supernatant of miR-378 expressing cells.

# Chapter 6

## 6-0. Appendix

### 6-1. Cell lines

Cell line	Cancer type
HCT116	Colorectal cancer
RKO	Colorectal cancer
MCF7	Luminal A breast cancer
ZR-75-1	Luminal A breast cancer
MDA-MB-231	Triple negative breast cancer
HEK 293T	Embryonic kidney cells
MCF10A	Non-tumorigenic epithelial mammary gland cells

### 6-2. MiRNA-specific primer sequences for RT-qPCR assay

MicroRNAs	MirBase accession no.	Primer sequences (5' to 3')
hsa-miR-616	MIMAT0004805	AGUCAUUGGAGGGUUUGAGCAG
hsa-miR-378	MIMAT0000731	CUCCUGACUCCAGGUCCUGUGU
hsa-miR-663a	MIMAT0003326	AGGCGGGGCGCCGCGGGACCGC
hsa-miR-625*	MIMAT0004808	GACUAUAGAACUUUCCCCUCA
hsa-miR-149*	MIMAT0004609	AGGGAGGGACGGGGGCUUGUC
hsa-miR-1908	MIMAT0007881	CGGCGGGGACGGCGAUUGGUC
hsa-miR-1915	MIMAT0007891	ACCUUGCCUUGCUGCCCGGGCC
hsa-miR-638	MIMAT0003308	AGGGAUCGCGGGCGGGUGGCGGCCU
hsa-miR-483	MIMAT0004761	AAGACGGGAGGAAAGAAGGGAG
hsa-miR-224	MIMAT0000281	UCAAGUCACUAGUGGUUCCGUUAG

### 6-3. Cell culture medium and chemical reagents

Reagent	Catalogue number	Supplier
Hank's Balanced salt solution	H6648	Sigma-Aldrich
DMEM	D6429	Sigma-Aldrich
RPMI 1460	11879	Invitrogen
McCoy's 5A	M9309	Sigma-Aldrich
Trypsin EDTA	T4174	Sigma-Aldrich
Foetal bovine serum	F7524	Sigma-Aldrich
L-Glutamine	G7513	Sigma-Aldrich
N-sodium pyruvate	S8636	Sigma-Aldrich
Penicillin Streptomycin	P0781	Sigma-Aldrich
Trizol	15596-018	Invitrogen
Chloroform	372978	Sigma-Aldrich
Isopropanol	19516	Sigma-Aldrich
Ethanol	E7023	Sigma-Aldrich
10X Trish Borate EDTA buffer	T4415	Sigma-Aldrich
Agarose	A9539	Sigma-Aldrich
Ethidium Bromide	H5041	Promega
6 X loading dye Blue Orange	G190A	Promega
100bp DNA ladder	N32315	New England
1kb DNA ladder	15615 - 016	Invitrogen
Micro Amp Optical96-well plate	N8010560	Applied Biosystems
4mM Caffeine	C0750-100G	Sigma-Aldrich
JetPEI transfection reagent	101-40N	Polyplus transfection

#### 6-4. Reverse transcription reagents

Reagent	Catalogue no.	Supplier
GAPDH forward primer	8895 - 041	Sigma-Aldrich
GAPDH reverse primer	8895 - 042	Sigma-Aldrich
XBP1 forward primer	SY130218766	Sigma-Aldrich
XBP1 reverse primer	SY130218904	Sigma-Aldrich
Green master mix	M711B	Promega
TaqMan master mix	4426710	Applied Biosystems
Oligo dT	C1108	Promega
MgCl <sub>2</sub>	A351H	Promega
5X Reaction Buffer	M289A	Promega
dNTP	C114B	Promega
RNase inhibitor	4469082	Applied Biosystems
Reverse transcriptase	A501C	Promega
Nuclease free water	AM9937	Ambion

### 6-5. IDT primer and probe sequences for UPR signalling pathway genes

Primer	Direction	5'to3' primer sequence
<b>GAPDH</b>	Probe	5'-/56FAM/CAGCAAGAG/ZEN/CACAAGAGAGAGAGA/3IABkFQ/-3'
	Primer 1	5'-AGGGTGGTGGACCTCAT-3'
	Primer 2	5'-TGAGTGTGGCAGGGACT-3'
<b>HERP</b>	Probe	5'-/56FAM/AGCTTTTAC/ZEN/GAGAGAACTCATGGCCT/3IABkFQ/-3'
	Primer 1	5'-CGCTGTCTTAACTCCTGGTTC-3'
	Primer 2	5'-CTGGAACAGCAAGTGGTAGA-3'
<b>PERK</b>	Probe	5'-/56-FAM/TTTCTTGAT/ZEN/GGAGAGAGCGGGCTGG/3IABkFQ/-3'
	Primer 1	5'-AGGACTTGCCTATGGAAACC-3'
	Primer 2	5'-CTGTTGCTCCAAGGTGTGAT-3'
<b>ATF4</b>	Probe	5'-/56-FAM/TGCTGTCCA/ZEN/TGGGCTTCTCTGATG/3IABkFQ/-3'
	Primer 1	5'-CTGCCTTGTACCCACATCTC-3'
	Primer 2	5'-CCGATGTCATAGTTCTTGGTCTG-3'
<b>ATF6</b>	Probe	5'-/56FAM/AGGACTG/ZEN/AGGATAGCAAGATGAGAA/3IABkFQ/-3'
	Primer 1	5'-AACTTTAGTCGGCCTGATGG-3'
	Primer 2	5'-GAATCAAAGCAAAAAGCCTGTCC-3'
<b>CHOP</b>	Probe	5'-/56-FAM/AAGCCAGAG/ZEN/AAGCAGGGTCAAGAG/3IABkFQ/-3'
	Primer 1	5'-GTACCTATGTTTCACCTCCTGG-3'
	Primer 2	5'-TGGAATCTGGAGAGTGAGGG-3'
<b>GRP78</b>	Probe	5'-/56-FAM/ACGACCCCT/ZEN/GACAAGACAATCACC/3IABkFQ/-3'
	Primer 1	5'-AGCCCACCGTAACAATCAAG-3'
	Primer 2	5'-CCAGTCAGATCAAATGTACCCAG-3'
<b>PPARGC1B</b>	Probe	5'-56-FAM/TCCATGGCT/ZEN/TCATACTTGCTTTTCCCT/3IABkFQ/-3'
	Primer 1	5'-GCCTCTTTCAGTAAGCTGTCA-3'
	Primer 2	5'-GCCAGATACTGACTACG-3'

## 6-6. IDT primer and probe sequences for miR-616 dependent genes

Primer	Direction	5'to3' primer sequence
<b>SUSD3</b>	Probe	5'/56-FAM/ACC ACA GCT /ZEN/TCA CC CAG ACC AT/3IABkFQ/3'
	Primer 1	5'-CCT CAA GCA CTT CAA CAA ACC-3'
	Primer 2	5'-GAT CCC AGG GTC CTT GTC-3'
<b>GALNT14</b>	Probe	5'/56-FAM/CCC CAG TG /ZEN/TTC TTG TCC TTT GCA /3IABkFQ/3'
	Primer 1	5'-GAG CTG TGC CTG TCA GTC-3'
	Primer 2	5'-ATG CTA TGT GCT CGA TGT GG-3'
<b>BCL2</b>	Probe	5'/56-FAM/AAC AAA TGC /ZEN/ATA AGG CAA CGA C/3IABkFQ/3'
	Primer 1	5'GCT ATA ACT GGA GAG TGC TGA AG3'
	Primer 2	5'AGT CTA CTT CCT CTG TGA TGT TG3'
<b>VAV1</b>	Probe	5'/56-FAM/CCA TAG ATC /ZEN/TCC CCT CGC CAC CA/3IABkFQ/3'
	Primer 1	5'GTG ACA TCA TCA AGA TCC TTA ACA AG3'
	Primer 2	5'CAG AAT AAT CTT CCT CCA CGT AGT3'
<b>MYC</b>	Probe	5'/56-FAM/TGG GCG GTG /ZEN/TCT CCT CAT GG/3IABkFQ/3'
	Primer 1	5'TCC TCG GAT TCT CTG CTC TC3'
	Primer 2	5'TCT TCC TCA TCT TCT TGT TCC TC3'
<b>LINC00052</b>	Probe	5'/56-FAM/TGC AGA CTG /ZEN/TAG GGC TTT GGG C/3IABkFQ/3'
	Primer 1	5'CCA GAA TGA AGA ATG GCA ACC3'
	Primer 2	5'GCA GAA TGA TGT AGC AAA GCA T3'
<b>ALCAM</b>	Probe	5'/56-FAM/TGC ATG CCT /ZEN/GTG TCA AAA CAT AC/3IABkFQ/3'
	Primer 1	5'TCT CAA GTC TTT AAT TAG AAT GTC TCA C3'
	Primer 2	5'CCT CAT TCT CCA TGA TAC ACG TA3'
<b>ID4</b>	Probe	5'/56-FAM/TGC GGT CAT /ZEN/CAG AAT TTT TGG GC/3IABkFQ/3'
	Primer 1	5'CAT AAT GGC AAA TCC TTC AAG CA3'
	Primer 2	5'ACA GTA GCT TAG CGT AAC ATA GC3'



## 6-7. IDT primer and probe sequences for miR-378dependent genes

Primer	Direction	5'to3' primer sequence
<b>SOCS2</b>	Probe	5'/56-FAM/AAA GAG GCA /ZEN/CCA GA ACT TTC TTA/3IABkFQ/3'
	Primer 1	5'GGA GCT CGG TCA GAC AG3'
	Primer 2	5'GAT ATT GTT AGT AGG TAG TCT GAA TGC3'
<b>GBX2</b>	Probe	5'/56-FAM/CGG AGA AGG /ZEN/CGA GCA GCG AG/3IABkFQ/3'
	Primer 1	5'GAG GAC GGC AAA GGC TTC3'
	Primer 2	5'GTC TTC CAC CTT TGA CTC GTC3'
<b>GAL</b>	Probe	5'/56-FAM/AGA TCC AGG /ZEN/AGG CGG TCG AGG /3IABkFQ/3'
	Primer 1	5'GCG CAC AAT CAT TGA GTT TCT G3'
	Primer 2	5'CAG GTT ACA GCA CAC AGA CA3'
<b>GALNT13</b>	Probe	5'/56-FAM/ATG C AGA /ZEN/GAC TCA CGT TGC GAC /3IABkFQ/3'
	Primer 1	5'ATG ACT TGT GCT TGG ATG TTT C3'
	Primer 2	5'CAG AAG GTT CAT CGA GAC ATT G3'
<b>H19</b>	Probe	5'/56-FAM/TGT TGG GCT /ZEN/GAT GAG TC TGG TTC /3IABkFQ/3'
	Primer 1	5'CTT TAC AAC CAC TGC ACT ACC T3'
	Primer 2	5'GCT GTT CCG ATG GTG TCT T3'
<b>IFIT1</b>	Probe	5'/56-FAM/CTA GC AAA /ZEN/AC CTG CAG AAC GGC /3IABkFQ/3'
	Primer 1	5'CCA CAA GAC AGA ATA GCC AGA T3'
	Primer 2	3'GCT CCA GAC TAT CCT TGA CCT3
<b>IFIT2</b>	Probe	3'/56-FAM/ATT GTT C /ZEN/ACT AT GGT TGC AGTGC/3IABkFQ/3'
	Primer 1	5'AGA GGA AGA TTT CTG AAG AGT GC3'
	Primer 2	5'CAT CAA GTT CCA GGT GAA ATG G3'
<b>DDX58</b>	Probe	5'/56-FAM/AGT GCC /ZEN/ATT ACA CTG TGC TTG GA/3IABkFQ/3'
	Primer 1	5'GCA GAA AGT GCA AAG CCT T3'
	Primer 2	5'GCT TGG GAT GTG GTC TAC TC3'

## 6-8. MiR-378 upregulated dependent genes

The 30 most upregulated genes analysed by RNA sequencing are shown.

	A	B	C	D	E	F	G	H	I	J	K	L	M	N
1	GeneID	geneLengt	Means-M	Means-M	log2Ratio	Up-Down	Probability	Symbol	Descriptio	KEGG Orth	GO Comp	GO Functi	GO Proces	Blast
2	494327	66	0.01	54.8075	12.42016	Up	1	MIR378A	1 -	-	-	-	-	-
3	136319	3900	0.01	1.115	6.8009	Up	0.970209	MTPN	3 K10380 1	GO:00430	GO:00054	GO:00064	gi 302	
4	1.02E+08	72	0.01	1.1	6.78136	Up	1	MIR6875	1 -	-	-	-	-	
5	1.01E+08	67	0.01	1.09	6.768184	Up	1	MIR4472	1 -	-	-	-	-	
6	1.02E+08	61	0.01	1.0825	6.758223	Up	1	MIR6845	1 -	-	-	-	-	
7	5304	591	0.0725	2.4525	5.080128	Up	0.98605	PIP	2 -	-	GO:00080	-	gi 450	
8	72	1216	1.4575	46.7225	5.00255	Up	0.990348	ACTG2	3 K12315 1	GO:00444	GO:00325	GO:00030	gi 947	
9	338324	4279	0.2625	7.2625	4.790077	Up	0.980166	S100A7A	3 -	GO:00432	GO:00469	GO:00434	gi 635	
10	3853	2450	0.1025	1.9025	4.214201	Up	0.960516	KRT6A	3 K07605 1	GO:00058	GO:00054	GO:00082	gi 503	
11	374918	771	0.09	1.485	4.044394	Up	0.963142	IGFL1	1 -	-	-	-	gi 383	
12	6279	512.81	20.8225	304.6	3.870701	Up	0.967815	S100A8	4 K17274 1	GO:00444	GO:00468	GO:00069	gi 426	
13	3872	1574	1.6625	23.23	3.804563	Up	0.95339	KRT17	2 K07604 1	GO:00058	GO:00054	GO:00064	gi 455	
14	6278	450	18.925	251.2225	3.7306	Up	0.974513	S100A7	3 -	GO:00432	GO:00469	GO:00434	gi 635	
15	6280	586	76.5825	915.465	3.579418	Up	0.953043	S100A9	3 K17274 1	GO:00432	GO:00600	GO:00069	gi 450	
MCF7_miR_CTRL-VS-MCF7_miR_378														
16	55601	6099	1.135	12.7975	3.495098	Up	0.955451	DDX60	5 K20103 1	-	GO:00036	-	gi 222	
17	6876	1177	6.12	65.9125	3.428949	Up	0.9596	TAGLN	1 K20526 1	GO:00444	GO:00080	GO:00485	gi 119	
18	84675	2483	0.15	1.3125	3.129283	Up	0.958208	TRIM55	1 K10654 1	GO:00432	GO:00469	GO:00230	gi 348	
19	10964	5910	0.185	1.5975	3.110219	Up	0.939985	IFI44L	3 -	GO:00444	-	GO:00023	gi 166	
20	3481	4539	1.125	9.67	3.103591	Up	0.955872	IGF2	2 K13769 1	GO:00444	GO:00051	GO:00096	gi 189	
21	3437	2516.71	3.6175	29.4025	3.022874	Up	0.97915	IFIT3	1 K14217 1	-	GO:00054	GO:00192	gi 315	
22	4600	2961	0.4975	3.7625	2.918923	Up	0.966078	MX2	1 K14754 1	GO:00432	GO:00171	GO:00517	gi 113	
23	3433	3505	1.0225	7.4325	2.861747	Up	0.960729	IFIT2	4 K14217 1	-	GO:00054	GO:00433	gi 341	
24	2633	3050	0.215	1.5575	2.856824	Up	0.953571	GBP1	2 K17339 1	GO:00160	GO:00171	GO:00192	gi 166	
25	6283	466	0.945	6.81	2.849269	Up	0.949368	S100A12	1 K17274 1	GO:00432	GO:00469	GO:00069	gi 503	
26	653145	1905	0.16	1.15	2.84549	Up	0.945311	ANXA8	1 K17096 1	-	GO:00468	GO:00075	gi 411	
27	5004	847	0.23	1.645	2.838382	Up	0.953656	ORM1	2 K17308 1	GO:00444	GO:00054	GO:00025	gi 167	
28	6699	641	0.5725	4.0325	2.816327	Up	0.952625	SPRR1B	2 K15601 1	GO:00058	GO:00055	GO:00302	gi 338	
29	3434	4410.47	6.6375	45.0575	2.763055	Up	0.969109	IFIT1	4 K14217 1	GO:00444	GO:00055	GO:00510	gi 400	
30	91351	6727.59	0.93	6.085	2.709955	Up	0.967604	DDX60L	2 K20103 1	-	-	-	gi 613	
MCF7_miR_CTRL-VS-MCF7_miR_378														

## 6-9. MiR-378 downregulated dependent genes

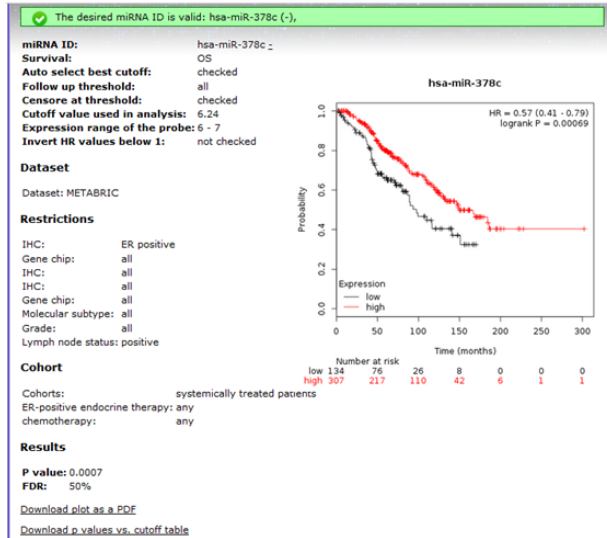
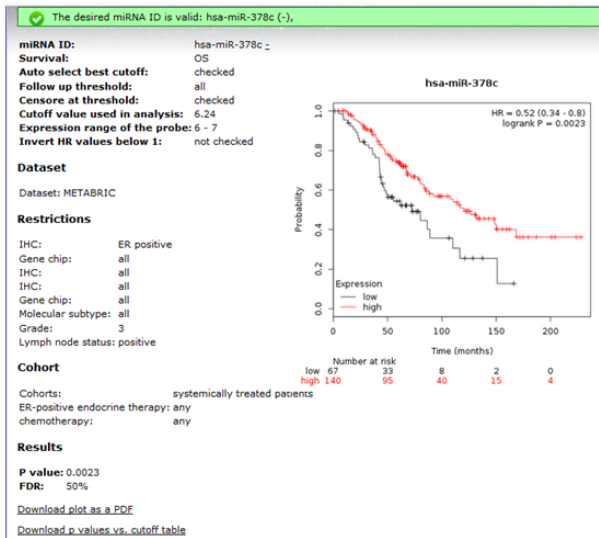
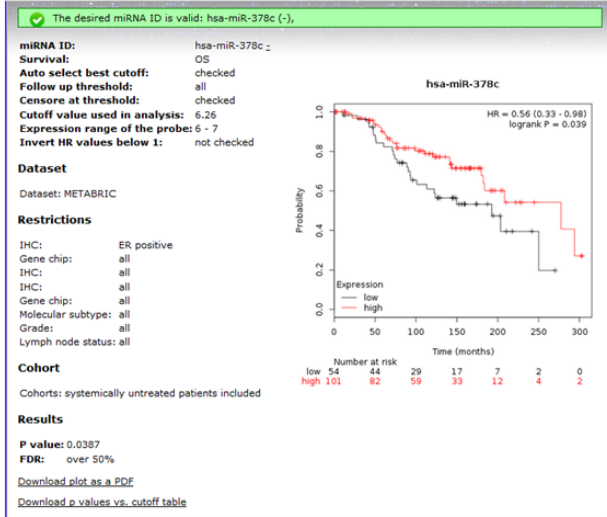
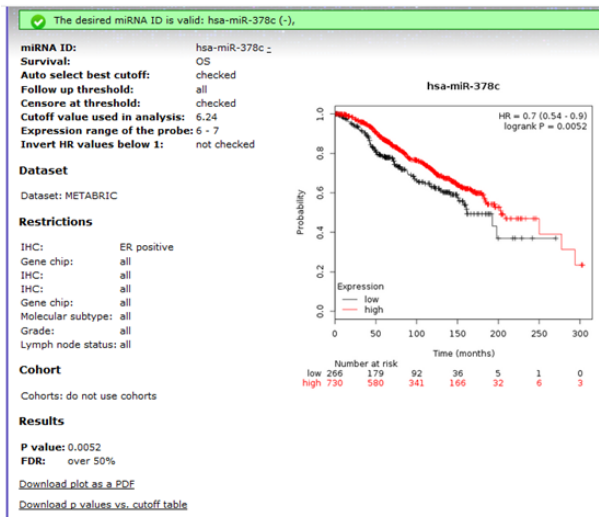
The 30 most downregulated genes analysed by RNA sequencing are shown.

	B	C	D	E	F	G	H	I	J	K	L	M	N	O
1	geneLengt	Means-M	Means-M	log2Ratio	Up-Down	Probability	Symbol	Descriptio	KEGG Orth	GO Comp	GO Functi	GO Proces	Blast nr	
2	71	2.2125	0.01	-7.78953	Down	1	SNORD361	1 -	-	-	-	-	-	
3	65	1.83	0.01	-7.5157	Down	1	MIR6727	1 -	-	-	-	-	-	
4	54	1.4875	0.01	-7.21675	Down	1	SNORD78	1 -	-	-	-	-	-	
5	55	1.3725	0.01	-7.10066	Down	0.991269	MIR4454	1 -	-	-	-	-	-	
6	81	1.285	0.01	-7.00562	Down	1	MIR922	1 -	-	-	-	-	-	
7	60	1.0975	0.01	-6.77808	Down	0.999656	MIR4722	1 -	-	-	-	-	-	
8	107	44.285	6.1925	-2.83822	Down	0.981159	RNU6-7	1 K05692 1	-	-	-	-	gi 537152882 gb	
9	107	44.285	6.1925	-2.83822	Down	0.981159	H19	1 K05692 1	-	-	-	-	gi 537152882 gb	
10	1795	2.9275	0.495	-2.56417	Down	0.99201	GBX2	1 K09321 1	GO:00432	GO:00010	GO:00015	gi 45593144 ref		
11	75	3.7075	0.6975	-2.41018	Down	0.934945	SNORD110	1 -	-	-	-	-	-	
12	163	3.49	0.705	-2.30753	Down	0.970491	GAL	1 K17540 1	-	-	-	-	gi 927196956 ref	
13	5637.86	13.265	2.695	-2.29927	Down	0.999996	SULF1	1 K14607 1	GO:00444	GO:00468	GO:00060	gi 46249932 gb		
14	66	2.1625	0.4575	-2.24086	Down	0.930383	GALNT13	1 -	-	-	-	-	-	
15	216	1.29	0.2875	-2.16574	Down	0.992013	SNORD138	1 -	-	-	-	-	-	

16	110	3.435	0.865	-1.98954	Down	0.923172	MIR3653	1 -	-	-	-	-	-	
17	85	1.0775	0.2775	-1.95713	Down	0.807072	MIR4742	1 -	-	-	-	-	-	
18	418	12.5625	3.435	-1.87074	Down	0.984171	SPANXA1	3 -	GO:00432	-	GO:00482	gi 14192937 ref		
19	1496	1.965	0.565	-1.79821	Down	0.970268	RPRM	2 K10128 1	GO:00444	GO:00054	GO:00224	gi 9790193 ref		
20	117	5.2	1.56	-1.73697	Down	0.982273	RNU5A-1	2 -	-	-	-	-	-	
21	74	3.405	1.0275	-1.72852	Down	0.93324	SNORD55	2 -	-	-	-	-	-	
22	627	2.9425	0.925	-1.66952	Down	0.96074	HBA1	4 K13822 1	GO:00432	GO:00228	GO:00156	gi 635029536 ref		
23	88	3.71	1.2425	-1.57817	Down	0.948089	SNORD140	2 -	-	-	-	-	-	
24	5622	2.3	0.7775	-1.56472	Down	0.970425	AHRR	1 K09094 1	GO:00319	GO:00600	GO:00063	gi 115430245 ref		
25	137	1.1525	0.4	-1.52669	Down	0.873129	SNORA55	1 -	-	-	-	-	-	
26	1014	1.6625	0.61	-1.44647	Down	0.974141	LOC10192	1 -	-	-	-	-	gi 119569977 gb	
27	2831	2.1525	0.8025	-1.42344	Down	0.973103	COL9A2	3 K08131 1	GO:00055	-	-	-	gi 1054873 gb	
28	97	3.405	1.28	-1.41151	Down	0.935986	SNORD880	1 -	-	-	-	-	-	
29	71	2.975	1.1325	-1.39338	Down	0.935993	MIR6748	1 -	-	-	-	-	-	
30	90	1.9075	0.7325	-1.38078	Down	0.950314	SNORD12	1 -	-	-	-	-	-	

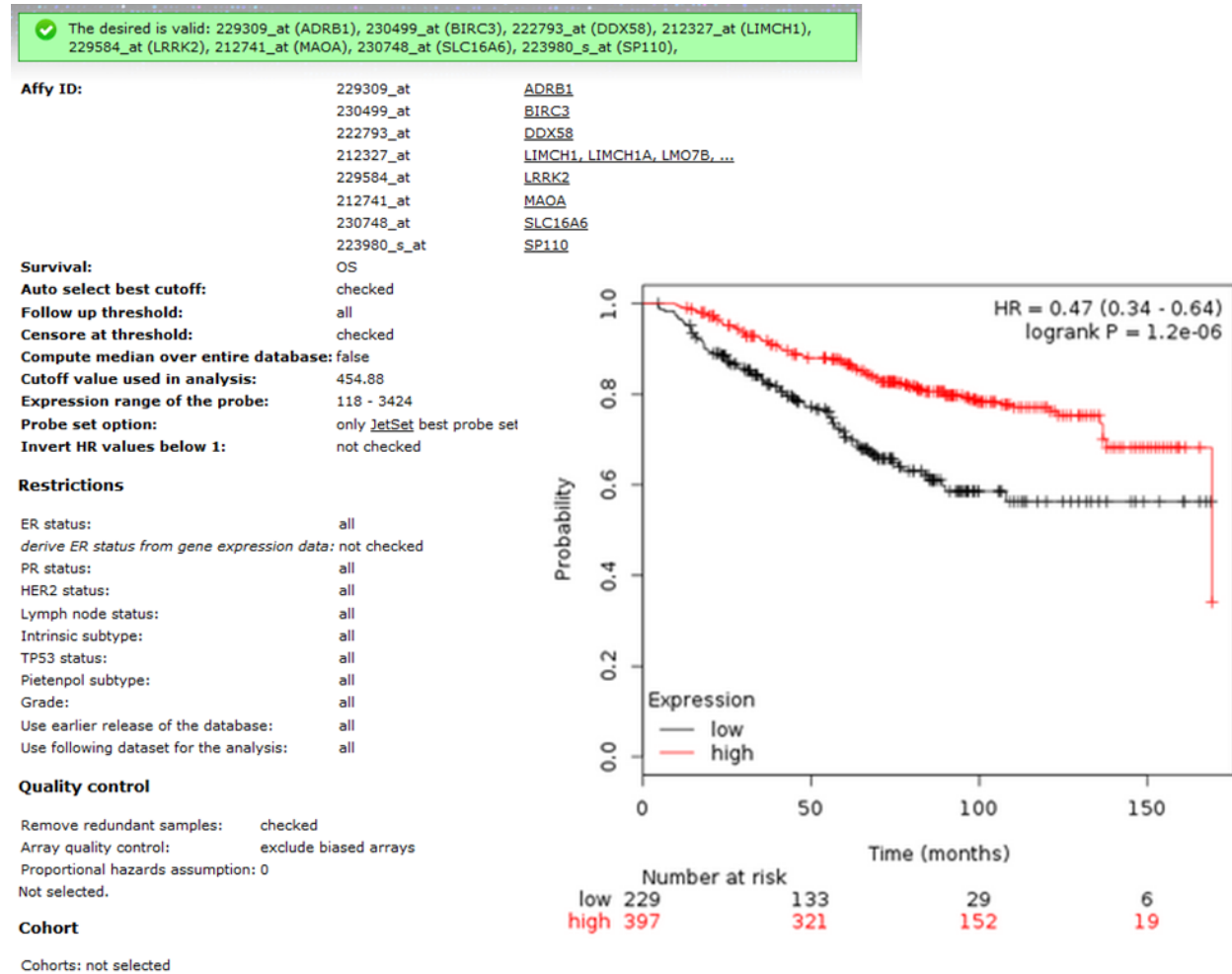
## 6-10. Kaplan-Meier plots for miR-378 in ER-positive breast cancers

High expression of miR-378 is associated with better overall survival in ER-positive breast cancer



## 6-11. Kaplan-Meier plots for selected miR-378 gene signature

Kaplan-Meier plots demonstrating a significant association between elevated expression of the miR-378 signature (red line) and longer relapse-free survival in 1809 patients using KM plotter.



HR = 0.47 (0.34 - 0.64)  
logrank P = 1.2e-06

Probability

Time (months)

Expression  
— low  
— high

	0	50	100	150
low	229	133	29	6
high	397	321	152	19

✓ The desired is valid: 229309\_at (ADRB1), 230499\_at (BIRC3), 222793\_at (DDX58), 212327\_at (LIMCH1), 229584\_at (LRRK2), 212741\_at (MAOA), 230748\_at (SLC16A6), 223980\_s\_at (SP110),

**Affy ID:** 229309\_at ADRB1  
 230499\_at BIRC3  
 222793\_at DDX58  
 212327\_at LIMCH1, LIMCH1A, LMO7B, ...  
 229584\_at LRRK2  
 212741\_at MAOA  
 230748\_at SLC16A6  
 223980\_s\_at SP110

**Survival:** RFS  
**Auto select best cutoff:** checked  
**Follow up threshold:** all  
**Censore at threshold:** checked  
**Compute median over entire database:** false  
**Cutoff value used in analysis:** 415.38  
**Expression range of the probe:** 111 - 3424  
**Probe set option:** only JetSet best probe set  
**Invert HR values below 1:** not checked

**Restrictions**

ER status:  
*derive ER status from gene expression*  
 PR status:  
 HER2 status:  
 Lymph node status:  
 Intrinsic subtype:  
 TP53 status:  
 Pietsenpol subtype:  
 Grade:  
 Use earlier release of the database:  
 Use following dataset for the analysis:

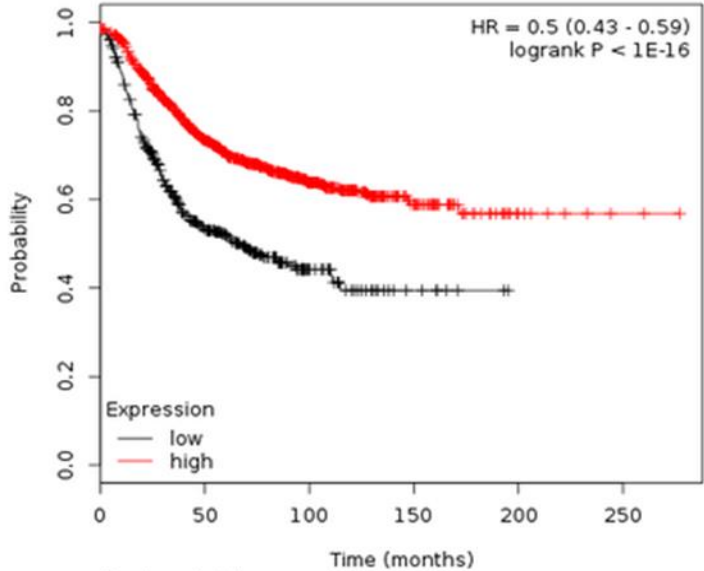
**Quality control**

Remove redundant samples: check  
 Array quality control: exclu  
 Proportional hazards assumption: 0  
 Not selected.

**Cohort**

Cohorts: not selected

**Results**



	low	high	453	180	39	8	0	0
low	453	180	39	8	0	0		
high	1311	797	306	60	10	2		

## 6-12. MiR-616 upregulated dependent genes

The 30 most upregulated genes analysed by RNA sequencing are shown.

	A	B	C	D	E	F	G	H	I	J	K	L	M	N
	GeneID	geneLength	Means-M	Means-M	log2Ratio	Up-Down	Probability	Symbol	Description	KEGG Orth	GO Comp	GO Functi	GO Proces	Blast
1	693201	97	0.225	443.1625	10.9437	Up	1	MIR616	1 -	-	-	-	-	-
2	26832	117	0.01	3.56	8.475733	Up	0.997767	RNU5B-1	3 -	-	-	-	-	-
3	26864	164	0.515	180.3325	8.451871	Up	1	RNVU1-7	2 K17540 1	-	-	-	-	gi 927
4	1.01E+08	80	0.01	2.48	7.954196	Up	1	MIR3198-	1 K04726 1	-	-	-	-	-
5	6023	277	0.1675	40.7825	7.927645	Up	1	RMRP	3 -	-	-	-	-	gi 431
6	1.02E+08	86	0.01	1.6325	7.350939	Up	1	ALCAM	1 -	-	-	-	-	-
7	1.02E+08	72	0.01	1.515	7.243174	Up	1	MIR6875	1 -	-	-	-	-	-
8	1E+08	73	0.01	1.48	7.209453	Up	0.999997	ID4	1 -	-	-	-	-	-
9	1.02E+08	669	0.01	1.3425	7.068778	Up	1	LOC10192	1 K17570 1	-	-	-	-	gi 432
10	85495	341	0.76	98.09	7.011963	Up	1	RPPH1	1 K10798 1	-	-	-	-	gi 426
11	1.02E+08	68	0.01	1.275	6.994353	Up	0.996106	MIR6734	1 -	-	-	-	-	-
12	1.01E+08	60	0.01	1.15	6.84549	Up	0.994923	RAB6C	1 -	-	-	-	-	-
13	1.01E+08	109	0.01	1.1175	6.804131	Up	1	SOCS2	1 -	-	-	-	-	-
14	1.02E+08	73	0.01	1.105	6.787903	Up	1	MIR6769A	1 -	-	-	-	-	-
15	1.02E+08	61	0.01	1.095	6.774787	Up	0.995327	MIR6845	1 -	-	-	-	-	-
16	125050	332	3.0625	321.405	6.713539	Up	1	RN7SK	2 K17570 1	-	-	-	-	gi 432
17	26807	62	0.01	1.0475	6.710806	Up	1	SNORD43	1 -	-	-	-	-	-
18	6060	164	0.84	38.8075	5.529802	Up	0.999954	RNU1-4	1 K17540 1	-	-	-	-	gi 927
19	26869	164	0.84	38.8075	5.529802	Up	0.999954	RNU1-3	1 K17540 1	-	-	-	-	gi 927
20	26870	164	0.84	38.8075	5.529802	Up	0.999954	RNU1-2	1 K17540 1	-	-	-	-	gi 927
21	26871	164	0.84	38.8075	5.529802	Up	0.999954	RNU1-1	2 K17540 1	-	-	-	-	gi 927
22	26863	164	0.84	38.8075	5.529802	Up	0.999954	RNVU1-18	1 K17540 1	-	-	-	-	gi 927
23	1E+08	5070	0.175	7.0275	5.327585	Up	0.999454	RNA28S5	2 K04257 1	-	GO:00010	GO:00063	gi 954	
24	780851	217	0.71	25.6025	5.172322	Up	0.999409	SNORD3A	1 -	-	-	-	-	gi 296
25	1E+08	1869	0.2775	6.985	4.6537	Up	0.999018	RNA18S5	2 K05692 1	-	-	-	-	gi 296
26	420	1386	0.2075	4.44	4.419376	Up	1	ART4	2 K06717 1	GO:00312	GO:00167	GO:00090	gi 397	
27	11012	1200.88	0.2875	6.1125	4.410129	Up	0.999056	KLK11	2 K09620 1	-	GO:00041	GO:00195	gi 216	
28	26834	141	0.25	5.15	4.364572	Up	0.997428	RNU4-2	2 K11414 1	-	-	-	-	gi 676
29	26835	144	0.36	6.65	4.207286	Up	0.997552	RNU4-1	1 K11414 1	-	-	-	-	gi 676



## 6-13. MiR-616 downregulated dependent genes

The 30 most downregulated genes analysed by RNA sequencing are shown.

GeneID	geneLengt	Means-M	Means-M	log2Ratio	Up-Down	Probability	Symbol	Descriptio	KEGG Orth	GO Comp	GO Functi	GO Proces	Blast
1.01E+08	63	22.545	0.01	-11.1386	Down	1	MIR4426	1 -	-	-	-	-	
1.01E+08	55	2.07	0.01	-7.69349	Down	1	MIR3929	1 -	-	-	-	-	
1.02E+08	65	1.83	0.01	-7.5157	Down	0.999791	MIR6727	1 -	-	-	-	-	
26798	70	1.545	0.01	-7.27146	Down	1	SNORD51	1 -	-	-	-	-	
26817	66	1.31	0.01	-7.03342	Down	1	GALNT14	1 -	-	-	-	-	
94163	69	1.2	0.01	-6.90689	Down	0.999995	SNORD38B	1 -	-	-	-	-	
1.02E+08	69	1.17	0.01	-6.87036	Down	0.999992	VAV1	1 -	-	-	-	-	
1.01E+08	60	1.0975	0.01	-6.77808	Down	1	MIR4722	1 -	-	-	-	-	
6279	450	20.8225	0.23	-6.50037	Down	0.999999	S100A8	4 K17274 1	GO:00444	GO:00468	GO:00069	gi 42	
3934	863	16.7325	0.21	-6.31612	Down	1	SUSD3	4 K01830 1	GO:00444	GO:00469	GO:00346	gi 11	
3576	1718	2.89	0.04	-6.17493	Down	1	CXCL8	3 K10030 1	GO:00444	GO:00051	GO:00069	gi 10	
6278	450	18.925	0.325	-5.86371	Down	1	S100A7	3 -	GO:00432	GO:00469	GO:00434	gi 63	
10537	1006	2.02	0.0475	-5.41028	Down	0.999412	MYC	3 K12157 1	GO:00432	GO:00324	GO:00069	gi 22	
6280	586	76.5825	2.0475	-5.22508	Down	1	S100A9	3 K17274 1	GO:00432	GO:00600	GO:00069	gi 45	
629	2646	6.575	0.225	-4.86899	Down	0.99945	CFB	5 K01335 1	GO:00160	GO:00041	GO:00069	gi 67	
6288	579	1.6575	0.08	-4.37287	Down	0.997503	SAA1	5 K17310 1	GO:00343	GO:00051	GO:00301	gi 40	
4939	3395.59	9.9175	0.4925	-4.33178	Down	0.996705	OAS2	1 K14216 1	GO:00432	GO:00036	GO:00192	gi 11	
3429	659.52	14.1625	0.705	-4.32831	Down	1	BCL2	4 -	GO:00444	-	GO:00430	gi 79	
1.01E+08	110	3.435	0.19	-4.17624	Down	0.998897	MIR3653	1 -	-	-	-	-	
27189	1048	1.1875	0.0675	-4.1369	Down	0.998516	IL17C	3 K05491 1	GO:00444	GO:00051	GO:00069	gi 70	
684	1048	9.6725	0.7275	-3.73287	Down	0.999992	BST2	3 K06731 1	GO:00160	GO:00600	GO:00069	gi 47	
1.01E+08	1085	1.98	0.1575	-3.65208	Down	0.999656	CFAP58-AS	1 -	-	-	-	gi 20	
718	5148	2.7475	0.22	-3.64254	Down	0.997378	LINC00052	3 K03990 1	-	-	-	gi 11	
7052	4964	3.01	0.2525	-3.57541	Down	0.999531	TGM2	1 K05625 1	-	GO:00431	GO:00301	gi 39	
1.02E+08	107	44.285	3.7225	-3.57247	Down	1	RNU6-7	1 K05692 1	-	-	-	gi 53	
1.02E+08	107	44.285	3.7225	-3.57247	Down	1	RNU6-8	1 K05692 1	-	-	-	gi 53	
4599	3444	6.43	0.5425	-3.56712	Down	0.999989	MX1	1 K14754 1	GO:00444	GO:00171	GO:00125	gi 22	
693206	96	2.255	0.195	-3.53158	Down	0.992257	MIR621	1 -	-	-	-	-	
3248	2774	2.755	0.2725	-3.33772	Down	0.999999	HPGD	1 K00069 1	GO:00319	GO:00512	GO:00000	gi 31	



## 6-14. Permission letter for figure 1-4.

https://s100.copyright.com/AppDispatchServlet

**ELSEVIER LICENSE  
TERMS AND CONDITIONS**

Oct 18, 2018

---

This Agreement between Mr. Vahid Arabkari ("You") and Elsevier ("Elsevier") consists of your license details and the terms and conditions provided by Elsevier and Copyright Clearance Center.

License Number	4451760461096
License date	Oct 18, 2018
Licensed Content Publisher	Elsevier
Licensed Content Publication	Cell
Licensed Content Title	Hallmarks of Cancer: The Next Generation
Licensed Content Author	Douglas Hanahan,Robert A. Weinberg
Licensed Content Date	Mar 4, 2011
Licensed Content Volume	144
Licensed Content Issue	5
Licensed Content Pages	29
Start Page	646
End Page	674
Type of Use	reuse in a thesis/dissertation
Portion	figures/tables/illustrations
Number of figures/tables /illustrations	1
Format	both print and electronic
Are you the author of this	No

## 6-15. Submitted manuscripts.

### **miRNA-378 is downregulated by XBP1 and inhibits growth and migration of luminal breast cancer cells**

Vahid Arabkari<sup>1</sup>, David Barua<sup>1</sup>, Muhammad Mosaraf Hossain<sup>1,2</sup>, Mark Webber<sup>1</sup>, Terry Smith<sup>3</sup>, Ananya Gupta<sup>4</sup> and Sanjeev Gupta<sup>1\*</sup>

<sup>1</sup>Discipline of Pathology, Lambe Institute for Translational Research, Clinical Science Institute, School of Medicine, National University of Ireland Galway, Ireland

<sup>2</sup>Department of Biochemistry and Molecular Biology, University of Chittagong, Chittagong, Bangladesh.

<sup>3</sup>Molecular Diagnostic Research Group, College of Science, National University of Ireland Galway, Ireland

<sup>4</sup>Discipline of Physiology, School of Medicine, National University of Ireland Galway, Ireland

Authors email address:

Vahid Arabkari ([v.arabkari1@nuigalway.ie](mailto:v.arabkari1@nuigalway.ie)), David Barua ([d.barua1@nuigalway.ie](mailto:d.barua1@nuigalway.ie)), Muhammad Mosaraf Hossain ([mosarafacme@gmail.com](mailto:mosarafacme@gmail.com)), Mark Webber ([mark.webber@nuigalway.ie](mailto:mark.webber@nuigalway.ie)), Terry Smith ([terry.smith@nuigalway.ie](mailto:terry.smith@nuigalway.ie)), Ananya Gupta ([Ananya.gupta@nuigalway.ie](mailto:Ananya.gupta@nuigalway.ie)), Sanjeev Gupta ([sanjeev.gupta@nuigalway.ie](mailto:sanjeev.gupta@nuigalway.ie))

Address correspondence to:

\* Sanjeev Gupta, PhD

School of Medicine

NUI Galway

Galway, Ireland

Tel: +353 (0)91 494415 ext 4415

Email: [sanjeev.gupta@nuigalway.ie](mailto:sanjeev.gupta@nuigalway.ie)

Keywords: endoplasmic reticulum stress, endocrine resistance, XBP1, miR-378, breast cancer

## Abstract

**Background:** Stressful conditions such as oxygen and nutrient deprivation, hypoxia, acidic pH in tumour microenvironment induce the unfolded protein response (UPR) which contributes to endocrine resistance in ER-positive breast cancer. Expression of spliced XBP1 (XBP1s) is increased during UPR and it is a key UPR component mediating endocrine resistance. Transcriptional activity XBP1s is a major component of its biological effects but the mediators of XBP1s in estrogen receptor-positive breast cancer are not well understood.

**Methods:** MCF-7, ZR-75-1, MDA-MB-231, and HCT116 cells were treated with three different endoplasmic reticulum (EnR) stressors and levels of miR-378, PARGC1b (host gene of miR-378) and UPR target genes were assessed by RT-qPCR and Western blot analyses. The role of XBP1s on miR-378 expression was assessed with overexpression or silencing techniques. Various techniques were utilized to assess the biological effect of miR-378, including MTS cell proliferation, colony formation assay, *in vitro* scratch assay and cell death analyses. Published microarray databases of breast cancer tissues were analysed for association of miR-378 and miR-378-specific gene signature with outcome in breast cancer.

**Results:** Here we show that XBP1s downregulates the expression of miR-378 and PPARGC1b (host gene of miR-378) during UPR. Ectopic expression of XBP1s repressed the expression of miR-378 and PPARGC1b and we observed an inverse relationship between the expression of XBP1 and PPARGC1b in breast cancer subset of TCGA. Our results show that overexpression of miR-378 significantly suppressed cell growth, colony formation and migration of estrogen receptor (ER)-positive breast cancer cells (MCF7, ZR-75-1). Further, we found that expression of miR-378 sensitized the cells to UPR-induced cell death and anti-estrogens. Higher expression of miR-378 was associated with better overall survival in ER-positive breast cancer. We found that miR-378 upregulates the expression of several genes that regulate type I interferon signalling and conditioned medium from miR-378 expressing cells inhibited the growth of parental MCF7 cells. Analysis of separate cohorts of breast cancer patients showed that a gene-signature derived from miR-378 upregulated genes showed a strong association with improved overall and recurrence free survival in breast cancer.

**Conclusions:** Overall our findings show an important role for the XBP1s-miR-378 signalling in ER-positive breast cancer and suggest that XBP1s may contribute to the development of endocrine-resistant breast cancer, in part, by downregulating the expression of miR-378.

**Pathology & Oncology Research**  
**Relative and Absolute Expression Analysis of MicroRNAs Associated with Luminal A Breast Cancer- A Comparison**  
 --Manuscript Draft--

<b>Manuscript Number:</b>	PORE-D-18-00030
<b>Full Title:</b>	Relative and Absolute Expression Analysis of MicroRNAs Associated with Luminal A Breast Cancer- A Comparison
<b>Article Type:</b>	Original Article
<b>Keywords:</b>	MicroRNAs, Luminal A breast cancer, Relative quantification, Absolute quantification
<b>Corresponding Author:</b>	Vahid Arabkari National University of Ireland Galway Galway, IRELAND
<b>Corresponding Author Secondary Information:</b>	
<b>Corresponding Author's Institution:</b>	National University of Ireland Galway
<b>Corresponding Author's Secondary Institution:</b>	
<b>First Author:</b>	Vahid Arabkari
<b>First Author Secondary Information:</b>	
<b>Order of Authors:</b>	Vahid Arabkari Eoin Clancy Róisín M Dwyer Michael J Kerin Olga Kalinina Emma Holian John Newell Terry J Smith
<b>Order of Authors Secondary Information:</b>	
<b>Funding Information:</b>	
<b>Abstract:</b>	<p>MicroRNAs, as small non-coding regulatory RNAs, play crucial roles in various aspects of breast cancer biology. They have prognostic and diagnostic value, which makes them very interesting molecules to investigate. Reverse transcriptase quantitative polymerase chain reaction (RT-qPCR) is the gold standard method to analyse miRNA expression in breast cancer patients. This study investigated two RT-qPCR methods (absolute and relative) to determine the expression of ten miRNAs in whole blood samples obtained from luminal A breast cancer patients compared to healthy controls. Whole blood samples were collected from 38 luminal A breast cancer patients and 20 healthy controls in Paxgene blood RNA tubes. Total RNA was extracted and analysed by relative and absolute RT-qPCR. For relative RT-qPCR, miR-16 was used as an endogenous control. For absolute RT-qPCR, standard curves were generated using synthetic miRNA oligonucleotides to determine the absolute copy number of each miRNA.</p> <p>Of the ten miRNAs that were analysed, the absolute RT-qPCR method identified six miRNAs (miR-16, miR-145, miR-155, miR-451a, miR-21 and miR-486) that were upregulated and one miRNA (miR-195) that was downregulated. ROC curve and AUC analysis of the data found that the combination of three miRNAs (miR-145, miR-195 and miR-486) had the best diagnostic value for luminal A breast cancer with an AUC of 0.875, with 76% sensitivity and 81% specificity. On the other hand, the relative RT-qPCR method identified two miRNAs (miR-155 and miR-486) that were upregulated</p>

*Powered by Editorial Manager® and ProduXion Manager® from Aries Systems Corporation*

	and miR-195, which was downregulated. Using this approach, the combination of three miRNAs (miR-155, miR-195 and miR-486) was showed to have an AUC of 0.657 with 65% sensitivity and 69% specificity. we conclude that miR-16 is not a suitable normalizer for the relative expression profiling of miRNAs in luminal A breast cancer patients. Compare to relative quantification, absolute quantification assay is better method to determine the expression level of circulating miRNAs in Luminal A breast cancer.
<b>Suggested Reviewers:</b>	Dr. Ian A CREE  Dr. Andrea LADÁNYI

1 ***Relative and Absolute Expression Analysis of MicroRNAs***  
2 ***Associated with Luminal A Breast Cancer– A Comparison***

3 Vahid Arabkari<sup>1,2\*</sup>, Eoin Clancy<sup>1</sup>, Róisín M. Dwyer<sup>3</sup>, Michael J. Kerin<sup>3</sup>, Olga Kalinina<sup>4</sup>, Emma  
4 Holian<sup>4</sup>, John Newell<sup>4</sup> and Terry J. Smith<sup>1\*</sup>

5

---

6 <sup>1</sup>Molecular Diagnostics Research Group, School of Natural Sciences and National Centre for Biomedical

7 Engineering Science, NUI Galway, Ireland

8 <sup>2</sup>Discipline of Pathology, School of Medicine, Lambe Institute for Translational Research, NUI Galway, Ireland

9 <sup>3</sup>Discipline of Surgery, School of Medicine, Lambe Institute for Translational Research, NUI Galway, Ireland

10 <sup>4</sup>Clinical Research Facility and School of Mathematics, Statistics and Applied Mathematics, NUI Galway, Ireland

11

12 \* Corresponding author

13 E-mail: terry.smith@nuigalway.ie (TJS) - v.arabkari1@nuigalway.ie (VA)

14

15 **Abstract**

16 MicroRNAs, as small non-coding regulatory RNAs, play crucial roles in various aspects of breast  
17 cancer biology. They have prognostic and diagnostic value, which makes them very interesting  
18 molecules to investigate. Reverse transcriptase quantitative polymerase chain reaction (RT-  
19 qPCR) is the gold standard method to analyse miRNA expression in breast cancer patients. This  
20 study investigated two RT-qPCR methods (absolute and relative) to determine the expression of  
21 ten miRNAs in whole blood samples obtained from luminal A breast cancer patients compared  
22 to healthy controls.

23 Whole blood samples were collected from 38 luminal A breast cancer patients and 20 healthy  
24 controls in Paxgene blood RNA tubes. Total RNA was extracted and analysed by relative and  
25 absolute RT-qPCR. For relative RT-qPCR, miR-16 was used as an endogenous control. For  
26 absolute RT-qPCR, standard curves were generated using synthetic miRNA oligonucleotides to  
27 determine the absolute copy number of each miRNA.

28 Of the ten miRNAs that were analysed, the absolute RT-qPCR method identified six miRNAs (miR-  
29 16, miR-145, miR-155, miR-451a, miR-21 and miR-486) that were upregulated and one miRNA  
30 (miR-195) that was downregulated. ROC curve and AUC analysis of the data found that the  
31 combination of three miRNAs (miR-145, miR-195 and miR-486) had the best diagnostic value for  
32 luminal A breast cancer with an AUC of 0.875, with 76% sensitivity and 81% specificity. On the  
33 other hand, the relative RT-qPCR method identified two miRNAs (miR-155 and miR-486) that  
34 were upregulated and miR-195, which was downregulated. Using this approach, the combination  
35 of three miRNAs (miR-155, miR-195 and miR-486) was showed to have an AUC of 0.657 with 65%

36 sensitivity and 69% specificity. we conclude that miR-16 is not a suitable normalizer for the  
37 relative expression profiling of miRNAs in luminal A breast cancer patients. Compare to relative  
38 quantification, absolute quantification assay is better method to determine the expression level  
39 of circulating miRNAs in Luminal A breast cancer.

40

41 **Key words:**

42 MicroRNAs, Luminal A breast cancer, Relative quantification, Absolute quantification.

43

## 44 Introduction

45 Human cancer is the among the top leading causes of death globally, based on World Health  
46 Organization (WHO) estimates in 2015 [1]. Globally, there were 14.1 million new cancer cases  
47 and 8.2 million deaths from cancer reported in 2012 [2]. These include, 3.45 million new cases  
48 and 1.75 million deaths within in the European Union during that same period [3]. In terms of its  
49 significance, breast cancer, as a heterogeneous disease, is one of the most common causes of  
50 death in women in developed countries with approximately 1.67 million new cases and 522,000  
51 deaths from breast cancer recorded in 2012 [2].

52 Breast cancer can be classified into four subtypes based on hormone receptor status [4, 5]. These  
53 subtypes include; Luminal A (ER and/or PR positive, HER2/neu negative), Luminal B (ER, PR, and  
54 HER2/neu triple positive), Basal-like or triple negative (ER, PR, and HER2/neu triple negative) and  
55 HER2 amplified (ER and PR negative, HER2/neu positive). Each of these subtypes has a different  
56 prognosis, biological behaviour and treatment regimen. Luminal A breast cancers, as the  
57 commonest subtype, have a good prognosis, and show satisfactory responses to hormone  
58 therapies [6, 7].

59 MicroRNAs (miRNAs) are small regulatory RNAs found in all tissues, including blood. It has been  
60 shown that miRNAs are linked to the etiology, progression and prognosis of cancer [8].  
61 Furthermore, miRNAs expression profiles can be used to classify cancer types [9]. The abundance  
62 of particular miRNAs, including circulating miRNAs, has been shown to be dysregulated in certain  
63 cancers [10]. Dysregulation of miRNAs has also been observed in tumours and in the blood of  
64 breast cancer patients, suggesting that they may have diagnostic potential in breast cancer [11-



65 14]. Iorio *et al.* (2005), identified 29 miRNAs that were differentially expressed in breast cancer  
66 tissue [10]. They found that the most consistently dysregulated miRNAs were miR-10b, miR-125b,  
67 miR145, miR-21, and miR-155. Of these, three (miR-10b, miR-125b and miR-145) were  
68 downregulated and two (miR-21 and miR-155) were upregulated [11]. Chan *et al.* (2013),  
69 examined the 20 most differentially expressed miRNAs in breast cancer tumours in a cohort (n  
70 =32) of breast cancer patients [15]. They found several miRNAs that were dysregulated in these  
71 patients, including; miR-145, miR-21, miR-10b, miR-1, miR-92a, miR-133a, and miR-133b. In  
72 another study by McDermott *et al.* (2014), specific miRNA expression profiles were identified in  
73 whole blood of luminal A-like (ER+PR+HER2/neu-) breast cancer subtype [14]. This study found  
74 that miR-29, miR-181a and miR-652 were significantly downregulated in the blood of patients  
75 compared to healthy individuals.

76 Reverse transcriptase real-time quantitative PCR (RT-qPCR) is the gold standard technology for  
77 profiling the expression of miRNAs. Using RT-qPCR, miRNAs can be profiled in terms of their  
78 absolute copy number (absolute quantitation) or relative to a predefined reference biomarker  
79 (relative quantitation). In this study, we analysed and compared the expression level of ten  
80 selected miRNAs with both absolute and relative RT-qPCR assays in whole blood from luminal A  
81 breast cancer patients.

82

83

84

85

## 86 **Materials and Methods**

### 87 **Sample Collection**

88 Whole blood from 38 luminal A breast cancer patients and 20 healthy females attending Galway  
89 University Hospital (GUH) was collected in PAXgene Blood RNA tubes (Qiagen, Germany). All  
90 patients have confirmed ER /PR positive and HER2/neu negative breast cancer. Control blood  
91 samples were collected from women without any history of malignancy, inflammatory or  
92 infectious diseases. Clinicopathological details of patient cohort are shown in Table S1.

### 93 **Ethics Statement**

94 The study was performed in accordance with the Clinical Research Ethics Committee, Galway  
95 University Hospital and written informed consent was obtained from all participants involved in  
96 this study.

### 97 **Total RNA Extraction**

98 Total RNA was extracted and purified using the PAXgene Blood RNA kit (Qiagen, Germany)  
99 according the manufacturer's instructions. Following purification, total RNA was quantified by  
100 UV spectrophotometry (NanoDrop, ThermoFisher) and analysed by capillary electrophoresis  
101 (RNA 6000 NanoChip Kit Series II, Agilent Technologies, USA) to determine its integrity, (RNA  
102 Integrity Number >8). Samples were then stored at -80°C until required.

103

104

## 105 **MicroRNA Reverse Transcription**

106 Ten miRNAs (miR-195, miR-16, miR-21, miR-451a, miR-486, miR-181a, miR-145, miR-155, miR-  
107 10b and miR-205) were chosen for analysis (Table S2). Each miRNA was separately reverse  
108 transcribed using 100 nanograms of total RNA from each sample using the TaqMan miRNA  
109 reverse transcription kit (Cat. No. 4366596, Life Technologies, Paisley, UK) according to the  
110 manufacturer's instructions. Briefly, the reverse transcription reaction consisted of 7 µL master  
111 mix [4.16 µL nuclease free water, 1.5 µL 10X RT buffer, 1 µL multiscribe RT enzyme (50 U/ µL),  
112 0.19 µL RNase inhibitor (20U/ µL) and 0.15 µL dNTP mix (100mM total)], 3 µL miRNA specific  
113 primer and 5 µL (100 ng) RNA were added to the PCR microtube (total volume 15 µL). Reverse  
114 transcription thermocycling conditions were 16°C for 30 min, 42°C for 30 min, 85°C for 5 min.  
115 The resultant cDNA was stored at -20°C until required.

## 116 **Standard Curves and Quantitative Real-Time PCR**

117 Complementary DNA (cDNA) was analysed by qPCR using specific miRNA TaqMan probes (Life  
118 technologies, Paisley, UK) and the Taqman Universal PCR master mix (Cat. No. 4440047, Life  
119 Technologies, Paisley, UK) according to the manufacturer's instructions (10 µL PCR master mix,  
120 7.67 µL nuclease free water, 1.33 µL cDNA and 1 µL 20X specific microRNA assay). QPCR reactions  
121 were performed on a LightCycler 480 real-time PCR instrument (Roche Diagnostics, UK). The  
122 thermocycling conditions were initial heating to 95°C for 10 min, followed by 40 cycles of 95°C  
123 for 15 seconds/60°C for 60 seconds. The threshold cycle ( $C_T$ ) was determined by the 'Second  
124 Derivative Maximum method' using the LightCycler instrument's software. All qPCR reactions  
125 were performed in triplicate.

126 The absolute copy number of each miRNA was determined using a standard curve. For this  
127 purpose, a 10-fold serial dilution series of synthetic miRNA oligonucleotides (IDT, Iowa, USA) was  
128 used to generate standard curves at various concentrations ( $1 \times 10^1 - 1 \times 10^8$  molecules per  
129 reaction).

### 130 **Statistical Analysis**

131 Using miR-16 as an endogenous control, the relative expression of each miRNA was determined  
132 using REST (Relative Expression Software Tool V2.0.13) [16, 17]. Absolute RT-qPCR (copy number)  
133 data were analysed using the software package SPSS 21.0 for windows and a one-way ANOVA  
134 test was performed to determine the p-value. Receiver operating characteristic (ROC) curves  
135 were generated to evaluate the diagnostic specificity and sensitivity of each miRNA and for  
136 combined miRNAs (using binary logistic regression).

137

138

139

140

141

142

143

144

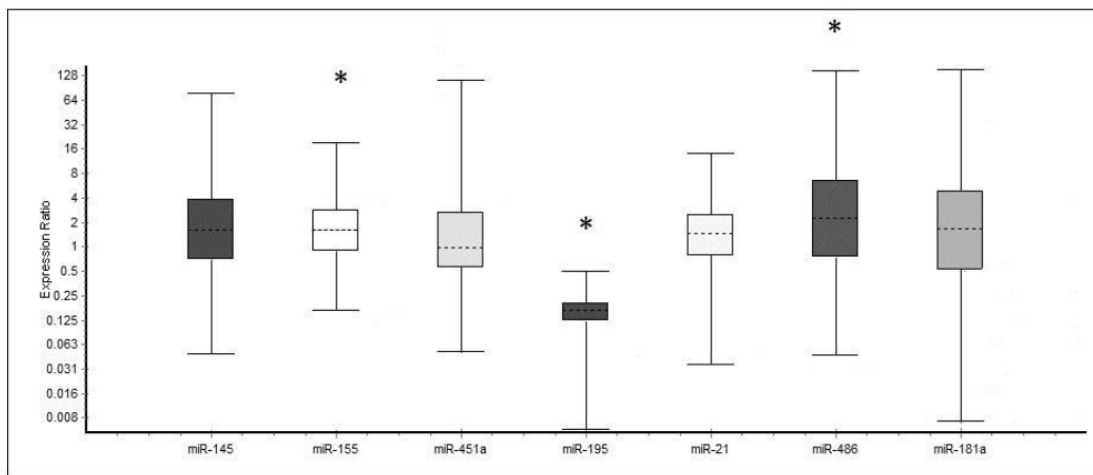
145 **Results**

146 All ten miRNAs were detected in all samples(n=58). Two miRNAs (miR-10b and miR-205) were  
147 present at high C<sub>T</sub> values (> 38) were eliminated from further analysis.

148 **Identification of Dysregulated miRNAs by relative quantification**

149 **method**

150 Using miR-16 as a normaliser, the relative expression profiles of seven miRNAs (miR-21, miR-145,  
151 miR-155, miR-181a, miR-195, miR-451a and miR-486) were determined (Fig 1 and summarised in  
152 Table 1). Two miRNAs (miR-486 and miR-155) were found to be upregulated (P<0.05), whilst one  
153 miRNA (miR-195) was found to be downregulated (P<0.05). MiR-21, miR-181a, miR-145 and miR-  
154 451a were not found to be differentially expressed in patients versus healthy controls (P>0.05).



155  
156 **Figure 1. Relative expression of seven circulating miRNAs in luminal A breast cancer patients by whisker-**  
157 **box plot (\*P < 0.05).**

158

159

**Table 1. Relative expression of circulating miRNAs in luminal A breast cancer patients.**

MicroRNA	Relative expression	95% C. I.	P value	Result
miR-145	1.610	0.146 - 21.07	0.058	--
miR-155	1.633	0.303 - 10.316	0.009	Up
miR-451a	1.621	0.150 - 61.838	0.208	--
miR-195	0.144	0.025 - 0.335	0.0006	Down
miR-21	1.353	0.127 - 6.790	0.103	--
miR-486	2.246	0.104 - 44.785	0.014	Up
miR-181a	1.524	0.042 - 32.547	0.223	--

160

C. I.; Confidence Interval, Up; upregulation, Down; downregulation, P value; P < 0.05 is considered statistically significant.

161

162

163

ROC curves and area under the ROC curves (AUCs) were generated for the miRNAs that were

164

found to be dysregulated by relative quantification (Fig 2). The AUCs for miR-155, miR-486 and

165

miR-195 were 0.795, 0.895 and 0.746 respectively. When combined, the three dysregulated

166

miRNAs (miR-155, miR-195 and miR-486) were determined to have an AUC of 0.657, with 65%

167

diagnostic sensitivity and 69% specificity.

168

169

170

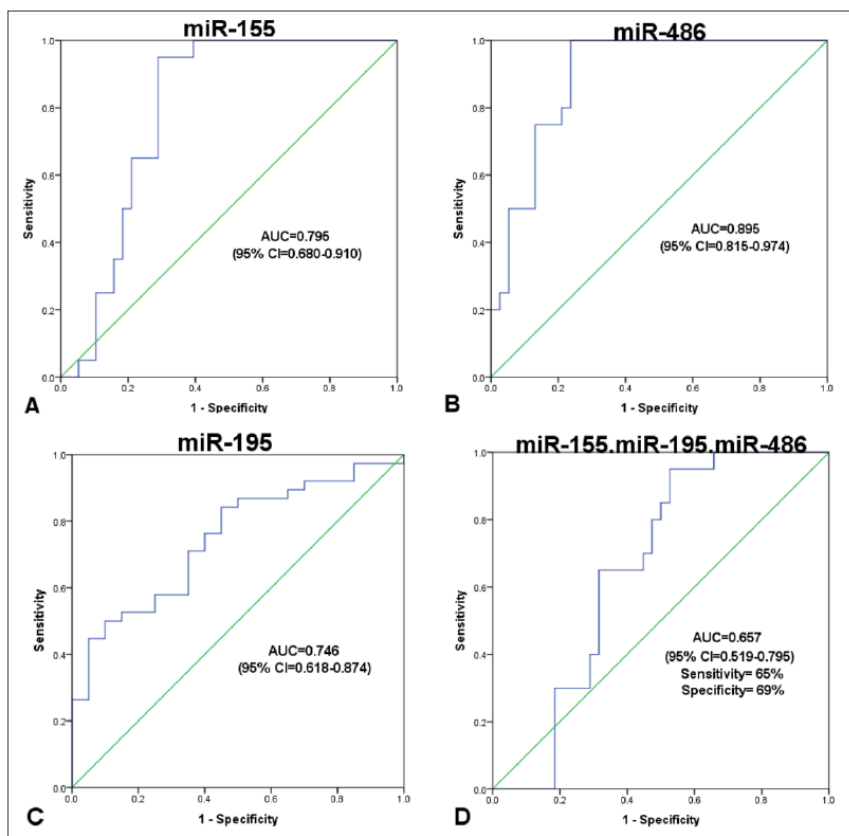
171

172

173

174

175



176

177 **Figure 2. ROC curve analysis for individually dysregulated (A-C) and combination of three circulating**  
 178 **miRNAs (D) in luminal A breast cancer patients by relative quantification assay.**

179

180

181

182

183

184

185

186

187

188 **Identification of Dysregulated miRNAs by absolute quantification**

189 **method**

190 Standard curves were generated using synthetic miRNA oligonucleotides. The curves were linear  
191 over the range of concentrations tested and amplification efficiencies varied between 1.839 and  
192 2.021 (Fig S1).

193 Figure 3 shows the absolute expression values of eight miRNAs (miR-16, miR-145, miR-155, miR-  
194 451a, miR-195, miR-21, miR-486 and miR-181a) in luminal A breast cancer patients (n=38)  
195 compared to controls (n=20). Of these eight miRNAs, six miRNAs (miR-16, miR-145, miR-155, miR-  
196 451a, miR-21 and miR-486) were found to be upregulated, and one miRNAs (miR-195) was found  
197 to be downregulated ( $P<0.05$ ). Mir-181a was not found to be differentially expressed ( $P>0.05$ ).

198

199

200

201

202

203

204

205

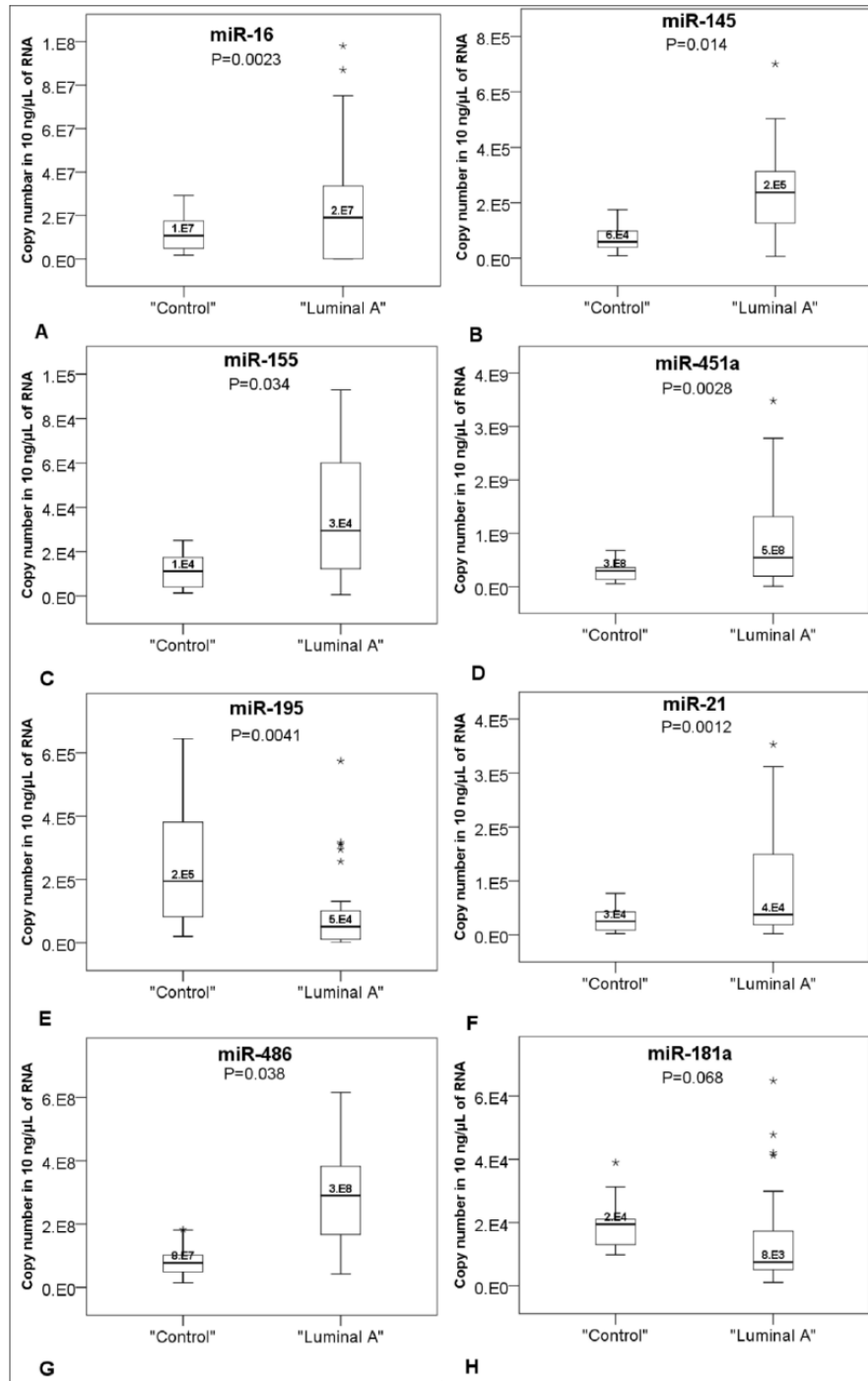
206

207

208

209





210

211 **Figure 3. Real-time PCR analysis for the absolute quantification of circulating miRNAs in luminal A breast**  
 212 **cancer patients by whisker-box plot.**

213 ROC curves and AUCs were established to evaluate the diagnostic value of these miRNAs for  
214 differentiating luminal A breast cancer patients from healthy controls. For the six miRNAs found  
215 to be upregulated at a statistically significant level (miR-16, miR-145, miR-155, miR-451a, miR-21  
216 and miR-486), the AUCs were 0.612, 0.826, 0.775, 0.734, 0.652 and 0.893 respectively. For the  
217 one downregulated miRNA (miR-195), the AUC was 0.807. In addition, the three miRNAs showing  
218 the best diagnostic value were examined in combination. Combining miR-145, miR-195 and miR-  
219 486 resulted in an AUC of 0.875 with 76% diagnostic sensitivity and 81% specificity (Fig 4).

220

221

222

223

224

225

226

227

228

229

230

231

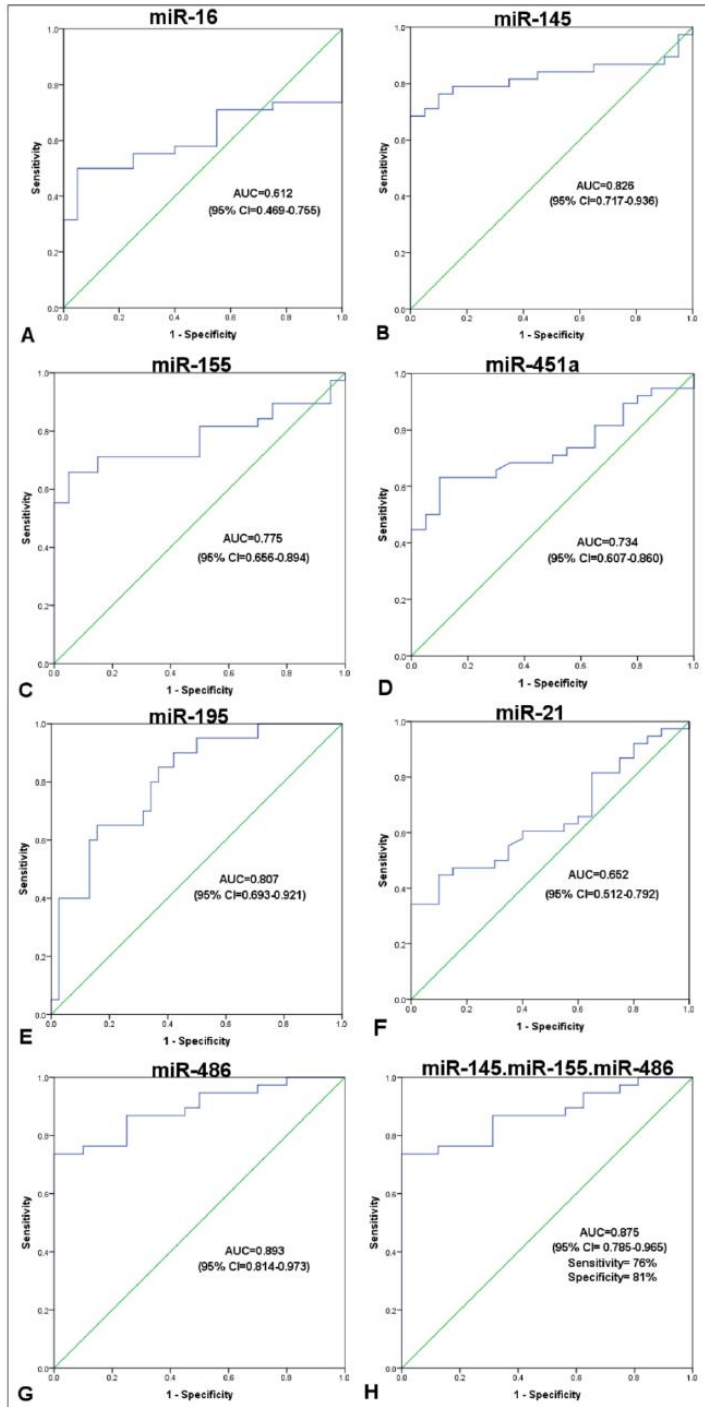
232

233

234

235

236



237

238 Figure 4. ROC curve analysis for individually dysregulated (A-G) and combination of three circulating  
 239 miRNAs (H) in luminal A breast cancer patients by absolute quantification assay.

## 240 **Discussion**

241 Characterising the circulating miRNAs associated with diverse types of human cancer may  
242 increase our ability to diagnose and classify them. Accordingly, miRNA expression profiles in  
243 breast cancer patients indicate that they may potentially be useful in diagnosing and classifying  
244 breast cancer into their different molecular subtypes.

245 Various techniques have been using to analyse microRNA expression profiles, such as microarray,  
246 next-generation sequencing, and reverse transcriptase quantitative PCR (RT-qPCR). The most  
247 popular and powerful method is RT-qPCR, which is based on the amplification of a  
248 complementary DNA (cDNA) template after reverse transcription of the total RNA [18]. There are  
249 two methods of RT-qPCR; relative and absolute quantification RT-qPCR assays. In relative RT-  
250 qPCR, a reference RNA (mRNA, rRNA, or miRNA) is used to normalise the  $C_T$  values of the target  
251 transcripts between patient and control groups. Two mathematical models are applied to  
252 determine the relative expression ratio of the target genes, including the Pfaffl [17] and the Livak/  
253  $\Delta\Delta C_t$  method [19]. Several variations such as sample biological differences, RNA integrity, RT  
254 reaction efficiency and the amount of cDNA template can affect the expression level of miRNAs  
255 [20, 21]. Thus, choosing a stably expressed reference molecule as a normaliser is crucial to obtain  
256 accurate and reliable results in any relative quantification assay

257 In contrast, absolute RT-qPCR can be used to determine the exact copy number of a miRNA.  
258 Traditionally, this has been achieved by relating the signal in an unknown sample to a standard  
259 curve [22, 23]. More recently, digital RT-PCR has been applied to the absolute quantitation of

260 miRNAs [24]. Digital PCR has the inherent advantage of not requiring external calibrators  
261 (standard curve) or normalisation to estimate the concentration of an unknown target [25].

262 Several groups have studied miRNA signatures in various matrices, including; breast tissue, whole  
263 blood, serum and plasma. Various normalisers have been used for the expression profiling of  
264 miRNAs associated with breast cancer, very often leading to conflicting results. For example, Mar-  
265 Aguilar *et al.* (2013) reported the upregulation of miR-145 in the serum of breast cancer patients  
266 using 18s ribosomal RNA as the reference gene [26]. In another study, Kodahl *et al.* (2014) found  
267 that miR-145 was downregulated in the serum of breast cancer patients using miR-10b and miR-  
268 30a as reference genes [27]. The most common reference RNAs that have been used for miRNA  
269 profiling of breast cancer are RNU6B, RNU48, 18s rRNA, Let-7a and cel-miR-39 [11, 13, 26, 28-  
270 34]. There are also a few studies that determined miRNA expression profiles in whole blood of  
271 breast cancer patients, which used miR-16 as the reference miRNA [14, 35].

272 Based on previously published studies, we chose ten circulating miRNAs previously identified as  
273 being dysregulated in breast cancer (miR-195, miR-16, miR-21, miR-451a, miR-486, miR-181a,  
274 miR-145, miR-155, miR-10b and miR-205) to investigate the luminal A breast cancer subtype [13-  
275 15, 34, 36-38]. Of these, miR-205 and miR-10b were eliminated from our analysis because of their  
276 high  $C_T$  values ( $> 38$ ). Mitchell *et al.* (2008) also reported that the miR-205 was not detectable in  
277 the serum of prostate cancer patients using an absolute RT-qPCR assay [39]. A few studies have  
278 reported that these two miRNAs were dysregulated in breast cancer patients. For instance, Liu  
279 *et al.* (2013) found that miR-205 was upregulated in the serum of breast cancer patients [40]. In  
280 another study, Filho and colleagues reported that miR-205 was downregulated in tissue samples  
281 obtained from luminal A and triple negative breast cancer patients [41]. Anfossi *et al.* (2014),

282 observed the upregulation of miR-10b in the blood of breast cancer patients [42]. Furthermore,  
283 Mangolini and colleagues investigated the expression level of some miRNAs in the serum of two  
284 independent cohorts of breast cancer patients. They found that the upregulation of miR-10b is  
285 associated with poor prognosis in patients [43].

286 Of the seven miRNAs analysed by relative quantification, three miRNAs were found to be  
287 dysregulated in Luminal A breast cancer patients. Two miRNAs were upregulated (miR-155 and  
288 miR-486) and one (miR-195) was downregulated. None of the other miRNAs (miR-145, miR-451a,  
289 miR-21 and miR-181a) were found to be dysregulated by this method ( $P > 0.05$ ).

290 On the other hand, for absolute quantification of miRNAs, standard curves were generated using  
291 synthetic miRNAs to enable the absolute copy number of each miRNA to be determined. MiR-  
292 205 and miR-10b were eliminated from our analysis because of the high  $C_T$  values ( $> 38$ ).

293 Of the eight miRNAs that had their absolute copy number determined, seven were found to be  
294 dysregulated in Luminal A breast cancer. Six of these were upregulated (miR-16, miR-145, miR-  
295 155, miR-451a, miR-21 and miR-486) and one was downregulated (miR-195). MiR-181a was not  
296 found to be differentially expressed between patients and controls ( $P > 0.05$ ).

297 The expression levels of miR-155 and miR-486 were found to be significantly increased in the  
298 patient group compare to healthy controls, using both absolute and relative quantification  
299 methods. Chan *et al.* (2013) reported that miR-486 was upregulated in the serum of breast  
300 cancer patients using miR-103 and miR-191 as endogenous controls [15]. However, in contrast,  
301 a few studies have found that miR-486 is downregulated in breast tissue, using small nuclear  
302 RNAs as normaliser [29, 44, 45].

303 MiR-155 is known as a multifunctional miRNA which is over-expressed in a number of different  
304 cancers, including; Acute Myeloid Leukaemia [46], Hodgkin's Lymphoma [47], Colon cancer [48],  
305 Cervical cancer [49] and Lung cancer[50]. Several studies have also described the function and  
306 upregulation of miR-155 in breast cancer tumours and serum [26, 30, 37, 51].

307 MiR-195 was found to be downregulated in the whole blood of patients by both methods in our  
308 study. Zhao *et al.* (2014) reported the downregulation of miR-195 in plasma of breast cancer  
309 patients using miR-16 as an endogenous control [52]. Several groups have also found that miR-  
310 195 is downregulated in breast tumours compare to healthy controls [13, 37, 53, 54]. However,  
311 Heneghan *et al.* showed that miR-195 is upregulated in blood sample of breast cancer patients  
312 [33].

313 Using absolute quantification, we found that miR-451a was increased in the whole blood of  
314 luminal A patients compared the control group. Hu *et al.* (2012) and Ng *et al.* (2013) reported  
315 that miR-451a was upregulated in the serum and plasma of breast cancer patients [55, 56].  
316 However, using relative quantification, we did not find that miR-451a was differentially  
317 expressed.

318 MiR-21 is a well-known oncomir and various studies have found that it is upregulated not only in  
319 breast cancer [11, 42, 56, 57] but also in a wide range of other cancers [48, 58-60]. Here, we  
320 observed upregulation of miR-21 in whole blood of luminal A breast cancer patients by the  
321 absolute quantification method.

322 We showed that miR-145 was upregulated in patients versus healthy controls using the absolute  
323 qPCR method. In two separate studies, Heneghan *et al.* (2010) and Park *et al.* (2014) found that  
324 miR-145 transcription was increased in the blood of breast cancer patients [33, 34].

325 McDermott *et al.* (2014) found that miR-181a was downregulated in luminal A breast cancer  
326 patients [14]. Here, we also observed that miR-181a was downregulated but its expression level  
327 was not statistically significant ( $P > 0.05$ ).

328 Our absolute RT-qPCR assay showed that miR-16 was upregulated in patients versus healthy  
329 controls. Stuckrath and colleagues (2015) reported that miR-16 was upregulated in the plasma  
330 of different subtypes of invasive breast cancer before and after chemotherapy [61]. In another  
331 study by Shin *et al.* (2015), they found that the expression level of miR-16 is higher in plasma of  
332 none triple negative breast cancer (none TNBC) patients compare to healthy controls [62]. Ng *et*  
333 *al.* (2013) and Chan *et al.* (2013) also found that miR-16 was upregulated in plasma and serum of  
334 breast cancer patients using RNU6B and miR-103/miR-191 as reference genes [15, 28]. In another  
335 study, which was carried out by Filho *et al.* (2014), miR-16 was found to be upregulated in tumour  
336 samples from triple negative and luminal A breast cancer patients [41].

337 In this study, we used miR-16 as an internal normalisation control for relative quantification  
338 qPCR, based on previous published reports [34-36, 52, 63]. To date, only miR-16 has been  
339 evaluated as a stable control in whole blood of breast cancer patients and healthy controls. Two  
340 separates studies have found miR-16 to be stably expressed in whole blood [33, 36]. In another  
341 study, McDermott *et al.* (2013) carried out a more in-depth study specifically concerned with the  
342 identification of appropriate miRNA endogenous controls for use in whole blood miRNA



343 quantification [64]. Of 377 human miRNAs, they concluded that miR-16 and miR-425 were the  
344 most stably expressed miRNAs in whole blood samples from breast cancer patients and healthy  
345 controls. All these studies used microarray and relative RT-qPCR assays to evaluate miRNA  
346 expression profiles. In our study, we found that miR-16 was increased ( $P = 0.0023$ ) in the whole  
347 blood of luminal A breast cancer patients compare to healthy controls using our absolute  
348 quantification assay. Absolute quantification permits the generation of highly reproducible and  
349 sensitive data for the expression profiling of miRNAs [22, 23]. As the standard curve is generated,  
350 the exact copy number of target genes is determined which allows a comparison of target gene  
351 expression between patient and control groups directly without the requirement to know the  
352 cDNA synthesis efficiency.

## 353 **Conclusions**

354 Using relative quantification, we observed the upregulation of two miRNAs (miR-155 and miR-  
355 486) and downregulation of one miRNA (miR-195) in the luminal A breast cancer versus healthy  
356 controls. When combined, these three miRNAs were found to have an AUC of 0.657 with  
357 diagnostic 65% sensitivity and 69% specificity.

358 Six miRNAs (miR-16, miR-145, miR-155, miR-451a, miR-21 and miR-486) were found to be  
359 upregulated and one miRNAs (miR-195) was found to be downregulated when analysed using  
360 absolute quantification. The combination of miR-145, miR-195 and miR-486 resulted in the best  
361 diagnostic value (AUC=0.875, sensitivity=76% and specificity=81%) for luminal A breast cancer.  
362 Importantly, we found that miR-16 is upregulated in patients compared to the control group by

363 the absolute quantification method. Consequently miR-16 is not a suitable normaliser for the  
364 relative expression profiling of miRNAs in luminal A breast cancer patients.

365

366

## 367 **Authors Contributions**

368 Conceived and designed the experiments: TJS VA. Performed the experiments: VA. Analysed the  
369 data: VA EH OK JN. Contributed reagents/materials/analysis tools: TJS RMD MJK. Wrote the  
370 paper: VA EC TJS.

371

372

373

374

375

376

377

378

379

380

381

382

383

384

385

386 1. WHO. World Health Organization. Global health

387 observatory data repository. 2015. Number of

388 deaths (World) by cause. . <http://www.who.int/mediacentre/factsheets/fs310/en/>. 2015.389 2. Ferlay J, Soerjomataram I, Dikshit R, Eser S, Mathers C, Rebelo M, et al. Cancer incidence and  
390 mortality worldwide: sources, methods and major patterns in GLOBOCAN 2012. *International journal of*  
391 *cancer Journal international du cancer*. 2015;136(5):E359-86. Epub 2014/09/16. doi: 10.1002/ijc.29210.  
392 PubMed PMID: 25220842.393 3. Ferlay J, Steliarova-Foucher E, Lortet-Tieulent J, Rosso S, Coebergh JW, Comber H, et al. Cancer  
394 incidence and mortality patterns in Europe: estimates for 40 countries in 2012. *European journal of*  
395 *cancer*. 2013;49(6):1374-403. doi: 10.1016/j.ejca.2012.12.027. PubMed PMID: 23485231.396 4. Perou CM, Sorlie T, Eisen MB, van de Rijn M, Jeffrey SS, Rees CA, et al. Molecular portraits of  
397 human breast tumours. *Nature*. 2000;406(6797):747-52. doi: 10.1038/35021093. PubMed PMID:  
398 10963602.399 5. Sorlie T, Wang Y, Xiao C, Johnsen H, Naume B, Samaha RR, et al. Distinct molecular mechanisms  
400 underlying clinically relevant subtypes of breast cancer: gene expression analyses across three different  
401 platforms. *BMC genomics*. 2006;7:127. doi: 10.1186/1471-2164-7-127. PubMed PMID: 16729877;  
402 PubMed Central PMCID: PMC1489944.403 6. Goldhirsch A, Wood WC, Coates AS, Gelber RD, Thurlimann B, Senn HJ. Strategies for subtypes--  
404 dealing with the diversity of breast cancer: highlights of the St. Gallen International Expert Consensus on  
405 the Primary Therapy of Early Breast Cancer 2011. *Annals of oncology : official journal of the European*  
406 *Society for Medical Oncology / ESMO*. 2011;22(8):1736-47. Epub 2011/06/29. doi:  
407 10.1093/annonc/mdr304. PubMed PMID: 21709140; PubMed Central PMCID: PMC3144634.408 7. Rouzier R, Perou CM, Symmans WF, Ibrahim N, Cristofanilli M, Anderson K, et al. Breast cancer  
409 molecular subtypes respond differently to preoperative chemotherapy. *Clinical cancer research : an*  
410 *official journal of the American Association for Cancer Research*. 2005;11(16):5678-85. Epub 2005/08/24.  
411 doi: 10.1158/1078-0432.ccr-04-2421. PubMed PMID: 16115903.412 8. Kumar MS, Lu J, Mercer KL, Golub TR, Jacks T. Impaired microRNA processing enhances cellular  
413 transformation and tumorigenesis. *Nature genetics*. 2007;39(5):673-7. doi: 10.1038/ng2003. PubMed  
414 PMID: 17401365.415 9. Lu J, Getz G, Miska EA, Alvarez-Saavedra E, Lamb J, Peck D, et al. MicroRNA expression profiles  
416 classify human cancers. *Nature*. 2005;435(7043):834-8. doi: 10.1038/nature03702. PubMed PMID:  
417 15944708.418 10. Zen K, Zhang C-Y. Circulating MicroRNAs: a novel class of biomarkers to diagnose and monitor  
419 human cancers. *Medicinal Research Reviews*. 2012;32(2):326-48. doi: 10.1002/med.20215.420 11. Iorio MV, Ferracin M, Liu CG, Veronese A, Spizzo R, Sabbioni S, et al. MicroRNA gene expression  
421 deregulation in human breast cancer. *Cancer research*. 2005;65(16):7065-70. doi: 10.1158/0008-  
422 5472.CAN-05-1783. PubMed PMID: 16103053.423 12. Heneghan HM, Miller N, Lowery AJ, Sweeney KJ, Kerin MJ. MicroRNAs as Novel Biomarkers for  
424 Breast Cancer. *Journal of oncology*. 2009;2009:950201. doi: 10.1155/2010/950201. PubMed PMID:  
425 19639033; PubMed Central PMCID: PMC2712985.426 13. Tahiri A, Leivonen SK, Luders T, Steinfeld I, Ragle Aure M, Geisler J, et al. Deregulation of cancer-  
427 related miRNAs is a common event in both benign and malignant human breast tumors. *Carcinogenesis*.  
428 2014;35(1):76-85. doi: 10.1093/carcin/bgt333. PubMed PMID: 24104550.

- 429 14. McDermott AM, Miller N, Wall D, Martyn LM, Ball G, Sweeney KJ, et al. Identification and  
430 validation of oncologic miRNA biomarkers for luminal A-like breast cancer. *PloS one*. 2014;9(1):e87032.  
431 Epub 2014/02/06. doi: 10.1371/journal.pone.0087032. PubMed PMID: 24498016; PubMed Central  
432 PMCID: PMC3909065.
- 433 15. Chan M, Liaw CS, Ji SM, Tan HH, Wong CY, Thike AA, et al. Identification of circulating microRNA  
434 signatures for breast cancer detection. *Clinical cancer research : an official journal of the American  
435 Association for Cancer Research*. 2013;19(16):4477-87. doi: 10.1158/1078-0432.CCR-12-3401. PubMed  
436 PMID: 23797906.
- 437 16. Pfaffl MW, Horgan GW, Dempfle L. Relative expression software tool (REST) for group-wise  
438 comparison and statistical analysis of relative expression results in real-time PCR. *Nucleic acids research*.  
439 2002;30(9):e36. Epub 2002/04/25. PubMed PMID: 11972351; PubMed Central PMCID: PMC113859.
- 440 17. Pfaffl MW. A new mathematical model for relative quantification in real-time RT-PCR. *Nucleic  
441 acids research*. 2001;29(9):e45. Epub 2001/05/09. PubMed PMID: 11328886; PubMed Central PMCID:  
442 PMC113859.
- 443 18. Klein D. Quantification using real-time PCR technology: applications and limitations. *Trends in  
444 molecular medicine*. 2002;8(6):257-60. Epub 2002/06/18. PubMed PMID: 12067606.
- 445 19. Livak KJ, Schmittgen TD. Analysis of relative gene expression data using real-time quantitative PCR  
446 and the  $2^{-\Delta\Delta C(T)}$  Method. *Methods (San Diego, Calif)*. 2001;25(4):402-8. Epub 2002/02/16. doi:  
447 10.1006/meth.2001.1262. PubMed PMID: 11846609.
- 448 20. Mannhalter C, Koizar D, Mitterbauer G. Evaluation of RNA isolation methods and reference genes  
449 for RT-PCR analyses of rare target RNA. *Clinical chemistry and laboratory medicine*. 2000;38(2):171-7.  
450 Epub 2000/06/02. doi: 10.1515/cclm.2000.026. PubMed PMID: 10834406.
- 451 21. Karge WH, 3rd, Schaefer EJ, Ordovas JM. Quantification of mRNA by polymerase chain reaction  
452 (PCR) using an internal standard and a nonradioactive detection method. *Methods in molecular biology*.  
453 1998;110:43-61. Epub 1999/01/26. doi: 10.1385/1-59259-582-0:43. PubMed PMID: 9918038.
- 454 22. Bustin SA. Absolute quantification of mRNA using real-time reverse transcription polymerase  
455 chain reaction assays. *Journal of molecular endocrinology*. 2000;25(2):169-93. Epub 2000/10/03. PubMed  
456 PMID: 11013345.
- 457 23. Pfaffl MW, Hageleit M. Validities of mRNA quantification using recombinant RNA and  
458 recombinant DNA external calibration curves in real-time RT-PCR. *Biotechnology Letters*. 2001;23(4):275-  
459 82. doi: 10.1023/a:1005658330108.
- 460 24. Hindson CM, Chevillet JR, Briggs HA, Gallichotte EN, Ruf IK, Hindson BJ, et al. Absolute  
461 quantification by droplet digital PCR versus analog real-time PCR. *Nature methods*. 2013;10(10):1003-5.  
462 Epub 2013/09/03. doi: 10.1038/nmeth.2633. PubMed PMID: 23995387; PubMed Central PMCID:  
463 PMC34118677.
- 464 25. Pohl G, Shih le M. Principle and applications of digital PCR. *Expert review of molecular diagnostics*.  
465 2004;4(1):41-7. Epub 2004/01/09. PubMed PMID: 14711348.
- 466 26. Mar-Aguilar F, Mendoza-Ramirez JA, Malagon-Santiago I, Espino-Silva PK, Santuario-Facio SK,  
467 Ruiz-Flores P, et al. Serum circulating microRNA profiling for identification of potential breast cancer  
468 biomarkers. *Disease markers*. 2013;34(3):163-9. PubMed PMID: Medline:23334650.
- 469 27. Kodahl AR, Lyng MB, Binder H, Cold S, Gravgaard K, Knoop AS, et al. Novel circulating microRNA  
470 signature as a potential non-invasive multi-marker test in ER-positive early-stage breast cancer: a case  
471 control study. *Molecular oncology*. 2014;8(5):874-83. Epub 2014/04/04. doi:  
472 10.1016/j.molonc.2014.03.002. PubMed PMID: 24694649.
- 473 28. Ng EK, Li R, Shin VY, Jin HC, Leung CP, Ma ES, et al. Circulating microRNAs as specific biomarkers  
474 for breast cancer detection. *PloS one*. 2013;8(1):e53141. Epub 2013/01/10. doi:  
475 10.1371/journal.pone.0053141. PubMed PMID: 23301032; PubMed Central PMCID: PMC3536802.



- 476 29. Rask L, Balslev E, Sokilde R, Hogdall E, Flyger H, Eriksen J, et al. Differential expression of miR-139,  
477 miR-486 and miR-21 in breast cancer patients sub-classified according to lymph node status. *Cellular*  
478 *oncology* (Dordrecht). 2014;37(3):215-27. Epub 2014/07/17. doi: 10.1007/s13402-014-0176-6. PubMed  
479 PMID: 25027758.
- 480 30. Sochor M, Basova P, Pesta M, Dusilkova N, Bartos J, Burda P, et al. Oncogenic microRNAs: miR-  
481 155, miR-19a, miR-181b, and miR-24 enable monitoring of early breast cancer in serum. *BMC cancer*.  
482 2014;14:448. doi: 10.1186/1471-2407-14-448. PubMed PMID: 24938880; PubMed Central PMCID:  
483 PMC4075993.
- 484 31. Madhavan D, Zucknick M, Wallwiener M, Cuk K, Modugno C, Scharpff M, et al. Circulating miRNAs  
485 as surrogate markers for circulating tumor cells and prognostic markers in metastatic breast cancer.  
486 *Clinical cancer research : an official journal of the American Association for Cancer Research*.  
487 2012;18(21):5972-82. Epub 2012/09/07. doi: 10.1158/1078-0432.ccr-12-1407. PubMed PMID: 22952344.
- 488 32. Godfrey AC, Xu Z, Weinberg CR, Getts RC, Wade PA, DeRoo LA, et al. Serum microRNA expression  
489 as an early marker for breast cancer risk in prospectively collected samples from the Sister Study cohort.  
490 *Breast cancer research : BCR*. 2013;15(3):R42. Epub 2013/05/28. doi: 10.1186/bcr3428. PubMed PMID:  
491 23705859; PubMed Central PMCID: PMC3706791.
- 492 33. Heneghan HM, Miller N, Lowery AJ, Sweeney KJ, Newell J, Kerin MJ. Circulating microRNAs as  
493 novel minimally invasive biomarkers for breast cancer. *Annals of surgery*. 2010;251(3):499-505. Epub  
494 2010/02/06. doi: 10.1097/SLA.0b013e3181cc939f. PubMed PMID: 20134314.
- 495 34. Park IH, Kang JH, Lee KS, Nam S, Ro J, Kim JH. Identification and clinical implications of circulating  
496 microRNAs for estrogen receptor-positive breast cancer. *Tumour biology : the journal of the International*  
497 *Society for Oncodevelopmental Biology and Medicine*. 2014. Epub 2014/09/03. doi: 10.1007/s13277-014-  
498 2525-5. PubMed PMID: 25179838.
- 499 35. Schrauder MG, Strick R, Schulz-Wendtland R, Strissel PL, Kahmann L, Loehberg CR, et al.  
500 Circulating micro-RNAs as potential blood-based markers for early stage breast cancer detection. *PloS*  
501 *one*. 2012;7(1):e29770. Epub 2012/01/14. doi: 10.1371/journal.pone.0029770. PubMed PMID: 22242178;  
502 PubMed Central PMCID: PMC3252341.
- 503 36. Heneghan HM, Miller N, Kelly R, Newell J, Kerin MJ. Systemic miRNA-195 differentiates breast  
504 cancer from other malignancies and is a potential biomarker for detecting noninvasive and early stage  
505 disease. *The oncologist*. 2010;15(7):673-82. Epub 2010/06/26. doi: 10.1634/theoncologist.2010-0103.  
506 PubMed PMID: 20576643; PubMed Central PMCID: PMC3228012.
- 507 37. Ouyang M, Li Y, Ye S, Ma J, Lu L, Lv W, et al. MicroRNA profiling implies new markers of  
508 chemoresistance of triple-negative breast cancer. *PloS one*. 2014;9(5):e96228. Epub 2014/05/03. doi:  
509 10.1371/journal.pone.0096228. PubMed PMID: 24788655; PubMed Central PMCID: PMC34008525.
- 510 38. Ng EK, Chong WW, Jin H, Lam EK, Shin VY, Yu J, et al. Differential expression of microRNAs in  
511 plasma of patients with colorectal cancer: a potential marker for colorectal cancer screening. *Gut*.  
512 2009;58(10):1375-81. doi: 10.1136/gut.2008.167817. PubMed PMID: 19201770.
- 513 39. Mitchell PS, Parkin RK, Kroh EM, Fritz BR, Wyman SK, Pogosova-Agadjanyan EL, et al. Circulating  
514 microRNAs as stable blood-based markers for cancer detection. *Proceedings of the National Academy of*  
515 *Sciences*. 2008;105(30):10513-8. doi: 10.1073/pnas.0804549105.
- 516 40. Liu J, Mao Q, Liu Y, Hao X, Zhang S, Zhang J. Analysis of miR-205 and miR-155 expression in the  
517 blood of breast cancer patients. *Chinese journal of cancer research = Chung-kuo yen cheng yen chiu*.  
518 2013;25(1):46-54. Epub 2013/02/02. doi: 10.3978/j.issn.1000-9604.2012.11.04. PubMed PMID:  
519 23372341; PubMed Central PMCID: PMC3555294.
- 520 41. Calvano Filho CM, Calvano-Mendes DC, Carvalho KC, Maciel GA, Ricci MD, Torres AP, et al. Triple-  
521 negative and luminal A breast tumors: differential expression of miR-18a-5p, miR-17-5p, and miR-20a-5p.  
522 *Tumour biology : the journal of the International Society for Oncodevelopmental Biology and Medicine*.  
523 2014;35(8):7733-41. Epub 2014/05/09. doi: 10.1007/s13277-014-2025-7. PubMed PMID: 24810926.

- 524 42. Anfossi S, Giordano A, Gao H, Cohen EN, Tin S, Wu Q, et al. High serum miR-19a levels are  
525 associated with inflammatory breast cancer and are predictive of favorable clinical outcome in patients  
526 with metastatic HER2+ inflammatory breast cancer. *PloS one*. 2014;9(1):e83113. Epub 2014/01/15. doi:  
527 10.1371/journal.pone.0083113. PubMed PMID: 24416156; PubMed Central PMCID: PMC3885405.
- 528 43. Mangolini A, Ferracin M, Zanzi MV, Saccenti E, Ebnaof SO, Poma VV, et al. Diagnostic and  
529 prognostic microRNAs in the serum of breast cancer patients measured by droplet digital PCR. *Biomarker  
530 research*. 2015;3:12. Epub 2015/06/30. doi: 10.1186/s40364-015-0037-0. PubMed PMID: 26120471;  
531 PubMed Central PMCID: PMC4483205.
- 532 44. Zhang G, Liu Z, Cui G, Wang X, Yang Z. MicroRNA-486-5p targeting PIM-1 suppresses cell  
533 proliferation in breast cancer cells. *Tumour biology : the journal of the International Society for  
534 Oncodevelopmental Biology and Medicine*. 2014;35(11):11137-45. Epub 2014/08/12. doi:  
535 10.1007/s13277-014-2412-0. PubMed PMID: 25104088.
- 536 45. Lerebours F, Cizeron-Clairac G, Susini A, Vacher S, Mouret-Fourme E, Belichard C, et al. miRNA  
537 expression profiling of inflammatory breast cancer identifies a 5-miRNA signature predictive of breast  
538 tumor aggressiveness. *International journal of cancer Journal international du cancer*. 2013;133(7):1614-  
539 23. Epub 2013/03/26. doi: 10.1002/ijc.28171. PubMed PMID: 23526361.
- 540 46. O'Connell RM, Rao DS, Chaudhuri AA, Boldin MP, Taganov KD, Nicoll J, et al. Sustained expression  
541 of microRNA-155 in hematopoietic stem cells causes a myeloproliferative disorder. *The Journal of  
542 experimental medicine*. 2008;205(3):585-94. Epub 2008/02/27. doi: 10.1084/jem.20072108. PubMed  
543 PMID: 18299402; PubMed Central PMCID: PMC2275382.
- 544 47. Kluiver J, Poppema S, de Jong D, Blokzijl T, Harms G, Jacobs S, et al. BIC and miR-155 are highly  
545 expressed in Hodgkin, primary mediastinal and diffuse large B cell lymphomas. *The Journal of pathology*.  
546 2005;207(2):243-9. Epub 2005/07/26. doi: 10.1002/path.1825. PubMed PMID: 16041695.
- 547 48. Volinia S, Calin GA, Liu C-G, Ambs S, Cimmino A, Petrocca F, et al. A microRNA expression signature  
548 of human solid tumors defines cancer gene targets. *Proceedings of the National Academy of Sciences of  
549 the United States of America*. 2006;103(7):2257-61. PubMed PMID: Medline:16461460.
- 550 49. Wang X, Tang S, Le SY, Lu R, Rader JS, Meyers C, et al. Aberrant expression of oncogenic and  
551 tumor-suppressive microRNAs in cervical cancer is required for cancer cell growth. *PloS one*.  
552 2008;3(7):e2557. Epub 2008/07/04. doi: 10.1371/journal.pone.0002557. PubMed PMID: 18596939;  
553 PubMed Central PMCID: PMC2438475.
- 554 50. Yanaihara N, Caplen N, Bowman E, Seike M, Kumamoto K, Yi M, et al. Unique microRNA molecular  
555 profiles in lung cancer diagnosis and prognosis. *Cancer cell*. 2006;9(3):189-98. Epub 2006/03/15. doi:  
556 10.1016/j.ccr.2006.01.025. PubMed PMID: 16530703.
- 557 51. Kong W, He L, Coppola M, Guo J, Esposito NN, Coppola D, et al. MicroRNA-155 regulates cell  
558 survival, growth, and chemosensitivity by targeting FOXO3a in breast cancer. *The Journal of biological  
559 chemistry*. 2016;291(43):22855. Epub 2016/11/09. doi: 10.1074/jbc.A110.101055. PubMed PMID:  
560 27825093; PubMed Central PMCID: PMC45077230.
- 561 52. Zhao FL, Dou YC, Wang XF, Han DC, Lv ZG, Ge SL, et al. Serum microRNA-195 is down-regulated in  
562 breast cancer: a potential marker for the diagnosis of breast cancer. *Molecular biology reports*.  
563 2014;41(9):5913-22. Epub 2014/08/12. doi: 10.1007/s11033-014-3466-1. PubMed PMID: 25103018.
- 564 53. Li D, Zhao Y, Liu C, Chen X, Qi Y, Jiang Y, et al. Analysis of MiR-195 and MiR-497 expression,  
565 regulation and role in breast cancer. *Clinical cancer research : an official journal of the American  
566 Association for Cancer Research*. 2011;17(7):1722-30. Epub 2011/02/26. doi: 10.1158/1078-0432.ccr-10-  
567 1800. PubMed PMID: 21350001.
- 568 54. Luo Q, Wei C, Li X, Li J, Chen L, Huang Y, et al. MicroRNA-195-5p is a potential diagnostic and  
569 therapeutic target for breast cancer. *Oncology reports*. 2014;31(3):1096-102. Epub 2014/01/10. doi:  
570 10.3892/or.2014.2971. PubMed PMID: 24402230; PubMed Central PMCID: PMC3926672.

571 55. Hu Z, Dong J, Wang LE, Ma H, Liu J, Zhao Y, et al. Serum microRNA profiling and breast cancer risk:  
572 the use of miR-484/191 as endogenous controls. *Carcinogenesis*. 2012;33(4):828-34. Epub 2012/02/03.  
573 doi: 10.1093/carcin/bgs030. PubMed PMID: 22298638.

574 56. Ng EKO, Li R, Shin VY, Jin HC, Leung CPH, Ma ESK, et al. Circulating microRNAs as specific  
575 biomarkers for breast cancer detection. *PloS one*. 2013;8(1):e53141. PubMed PMID: Medline:23301032.

576 57. Calvano Filho CM, Calvano-Mendes DC, Carvalho KC, Maciel GA, Ricci MD, Torres AP, et al. Triple-  
577 negative and luminal A breast tumors: differential expression of miR-18a-5p, miR-17-5p, and miR-20a-5p.  
578 *Tumour biology : the journal of the International Society for Oncodevelopmental Biology and Medicine*.  
579 2014. Epub 2014/05/09. doi: 10.1007/s13277-014-2025-7. PubMed PMID: 24810926.

580 58. Iorio MV, Visone R, Di Leva G, Donati V, Petrocca F, Casalini P, et al. MicroRNA signatures in human  
581 ovarian cancer. *Cancer research*. 2007;67(18):8699-707. Epub 2007/09/19. doi: 10.1158/0008-5472.can-  
582 07-1936. PubMed PMID: 17875710.

583 59. Asangani IA, Rasheed SA, Nikolova DA, Leupold JH, Colburn NH, Post S, et al. MicroRNA-21 (miR-  
584 21) post-transcriptionally downregulates tumor suppressor Pdc4 and stimulates invasion, intravasation  
585 and metastasis in colorectal cancer. *Oncogene*. 2008;27(15):2128-36. Epub 2007/10/31. doi:  
586 10.1038/sj.onc.1210856. PubMed PMID: 17968323.

587 60. Chan JA, Krichevsky AM, Kosik KS. MicroRNA-21 is an antiapoptotic factor in human glioblastoma  
588 cells. *Cancer research*. 2005;65(14):6029-33. Epub 2005/07/19. doi: 10.1158/0008-5472.can-05-0137.  
589 PubMed PMID: 16024602.

590 61. Stuckrath I, Rack B, Janni W, Jager B, Pantel K, Schwarzenbach H. Aberrant plasma levels of  
591 circulating miR-16, miR-107, miR-130a and miR-146a are associated with lymph node metastasis and  
592 receptor status of breast cancer patients. *Oncotarget*. 2015;6(15):13387-401. Epub 2015/06/03. doi:  
593 10.18632/oncotarget.3874. PubMed PMID: 26033453; PubMed Central PMCID: PMC4537022.

594 62. Shin VY, Siu JM, Cheuk I, Ng EK, Kwong A. Circulating cell-free miRNAs as biomarker for triple-  
595 negative breast cancer. *British journal of cancer*. 2015;112(11):1751-9. Epub 2015/04/24. doi:  
596 10.1038/bjc.2015.143. PubMed PMID: 25906045; PubMed Central PMCID: PMC4647231.

597 63. Guo LJ, Zhang QY. Decreased serum miR-181a is a potential new tool for breast cancer screening.  
598 *International journal of molecular medicine*. 2012;30(3):680-6. Epub 2012/06/14. doi:  
599 10.3892/ijmm.2012.1021. PubMed PMID: 22692639.

600 64. McDermott AM, Kerin MJ, Miller N. Identification and validation of miRNAs as endogenous  
601 controls for RQ-PCR in blood specimens for breast cancer studies. *PloS one*. 2013;8(12):e83718. PubMed  
602 PMID: Medline:24391813.

603

604

605

606

607

608

609

610

611

612

613 **Supporting information**

614 **S1 Table. Patient and control characteristics.**

	Luminal A (n=38)	Controls (n=20)
<b>Mean Patient Age (yr)</b>	59.13	66.15
<b>Menopausal Status</b>		
Pre	13	8
Post	25	12
<b>Histological Subtype</b>		
Inv. Ductal	28	
Inv. Lobular	10	
<b>Nodal Status</b>		
-	18	
+	20	
<b>Tumor Grade</b>		
2	29	
3	9	
<b>UICC Stage</b>		
1A	9	
2A	7	
3A	12	
1B	3	
2B	7	
<b>Hormone Receptor</b>		
ER +	38	
PR +	38	
HER2/neu +	0	

615 Yrs, Year; Inv, Invasion; UICC, Stage of breast tumor according to the International Union Against Cancer  
616 staging criteria; ER, Estrogen receptor; PR, Progesterone receptor; HER2/neu, Human epidermal growth  
617 factor receptor; -, negative; +, positive; \*All control subjects had no personal or family history of breast  
618 or ovarian cancer and were clinically well at the time of sampling.

619

620

621

622

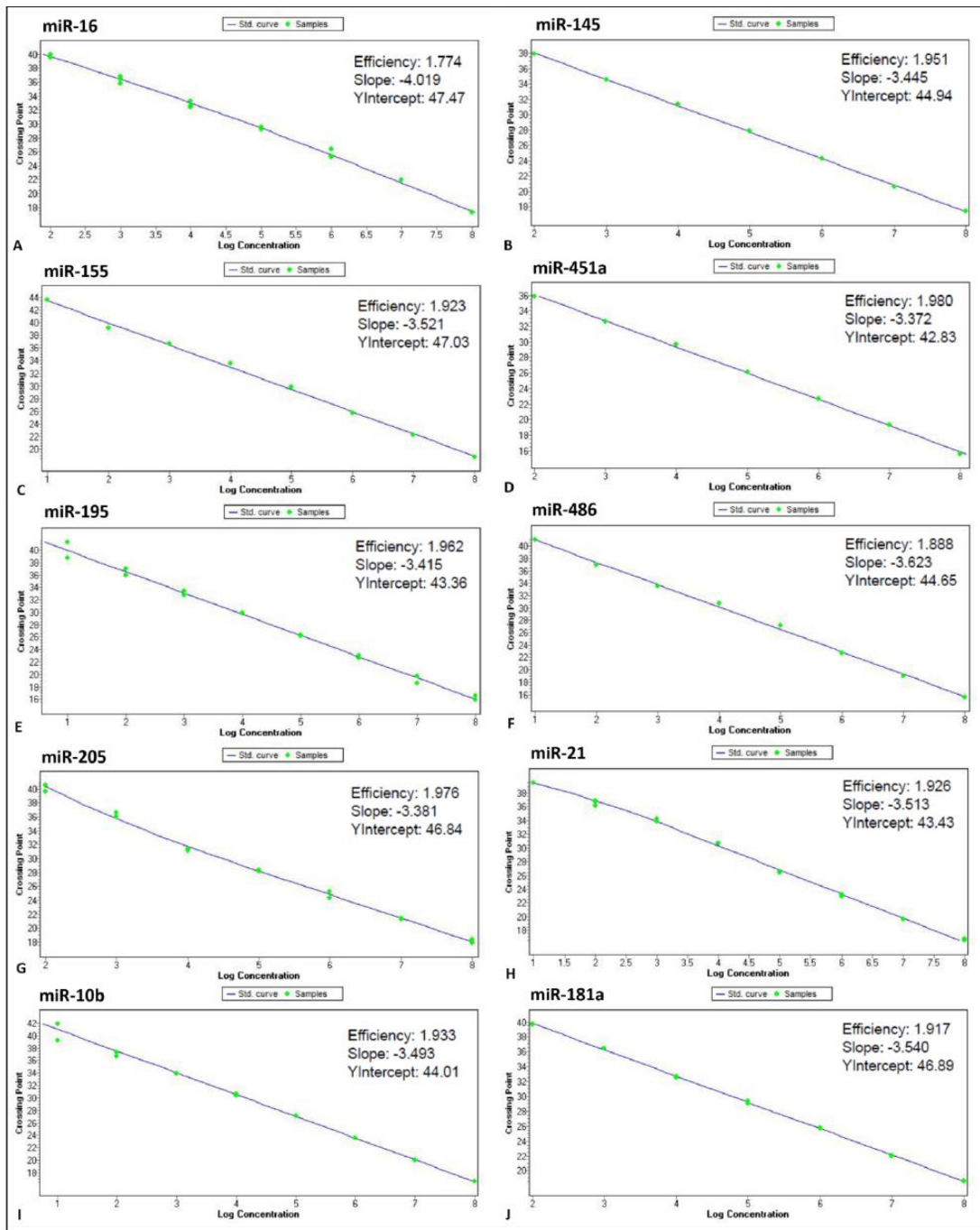
623

624

625



S1 Figure. Standard curve for ten synthetic miRNA oligonucleotides (A-J).



627

628

629

**S2 Table: MiRNA-specific primer sequences for RT-qPCR assay.**

<b>MicroRNAs</b>	<b>MirBase accession no.</b>	<b>Primer sequences (5' to 3')</b>
hsa-miR-16	MIMAT0000069	TAGCAGCACGTAAATATTGGCG
hsa-miR-486	MIMAT0004762	CGGGGCAGCTCAGTACAGGAT
hsa-miR-145	MIMAT0000437	GTCCAGTTTTCCAGGAATCCCT
hsa-miR-451a	MIMAT0001631	AAACCGTTACCATTACTGAGTT
hsa-miR-21	MIMAT0000076	TAGCTTATCAGACTGATGTTGA
hsa-miR-195	MIMAT0000461	TAGCAGCACAGAAATATTGGC
hsa-miR-205	MIMAT0000266	TCCTTCATTCCACCGGAGTCTG
hsa-miR-155	MIMAT0000646	TTAATGCTAATCGTGATAGGGGT
has-miR-181a	MIMAT0000256	AACATTCAACGCTGTCGGTGAGT
hsa-miR-10b	MIMAT0004556	ACAGATTTCGATTCTAGGGGAAT

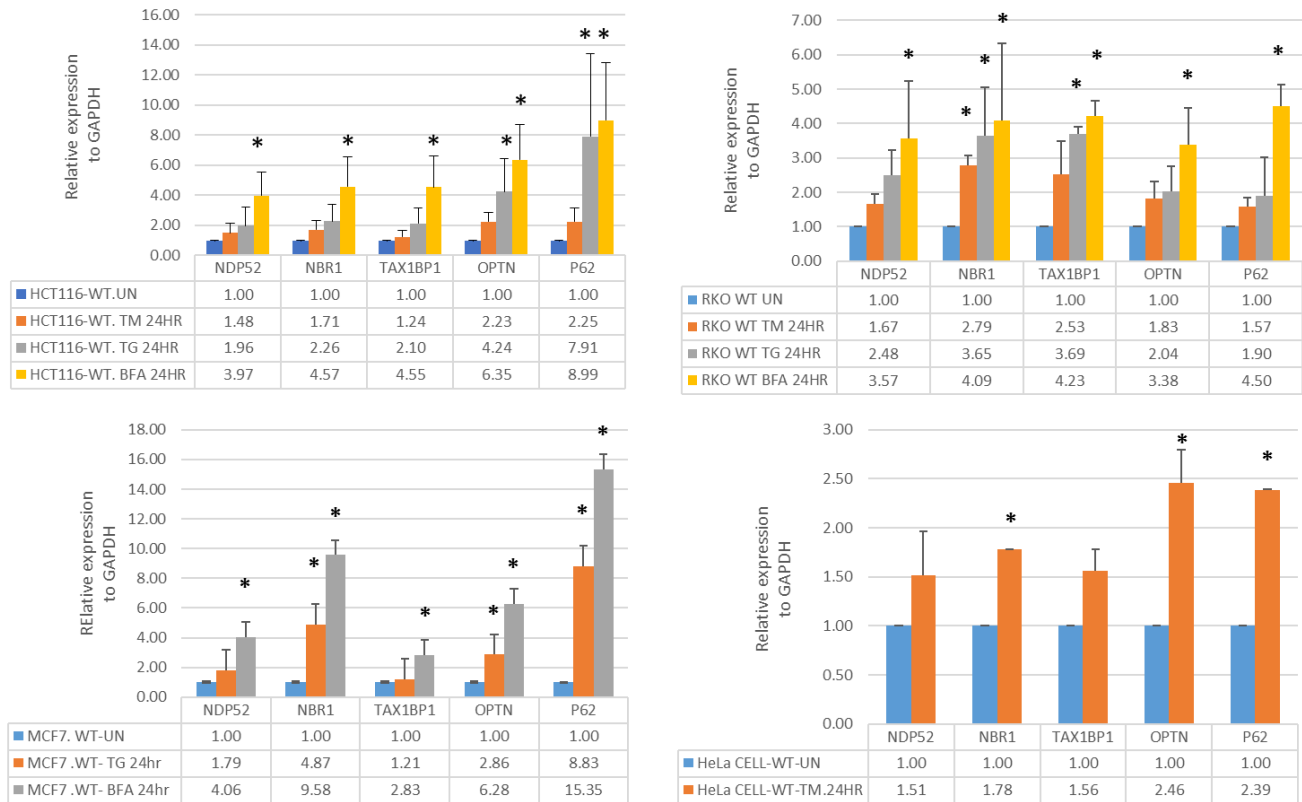
630

## 6-16. Results for two uncompleted projects.

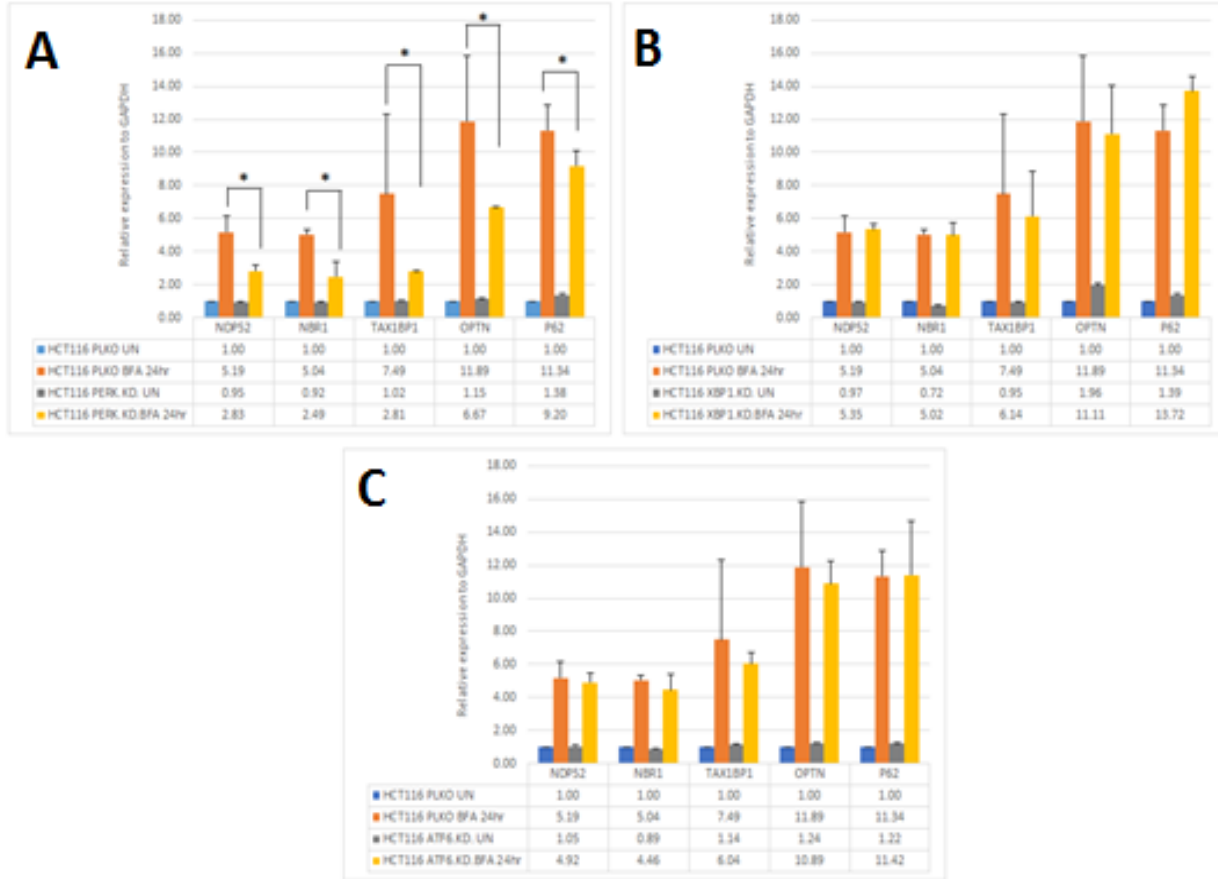
I carried out two other projects in Dr Sanjeev Gupta's laboratory including;

- 1- Regulation of mitophagy receptors during UPR.
- 2- Regulation of DCLK1 gene expression during UPR.

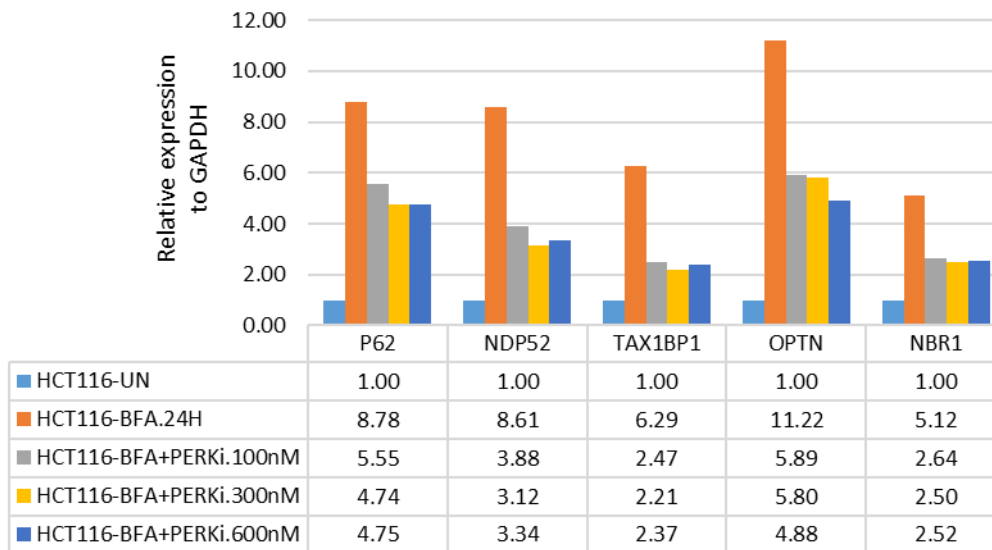
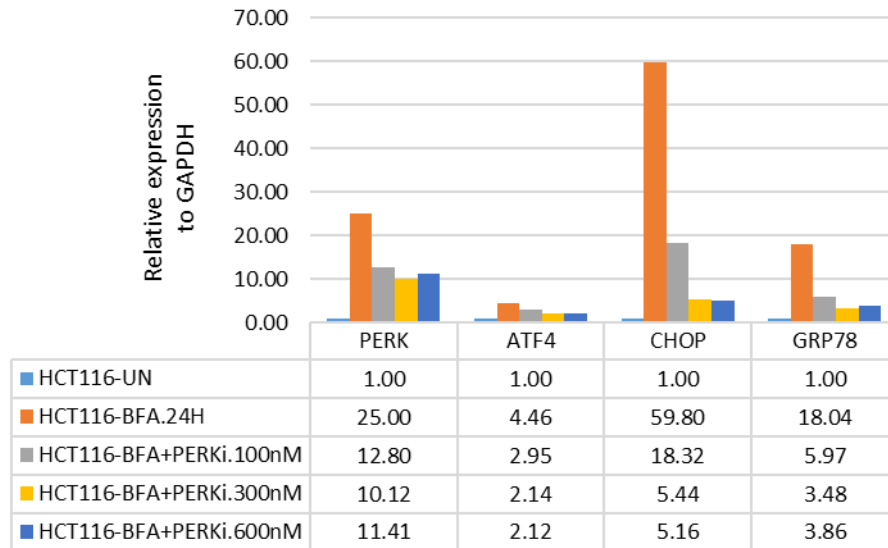
The results from these two projects are addressed here, a. All raw data and results are also documented in my laboratory notebook (number 1837).



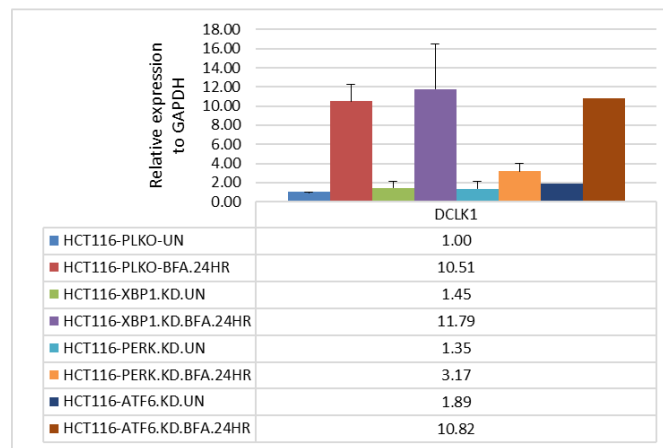
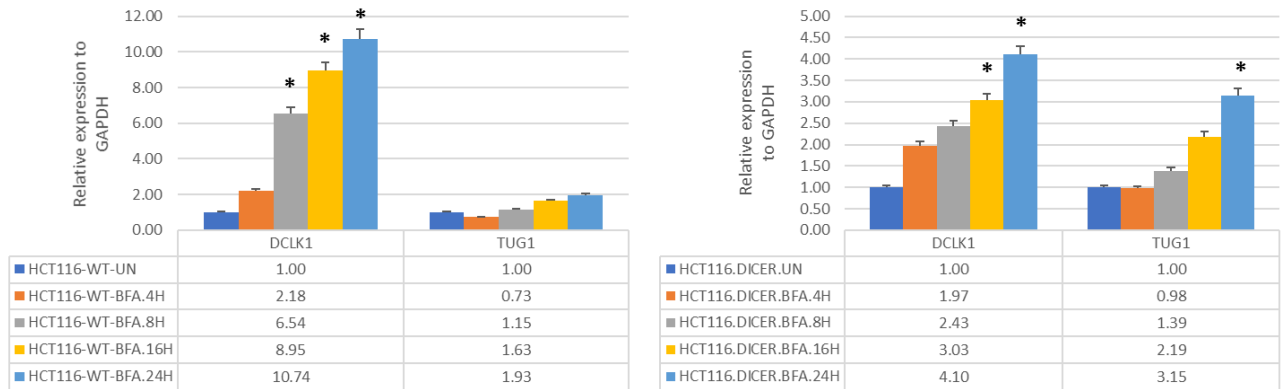
Expression profile of five autophagy receptor mRNAs in four cancer cell lines treated with 1µM of Tg, 500 ng/ml of Tm, 500ng/ml of Bfa for 24 h. Data are presented as the mean ± standard deviation, (n=3, \* P < 0.05).



Expression profile of five autophagy receptor mRNAs in A) HCT116. PERK.KD cells, B) HCT116. XBP1.KD cells and C) HCT116. ATF6.KD cells treated with 500ng/ml of Bfa for 24 h. Data are presented as the mean  $\pm$  standard deviation, (n=3, \* P < 0.05).



Expression profile of some UPR and five autophagy receptor mRNAs in HCT116 cells treated with 500ng/ml of Bfa, 100nM, 300nM and 600nM of GSK PERK inhibitor for 24 h.



Expression profile of DCLK1 and TUG1 mRNAs in arental HCT116, Dicer mutant HCT116 and HCT116. PERK.KD cells treated with 500ng/ml of Bfa for 4, 8, 16 and 24 h. Data are presented as the mean  $\pm$  standard deviation, (n=3, \* P < 0.05).

# Bibliography

1. Schwarz, D.S. and M.D. Blower, *The endoplasmic reticulum: structure, function and response to cellular signaling*. Cell Mol Life Sci, 2016. **73**(1): p. 79-94.
2. Bravo, R., et al., *Endoplasmic reticulum and the unfolded protein response: dynamics and metabolic integration*. Int Rev Cell Mol Biol, 2013. **301**: p. 215-90.
3. de la Cadena, S.G., et al., *Glucose deprivation induces reticulum stress by the PERK pathway and caspase-7- and calpain-mediated caspase-12 activation*. Apoptosis, 2014. **19**(3): p. 414-27.
4. Nagelkerke, A., et al., *Hypoxia stimulates migration of breast cancer cells via the PERK/ATF4/LAMP3-arm of the unfolded protein response*. Breast Cancer Res, 2013. **15**(1): p. R2.
5. Wang, M. and R.J. Kaufman, *The impact of the endoplasmic reticulum protein-folding environment on cancer development*. Nat Rev Cancer, 2014. **14**(9): p. 581-97.
6. Hughes, D. and G.R. Mallucci, *The unfolded protein response in neurodegenerative disorders - therapeutic modulation of the PERK pathway*. Febs j, 2018.
7. Belmadani, S. and K. Matrougui, *The Unraveling Truth About IRE1 and MicroRNAs in Diabetes*. Diabetes, 2017. **66**(1): p. 23-24.
8. Chan, S.W., *The unfolded protein response in virus infections*. Front Microbiol, 2014. **5**: p. 518.
9. Jung, T.W. and K.M. Choi, *Pharmacological Modulators of Endoplasmic Reticulum Stress in Metabolic Diseases*. Int J Mol Sci, 2016. **17**(2).
10. Ron, D. and P. Walter, *Signal integration in the endoplasmic reticulum unfolded protein response*. Nat Rev Mol Cell Biol, 2007. **8**(7): p. 519-29.
11. Hetz, C. and F.R. Papa, *The Unfolded Protein Response and Cell Fate Control*. Mol Cell, 2018. **69**(2): p. 169-181.
12. Hetz, C., *The unfolded protein response: Controlling cell fate decisions under ER stress and beyond*. Nature Reviews Molecular Cell Biology, 2012. **13**(2): p. 89-102.
13. Tabas, I. and D. Ron, *Integrating the mechanisms of apoptosis induced by endoplasmic reticulum stress*. Nat Cell Biol, 2011. **13**(3): p. 184-90.
14. Rojas-Rivera, D., et al., *ER stress sensing mechanism: Putting off the brake on UPR transducers*. Oncotarget, 2018. **9**(28): p. 19461-19462.
15. Yoshida, H., et al., *XBP1 mRNA is induced by ATF6 and spliced by IRE1 in response to ER stress to produce a highly active transcription factor*. Cell, 2001. **107**(7): p. 881-91.
16. Vekich, J.A., et al., *Protein disulfide isomerase-associated 6 is an ATF6-inducible ER stress response protein that protects cardiac myocytes from ischemia/reperfusion-mediated cell death*. J Mol Cell Cardiol, 2012. **53**(2): p. 259-67.
17. Wang, Y., et al., *Activation of ATF6 and an ATF6 DNA binding site by the endoplasmic reticulum stress response*. J Biol Chem, 2000. **275**(35): p. 27013-20.
18. Kokame, K., H. Kato, and T. Miyata, *Identification of ERSE-II, a new cis-acting element responsible for the ATF6-dependent mammalian unfolded protein response*. J Biol Chem, 2001. **276**(12): p. 9199-205.
19. Yamamoto, K., et al., *Differential contributions of ATF6 and XBP1 to the activation of endoplasmic reticulum stress-responsive cis-acting elements ERSE, UPRE and ERSE-II*. J Biochem, 2004. **136**(3): p. 343-50.
20. Yoshida, H., et al., *Endoplasmic reticulum stress-induced formation of transcription factor complex ERSF including NF-Y (CBF) and activating transcription factors 6alpha and 6beta that activates the mammalian unfolded protein response*. Mol Cell Biol, 2001. **21**(4): p. 1239-48.

21. Korennykh, A. and P. Walter, *Structural basis of the unfolded protein response*. *Annu Rev Cell Dev Biol*, 2012. **28**: p. 251-77.
22. Morishima, N., K. Nakanishi, and A. Nakano, *Activating transcription factor-6 (ATF6) mediates apoptosis with reduction of myeloid cell leukemia sequence 1 (Mcl-1) protein via induction of WW domain binding protein 1*. *J Biol Chem*, 2011. **286**(40): p. 35227-35.
23. Wang, M. and R.J. Kaufman, *Protein misfolding in the endoplasmic reticulum as a conduit to human disease*. *Nature*, 2016. **529**(7586): p. 326-35.
24. Wek, R.C., H.Y. Jiang, and T.G. Anthony, *Coping with stress: eIF2 kinases and translational control*. *Biochem Soc Trans*, 2006. **34**(Pt 1): p. 7-11.
25. Vattem, K.M. and R.C. Wek, *Reinitiation involving upstream ORFs regulates ATF4 mRNA translation in mammalian cells*. *Proc Natl Acad Sci U S A*, 2004. **101**(31): p. 11269-74.
26. Connor, J.H., et al., *Growth arrest and DNA damage-inducible protein GADD34 assembles a novel signaling complex containing protein phosphatase 1 and inhibitor 1*. *Mol Cell Biol*, 2001. **21**(20): p. 6841-50.
27. Tong, K.I., et al., *Two-site substrate recognition model for the Keap1-Nrf2 system: a hinge and latch mechanism*. *Biol Chem*, 2006. **387**(10-11): p. 1311-20.
28. Kobayashi, M. and M. Yamamoto, *Molecular mechanisms activating the Nrf2-Keap1 pathway of antioxidant gene regulation*. *Antioxid Redox Signal*, 2005. **7**(3-4): p. 385-94.
29. Cullinan, S.B., et al., *Nrf2 is a direct PERK substrate and effector of PERK-dependent cell survival*. *Mol Cell Biol*, 2003. **23**(20): p. 7198-209.
30. Chorley, B.N., et al., *Identification of novel NRF2-regulated genes by ChIP-Seq: influence on retinoid X receptor alpha*. *Nucleic Acids Res*, 2012. **40**(15): p. 7416-29.
31. Deng, J., et al., *Translational repression mediates activation of nuclear factor kappa B by phosphorylated translation initiation factor 2*. *Mol Cell Biol*, 2004. **24**(23): p. 10161-8.
32. Rozpedek, W., et al., *The Role of the PERK/eIF2alpha/ATF4/CHOP Signaling Pathway in Tumor Progression During Endoplasmic Reticulum Stress*. *Curr Mol Med*, 2016. **16**(6): p. 533-44.
33. McCullough, K.D., et al., *Gadd153 sensitizes cells to endoplasmic reticulum stress by down-regulating Bcl2 and perturbing the cellular redox state*. *Mol Cell Biol*, 2001. **21**(4): p. 1249-59.
34. Marciniak, S.J., et al., *CHOP induces death by promoting protein synthesis and oxidation in the stressed endoplasmic reticulum*. *Genes Dev*, 2004. **18**(24): p. 3066-77.
35. Cazanave, S.C., et al., *CHOP and AP-1 cooperatively mediate PUMA expression during lipoapoptosis*. *Am J Physiol Gastrointest Liver Physiol*, 2010. **299**(1): p. G236-43.
36. Ghosh, A.P., et al., *CHOP potentially co-operates with FOXO3a in neuronal cells to regulate PUMA and BIM expression in response to ER stress*. *PLoS One*, 2012. **7**(6): p. e39586.
37. Hetz, C., *The unfolded protein response: controlling cell fate decisions under ER stress and beyond*. *Nat Rev Mol Cell Biol*, 2012. **13**(2): p. 89-102.
38. Gardner, B.M. and P. Walter, *Unfolded proteins are Ire1-activating ligands that directly induce the unfolded protein response*. *Science*, 2011. **333**(6051): p. 1891-4.
39. Lu, Y., F.X. Liang, and X. Wang, *A synthetic biology approach identifies the mammalian UPR RNA ligase RtcB*. *Mol Cell*, 2014. **55**(5): p. 758-70.
40. Sriburi, R., et al., *XBP1: a link between the unfolded protein response, lipid biosynthesis, and biogenesis of the endoplasmic reticulum*. *J Cell Biol*, 2004. **167**(1): p. 35-41.
41. Hetz, C., et al., *The unfolded protein response: integrating stress signals through the stress sensor IRE1alpha*. *Physiol Rev*, 2011. **91**(4): p. 1219-43.
42. Lee, A.H., N.N. Iwakoshi, and L.H. Glimcher, *XBP-1 regulates a subset of endoplasmic reticulum resident chaperone genes in the unfolded protein response*. *Mol Cell Biol*, 2003. **23**(21): p. 7448-59.



43. Maurel, M., et al., *Getting RIDD of RNA: IRE1 in cell fate regulation*. Trends Biochem Sci, 2014. **39**(5): p. 245-54.
44. Hollien, J., et al., *Regulated Ire1-dependent decay of messenger RNAs in mammalian cells*. J Cell Biol, 2009. **186**(3): p. 323-31.
45. Imagawa, Y., et al., *RNase domains determine the functional difference between IRE1 $\alpha$  and IRE1 $\beta$* . FEBS Letters, 2008. **582**(5): p. 656-660.
46. Iqbal, J., et al., *IRE1 $\beta$  Inhibits Chylomicron Production by Selectively Degrading MTP mRNA*. Cell Metabolism, 2008. **7**(5): p. 445-455.
47. Upton, J.P., et al., *IRE1 $\alpha$  cleaves select microRNAs during ER stress to derepress translation of proapoptotic Caspase-2*. Science, 2012. **338**(6108): p. 818-22.
48. Urano, F., et al., *Coupling of stress in the ER to activation of JNK protein kinases by transmembrane protein kinase IRE1*. Science, 2000. **287**(5453): p. 664-6.
49. Ferlay, J., et al., *Cancer incidence and mortality worldwide: sources, methods and major patterns in GLOBOCAN 2012*. Int J Cancer, 2015. **136**(5): p. E359-86.
50. Ferlay, J., et al., *Cancer incidence and mortality patterns in Europe: estimates for 40 countries in 2012*. Eur J Cancer, 2013. **49**(6): p. 1374-403.
51. Hanahan, D. and R.A. Weinberg, *The hallmarks of cancer*. Cell, 2000. **100**(1): p. 57-70.
52. Hanahan, D. and R.A. Weinberg, *Hallmarks of cancer: the next generation*. Cell, 2011. **144**(5): p. 646-74.
53. Ferlay J, S.I., Ervik M, Dikshit R, Eser S, Mathers C, Rebelo M, Parkin DM, Forman D, Bray, F, *Cancer Incidence and Mortality Worldwide: IARC CancerBase No. 11 [Internet]*. GLOBOCAN 2012 2013. **v1.0**: p. <http://globocan.iarc.fr>.
54. Althuis, M.D., et al., *Global trends in breast cancer incidence and mortality 1973-1997*. Int J Epidemiol, 2005. **34**(2): p. 405-12.
55. NCRI., *Cancer Factsheet Female breast 2015* [Available from: [http://www.ncri.ie/sites/ncri/files/factsheets/FACTSHEET\\_breast\\_0.pdf](http://www.ncri.ie/sites/ncri/files/factsheets/FACTSHEET_breast_0.pdf)], 2015.
56. Bray, F., P. McCarron, and D.M. Parkin, *The changing global patterns of female breast cancer incidence and mortality*. Breast Cancer Res, 2004. **6**(6): p. 229-39.
57. Jemal, A., et al., *Global patterns of cancer incidence and mortality rates and trends*. Cancer Epidemiol Biomarkers Prev, 2010. **19**(8): p. 1893-907.
58. Bertos, N.R. and M. Park, *Breast cancer - one term, many entities?* J Clin Invest, 2011. **121**(10): p. 3789-96.
59. Perou, C.M., et al., *Molecular portraits of human breast tumours*. Nature, 2000. **406**(6797): p. 747-52.
60. Sorlie, T., et al., *Gene expression patterns of breast carcinomas distinguish tumor subclasses with clinical implications*. Proc Natl Acad Sci U S A, 2001. **98**(19): p. 10869-74.
61. Gruvberger, S., et al., *Estrogen receptor status in breast cancer is associated with remarkably distinct gene expression patterns*. Cancer Res, 2001. **61**(16): p. 5979-84.
62. Sotiriou, C., et al., *Breast cancer classification and prognosis based on gene expression profiles from a population-based study*. Proc Natl Acad Sci U S A, 2003. **100**(18): p. 10393-8.
63. Sorlie, T., et al., *Repeated observation of breast tumor subtypes in independent gene expression data sets*. Proc Natl Acad Sci U S A, 2003. **100**(14): p. 8418-23.
64. Takada, K., et al., *Analysis of HER Family (HER1-4) Expression as a Biomarker in Combination Therapy with Pertuzumab, Trastuzumab and Docetaxel for Advanced HER2-positive Breast Cancer*. Anticancer Res, 2018. **38**(4): p. 2285-2294.
65. Bivin, W.W., et al., *GRB7 Expression and Correlation With HER2 Amplification in Invasive Breast Carcinoma*. Appl Immunohistochem Mol Morphol, 2017. **25**(8): p. 553-558.

66. Iqbal, N. and N. Iqbal, *Human Epidermal Growth Factor Receptor 2 (HER2) in Cancers: Overexpression and Therapeutic Implications*. Mol Biol Int, 2014. **2014**: p. 852748.
67. !!! INVALID CITATION !!! [62, 65, 70].
68. Carey, L.A., et al., *Race, breast cancer subtypes, and survival in the Carolina Breast Cancer Study*. JAMA, 2006. **295**(21): p. 2492-502.
69. Ali, H.R., et al., *Genome-driven integrated classification of breast cancer validated in over 7,500 samples*. Genome Biol, 2014. **15**(8): p. 431.
70. Al-Hussaini, H., et al., *Notch signaling pathway as a therapeutic target in breast cancer*. Mol Cancer Ther, 2011. **10**(1): p. 9-15.
71. Lu, W., C. Lin, and Y. Li, *Rottlerin induces Wnt co-receptor LRP6 degradation and suppresses both Wnt/beta-catenin and mTORC1 signaling in prostate and breast cancer cells*. Cell Signal, 2014. **26**(6): p. 1303-9.
72. Huth, L., et al., *BDNF is associated with SFRP1 expression in luminal and basal-like breast cancer cell lines and primary breast cancer tissues: a novel role in tumor suppression?* PLoS One, 2014. **9**(7): p. e102558.
73. Chen, Y.J., et al., *Small-molecule synthetic compound norcantharidin reverses multi-drug resistance by regulating Sonic hedgehog signaling in human breast cancer cells*. PLoS One, 2012. **7**(5): p. e37006.
74. Candelaria, N.R., K. Liu, and C.Y. Lin, *Estrogen receptor alpha: molecular mechanisms and emerging insights*. J Cell Biochem, 2013. **114**(10): p. 2203-8.
75. Chakravarty, D., et al., *Extranuclear functions of ER impact invasive migration and metastasis by breast cancer cells*. Cancer Res, 2010. **70**(10): p. 4092-101.
76. Mayer, E.L. and I.E. Krop, *Advances in targeting SRC in the treatment of breast cancer and other solid malignancies*. Clin Cancer Res, 2010. **16**(14): p. 3526-32.
77. Strom, A., et al., *Estrogen receptor beta inhibits 17beta-estradiol-stimulated proliferation of the breast cancer cell line T47D*. Proc Natl Acad Sci U S A, 2004. **101**(6): p. 1566-71.
78. Speirs, V., et al., *Oestrogen receptor beta: what it means for patients with breast cancer*. Lancet Oncol, 2004. **5**(3): p. 174-81.
79. Lindberg, K., et al., *Expression of estrogen receptor beta increases integrin alpha1 and integrin beta1 levels and enhances adhesion of breast cancer cells*. J Cell Physiol, 2010. **222**(1): p. 156-67.
80. Haldosen, L.A., C. Zhao, and K. Dahlman-Wright, *Estrogen receptor beta in breast cancer*. Mol Cell Endocrinol, 2014. **382**(1): p. 665-672.
81. Holgado, E., et al., *Is there a role for immunotherapy in HER2-positive breast cancer?* NPJ Breast Cancer, 2018. **4**: p. 21.
82. Mora Vidal, R., et al., *Epidermal Growth Factor Receptor Family Inhibition Identifies P38 Mitogen-activated Protein Kinase as a Potential Therapeutic Target in Bladder Cancer*. Urology, 2018. **112**: p. 225.e1-225.e7.
83. Dixon-Clarke, S., et al., *Cyclin-Dependent Kinase 12 (CDK12), Human Kinase Domain; A Target Enabling Package*. 2018, University of Oxford.
84. Joshaghani, H.R., et al., *A3 adenosine receptor agonist induce G1 cell cycle arrest via Cyclin D and cyclin-dependent kinase 4 pathways in OVCAR-3 and Caov-4 cell lines*. J Cancer Res Ther, 2017. **13**(1): p. 107-112.
85. Sutherland, R.L. and E.A. Musgrove, *Cyclins and breast cancer*. J Mammary Gland Biol Neoplasia, 2004. **9**(1): p. 95-104.
86. Gonzalez-Angulo, A.M., et al., *Downregulation of the cyclin-dependent kinase inhibitor p27kip1 might correlate with poor disease-free and overall survival in inflammatory breast cancer*. Clin Breast Cancer, 2006. **7**(4): p. 326-30.

87. Stendahl, M., et al., *Cyclin D1 overexpression is a negative predictive factor for tamoxifen response in postmenopausal breast cancer patients*. Br J Cancer, 2004. **90**(10): p. 1942-8.
88. Weng, A.P., et al., *Activating mutations of NOTCH1 in human T cell acute lymphoblastic leukemia*. Science, 2004. **306**(5694): p. 269-71.
89. Stylianou, S., R.B. Clarke, and K. Brennan, *Aberrant activation of notch signaling in human breast cancer*. Cancer Res, 2006. **66**(3): p. 1517-25.
90. Reedijk, M., et al., *High-level coexpression of JAG1 and NOTCH1 is observed in human breast cancer and is associated with poor overall survival*. Cancer Res, 2005. **65**(18): p. 8530-7.
91. Baker, A., et al., *Notch-1-PTEN-ERK1/2 signaling axis promotes HER2+ breast cancer cell proliferation and stem cell survival*. Oncogene, 2018. **37**(33): p. 4489-4504.
92. Logan, C.Y. and R. Nusse, *The Wnt signaling pathway in development and disease*. Annu Rev Cell Dev Biol, 2004. **20**: p. 781-810.
93. Murakami, T., et al., *Distinct WNT/beta-catenin signaling activation in the serrated neoplasia pathway and the adenoma-carcinoma sequence of the colorectum*. Mod Pathol, 2015. **28**(1): p. 146-58.
94. Khramtsov, A.I., et al., *Wnt/beta-catenin pathway activation is enriched in basal-like breast cancers and predicts poor outcome*. Am J Pathol, 2010. **176**(6): p. 2911-20.
95. Bilir, B., O. Kucuk, and C.S. Moreno, *Wnt signaling blockage inhibits cell proliferation and migration, and induces apoptosis in triple-negative breast cancer cells*. J Transl Med, 2013. **11**: p. 280.
96. Zhou, X.L., et al., *Downregulation of Dickkopf-1 is responsible for high proliferation of breast cancer cells via losing control of Wnt/beta-catenin signaling*. Acta Pharmacol Sin, 2010. **31**(2): p. 202-10.
97. Stevens, K.N., C.M. Vachon, and F.J. Couch, *Genetic susceptibility to triple-negative breast cancer*. Cancer Res, 2013. **73**(7): p. 2025-30.
98. Van Heetvelde, M., et al., *Accurate detection and quantification of epigenetic and genetic second hits in BRCA1 and BRCA2-associated hereditary breast and ovarian cancer reveals multiple co-acting second hits*. Cancer Lett, 2018. **425**: p. 125-133.
99. Godet, I. and D.M. Gilkes, *BRCA1 and BRCA2 mutations and treatment strategies for breast cancer*. Integr Cancer Sci Ther, 2017. **4**(1).
100. Winter, C., et al., *Targeted sequencing of BRCA1 and BRCA2 across a large unselected breast cancer cohort suggests that one-third of mutations are somatic*. Ann Oncol, 2016. **27**(8): p. 1532-8.
101. van der Groep, P., et al., *Re: Germline BRCA1 mutations and a basal epithelial phenotype in breast cancer*. J Natl Cancer Inst, 2004. **96**(9): p. 712-3; author reply 714.
102. Richardson, A.L., et al., *X chromosomal abnormalities in basal-like human breast cancer*. Cancer Cell, 2006. **9**(2): p. 121-32.
103. Crawford, B., et al., *Multi-gene panel testing for hereditary cancer predisposition in unsolved high-risk breast and ovarian cancer patients*. Breast Cancer Res Treat, 2017. **163**(2): p. 383-390.
104. Antoniou, A.C., et al., *Breast-cancer risk in families with mutations in PALB2*. N Engl J Med, 2014. **371**(6): p. 497-506.
105. Orlando, L., et al., *Molecularly targeted endocrine therapies for breast cancer*. Cancer Treat Rev, 2010. **36 Suppl 3**: p. S67-71.
106. An, K.C., *Selective Estrogen Receptor Modulators*. Asian Spine J, 2016. **10**(4): p. 787-91.
107. Romano, A., et al., *Identification of novel ER- $\alpha$  target genes in breast cancer cells: Gene- and cell-selective co-regulator recruitment at target promoters determines the response to 17 $\beta$ -estradiol and tamoxifen*. Molecular and Cellular Endocrinology, 2010. **314**(1): p. 90-100.

108. Wardley, A.M., *Fulvestrant: a review of its development, pre-clinical and clinical data*. *Int J Clin Pract*, 2002. **56**(4): p. 305-9.
109. Rydén, L., et al., *Aromatase inhibitors alone or sequentially combined with tamoxifen in postmenopausal early breast cancer compared with tamoxifen or placebo – Meta-analyses on efficacy and adverse events based on randomized clinical trials*. *The Breast*, 2016. **26**: p. 106-114.
110. Chumsri, S., et al., *Aromatase, aromatase inhibitors, and breast cancer*. *The Journal of Steroid Biochemistry and Molecular Biology*, 2011. **125**(1): p. 13-22.
111. (EBCTCG)†, E.B.C.T.C.G., *Aromatase inhibitors versus tamoxifen in early breast cancer: patient-level meta-analysis of the randomised trials*. *The Lancet*, 2015. **386**(10001): p. 1341-1352.
112. Ahmed, S., A. Sami, and J. Xiang, *HER2-directed therapy: current treatment options for HER2-positive breast cancer*. *Breast Cancer*, 2015. **22**(2): p. 101-16.
113. Arnould, L., et al., *Trastuzumab-based treatment of HER2-positive breast cancer: an antibody-dependent cellular cytotoxicity mechanism?* *Br J Cancer*, 2006. **94**(2): p. 259-67.
114. Capelan, M., et al., *Pertuzumab: new hope for patients with HER2-positive breast cancer*. *Ann Oncol*, 2013. **24**(2): p. 273-82.
115. Montemurro, F., G. Valabrega, and M. Aglietta, *Lapatinib: a dual inhibitor of EGFR and HER2 tyrosine kinase activity*. *Expert Opin Biol Ther*, 2007. **7**(2): p. 257-68.
116. Piccart-Gebhart, M., et al., *Adjuvant Lapatinib and Trastuzumab for Early Human Epidermal Growth Factor Receptor 2-Positive Breast Cancer: Results From the Randomized Phase III Adjuvant Lapatinib and/or Trastuzumab Treatment Optimization Trial*. *J Clin Oncol*, 2016. **34**(10): p. 1034-42.
117. Isakoff, S.J., *Triple-negative breast cancer: role of specific chemotherapy agents*. *Cancer J*, 2010. **16**(1): p. 53-61.
118. Wahba, H.A. and H.A. El-Hadaad, *Current approaches in treatment of triple-negative breast cancer*. *Cancer Biol Med*, 2015. **12**(2): p. 106-16.
119. (EBCTCG), E.B.C.T.C.G., *Effects of chemotherapy and hormonal therapy for early breast cancer on recurrence and 15-year survival: an overview of the randomised trials*. *Lancet*, 2005. **365**(9472): p. 1687-717.
120. Fan, W., J. Chang, and P. Fu, *Endocrine therapy resistance in breast cancer: current status, possible mechanisms and overcoming strategies*. *Future Med Chem*, 2015. **7**(12): p. 1511-9.
121. Costa, R.L.B., H.S. Han, and W.J. Gradishar, *Targeting the PI3K/AKT/mTOR pathway in triple-negative breast cancer: a review*. *Breast Cancer Res Treat*, 2018. **169**(3): p. 397-406.
122. Bosch, A., et al., *PI3K inhibition results in enhanced estrogen receptor function and dependence in hormone receptor-positive breast cancer*. *Sci Transl Med*, 2015. **7**(283): p. 283ra51.
123. Yardley, D.A., et al., *Everolimus plus exemestane in postmenopausal patients with HR(+) breast cancer: BOLERO-2 final progression-free survival analysis*. *Adv Ther*, 2013. **30**(10): p. 870-84.
124. Ribas, R., et al., *AKT Antagonist AZD5363 Influences Estrogen Receptor Function in Endocrine-Resistant Breast Cancer and Synergizes with Fulvestrant (ICI182780) In Vivo*. *Mol Cancer Ther*, 2015. **14**(9): p. 2035-48.
125. Finn, R.S., A. Aleshin, and D.J. Slamon, *Targeting the cyclin-dependent kinases (CDK) 4/6 in estrogen receptor-positive breast cancers*. *Breast Cancer Res*, 2016. **18**(1): p. 17.
126. Turner, N.C., et al., *Palbociclib in Hormone-Receptor-Positive Advanced Breast Cancer*. *N Engl J Med*, 2015. **373**(3): p. 209-19.
127. Giampietri, C., et al., *Cancer Microenvironment and Endoplasmic Reticulum Stress Response*. *Mediators Inflamm*, 2015. **2015**: p. 417281.
128. Chevet, E., C. Hetz, and A. Samali, *Endoplasmic reticulum stress-activated cell reprogramming in oncogenesis*. *Cancer Discov*, 2015. **5**(6): p. 586-97.

129. Lorusso, G. and C. Rugg, *The tumor microenvironment and its contribution to tumor evolution toward metastasis*. *Histochem Cell Biol*, 2008. **130**(6): p. 1091-103.
130. Bettigole, S.E. and L.H. Glimcher, *Endoplasmic reticulum stress in immunity*. *Annu Rev Immunol*, 2015. **33**: p. 107-38.
131. Spiotto, M.T., et al., *Imaging the unfolded protein response in primary tumors reveals microenvironments with metabolic variations that predict tumor growth*. *Cancer Res*, 2010. **70**(1): p. 78-88.
132. Parsons, D.W., et al., *An integrated genomic analysis of human glioblastoma multiforme*. *Science*, 2008. **321**(5897): p. 1807-12.
133. Guichard, C., et al., *Integrated analysis of somatic mutations and focal copy-number changes identifies key genes and pathways in hepatocellular carcinoma*. *Nat Genet*, 2012. **44**(6): p. 694-8.
134. Maestre, L., et al., *Expression pattern of XBP1(S) in human B-cell lymphomas*. *Haematologica*, 2009. **94**(3): p. 419-22.
135. Chen, X., et al., *XBP1 promotes triple-negative breast cancer by controlling the HIF1alpha pathway*. *Nature*, 2014. **508**(7494): p. 103-7.
136. Romero-Ramirez, L., et al., *XBP1 is essential for survival under hypoxic conditions and is required for tumor growth*. *Cancer Res*, 2004. **64**(17): p. 5943-7.
137. Drogat, B., et al., *IRE1 signaling is essential for ischemia-induced vascular endothelial growth factor-A expression and contributes to angiogenesis and tumor growth in vivo*. *Cancer Res*, 2007. **67**(14): p. 6700-7.
138. Hart, L.S., et al., *ER stress-mediated autophagy promotes Myc-dependent transformation and tumor growth*. *J Clin Invest*, 2012. **122**(12): p. 4621-34.
139. Kim, J.Y., et al., *Activation of the PERK-eIF2alpha Pathway Is Associated with Tumor-infiltrating Lymphocytes in HER2-Positive Breast Cancer*. *Anticancer Res*, 2016. **36**(6): p. 2705-11.
140. Horiguchi, M., et al., *Stress-regulated transcription factor ATF4 promotes neoplastic transformation by suppressing expression of the INK4a/ARF cell senescence factors*. *Cancer Res*, 2012. **72**(2): p. 395-401.
141. Wang, X.J., et al., *Nrf2 enhances resistance of cancer cells to chemotherapeutic drugs, the dark side of Nrf2*. *Carcinogenesis*, 2008. **29**(6): p. 1235-43.
142. Shuda, M., et al., *Activation of the ATF6, XBP1 and grp78 genes in human hepatocellular carcinoma: a possible involvement of the ER stress pathway in hepatocarcinogenesis*. *J Hepatol*, 2003. **38**(5): p. 605-14.
143. Arai, M., et al., *Transformation-associated gene regulation by ATF6alpha during hepatocarcinogenesis*. *FEBS Lett*, 2006. **580**(1): p. 184-90.
144. Higa, A., et al., *Endoplasmic reticulum stress-activated transcription factor ATF6alpha requires the disulfide isomerase PDIA5 to modulate chemoresistance*. *Mol Cell Biol*, 2014. **34**(10): p. 1839-49.
145. Gomez, B.P., et al., *Human X-box binding protein-1 confers both estrogen independence and antiestrogen resistance in breast cancer cell lines*. *FASEB J*, 2007. **21**(14): p. 4013-27.
146. Davies, M.P., et al., *Expression and splicing of the unfolded protein response gene XBP-1 are significantly associated with clinical outcome of endocrine-treated breast cancer*. *Int J Cancer*, 2008. **123**(1): p. 85-8.
147. Cancer Genome Atlas, N., *Comprehensive molecular portraits of human breast tumours*. *Nature*, 2012. **490**(7418): p. 61-70.
148. Scriven, P., et al., *Activation and clinical significance of the unfolded protein response in breast cancer*. *Br J Cancer*, 2009. **101**(10): p. 1692-8.
149. Zhao, N., et al., *Pharmacological targeting of MYC-regulated IRE1/XBP1 pathway suppresses MYC-driven breast cancer*. *J Clin Invest*, 2018. **128**(4): p. 1283-1299.

150. *Comprehensive molecular portraits of human breast tumours*. Nature, 2012. **490**(7418): p. 61-70.
151. Sengupta, S., C.G. Sharma, and V.C. Jordan, *Estrogen regulation of X-box binding protein-1 and its role in estrogen induced growth of breast and endometrial cancer cells*. Horm Mol Biol Clin Investig, 2010. **2**(2): p. 235-243.
152. Ming, J., et al., *A novel chemical, STF-083010, reverses tamoxifen-related drug resistance in breast cancer by inhibiting IRE1/XBP1*. Oncotarget, 2015. **6**(38): p. 40692-703.
153. Hu, R., et al., *NF-kappaB signaling is required for XBP1 (unspliced and spliced)-mediated effects on antiestrogen responsiveness and cell fate decisions in breast cancer*. Mol Cell Biol, 2015. **35**(2): p. 379-90.
154. Andruska, N., et al., *Anticipatory estrogen activation of the unfolded protein response is linked to cell proliferation and poor survival in estrogen receptor alpha-positive breast cancer*. Oncogene, 2015. **34**(29): p. 3760-9.
155. Gupta, A., et al., *NCOA3 coactivator is a transcriptional target of XBP1 and regulates PERK-eIF2alpha-ATF4 signalling in breast cancer*. Oncogene, 2016. **35**(45): p. 5860-5871.
156. Bobrovnikova-Marjon, E., et al., *PERK promotes cancer cell proliferation and tumor growth by limiting oxidative DNA damage*. Oncogene, 2010. **29**(27): p. 3881-95.
157. Del Vecchio, C.A., et al., *De-differentiation confers multidrug resistance via noncanonical PERK-Nrf2 signaling*. PLoS Biol, 2014. **12**(9): p. e1001945.
158. Bi, M., et al., *ER stress-regulated translation increases tolerance to extreme hypoxia and promotes tumor growth*. Embo j, 2005. **24**(19): p. 3470-81.
159. Sawada, R., J.B. Lowe, and M. Fukuda, *E-selectin-dependent adhesion efficiency of colonic carcinoma cells is increased by genetic manipulation of their cell surface lysosomal membrane glycoprotein-1 expression levels*. J Biol Chem, 1993. **268**(17): p. 12675-81.
160. Pike, L.R., et al., *Transcriptional up-regulation of ULK1 by ATF4 contributes to cancer cell survival*. Biochem J, 2013. **449**(2): p. 389-400.
161. Feng, Y.X., et al., *Epithelial-to-mesenchymal transition activates PERK-eIF2alpha and sensitizes cells to endoplasmic reticulum stress*. Cancer Discov, 2014. **4**(6): p. 702-15.
162. Greenman, C., et al., *Patterns of somatic mutation in human cancer genomes*. Nature, 2007. **446**(7132): p. 153-8.
163. Okada, T., et al., *Distinct roles of activating transcription factor 6 (ATF6) and double-stranded RNA-activated protein kinase-like endoplasmic reticulum kinase (PERK) in transcription during the mammalian unfolded protein response*. Biochem J, 2002. **366**(Pt 2): p. 585-94.
164. Ruan, Q., et al., *Development of an anti-angiogenic therapeutic model combining scAAV2-delivered siRNAs and noninvasive photoacoustic imaging of tumor vasculature development*. Cancer Lett, 2013. **332**(1): p. 120-9.
165. Fu, Y., J. Li, and A.S. Lee, *GRP78/BiP inhibits endoplasmic reticulum BIK and protects human breast cancer cells against estrogen starvation-induced apoptosis*. Cancer Res, 2007. **67**(8): p. 3734-40.
166. Zhang, D., et al., *Proteomic characterization of differentially expressed proteins in breast cancer: Expression of hnRNP H1, RKIP and GRP78 is strongly associated with HER-2/neu status*. Proteomics Clin Appl, 2008. **2**(1): p. 99-107.
167. Tyson W. Lager, H.C.C., Ian H. Guldner, Michael Z. Wu, Yuriko Hishida, Tomoaki Hishida, Sergio Ruiz, Amanda E. , *Aberrant cell surface expression of GRP78 in breast cancer cells marks a stem-like population that has increased metastatic potential in vivo*. Cancer Research, 2018(10.1158/1538-7445.).

168. Zhou, H., et al., *Novel mechanism of anti-apoptotic function of 78-kDa glucose-regulated protein (GRP78): endocrine resistance factor in breast cancer, through release of B-cell lymphoma 2 (BCL-2) from BCL-2-interacting killer (BIK)*. J Biol Chem, 2011. **286**(29): p. 25687-96.
169. Reddy, R.K., et al., *Endoplasmic reticulum chaperone protein GRP78 protects cells from apoptosis induced by topoisomerase inhibitors: role of ATP binding site in suppression of caspase-7 activation*. J Biol Chem, 2003. **278**(23): p. 20915-24.
170. Chang, Y.W., et al., *Deacetylation of HSPA5 by HDAC6 leads to GP78-mediated HSPA5 ubiquitination at K447 and suppresses metastasis of breast cancer*. Oncogene, 2016. **35**(12): p. 1517-28.
171. Notte, A., et al., *Taxol-induced unfolded protein response activation in breast cancer cells exposed to hypoxia: ATF4 activation regulates autophagy and inhibits apoptosis*. Int J Biochem Cell Biol, 2015. **62**: p. 1-14.
172. Wang, J., et al., *Blockade of GRP78 sensitizes breast cancer cells to microtubules-interfering agents that induce the unfolded protein response*. J Cell Mol Med, 2009. **13**(9b): p. 3888-97.
173. Kim, K.W., et al., *Endoplasmic reticulum stress mediates radiation-induced autophagy by perker-*EIF2alpha* in caspase-3/7-deficient cells*. Oncogene, 2010. **29**(22): p. 3241-51.
174. Wang, S., et al., *ATF4 Gene Network Mediates Cellular Response to the Anticancer PAD Inhibitor YW3-56 in Triple-Negative Breast Cancer Cells*. Mol Cancer Ther, 2015. **14**(4): p. 877-88.
175. Cruickshanks, N., et al., *Lapatinib and obatoclax kill breast cancer cells through reactive oxygen species-dependent endoplasmic reticulum stress*. Mol Pharmacol, 2012. **82**(6): p. 1217-29.
176. Nagelkerke, A., et al., *The PERK/ATF4/LAMP3-arm of the unfolded protein response affects radioresistance by interfering with the DNA damage response*. Radiother Oncol, 2013. **108**(3): p. 415-21.
177. Cook, K.L., et al., *Endoplasmic Reticulum Stress Protein GRP78 Modulates Lipid Metabolism to Control Drug Sensitivity and Antitumor Immunity in Breast Cancer*. Cancer Res, 2016. **76**(19): p. 5657-5670.
178. Logue, S.E., et al., *Inhibition of IRE1 RNase activity modulates the tumor cell secretome and enhances response to chemotherapy*. Nat Commun, 2018. **9**(1): p. 3267.
179. Axten, J.M., et al., *Discovery of GSK2656157: An Optimized PERK Inhibitor Selected for Preclinical Development*. ACS Med Chem Lett, 2013. **4**(10): p. 964-8.
180. Smith, A.L., et al., *Discovery of 1H-pyrazol-3(2H)-ones as potent and selective inhibitors of protein kinase R-like endoplasmic reticulum kinase (PERK)*. J Med Chem, 2015. **58**(3): p. 1426-41.
181. Gallagher, C.M., et al., *Ceapins are a new class of unfolded protein response inhibitors, selectively targeting the ATF6alpha branch*. Elife, 2016. **5**.
182. Cerezo, M., et al., *Compounds Triggering ER Stress Exert Anti-Melanoma Effects and Overcome BRAF Inhibitor Resistance*. Cancer Cell, 2016. **29**(6): p. 805-819.
183. Macias, A.T., et al., *Adenosine-derived inhibitors of 78 kDa glucose regulated protein (Grp78) ATPase: insights into isoform selectivity*. J Med Chem, 2011. **54**(12): p. 4034-41.
184. Xu, W., et al., *Quantum dot-conjugated anti-GRP78 scFv inhibits cancer growth in mice*. Molecules, 2012. **17**(1): p. 796-808.
185. Liu, R., et al., *Monoclonal antibody against cell surface GRP78 as a novel agent in suppressing PI3K/AKT signaling, tumor growth, and metastasis*. Clin Cancer Res, 2013. **19**(24): p. 6802-11.
186. Rasche, L., et al., *GRP78-directed immunotherapy in relapsed or refractory multiple myeloma - results from a phase 1 trial with the monoclonal immunoglobulin M antibody PAT-SM6*. Haematologica, 2015. **100**(3): p. 377-84.
187. Kawiak, A., et al., *Plumbagin sensitizes breast cancer cells to tamoxifen-induced cell death through GRP78 inhibition and Bik upregulation*. Sci Rep, 2017. **7**: p. 43781.

188. Lee, R.C., R.L. Feinbaum, and V. Ambros, *The C. elegans heterochronic gene lin-4 encodes small RNAs with antisense complementarity to lin-14*. Cell, 1993. **75**(5): p. 843-54.
189. Carrington, J.C. and V. Ambros, *Role of microRNAs in plant and animal development*. Science, 2003. **301**(5631): p. 336-8.
190. Swaminathan, G., S. Navas-Martín, and J. Martín-García, *MicroRNAs and HIV-1 Infection: Antiviral Activities and Beyond*. Journal of Molecular Biology, 2014. **426**(6): p. 1178-1197.
191. Zhou, A., et al., *Interplay between microRNAs and host pathogen recognition receptors (PRRs) signaling pathways in response to viral infection*. Virus Research, 2014. **184**(0): p. 1-6.
192. Lu, J. and A.G. Clark, *Impact of microRNA regulation on variation in human gene expression*. Genome Res, 2012. **22**(7): p. 1243-54.
193. Miska, E.A., *How microRNAs control cell division, differentiation and death*. Curr Opin Genet Dev, 2005. **15**(5): p. 563-8.
194. Plasterk, R.H., *Micro RNAs in animal development*. Cell, 2006. **124**(5): p. 877-81.
195. Wienholds, E., et al., *The microRNA-producing enzyme Dicer1 is essential for zebrafish development*. Nature genetics, 2003. **35**(3): p. 217-8.
196. Stoorvogel, W., *Functional transfer of microRNA by exosomes*. Blood, 2012. **119**(3): p. 646-8.
197. Hunter, M.P., et al., *Detection of microRNA expression in human peripheral blood microvesicles*. PloS one, 2008. **3**(11): p. e3694.
198. Arroyo, J.D., et al., *Argonaute2 complexes carry a population of circulating microRNAs independent of vesicles in human plasma*. Proceedings of the National Academy of Sciences of the United States of America, 2011. **108**(12): p. 5003-8.
199. Fromm, B., et al., *A Uniform System for the Annotation of Vertebrate microRNA Genes and the Evolution of the Human microRNAome*. Annu Rev Genet, 2015. **49**: p. 213-42.
200. Desvignes, T., et al., *miRNA Nomenclature: A View Incorporating Genetic Origins, Biosynthetic Pathways, and Sequence Variants*. Trends Genet, 2015. **31**(11): p. 613-626.
201. de Rie, D., et al., *An integrated expression atlas of miRNAs and their promoters in human and mouse*. Nat Biotechnol, 2017. **35**(9): p. 872-878.
202. Ha, M. and V.N. Kim, *Regulation of microRNA biogenesis*. Nat Rev Mol Cell Biol, 2014. **15**(8): p. 509-24.
203. Bartel, D.P., *MicroRNAs: genomics, biogenesis, mechanism, and function*. Cell, 2004. **116**(2): p. 281-97.
204. Fukunaga, R., et al., *Dicer partner proteins tune the length of mature miRNAs in flies and mammals*. Cell, 2012. **151**(3): p. 533-46.
205. Lee, Y., et al., *The nuclear RNase III Drosha initiates microRNA processing*. Nature, 2003. **425**(6956): p. 415-9.
206. Alarcon, C.R., et al., *N6-methyladenosine marks primary microRNAs for processing*. Nature, 2015. **519**(7544): p. 482-5.
207. Sontheimer, E.J., *Assembly and function of RNA silencing complexes*. Nat Rev Mol Cell Biol, 2005. **6**(2): p. 127-38.
208. Chendrimada, T.P., et al., *TRBP recruits the Dicer complex to Ago2 for microRNA processing and gene silencing*. Nature, 2005. **436**(7051): p. 740-4.
209. Meijer, H.A., E.M. Smith, and M. Bushell, *Regulation of miRNA strand selection: follow the leader?* Biochem Soc Trans, 2014. **42**(4): p. 1135-40.
210. Zhou, X., et al., *Characterization and identification of microRNA core promoters in four model species*. PLoS Comput Biol, 2007. **3**(3): p. e37.
211. Treiber, T., N. Treiber, and G. Meister, *Regulation of microRNA biogenesis and its crosstalk with other cellular pathways*. Nat Rev Mol Cell Biol, 2018.



212. Ruby, J.G., C.H. Jan, and D.P. Bartel, *Intronic microRNA precursors that bypass Drosha processing*. *Nature*, 2007. **448**(7149): p. 83-6.
213. Ramalingam, P., et al., *Biogenesis of intronic miRNAs located in clusters by independent transcription and alternative splicing*. *Rna*, 2014. **20**(1): p. 76-87.
214. Xie, M., et al., *Mammalian 5'-capped microRNA precursors that generate a single microRNA*. *Cell*, 2013. **155**(7): p. 1568-80.
215. Babiarz, J.E., et al., *Mouse ES cells express endogenous shRNAs, siRNAs, and other Microprocessor-independent, Dicer-dependent small RNAs*. *Genes Dev*, 2008. **22**(20): p. 2773-85.
216. O'Brien, J., et al., *Overview of MicroRNA Biogenesis, Mechanisms of Actions, and Circulation*. *Front Endocrinol (Lausanne)*, 2018. **9**: p. 402.
217. Broughton, J.P., et al., *Pairing beyond the Seed Supports MicroRNA Targeting Specificity*. *Mol Cell*, 2016. **64**(2): p. 320-333.
218. Ma, F., et al., *MicroRNA-466l upregulates IL-10 expression in TLR-triggered macrophages by antagonizing RNA-binding protein tristetraprolin-mediated IL-10 mRNA degradation*. *J Immunol*, 2010. **184**(11): p. 6053-9.
219. Zhang, L., et al., *Systematic identification of C. elegans miRISC proteins, miRNAs, and mRNA targets by their interactions with GW182 proteins AIN-1 and AIN-2*. *Mol Cell*, 2007. **28**(4): p. 598-613.
220. Vasudevan, S., *Posttranscriptional upregulation by microRNAs*. *Wiley Interdiscip Rev RNA*, 2012. **3**(3): p. 311-30.
221. Vasudevan, S., Y. Tong, and J.A. Steitz, *Switching from repression to activation: microRNAs can up-regulate translation*. *Science*, 2007. **318**(5858): p. 1931-4.
222. Huang, V., et al., *Upregulation of Cyclin B1 by miRNA and its implications in cancer*. *Nucleic Acids Res*, 2012. **40**(4): p. 1695-707.
223. Krutzfeldt, J., et al., *Specificity, duplex degradation and subcellular localization of antagomirs*. *Nucleic Acids Res*, 2007. **35**(9): p. 2885-92.
224. Vester, B. and J. Wengel, *LNA (locked nucleic acid): high-affinity targeting of complementary RNA and DNA*. *Biochemistry*, 2004. **43**(42): p. 13233-41.
225. Van Zandwijk, N., Pavlakis, N., Kao, S., Clarke, S., Lee, A., Brahmbhatt, H., Macdiarmid, J., Pattison, S., Leslie, F., Huynh, Y., Linton, A., Reid, G., *MesomiR 1: A Phase I study of TargomiRs in patients with refractory malignant pleural mesothelioma (MPM) and lung cancer (NSCLC)* *Ann. Oncol.*, 2015. **26**.
226. Wiggins, J.F., et al., *Development of a lung cancer therapeutic based on the tumor suppressor microRNA-34*. *Cancer Res*, 2010. **70**(14): p. 5923-30.
227. Liu, C., et al., *The microRNA miR-34a inhibits prostate cancer stem cells and metastasis by directly repressing CD44*. *Nat Med*, 2011. **17**(2): p. 211-5.
228. Cortez, M.A., et al., *Therapeutic delivery of miR-200c enhances radiosensitivity in lung cancer*. *Mol Ther*, 2014. **22**(8): p. 1494-1503.
229. Ma, L., et al., *Therapeutic silencing of miR-10b inhibits metastasis in a mouse mammary tumor model*. *Nat Biotechnol*, 2010. **28**(4): p. 341-7.
230. Garofalo, M., et al., *miR-221&222 regulate TRAIL resistance and enhance tumorigenicity through PTEN and TIMP3 downregulation*. *Cancer Cell*, 2009. **16**(6): p. 498-509.
231. Kota, J., et al., *Therapeutic microRNA delivery suppresses tumorigenesis in a murine liver cancer model*. *Cell*, 2009. **137**(6): p. 1005-17.
232. Rupaimoole, R., et al., *Hypoxia-upregulated microRNA-630 targets Dicer, leading to increased tumor progression*. *Oncogene*, 2016. **35**(33): p. 4312-20.
233. Nishimura, M., et al., *Therapeutic synergy between microRNA and siRNA in ovarian cancer treatment*. *Cancer Discov*, 2013. **3**(11): p. 1302-15.

234. Calin, G.A., et al., *MiR-15a and miR-16-1 cluster functions in human leukemia*. Proc Natl Acad Sci U S A, 2008. **105**(13): p. 5166-71.
235. Babar, I.A., et al., *Nanoparticle-based therapy in an in vivo microRNA-155 (miR-155)-dependent mouse model of lymphoma*. Proc Natl Acad Sci U S A, 2012. **109**(26): p. E1695-704.
236. Ibrahim, A.F., et al., *MicroRNA replacement therapy for miR-145 and miR-33a is efficacious in a model of colon carcinoma*. Cancer Res, 2011. **71**(15): p. 5214-24.
237. Tomczak, K., P. Czerwinska, and M. Wiznerowicz, *The Cancer Genome Atlas (TCGA): an immeasurable source of knowledge*. Contemp Oncol (Pozn), 2015. **19**(1a): p. A68-77.
238. Zimmerman, A.L. and S. Wu, *MicroRNAs, cancer and cancer stem cells*. Cancer Lett, 2011. **300**(1): p. 10-9.
239. Calin, G.A., et al., *Frequent deletions and down-regulation of micro- RNA genes miR15 and miR16 at 13q14 in chronic lymphocytic leukemia*. Proc Natl Acad Sci U S A, 2002. **99**(24): p. 15524-9.
240. Cimmino, A., et al., *miR-15 and miR-16 induce apoptosis by targeting BCL2*. Proc Natl Acad Sci U S A, 2005. **102**(39): p. 13944-9.
241. Kumar, M.S., et al., *Impaired microRNA processing enhances cellular transformation and tumorigenesis*. Nat Genet, 2007. **39**(5): p. 673-7.
242. Lu, J., et al., *MicroRNA expression profiles classify human cancers*. Nature, 2005. **435**(7043): p. 834-8.
243. Ng, E.K., et al., *Circulating microRNAs as specific biomarkers for breast cancer detection*. PLoS One, 2013. **8**(1): p. e53141.
244. Tahiri, A., et al., *Deregulation of cancer-related miRNAs is a common event in both benign and malignant human breast tumors*. Carcinogenesis, 2014. **35**(1): p. 76-85.
245. Mattie, M.D., et al., *Optimized high-throughput microRNA expression profiling provides novel biomarker assessment of clinical prostate and breast cancer biopsies*. Mol Cancer, 2006. **5**: p. 24.
246. Boeri, M., et al., *MicroRNA signatures in tissues and plasma predict development and prognosis of computed tomography detected lung cancer*. Proc Natl Acad Sci U S A, 2011. **108**(9): p. 3713-8.
247. Roldo, C., et al., *MicroRNA expression abnormalities in pancreatic endocrine and acinar tumors are associated with distinctive pathologic features and clinical behavior*. J Clin Oncol, 2006. **24**(29): p. 4677-84.
248. Ng, E.K., et al., *Differential expression of microRNAs in plasma of patients with colorectal cancer: a potential marker for colorectal cancer screening*. Gut, 2009. **58**(10): p. 1375-81.
249. Iorio, M.V., et al., *MicroRNA signatures in human ovarian cancer*. Cancer Res, 2007. **67**(18): p. 8699-707.
250. Volinia, S., et al., *A microRNA expression signature of human solid tumors defines cancer gene targets*. Proceedings of the National Academy of Sciences of the United States of America, 2006. **103**(7): p. 2257-61.
251. Mitchell, P.S., et al., *Circulating microRNAs as stable blood-based markers for cancer detection*. Proc Natl Acad Sci U S A, 2008. **105**(30): p. 10513-8.
252. Calin, G.A., et al., *Human microRNA genes are frequently located at fragile sites and genomic regions involved in cancers*. Proceedings of the National Academy of Sciences of the United States of America, 2004. **101**(9): p. 2999-3004.
253. Sevignani, C., et al., *MicroRNA genes are frequently located near mouse cancer susceptibility loci*. Proc Natl Acad Sci U S A, 2007. **104**(19): p. 8017-22.
254. Hammond, S.M., *MicroRNAs as oncogenes*. Current Opinion in Genetics & Development, 2006. **16**(1): p. 4-9.

255. Garzon, R., et al., *MicroRNA expression and function in cancer*. Trends in Molecular Medicine, 2006. **12**(12): p. 580-587.
256. Dedes, K.J., et al., *Down-regulation of the miRNA master regulators Drosha and Dicer is associated with specific subgroups of breast cancer*. Eur J Cancer, 2011. **47**(1): p. 138-50.
257. Faggad, A., et al., *Down-regulation of the microRNA processing enzyme Dicer is a prognostic factor in human colorectal cancer*. Histopathology, 2012. **61**(4): p. 552-61.
258. Karube, Y., et al., *Reduced expression of Dicer associated with poor prognosis in lung cancer patients*. Cancer Sci, 2005. **96**(2): p. 111-5.
259. Melo, S.A., et al., *A genetic defect in exportin-5 traps precursor microRNAs in the nucleus of cancer cells*. Cancer Cell, 2010. **18**(4): p. 303-15.
260. Kim, M.S., et al., *Somatic mutations and losses of expression of microRNA regulation-related genes AGO2 and TNRC6A in gastric and colorectal cancers*. J Pathol, 2010. **221**(2): p. 139-46.
261. Adams, B.D., K.P. Claffey, and B.A. White, *Argonaute-2 expression is regulated by epidermal growth factor receptor and mitogen-activated protein kinase signaling and correlates with a transformed phenotype in breast cancer cells*. Endocrinology, 2009. **150**(1): p. 14-23.
262. Kent, O.A. and J.T. Mendell, *A small piece in the cancer puzzle: microRNAs as tumor suppressors and oncogenes*. Oncogene, 2006. **25**(46): p. 6188-96.
263. Kashyap, D., et al., *Oncogenic and Tumor-Suppressive Roles of MicroRNAs with Special Reference to Apoptosis: Molecular Mechanisms and Therapeutic Potential*. Molecular Diagnosis & Therapy, 2018. **22**(2): p. 179-201.
264. Spizzo, R., et al., *SnapShot: MicroRNAs in Cancer*. Cell, 2009. **137**(3): p. 586-586 e1.
265. Calin, G.A. and C.M. Croce, *MicroRNA signatures in human cancers*. Nat Rev Cancer, 2006. **6**(11): p. 857-66.
266. Opferman, J.T. and A. Kothari, *Anti-apoptotic BCL-2 family members in development*. Cell Death Differ, 2018. **25**(1): p. 37-45.
267. Singh, R. and N. Saini, *Downregulation of BCL2 by miRNAs augments drug-induced apoptosis--a combined computational and experimental approach*. J Cell Sci, 2012. **125**(Pt 6): p. 1568-78.
268. Hu, X., et al., *The heterochronic microRNA let-7 inhibits cell motility by regulating the genes in the actin cytoskeleton pathway in breast cancer*. Mol Cancer Res, 2013. **11**(3): p. 240-50.
269. Zeng, M., et al., *miR-378 suppresses the proliferation, migration and invasion of colon cancer cells by inhibiting SDAD1*. Cell Mol Biol Lett, 2017. **22**: p. 12.
270. Wang, Z., et al., *MicroRNA-378-5p suppresses cell proliferation and induces apoptosis in colorectal cancer cells by targeting BRAF*. Cancer Cell Int, 2015. **15**: p. 40.
271. Wang, K.Y., et al., *MicroRNA-378 inhibits cell growth and enhances L-OHP-induced apoptosis in human colorectal cancer*. IUBMB Life, 2014. **66**(9): p. 645-54.
272. Zhang, G.J., et al., *MiR-378 is an independent prognostic factor and inhibits cell growth and invasion in colorectal cancer*. BMC Cancer, 2014. **14**: p. 109.
273. Avgeris, M., K. Stravodimos, and A. Scorilas, *Loss of miR-378 in prostate cancer, a common regulator of KLK2 and KLK4, correlates with aggressive disease phenotype and predicts the short-term relapse of the patients*. Biol Chem, 2014. **395**(9): p. 1095-104.
274. Chen, Q.G., et al., *MiR-378 suppresses prostate cancer cell growth through downregulation of MAPK1 in vitro and in vivo*. Tumour Biol, 2016. **37**(2): p. 2095-103.
275. Qiu, P., et al., *MicroRNA-378 regulates cell proliferation and migration by repressing RNF31 in pituitary adenoma*. Oncol Lett, 2018. **15**(1): p. 789-794.
276. Zhang, Z.Y., et al., *Regulation of UHRF1 by microRNA-378 modulates medulloblastoma cell proliferation and apoptosis*. Oncol Rep, 2017. **38**(5): p. 3078-3084.
277. Kuang, X., et al., *miR-378 inhibits cell growth and enhances apoptosis in human myelodysplastic syndromes*. Int J Oncol, 2016. **49**(5): p. 1921-1930.

278. Olive, V., I. Jiang, and L. He, *mir-17-92, a cluster of miRNAs in the midst of the cancer network*. Int J Biochem Cell Biol, 2010. **42**(8): p. 1348-54.
279. Xiang, J. and J. Wu, *Feud or Friend? The Role of the miR-17-92 Cluster in Tumorigenesis*. Curr Genomics, 2010. **11**(2): p. 129-35.
280. Wang, N., Y. Li, and J. Zhou, *miR-31 Functions as an Oncomir Which Promotes Epithelial-Mesenchymal Transition via Regulating BAP1 in Cervical Cancer*. Biomed Res Int, 2017. **2017**: p. 6361420.
281. Song, Q., et al., *miR-548d-3p/TP53BP2 axis regulates the proliferation and apoptosis of breast cancer cells*. Cancer Med, 2016. **5**(2): p. 315-24.
282. Tan, D., et al., *MicroRNA-378 enhances migration and invasion in cervical cancer by directly targeting autophagy-related protein 12*. Mol Med Rep, 2018. **17**(5): p. 6319-6326.
283. Li, S., et al., *miR-378 functions as an onco-miRNA by targeting the ST7L/Wnt/beta-catenin pathway in cervical cancer*. Int J Mol Med, 2017. **40**(4): p. 1047-1056.
284. Ji, K.X., et al., *MiR-378 promotes the cell proliferation of non-small cell lung cancer by inhibiting FOXG1*. Eur Rev Med Pharmacol Sci, 2018. **22**(4): p. 1011-1019.
285. Ho, C.S., S.M. Noor, and N.H. Nagoor, *MiR-378 and MiR-1827 Regulate Tumor Invasion, Migration and Angiogenesis in Human Lung Adenocarcinoma by Targeting RBX1 and CRKL, Respectively*. J Cancer, 2018. **9**(2): p. 331-345.
286. Skrzypek, K., et al., *Interplay between heme oxygenase-1 and miR-378 affects non-small cell lung carcinoma growth, vascularization, and metastasis*. Antioxid Redox Signal, 2013. **19**(7): p. 644-60.
287. Li, W., et al., *MicroRNA-378 enhances radiation response in ectopic and orthotopic implantation models of glioblastoma*. J Neurooncol, 2018. **136**(1): p. 63-71.
288. Lee, D.Y., et al., *MicroRNA-378 promotes cell survival, tumor growth, and angiogenesis by targeting SuFu and Fus-1 expression*. Proc Natl Acad Sci U S A, 2007. **104**(51): p. 20350-5.
289. Deng, Z., et al., *The intermediate filament vimentin mediates microRNA miR-378 function in cellular self-renewal by regulating the expression of the Sox2 transcription factor*. J Biol Chem, 2013. **288**(1): p. 319-31.
290. Yu, B.L., et al., *MicroRNA-378 functions as an onco-miR in nasopharyngeal carcinoma by repressing TOB2 expression*. Int J Oncol, 2014. **44**(4): p. 1215-22.
291. Ma, S., et al., *MicroRNA-616 induces androgen-independent growth of prostate cancer cells by suppressing expression of tissue factor pathway inhibitor TFPI-2*. Cancer Res, 2011. **71**(2): p. 583-92.
292. Zhang, D., et al., *MicroRNA-616 promotes the migration, invasion and epithelial-mesenchymal transition of HCC by targeting PTEN*. Oncol Rep, 2016. **35**(1): p. 366-74.
293. Bai, Q.L., et al., *MiR-616 promotes proliferation and inhibits apoptosis in glioma cells by suppressing expression of SOX7 via the Wnt signaling pathway*. Eur Rev Med Pharmacol Sci, 2017. **21**(24): p. 5630-5637.
294. Wang, D., et al., *MicroRNA-616 promotes the growth and metastasis of non-small cell lung cancer by targeting SOX7*. Oncol Rep, 2017. **38**(4): p. 2078-2086.
295. Chen, Z., et al., *MicroRNA-616 promotes the progression of ovarian cancer by targeting TIMP2*. Oncol Rep, 2018. **39**(6): p. 2960-2968.
296. Fabbri, M., et al., *Regulatory mechanisms of microRNAs involvement in cancer*. Expert Opin Biol Ther, 2007. **7**(7): p. 1009-19.
297. Zhang, L., et al., *microRNAs exhibit high frequency genomic alterations in human cancer*. Proc Natl Acad Sci U S A, 2006. **103**(24): p. 9136-41.
298. Ottman, R., et al., *The other face of miR-17-92a cluster, exhibiting tumor suppressor effects in prostate cancer*. Oncotarget, 2016.

299. Li, S., et al., *The tumor suppressor role of miR-155-5p in gastric cancer*. *Oncol Lett*, 2018. **16**(2): p. 2709-2714.
300. Jiang, S., et al., *MicroRNA-155 functions as an OncomiR in breast cancer by targeting the suppressor of cytokine signaling 1 gene*. *Cancer Res*, 2010. **70**(8): p. 3119-27.
301. Gabriely, G., N.M. Teplyuk, and A.M. Krichevsky, *Context effect: microRNA-10b in cancer cell proliferation, spread and death*. *Autophagy*, 2011. **7**(11): p. 1384-6.
302. Blenkiron, C., et al., *MicroRNA expression profiling of human breast cancer identifies new markers of tumor subtype*. *Genome Biol*, 2007. **8**(10): p. R214.
303. Lowery, A.J., et al., *MicroRNA signatures predict oestrogen receptor, progesterone receptor and HER2/neu receptor status in breast cancer*. *Breast Cancer Res*, 2009. **11**(3): p. R27.
304. de Rinaldis, E., et al., *Integrated genomic analysis of triple-negative breast cancers reveals novel microRNAs associated with clinical and molecular phenotypes and sheds light on the pathways they control*. *BMC Genomics*, 2013. **14**: p. 643.
305. Dvinge, H., et al., *The shaping and functional consequences of the microRNA landscape in breast cancer*. *Nature*, 2013. **497**(7449): p. 378-82.
306. Riaz, M., et al., *miRNA expression profiling of 51 human breast cancer cell lines reveals subtype and driver mutation-specific miRNAs*. *Breast Cancer Res*, 2013. **15**(2): p. R33.
307. Byrd, A.E. and J.W. Brewer, *Micro(RNA)managing endoplasmic reticulum stress*. *IUBMB Life*, 2013. **65**(5): p. 373-81.
308. Maurel, M. and E. Chevet, *Endoplasmic reticulum stress signaling: the microRNA connection*. *Am J Physiol Cell Physiol*, 2013. **304**(12): p. C1117-26.
309. Dai, R., et al., *miR-221/222 suppression protects against endoplasmic reticulum stress-induced apoptosis via p27(Kip1)- and MEK/ERK-mediated cell cycle regulation*. *Biol Chem*, 2010. **391**(7): p. 791-801.
310. Li, G., et al., *Role of miR-204 in the regulation of apoptosis, endoplasmic reticulum stress response, and inflammation in human trabecular meshwork cells*. *Invest Ophthalmol Vis Sci*, 2011. **52**(6): p. 2999-3007.
311. Chhabra, R., R. Dubey, and N. Saini, *Gene expression profiling indicate role of ER stress in miR-23a~27a~24-2 cluster induced apoptosis in HEK293T cells*. *RNA Biol*, 2011. **8**(4): p. 648-64.
312. Yang, F., et al., *Modulation of the unfolded protein response is the core of microRNA-122-involved sensitivity to chemotherapy in hepatocellular carcinoma*. *Neoplasia*, 2011. **13**(7): p. 590-600.
313. Bartoszewski, R., et al., *The unfolded protein response (UPR)-activated transcription factor X-box-binding protein 1 (XBP1) induces microRNA-346 expression that targets the human antigen peptide transporter 1 (TAP1) mRNA and governs immune regulatory genes*. *J Biol Chem*, 2011. **286**(48): p. 41862-70.
314. Behrman, S., D. Acosta-Alvear, and P. Walter, *A CHOP-regulated microRNA controls rhodopsin expression*. *J Cell Biol*, 2011. **192**(6): p. 919-27.
315. Byrd, A.E., I.V. Aragon, and J.W. Brewer, *MicroRNA-30c-2\* limits expression of proadaptive factor XBP1 in the unfolded protein response*. *J Cell Biol*, 2012. **196**(6): p. 689-98.
316. Belmont, P.J., et al., *Regulation of microRNA expression in the heart by the ATF6 branch of the ER stress response*. *J Mol Cell Cardiol*, 2012. **52**(5): p. 1176-82.
317. Gupta, S., et al., *Perk-dependent repression of miR-106b-25 cluster is required for ER stress-induced apoptosis*. *Cell Death Dis*, 2012. **3**: p. e333.
318. Chitnis, N.S., et al., *miR-211 is a prosurvival microRNA that regulates chop expression in a PERK-dependent manner*. *Mol Cell*, 2012. **48**(3): p. 353-64.

319. Lerner, A.G., et al., *IRE1alpha induces thioredoxin-interacting protein to activate the NLRP3 inflammasome and promote programmed cell death under irremediable ER stress*. *Cell Metab*, 2012. **16**(2): p. 250-64.
320. Afonyushkin, T., O.V. Oskolkova, and V.N. Bochkov, *Permissive role of miR-663 in induction of VEGF and activation of the ATF4 branch of unfolded protein response in endothelial cells by oxidized phospholipids*. *Atherosclerosis*, 2012. **225**(1): p. 50-5.
321. Duan, Q., et al., *ER stress negatively modulates the expression of the miR-199a/214 cluster to regulates tumor survival and progression in human hepatocellular cancer*. *PLoS One*, 2012. **7**(2): p. e31518.
322. Dai, B.H., et al., *microRNA-199a-5p protects hepatocytes from bile acid-induced sustained endoplasmic reticulum stress*. *Cell Death Dis*, 2013. **4**: p. e604.
323. Maurel, M., et al., *MicroRNA-1291-mediated silencing of IRE1alpha enhances Glypican-3 expression*. *Rna*, 2013. **19**(6): p. 778-88.
324. Zhou, Y., et al., *Downregulation of microRNA199a5p protects cardiomyocytes in cyanotic congenital heart disease by attenuating endoplasmic reticulum stress*. *Mol Med Rep*, 2017. **16**(3): p. 2992-3000.
325. Ahmadi, A., et al., *miR-199a-5p and miR-495 target GRP78 within UPR pathway of lung cancer*. *Gene*, 2017. **620**: p. 15-22.
326. Bao, Q., et al., *MicroRNA-297 promotes cardiomyocyte hypertrophy via targeting sigma-1 receptor*. *Life Sciences*, 2017. **175**: p. 1-10.
327. Huang, Y.H., et al., *MicroRNA-29a mitigation of endoplasmic reticulum and autophagy aberrance counteracts in obstructive jaundice-induced fibrosis in mice*. *Exp Biol Med (Maywood)*, 2018. **243**(1): p. 13-21.
328. Sohn, E.J., *MicroRNA 200c-3p regulates autophagy via upregulation of endoplasmic reticulum stress in PC-3 cells*. *Cancer Cell International*, 2018. **18**(1): p. 2.
329. Gupta, A., et al., *PERK regulated miR-424(322)-503 cluster fine-tunes activation of IRE1 and ATF6 during Unfolded Protein Response*. *Sci Rep*, 2015. **5**: p. 18304.
330. Moenner, M., et al., *Integrated endoplasmic reticulum stress responses in cancer*. *Cancer Res*, 2007. **67**(22): p. 10631-4.
331. Healy, S.J., et al., *Targeting the endoplasmic reticulum-stress response as an anticancer strategy*. *Eur J Pharmacol*, 2009. **625**(1-3): p. 234-46.
332. Malhotra, J.D. and R.J. Kaufman, *The endoplasmic reticulum and the unfolded protein response*. *Semin Cell Dev Biol*, 2007. **18**(6): p. 716-31.
333. Bartoszewska, S., et al., *Regulation of the unfolded protein response by microRNAs*. *Cell Mol Biol Lett*, 2013. **18**(4): p. 555-78.
334. Bassik, M.C. and M. Kampmann, *Knocking out the door to tunicamycin entry*. *Proc Natl Acad Sci U S A*, 2011. **108**(29): p. 11731-2.
335. Sehgal, P., et al., *Inhibition of the sarco/endoplasmic reticulum (ER) Ca(2+)-ATPase by thapsigargin analogs induces cell death via ER Ca(2+) depletion and the unfolded protein response*. *J Biol Chem*, 2017. **292**(48): p. 19656-19673.
336. Colanzi, A., et al., *Molecular mechanism and functional role of brefeldin A-mediated ADP-ribosylation of CtBP1/BARS*. *Proc Natl Acad Sci U S A*, 2013. **110**(24): p. 9794-9.
337. Cross, B.C., et al., *The molecular basis for selective inhibition of unconventional mRNA splicing by an IRE1-binding small molecule*. *Proc Natl Acad Sci U S A*, 2012. **109**(15): p. E869-78.
338. Goodsell, D.S., *The molecular perspective: tamoxifen and the estrogen receptor*. *Stem Cells*, 2002. **20**(3): p. 267-8.
339. Lai, A.C. and C.M. Crews, *Induced protein degradation: an emerging drug discovery paradigm*. *Nat Rev Drug Discov*, 2017. **16**(2): p. 101-114.

340. Wang, H., et al., *Multiple mechanisms underlying acquired resistance to taxanes in selected docetaxel-resistant MCF-7 breast cancer cells*. BMC Cancer, 2014. **14**: p. 37.
341. Livak, K.J. and T.D. Schmittgen, *Analysis of relative gene expression data using real-time quantitative PCR and the 2(-Delta Delta C(T)) Method*. Methods, 2001. **25**(4): p. 402-8.
342. Franken, N.A., et al., *Clonogenic assay of cells in vitro*. Nat Protoc, 2006. **1**(5): p. 2315-9.
343. Liang, C.C., A.Y. Park, and J.L. Guan, *In vitro scratch assay: a convenient and inexpensive method for analysis of cell migration in vitro*. Nat Protoc, 2007. **2**(2): p. 329-33.
344. Adan, A., Y. Kiraz, and Y. Baran, *Cell Proliferation and Cytotoxicity Assays*. Curr Pharm Biotechnol, 2016. **17**(14): p. 1213-1221.
345. Wang, Z., M. Gerstein, and M. Snyder, *RNA-Seq: a revolutionary tool for transcriptomics*. Nat Rev Genet, 2009. **10**(1): p. 57-63.
346. Mortazavi, A., et al., *Mapping and quantifying mammalian transcriptomes by RNA-Seq*. Nat Methods, 2008. **5**(7): p. 621-8.
347. Kim, D., B. Langmead, and S.L. Salzberg, *HISAT: a fast spliced aligner with low memory requirements*. Nat Methods, 2015. **12**(4): p. 357-60.
348. Langmead, B., et al., *Ultrafast and memory-efficient alignment of short DNA sequences to the human genome*. Genome Biol, 2009. **10**(3): p. R25.
349. Rhodes, D.R., et al., *Oncomine 3.0: Genes, Pathways, and Networks in a Collection of 18,000 Cancer Gene Expression Profiles*. Neoplasia, 2007. **9**(2): p. 166-180.
350. Karali, E., et al., *VEGF Signals through ATF6 and PERK to promote endothelial cell survival and angiogenesis in the absence of ER stress*. Mol Cell, 2014. **54**(4): p. 559-72.
351. Hetz, C., et al., *The Unfolded Protein Response: Integrating Stress Signals through the Stress Sensor Ire1 Alpha*. Physiological Reviews, 2011. **91**(4): p. 1219-1243.
352. Sha, H., et al., *Stressed out about obesity: IRE1alpha-XBP1 in metabolic disorders*. Trends Endocrinol Metab, 2011. **22**(9): p. 374-81.
353. Ning, J., et al., *Constitutive role for IRE1alpha-XBP1 signaling pathway in the insulin-mediated hepatic lipogenic program*. Endocrinology, 2011. **152**(6): p. 2247-55.
354. Jurczak, M.J., et al., *Dissociation of inositol-requiring enzyme (IRE1alpha)-mediated c-Jun N-terminal kinase activation from hepatic insulin resistance in conditional X-box-binding protein-1 (XBP1) knock-out mice*. J Biol Chem, 2012. **287**(4): p. 2558-67.
355. Ikeda, K., et al., *miR-378a-3p modulates tamoxifen sensitivity in breast cancer MCF-7 cells through targeting GOLT1A*. Sci Rep, 2015. **5**: p. 13170.
356. Ek, J., et al., *Mutation analysis of peroxisome proliferator-activated receptor-gamma coactivator-1 (PGC-1) and relationships of identified amino acid polymorphisms to Type II diabetes mellitus*. Diabetologia, 2001. **44**(12): p. 2220-6.
357. Kressler, D., et al., *The PGC-1-related protein PERC is a selective coactivator of estrogen receptor alpha*. J Biol Chem, 2002. **277**(16): p. 13918-25.
358. Handschin, C. and B.M. Spiegelman, *Peroxisome proliferator-activated receptor gamma coactivator 1 coactivators, energy homeostasis, and metabolism*. Endocr Rev, 2006. **27**(7): p. 728-35.
359. Rhodes, D.R., et al., *ONCOMINE: a cancer microarray database and integrated data-mining platform*. Neoplasia, 2004. **6**(1): p. 1-6.
360. Pirooznia, M., V. Nagarajan, and Y. Deng, *GeneVenn - A web application for comparing gene lists using Venn diagrams*. Bioinformatics, 2007. **1**(10): p. 420-2.
361. Evans, H., et al., *Genomic organization and localization of the gene encoding human preprogalanin*. Genomics, 1993. **18**(3): p. 473-7.
362. Berger, A., et al., *Galanin and galanin receptors in human cancers*. Neuropeptides, 2005. **39**(3): p. 353-9.

363. Zhang, Y., et al., *Cloning and characterization of a new human UDP-N-acetyl-alpha-D-galactosamine:polypeptide N-acetylgalactosaminyltransferase, designated pp-GalNAc-T13, that is specifically expressed in neurons and synthesizes GalNAc alpha-serine/threonine antigen*. J Biol Chem, 2003. **278**(1): p. 573-84.
364. Nogimori, K., et al., *Increased expression levels of ppGalNAc-T13 in lung cancers: Significance in the prognostic diagnosis*. Int J Oncol, 2016. **49**(4): p. 1369-76.
365. Berteaux, N., et al., *A novel H19 antisense RNA overexpressed in breast cancer contributes to paternal IGF2 expression*. Mol Cell Biol, 2008. **28**(22): p. 6731-45.
366. Adriaenssens, E., et al., *H19 overexpression in breast adenocarcinoma stromal cells is associated with tumor values and steroid receptor status but independent of p53 and Ki-67 expression*. Am J Pathol, 1998. **153**(5): p. 1597-607.
367. Berteaux, N., et al., *H19 mRNA-like noncoding RNA promotes breast cancer cell proliferation through positive control by E2F1*. J Biol Chem, 2005. **280**(33): p. 29625-36.
368. Nakayama, Y., et al., *Gbx2 functions as a transcriptional repressor to regulate the specification and morphogenesis of the mid-hindbrain junction in a dosage- and stage-dependent manner*. Mechanisms of Development, 2013. **130**(11): p. 532-552.
369. Gao, A.C., W. Lou, and J.T. Isaacs, *Enhanced GBX2 expression stimulates growth of human prostate cancer cells via transcriptional up-regulation of the interleukin 6 gene*. Clin Cancer Res, 2000. **6**(2): p. 493-7.
370. Gale, M., Jr., *Understanding the Expanding Roles of Interferon and Cytokines in Health and Disease*. J Interferon Cytokine Res, 2018. **38**(5): p. 195-196.
371. Pytel, D., et al., *PERK Is a Haploinsufficient Tumor Suppressor: Gene Dose Determines Tumor-Suppressive Versus Tumor Promoting Properties of PERK in Melanoma*. PLoS Genet, 2016. **12**(12): p. e1006518.
372. Pytel, D., I. Majsterek, and J.A. Diehl, *Tumor progression and the different faces of the PERK kinase*. Oncogene, 2016. **35**(10): p. 1207-15.
373. Oyadomari, S. and M. Mori, *Roles of CHOP/GADD153 in endoplasmic reticulum stress*. Cell Death Differ, 2004. **11**(4): p. 381-9.
374. Yang, Y., et al., *Transcription Factor C/EBP Homologous Protein in Health and Diseases*. Front Immunol, 2017. **8**: p. 1612.
375. Jauhainen, A., et al., *Distinct cytoplasmic and nuclear functions of the stress induced protein DDIT3/CHOP/GADD153*. PLoS One, 2012. **7**(4): p. e33208.
376. Xu, G., et al., *miR-204 Targets PERK and Regulates UPR Signaling and beta-Cell Apoptosis*. Mol Endocrinol, 2016. **30**(8): p. 917-24.
377. Dweep, H. and N. Gretz, *miRWalk2.0: a comprehensive atlas of microRNA-target interactions*. Nat Methods, 2015. **12**(8): p. 697.
378. Radha, G. and S.C. Raghavan, *BCL2: A promising cancer therapeutic target*. Biochim Biophys Acta Rev Cancer, 2017. **1868**(1): p. 309-314.
379. Delbridge, A.R., et al., *Thirty years of BCL-2: translating cell death discoveries into novel cancer therapies*. Nat Rev Cancer, 2016. **16**(2): p. 99-109.
380. Wang, H., et al., *Cloning and characterization of a novel UDP-GalNAc:polypeptide N-acetylgalactosaminyltransferase, pp-GalNAc-T14*. Biochem Biophys Res Commun, 2003. **300**(3): p. 738-44.
381. Huanna, T., et al., *GALNT14 mediates tumor invasion and migration in breast cancer cell MCF-7*. Mol Carcinog, 2015. **54**(10): p. 1159-71.
382. Salameh, A., et al., *HER3 and LINC00052 interplay promotes tumor growth in breast cancer*. Oncotarget, 2017. **8**(4): p. 6526-6539.



383. Shan, Y., et al., *LINC00052 Promotes Gastric Cancer Cell Proliferation and Metastasis via Activating the Wnt/beta-Catenin Signaling Pathway*. *Oncol Res*, 2017. **25**(9): p. 1589-1599.
384. Zhu, L., et al., *LINC00052 upregulates EPB41L3 to inhibit migration and invasion of hepatocellular carcinoma by binding miR-452-5p*. *Oncotarget*, 2017. **8**(38): p. 63724-63737.
385. Shalom, B., et al., *Vav1 mutations identified in human cancers give rise to different oncogenic phenotypes*. *Oncogenesis*, 2018. **7**(10): p. 80.
386. Lazer, G., et al., *The haematopoietic specific signal transducer Vav1 is aberrantly expressed in lung cancer and plays a role in tumorigenesis*. *J Pathol*, 2009. **219**(1): p. 25-34.
387. Fernandez-Zapico, M.E., et al., *Ectopic expression of VAV1 reveals an unexpected role in pancreatic cancer tumorigenesis*. *Cancer Cell*, 2005. **7**(1): p. 39-49.
388. Grassilli, S., et al., *Vav1 downmodulates Akt in different breast cancer subtypes: a new promising chance to improve breast cancer outcome*. *Mol Oncol*, 2018. **12**(7): p. 1012-1025.
389. Wolpaw, A.J. and C.V. Dang, *MYC-induced metabolic stress and tumorigenesis*. *Biochim Biophys Acta Rev Cancer*, 2018. **1870**(1): p. 43-50.
390. Hanson, K.D., et al., *Effects of c-myc expression on cell cycle progression*. *Mol Cell Biol*, 1994. **14**(9): p. 5748-55.
391. Wang, S. and R.J. Kaufman, *The impact of the unfolded protein response on human disease*. *J Cell Biol*, 2012. **197**(7): p. 857-67.
392. Acosta-Alvear, D., et al., *XBP1 controls diverse cell type- and condition-specific transcriptional regulatory networks*. *Mol Cell*, 2007. **27**(1): p. 53-66.
393. Koumenis, C., et al., *Regulation of protein synthesis by hypoxia via activation of the endoplasmic reticulum kinase PERK and phosphorylation of the translation initiation factor eIF2alpha*. *Mol Cell Biol*, 2002. **22**(21): p. 7405-16.
394. Megiorni, F., et al., *Deep Sequencing the microRNA profile in rhabdomyosarcoma reveals down-regulation of miR-378 family members*. *BMC Cancer*, 2014. **14**: p. 880.
395. Li, W., et al., *MicroRNA-378 enhances inhibitory effect of curcumin on glioblastoma*. *Oncotarget*, 2017. **8**(43): p. 73938-73946.
396. Zhang, N., et al., *MicroRNA-378 Alleviates Cerebral Ischemic Injury by Negatively Regulating Apoptosis Executioner Caspase-3*. *Int J Mol Sci*, 2016. **17**(9).
397. Li, Y., et al., *MicroRNA-378 protects against intestinal ischemia/reperfusion injury via a mechanism involving the inhibition of intestinal mucosal cell apoptosis*. *Cell Death Dis*, 2017. **8**(10): p. e3127.
398. Kim, Y.K. and V.N. Kim, *Processing of intronic microRNAs*. *Embo j*, 2007. **26**(3): p. 775-83.
399. Liu, W., et al., *Hepatic miR-378 targets p110alpha and controls glucose and lipid homeostasis by modulating hepatic insulin signalling*. *Nat Commun*, 2014. **5**: p. 5684.
400. Lin, J., et al., *PGC-1beta in the regulation of hepatic glucose and energy metabolism*. *J Biol Chem*, 2003. **278**(33): p. 30843-8.
401. Krist, B., et al., *The Role of miR-378a in Metabolism, Angiogenesis, and Muscle Biology*. *Int J Endocrinol*, 2015. **2015**: p. 281756.
402. Shao, M., et al., *Hepatic IRE1alpha regulates fasting-induced metabolic adaptive programs through the XBP1s-PPARalpha axis signalling*. *Nat Commun*, 2014. **5**: p. 3528.
403. Browne, G., et al., *MicroRNA-378-mediated suppression of Runx1 alleviates the aggressive phenotype of triple-negative MDA-MB-231 human breast cancer cells*. *Tumour Biol*, 2016. **37**(7): p. 8825-39.
404. Winsel, S., et al., *Excess of miRNA-378a-5p perturbs mitotic fidelity and correlates with breast cancer tumorigenesis in vivo*. *Br J Cancer*, 2014. **111**(11): p. 2142-51.
405. Clarke, R., et al., *Anti-estrogen resistance in breast cancer and the role of estrogen receptor signaling*. *Oncogene*, 2003. **22**(47): p. 7316-39.

406. Kressler, D., M.B. Hock, and A. Kralli, *Coactivators PGC-1beta and SRC-1 interact functionally to promote the agonist activity of the selective estrogen receptor modulator tamoxifen*. J Biol Chem, 2007. **282**(37): p. 26897-907.
407. Wang, P., et al., *Identification of resting and type I IFN-activated human NK cell miRNomes reveals microRNA-378 and microRNA-30e as negative regulators of NK cell cytotoxicity*. J Immunol, 2012. **189**(1): p. 211-21.
408. Sonoda, J., et al., *Nuclear receptor ERR alpha and coactivator PGC-1 beta are effectors of IFN-gamma-induced host defense*. Genes Dev, 2007. **21**(15): p. 1909-20.
409. Gregory, R.I., et al., *Human RISC couples microRNA biogenesis and posttranscriptional gene silencing*. Cell, 2005. **123**(4): p. 631-40.
410. Ameres, S.L. and P.D. Zamore, *Diversifying microRNA sequence and function*. Nat Rev Mol Cell Biol, 2013. **14**(8): p. 475-88.
411. Ma, H., et al., *MicroRNA-17~92 inhibits colorectal cancer progression by targeting angiogenesis*. Cancer Lett, 2016. **376**(2): p. 293-302.
412. Brummer, A. and J. Hausser, *MicroRNA binding sites in the coding region of mRNAs: extending the repertoire of post-transcriptional gene regulation*. Bioessays, 2014. **36**(6): p. 617-26.
413. Schnall-Levin, M., et al., *Conserved microRNA targeting in Drosophila is as widespread in coding regions as in 3'UTRs*. Proc Natl Acad Sci U S A, 2010. **107**(36): p. 15751-6.
414. Tay, Y., et al., *MicroRNAs to Nanog, Oct4 and Sox2 coding regions modulate embryonic stem cell differentiation*. Nature, 2008. **455**(7216): p. 1124-8.
415. Duursma, A.M., et al., *miR-148 targets human DNMT3b protein coding region*. RNA, 2008. **14**(5): p. 872-7.
416. Qin, W., et al., *miR-24 regulates apoptosis by targeting the open reading frame (ORF) region of FAF1 in cancer cells*. PLoS One, 2010. **5**(2): p. e9429.
417. Ott, C.E., et al., *MicroRNAs differentially expressed in postnatal aortic development downregulate elastin via 3' UTR and coding-sequence binding sites*. PLoS One, 2011. **6**(1): p. e16250.
418. Jung, H.M., et al., *Tumor suppressor miR-375 regulates MYC expression via repression of CIP2A coding sequence through multiple miRNA-mRNA interactions*. Mol Biol Cell, 2013. **24**(11): p. 1638-48, S1-7.
419. Agarwal, V., et al., *Predicting effective microRNA target sites in mammalian mRNAs*. Elife, 2015. **4**.
420. Rehmsmeier, M., et al., *Fast and effective prediction of microRNA/target duplexes*. RNA, 2004. **10**(10): p. 1507-17.
421. Hornstein, I., et al., *The haematopoietic specific signal transducer Vav1 is expressed in a subset of human neuroblastomas*. J Pathol, 2003. **199**(4): p. 526-33.
422. Du, M.J., et al., *Estrogen induces Vav1 expression in human breast cancer cells*. PLoS One, 2014. **9**(6): p. e99052.
423. Dang, C.V., *MYC on the path to cancer*. Cell, 2012. **149**(1): p. 22-35.
424. Dalla-Favera, R., et al., *Human c-myc onc gene is located on the region of chromosome 8 that is translocated in Burkitt lymphoma cells*. Proc Natl Acad Sci U S A, 1982. **79**(24): p. 7824-7.
425. Lane, J., et al., *The expression and prognostic value of the guanine nucleotide exchange factors (GEFs) Trio, Vav1 and TIAM-1 in human breast cancer*. Int Semin Surg Oncol, 2008. **5**: p. 23.
426. Sebban, S., et al., *Vav1 fine tunes p53 control of apoptosis versus proliferation in breast cancer*. PLoS One, 2013. **8**(1): p. e54321.
427. Huang, M.Y., et al., *CDC25A, VAV1, TP73, BRCA1 and ZAP70 gene overexpression correlates with radiation response in colorectal cancer*. Oncol Rep, 2011. **25**(5): p. 1297-306.

428. Taub, R., et al., *Translocation of the c-myc gene into the immunoglobulin heavy chain locus in human Burkitt lymphoma and murine plasmacytoma cells*. Proc Natl Acad Sci U S A, 1982. **79**(24): p. 7837-41.
429. He, L., et al., *Loss of FBP function arrests cellular proliferation and extinguishes c-myc expression*. Embo j, 2000. **19**(5): p. 1034-44.
430. Deming, S.L., et al., *C-myc amplification in breast cancer: a meta-analysis of its occurrence and prognostic relevance*. Br J Cancer, 2000. **83**(12): p. 1688-95.
431. Blancato, J., et al., *Correlation of amplification and overexpression of the c-myc oncogene in high-grade breast cancer: FISH, in situ hybridisation and immunohistochemical analyses*. Br J Cancer, 2004. **90**(8): p. 1612-9.
432. Cannell, I.G., et al., *p38 MAPK/MK2-mediated induction of miR-34c following DNA damage prevents Myc-dependent DNA replication*. Proc Natl Acad Sci U S A, 2010. **107**(12): p. 5375-80.
433. Wang, Y.B., et al., *MicroRNA-184 inhibits proliferation and promotes apoptosis of human colon cancer SW480 and HCT116 cells by downregulating C-MYC and BCL-2*. J Cell Biochem, 2018. **119**(2): p. 1702-1715.
434. Si, W., et al., *A miR-20a/MAPK1/c-Myc regulatory feedback loop regulates breast carcinogenesis and chemoresistance*. Cell Death Differ, 2018. **25**(2): p. 406-420.
435. Clarke, R., et al., *Hormonal carcinogenesis in breast cancer: cellular and molecular studies of malignant progression*. Breast Cancer Res Treat, 1994. **31**(2-3): p. 237-48.
436. Wang, C., et al., *Estrogen induces c-myc gene expression via an upstream enhancer activated by the estrogen receptor and the AP-1 transcription factor*. Mol Endocrinol, 2011. **25**(9): p. 1527-38.
437. McNeil, C.M., et al., *c-Myc overexpression and endocrine resistance in breast cancer*. J Steroid Biochem Mol Biol, 2006. **102**(1-5): p. 147-55.
438. Miller, T.W., et al., *A gene expression signature from human breast cancer cells with acquired hormone independence identifies MYC as a mediator of antiestrogen resistance*. Clin Cancer Res, 2011. **17**(7): p. 2024-34.
439. Clarke, R., et al., *Endoplasmic reticulum stress, the unfolded protein response, and gene network modeling in antiestrogen resistant breast cancer*. Horm Mol Biol Clin Investig, 2011. **5**(1): p. 35-44.
440. Urra, H., et al., *Endoplasmic Reticulum Stress and the Hallmarks of Cancer*. Trends Cancer, 2016. **2**(5): p. 252-262.